

STUDIES OF THE ACTIVATION OF THE COENZYME B<sub>12</sub> PRECURSOR  $\alpha$ -RIBAZOLE  
AND ITS UNEXPECTED SYNTHESIS IN *SALMONELLA ENTERICA*

by

THEODORIC AARON MATTES

(Under the Direction of Jorge Escalante-Semerena)

ABSTRACT

Cobamides (Cbas) are cobalt-containing tetrapyrroles that are synthesized only by some bacteria and archaea. Cbas are distinguished from each other by the chemical identity of the lower ligand base. The lower ligand must be activated to a **unique nucleotide** before its attachment to the central ring of the cobamide precursor cobinamide-GDP. This nucleotide exhibits an alpha N-glycosidic linkage between the base and the C1 of the ribosyl moiety. Classically, this activation proceeds directly via a single enzyme, the phosphoribosyltransferase CobT. However, some Firmicutes utilize an alternative route to synthesize the ribotide: a transporter, CblT, to scavenge the  $\alpha$ -N-link riboside (i.e.,  $\alpha$ -Ribazole,  $\alpha$ -R) from the environment; and a kinase, CblS, to phosphorylate the riboside to the ribotide upon transport.

Here, we report that expression of CblS and CblT from *G. kaustophilus* restores growth in an *S. enterica* strain lacking CobT under conditions where Cba synthesis is required, even in the absence of the  $\alpha$ -riboside. This unexpected finding suggests that *S. enterica* synthesizes  $\alpha$ -R endogenously.

A continuous spectrophotometric assay revealed that CblS is specific for  $\alpha$ -N-linked ribosides. Feeding experiments reveal that while most  $\alpha$ -ribosides are utilized directly by *S. enterica* when

it depends on the kinase for the synthesis of  $\alpha$ -ribotides, the  $\alpha$ -riboside  $\alpha$ -adenosine is neither synthesized nor transported by *S. enterica*. Site-directed mutagenesis of conserved residues generated variants of the CblS kinase which could be used to probe for  $\alpha$ -R synthesis in *S. enterica*.

Attempts to understand how *S. enterica* synthesizes DMB and activates the base to  $\alpha$ -R revealed a complex interplay between purine metabolism and DMB scavenging as the loss of genes involved in nucleoside salvaging and purine biosynthesis resulted in strains unable to scavenge DMB. We report that the uptake of the bases 5-hydroxybenzimidazole or 5-methoxybenzimidazole lead to the synthesis of the 5,6-dimethylbenzimidazole (DMB)-containing Cba, indicating that the purine synthesis intermediate aminoimidazole-ribotide (AIR) may be the origin of DMB instead of reduced FMN, as has been proposed.

INDEX WORDS: Cobamide,  $\alpha$ -Ribotide,  $\alpha$ -Ribazole, 5,6-dimethylbenzimidazole, CblS, kinase, coenzyme B<sub>12</sub>, nucleotide synthesis, purines, *Salmonella enterica*, *Geobacillus kaustophilus*, *Firmicutes*

STUDIES OF THE ACTIVATION OF THE COENZYME B<sub>12</sub> PRECURSOR  $\alpha$ -RIBAZOLE  
AND ITS UNEXPECTED SYNTHESIS IN *SALMONELLA ENTERICA*

by

THEODORIC AARON MATTES

BS, **The** University of Nebraska-Lincoln, 2010

A Dissertation Submitted to the Graduate Faculty of The University of Georgia in Partial  
Fulfillment of the Requirements for the Degree

DOCTOR OF PHILOSOPHY

ATHENS, GEORGIA

2018

© 2018

Theodoric Aaron Mattes

All Rights Reserved

STUDIES OF THE ACTIVATION OF THE COENZYME B<sub>12</sub> PRECURSOR  $\alpha$ -RIBAZOLE  
AND ITS UNEXPECTED SYNTHESIS IN *SALMONELLA ENTERICA*

by

THEODORIC AARON MATTES

Major Professor: Jorge C Escalante-Semerena  
Committee: Diana M Downs  
Robert J Maier  
Vincent J Starai

Electronic Version Approved:

Suzanne Barbour  
Dean of the Graduate School  
The University of Georgia  
August 2018

*This thesis is dedicated in loving memory to  
Dr. Erich Peter Press, D.D.S., my maternal grandfather.*

*I love you and miss you, P'pa.*

## ACKNOWLEDGEMENTS

I would first like to thank my parents, **Victor and Linda**, for all their love and support. Between summer camps, trips to the library, and family vacations, you embraced my fascination with nature, and even indulged my earliest science experiments. When I got a microscope, you helped me find samples and prepare glass slides. You helped find me a blacksmith to build a log clamp I'd designed myself. And even when I accidentally cooked a frog, you still didn't stop me from pursuing my curiosity. This PhD is every bit your work as mine. I love you both.

**My siblings, Ben, Peter, and Katy**, who won't tell me they're proud of me, but I know they are, thank you for putting up with me liking weird stuff, and for opening your homes for me to escape from graduate school when I needed a break. I appreciate you all for being there for me all these years, even in the earliest days. You pushed me to be myself, and I know I wouldn't have this PhD without that drive to be different. So, thank you. And thank you for bringing **Shawna, Chad, Bekah, and baby Logan** into my life as well. Truly, truly, thank you, all of you.

**Dr. Clayton Kelling**, who started me on this journey ten years ago by telling me going to veterinary school was a waste of time and money if all I wanted to do was research.

**Dr. Greg Somerville**, who let me into his group, encouraged my curiosity, and ultimately led me to graduate school. Thank you Greg, for being the best mentor I could've asked for.

The **MDTP program at the University of Wisconsin-Madison**, for inviting me to pursue a PhD. While my stay was short, its impact will weigh heavy for many, many years.

To **Microsoft**, whose Windows operating system and Office software powered this thesis project, despite being surrounded by Macs.

To the **Microbiology Department here at the University of Georgia**, thank you for welcoming our lab as we escaped bad weather, on many fronts. I've made many memories here, developed great friendships, and witnessed amazing science being done. I believe it has been worth every day to be here, and the department should be proud of itself for that.

To the **Microbiology office staff**, especially Janice, thank you so much for all your efforts to keep this department afloat and to keep graduate students like me on track, even when our paperwork goes missing.

To all the friends who are still here, and those who have already left, thank you for filling the last eight years with your personalities and your support.

To the **distinguished alumni, all 31 of them**, who went before me under Jorge's tutelage and did so much to build out the knowledge found in the second chapter of this thesis, thank you, all of you. Your work kept the B<sub>12</sub> project funded for 30 years, and here's hoping our work keeps that going. And for those of you who I worked with, **Sandy, Tara, Heidi, Chi, Alex, Caryn, Ted, Kristy, and Norbert**, I couldn't have asked for a better group to begin my development as a scientist under. To my current colleagues, **Chelsey, Rachel, Tori, Flavia, Anatasia, and Libby**, thank you for making the lab what it is today. I'll miss working with all of you. We've survived floods and assorted facilities disasters, and I'll remember our time here fondly.

To my committee members, **Dr. Heidi Goodrich-Blair (Wisconsin), Dr. Doug Weibel (Wisconsin), Dr. Paul Weimer (Wisconsin), Dr. Diana Downs (Wisconsin and Georgia), Dr. Rob Maier (Georgia), and Dr. Vinny Starai (Georgia)**, thank you all for your help and advice over the last eight years. Thank you in particular to **Dr. Downs**, whose expertise on thiamine synthesis has proven rather essential as we work towards understanding how  $\alpha$ -ribosides are made.

To our lab manager **Jessie Will**, thank you for everything you do to keep the lab from descending into total anarchy and chaos. I know things will be a lot quieter when I'm gone. I recommend podcasts, they're great for filling the silence.

For my penultimate appreciation, to the man who taught me data is plural, an unending thank you to my advisor, **Jorge**. I know you sigh heavily when we thank you, because you're just "doing your job", but it still matters to us. Thirty years of B<sub>12</sub> funding isn't just because of the work we did, but because you inspired us, each in our own way, to raise the bar. I know my project didn't hit all the goals we'd hoped it would eight years ago, but I think we've learned a fair amount regardless. You've given me the freedom and the latitude to find my footing as a scientist, and for that, I'll always be grateful. Thank you.

Finally, I would like to note that this dissertation and the PhD that hopefully follows is only the second-best thing I've found here in Georgia. While words are never, ever enough, I'd like to thank my partner and my best friend, **Rachel**. Her love and support has been unflinching, even over the stress of the last year as I've worked to complete this thesis and find a job. Thank you for everything, Rachel. I can't imagine how I would've done this without you. I love you, and I'm excited for our future. You're next!

## TABLE OF CONTENTS

	Page
ACKNOWLEDGEMENTS .....	v
LIST OF TABLES .....	xii
LIST OF FIGURES .....	xiv
CHAPTER	
1 INTRODUCTION .....	1
OVERVIEW .....	1
DISSERTATION OUTLINE.....	2
REFERENCES .....	5
2 LITERATURE REVIEW: COBALAMIN BIOSYNTHESIS AND INSERTION..	8
ABSTRACT.....	9
INTRODUCTION .....	10
CONCLUDING REMARKS .....	53
ACKNOWLEDGEMENTS .....	53
REFERENCES .....	54
3 <i>SALMONELLA ENTERICA</i> SYNTHESIZES	
5,6-DIMETHYLBENZIMIDAZOYL-(DMB)- $\alpha$ -RIBOSIDE. WHY SOME	
<i>FIRMICUTES</i> DO NOT REQUIRE THE CANONICAL DMB ACTIVATION	
SYSTEM TO SYNTHESIZE ADENOSYLCOBALAMIN .....	90
ABSTRACT.....	91

INTRODUCTION .....	92
RESULTS .....	95
DISCUSSION .....	109
EXPERIMENTAL PROCEDURES .....	113
ACKNOWLEDGEMENTS .....	121
REFERENCES .....	121
4 FACILE ISOLATION OF $\alpha$ -RIBAZOLE FROM VITAMIN B <sub>12</sub> HYDROLYSATES USING BORONATE AFFINITY CHROMATOGRAPHY .....	128
ABSTRACT.....	129
INTRODUCTION .....	130
MATERIALS AND METHODS.....	132
RESULTS AND DISCUSSION .....	134
CONCLUSIONS.....	138
ACKNOWLEDGEMENTS .....	139
REFERENCES .....	139
5 FUNCTIONAL STUDIES OF $\alpha$ -RIBOSIDE ACTIVATION BY THE KINASE CBLS FROM <i>GEOBACILLUS KAUSTOPHILUS</i> CONFIRM THE EXCLUSIVE SYNTHESIS OF 5,6-DIMETHYLBENZIMIDAZOLYL-A-RIBOSIDE BY <i>SALMONELLA ENTERICA</i> .....	142
ABSTRACT.....	143
INTRODUCTION .....	144
MATERIALS AND METHODS.....	147

RESULTS .....	158
DISCUSSION .....	185
ACKNOWLEDGEMENTS.....	187
REFERENCES .....	187
6 INVESTIGATIONS INTO THE ORIGINS OF 5,6-DIMETHYLBENZIMIDAZOLE AND ITS $\alpha$ -RIBOSIDE $\alpha$ -RIBAZOLE IN <i>SALMONELLA ENTERICA</i> .....	192
ABSTRACT.....	193
INTRODUCTION .....	194
MATERIALS AND METHODS.....	196
RESULTS .....	207
DISCUSSION .....	230
ACKNOWLEDGEMENTS.....	236
REFERENCES .....	237
7 CONCLUSIONS.....	245
SUMMARY.....	245
RECOMMENDATIONS FOR FUTURE WORK .....	250
CONCLUSION.....	253
REFERENCES .....	253

## APPENDICES

- A SUPPLEMENTAL INFORMATION FOR “SALMONELLA ENTERICA  
SYNTHESIZES 5,6-DIMETHYLBENZIMIDAZOYL-(DMB)- $\alpha$ -RIBOSIDE.  
WHY SOME *FIRMICUTES* DO NOT REQUIRE THE CANONICAL DMB

	ACTIVATION SYSTEM TO SYNTHESIZE ADENOSYLCOBALAMIN” ....	255
B	SUPPLEMENTAL INFORMATION FOR “FACILE ISOLATION OF $\alpha$ -RIBAZOLE FROM VITAMIN B <sub>12</sub> HYDROLYSATES USING BORONATE AFFINITY CHROMATOGRAPHY .....	258
	REFERENCES .....	268
C	SUPPLEMENTAL INFORMATION FOR “FUNCTIONAL STUDIES OF $\alpha$ -RIBOSIDE ACTIVATION BY THE KINASE CBLs FROM <i>GEOBACILLUS</i> <i>KAUSTOPHILUS</i> ” .....	271
D	SUPPLEMENTAL INFORMATION FOR “INVESTIGATIONS INTO THE ORIGINS OF 5,6-DIMETHYLBENZIMIDAZOLE AND ITS $\alpha$ -RIBOSIDE $\alpha$ -RIBAZOLE IN <i>SALMONELLA ENTERICA</i> ” .....	278

## LIST OF TABLES

	Page
Table 3-1. Strains and plasmids used in this study. ....	114
Table 3-2. Oligonucleotides used in this study. ....	115
Table 4-1. Comparison of the estimated amount of $\alpha$ -R released under different hydrolysis conditions. ....	135
Table 4-2. A comparison to the previously published yield as determined by absorbance. ....	138
Table 5-1. Strains and plasmids used in this study. ....	152
Table 5-2. Oligonucleotides used in this study. ....	153
Table 5-3. Wavelengths and extinction coefficients of bases dissolved in DMSO. ....	153
Table 5-4. Michaelis-Menten kinetic parameters for Gk CblS on $\alpha$ -R and ATP. ....	164
Table 5-5. Generation time comparisons of Gk CblS variants. ....	184
Table 6-1. Strains used in this study. ....	200-201
Table 6-2. Plasmids used in this study. ....	202
Table 6-3. Oligonucleotides used for generating Wanner insertions in this study. ....	203
Table 6-4. Sequencing oligonucleotides used in this study. ....	204
Table 6-5. Cloning oligonucleotides used in this study. ....	205-206
Table 6-6. Generation time of the PNP and hydrolase deletion strains. ....	211
Table 6-7. Generation times in response to pTAC85 vectors on minimal medium. ....	214
Table 6-8. Generation times of <i>pur</i> gene knockouts. ....	227
Table B1. Bacterial strains and plasmids used in this study. ....	263

Table C1. Riboside (300 pM) feeding generation times (h) for JE17827 (empty vector), JE21364 ( <i>cblS</i> <sup>+</sup> ), and JE17830 ( <i>cblT</i> <sup>+</sup> , <i>cblS</i> <sup>+</sup> ) .....	272
Table C2. Riboside (300 nM) feeding generation times (h) for JE17827 (empty vector), JE21364 ( <i>cblS</i> <sup>+</sup> ), and JE17830 ( <i>cblT</i> <sup>+</sup> , <i>cblS</i> <sup>+</sup> ) .....	272
Table C3. $\alpha$ -Ado Feeding generation times (h) for JE17827 (empty vector) and JE17830 ( <i>cblT</i> <sup>+</sup> , <i>cblS</i> <sup>+</sup> ) .....	273
Table D1. Plasmid-carrying strains used in Chapter 6 .....	279-282

## LIST OF FIGURES

	Page
Figure 2-1. Flow diagram from uroporphyrinogen III to adenosylcobalamin.....	13
Figure 2-2. The transformation of uroporphyrinogen III into precorrin-2.....	14
Figure 2-3. The anaerobic pathway for corrin ring synthesis. ....	16
Figure 2-4. The aerobic pathway for corrin ring synthesis.....	20
Figure 2-5. The transformation of cobyrinic acid <i>a,c</i> -diamide into adenosylcobyrinic acid.....	23
Figure 2-6. AdoCba structure and lower ligand diversity.....	25
Figure 2-7. 4- and 5-coordinate Co(II)balamin in the active site of a CobA class ACAT. ....	30
Figure 2-8. 4- and 5-coordinate Co(II)balamin in the active site of a PduO class ACAT. ....	32
Figure 2-9. Binding motifs and sequences unique to the ACATs. ....	36
Figure 2-10. The nucleotide loop assembly pathway for AdoCba biosynthesis in bacteria and archaea. ....	39
Figure 3-1. Late steps in AdoCbl biosynthesis.....	93
Figure 3-2. <i>GkCbIS</i> is necessary and sufficient for incorporation of endogenously generated $\alpha$ -R into AdoCba.....	98
Figure 3-3. Purified His <sub>6</sub> - <i>GkCbIS</i> .....	100
Figure 3-4. <i>GkCbIS</i> converts $\alpha$ -R to $\alpha$ -RP at the expense of ATP.....	102
Figure 3-5. RP-HPLC Analysis of corrinoid extracts.....	107
Figure 3-6. $\alpha$ -RP biosynthesis model via direct DMB activation or $\alpha$ -R scavenging. ....	108, 146
Figure 4-1. Structure of CoB <sub>12</sub> , its precursors, and the known routes to $\alpha$ -R-5'-P. ....	131

Figure 4-2. Schematic of the process for the isolation of $\alpha$ -R synthesis from CNB <sub>12</sub>	
hydrolysates. ....	137
Figure 5-1. Optimizing the coupled kinase assay for use with <i>Gk</i> CblS .....	160
Figure 5-2. <i>Gk</i> CblS is a monomer in solution .....	163
Figure 5-3. Determining the Michaelis-Menten kinetic parameters for <i>Gk</i> CblS on $\alpha$ -R and	
ATP .....	164
Figure 5-4. Specific activity of <i>Gk</i> CblS on different ribosides at 1.75 mM ATP. ....	168
Figure 5-5. <i>Gk</i> CblS phosphorylates $\alpha$ -Ado .....	169
Figure 5-6. The kinase requires picomolar amounts of $\alpha$ -R to restore growth in a $\Delta cobT \Delta cobB$	
strain.....	173
Figure 5-7. The CblS kinase can activate $\alpha$ -ribosides in <i>S. enterica</i> .....	174
Figure 5-8. Cell extracts of $\Delta cobT \Delta cobB / pGkCblTS^+$ can activate $\alpha$ -Ado <i>in vitro</i> .....	176
Figure 5-9. Cell extracts of $\Delta cobT \Delta cobB / pGkCblTS^+$ can activate $\alpha$ -R <i>in vitro</i> . ....	177
Figure 5-10. Corrinoïd extractions reveal that pseudoCbl is synthesized when $\Delta cobT \Delta cobB /$	
<p><i>pGkCblTS<sup>+</sup></i> is fed <math>\alpha</math>-Ado. ....</p>	179
Figure 5-11. Annotation of a Clustal Omega alignment of CblS reveals conserved residues in the	
ATP binding domain.....	182
Figure 6-1. The growth rate of JE17830 varies with the concentration of DMB under limiting	
conditions.....	218
Figure 6-2. Comparison of generation time (in hours) when fed various bases .....	219
Figure 6-3. Corrinoïd extractions reveal that CNCbl is synthesized when $\Delta cobT \Delta cobB /$	
<p><i>pGkCblTS<sup>+</sup></i> (JE17830) is fed hydroxyBza or methoxyBza. ....</p>	223

Figure 6-4. Purine biosynthetic pathway in <i>S. enterica</i> and its possible connections to DMB biosynthesis.....	229
Figure 6-5. A new model for Cbl biosynthesis in <i>S. enterica</i> $\Delta cobT$ / pGkCblS <sup>+</sup> .....	224
Figure 7-1. A model for the multiple routes to $\alpha$ -RP demonstrated in <i>S. enterica</i> .....	249
Figure A-1. <i>cblT</i> and <i>cblS</i> are found within the <i>cob</i> operon of <i>G. kaustophilus</i> .....	256
Figure A-2. UV-visible spectrum of an unknown compound present in all extracted corrinoid mixtures.....	257
Figure B-1. UV-Vis spectral scan of water.....	264
Figure B-2. UV-Vis spectral scan of DMSO .....	265
Figure B-3. Corrinoid scavenging growth assay controls.....	266
Figure B-4. Mass spectrometric analysis of final product .....	267
Figure B-5. $\alpha$ -R Scavenging Bioassay Results.....	268
Figure C-1. MALDI analysis of synthesized ribosides.....	275
Figure C-2. <i>Gk</i> CblS activates $\alpha$ -HOB-R, $\alpha$ -MOB-R, and $\alpha$ -Bnz-R.....	276

## CHAPTER 1

### INTRODUCTION

#### OVERVIEW

Coenzyme B<sub>12</sub> (CoB<sub>12</sub>) is a unique, complex molecule consisting of a cobalt-containing cyclic tetrapyrrole (similar to other metal-binding tetrapyrroles like heme or chlorophyll), with both an upper and lower ligand, a feature not found in any other coenzyme (1). Its biosynthesis, reviewed in (1), is limited to some archaea and bacteria; and involves the synthesis and activity of dozens of enzymes to achieve the construction of this complex molecule. The enzymes must: form the specialized cyclic tetrapyrrole (1); insert a single cobalt ion (1); reduce that cobalt in order to attach a 5' deoxyadenosine as an upper ligand (2); prepare the tetrapyrrole for attachment of a lower ligand by attaching and guanylyating an amino-propanol moiety (3); synthesize an  $\alpha$ -N-linked nucleotide to serve as the lower ligand (4); and finally condense the prepared tetrapyrrole and the lower ligand (5). A phosphate is cleaved from the lower ligand nucleotide to complete the molecule (6). Some organisms have developed ways to bypass steps of this synthesis through scavenging (7) and remodeling (8).

In *Salmonella enterica* (which can synthesize CoB<sub>12</sub> *de novo*) and many other CoB<sub>12</sub> synthesizing organisms, the synthesis of the lower ligand nucleotide typically proceeds through the direct activation of the nucleobase to the  $\alpha$ -ribose via the enzyme 5,6-dimethylbenzimidazole: nicotinate mononucleotide phosphoribosyltransferase (DMB:NaMN PRTase) (5), encoded by *cobT* in *S. enterica* (9). However, in some *Firmicutes*, they lack this route to activation (10). Instead, they appear to be able to scavenge the  $\alpha$ -N-linked riboside from

the environment by a specialized transporter (CblT), which can then be phosphorylated (activated) to the  $\alpha$ -ribotide by a specialized kinase (CblS) (10). How the riboside is synthesized is unknown, though there is some evidence of its presence in the environment (11).

There are two known routes to synthesis of the base 5,6-dimethylbenzimidazole (DMB), which serves as the base of the lower ligand in the form of CoB<sub>12</sub> utilized by all animals. In the aerobic route, a single protein, BluB, catalyzes the conversion of reduced flavin mononucleotide to DMB using molecular oxygen (12-14). In the anaerobic route, found in *Eubacterium limosum*, the purine intermediate 5-aminoimidazole ribotide reacts with S-adenosylmethionine to synthesize 5-hydroxybenzimidazole (15), which is then modified by a series of enzymes to DMB (16). *Salmonella enterica* lacks homologs enabling either pathway, yet, under aerobic conditions, *S. enterica* synthesizes the DMB-containing CoB<sub>12</sub> molecule. Note that bases other than DMB can be utilized as that lower ligand base (17-19), but only DMB is found as the lower ligand in CoB<sub>12</sub> in humans (20).

This work discussed in this dissertation evolves our understanding of this unique pathway. In the progress of these studies, we discovered that *S. enterica* could synthesize the  $\alpha$ -riboside  $\alpha$ -ribazole ( $\alpha$ -R) endogenously in the absence of CobT, which was unexpected. We used this finding to study i) how *S. enterica* synthesizes DMB, and ii) how bacteria synthesize  $\alpha$ -ribosides, using *S. enterica* as a model.

## **DISSERTATION OUTLINE**

The effort to understand this phenomenon is described in this dissertation. An improved, rapid method for synthesizing the  $\alpha$ -riboside  $\alpha$ -R from vitamin B<sub>12</sub> was prepared to enable the development of an assay for the CblS kinase. This assay revealed that the kinase recognized any riboside carrying an  $\alpha$ -N-glycosidic bond, including  $\alpha$ -adenosine. Alanine scanning of

conserved residues of CblS generated variants which will help in studying the synthesis of  $\alpha$ -R in *S. enterica*. The remainder of this work describes investigates how *S. enterica* synthesizes DMB and  $\alpha$ -R.

In Chapter 2, we discuss the published research concerning the complex biosynthesis of CoB<sub>12</sub> in bacteria and archaea. This review emphasizes the diversity and complexity of this crucial biosynthetic pathway. It also highlights the current questions in the field.

In Chapter 3, we reported the finding that when the transporter CblT and kinase CblS from *G. kaustophilus* replace CobT in *S. enterica*, *S. enterica* synthesizes  $\alpha$ -R endogenously. Under conditions requiring synthesis of CoB<sub>12</sub> for growth, expression of these proteins not only restored growth, but force the cell to synthesize only the DMB-containing cobamide. Attempts to use the kinase CblS to perform the DMB: PRTase activity failed, confirming that *S. enterica* could be synthesizing  $\alpha$ -R endogenously. By limiting the amount of the tetrapyrrole precursor provided, the strain became auxotrophic for DMB or  $\alpha$ -R. These findings lay the groundwork for the remainder of this dissertation.

In Chapter 4, we reported a new method for synthesizing  $\alpha$ -R from vitamin B<sub>12</sub>, the cyanated form of the DMB-containing CoB<sub>12</sub>. In the original method, B<sub>12</sub> hydrolysates containing  $\alpha$ -R were separated over a C18 resin, and then cleaned up further by high-pressure liquid chromatography. Due to similar binding affinities for the C18 resin, the leftover B<sub>12</sub> and  $\alpha$ -R co-elute, resulting in the need for additional clean-up. We were able to avoid additional clean-up by switching to boronate affinity chromatography, resulting in a single-step chromatography purification. By using this method, we can rapidly synthesize  $\alpha$ -R for probing kinase activity both *in vitro* and in *S. enterica*.

In Chapter 5, we report the development of a continuous spectrophotometric assay for the *G. kaustophilus* CblS kinase, which we use to determine the apparent  $K_m$  for  $\alpha$ -R and ATP. We use those values to test CblS against other synthesized  $\alpha$ -ribosides as well as  $\beta$ -ribosides. We found that CblS could phosphorylate all of the  $\alpha$ -ribosides we synthesized. We then attempted to feed the  $\alpha$ -ribosides to a strain which uses CblS instead of the DMB: NaMN PRTase CobT, under conditions which require the  $\alpha$ -ribosides to restore B<sub>12</sub> biosynthesis. We found that all but  $\alpha$ -adenosine could permit growth in *S. enterica*. Testing with cell extracts from that strain did not show any impairment in the activation of the enzyme, leading us to propose that the issue is transport, rather than any endogenous degradation, that prevents utilization of  $\alpha$ -adenosine. We also reported on some variants of CblS, two of which may be useful in the future for generating complementary suppressor mutations in *S. enterica*.

In Chapter 6, we report that disruption of the nucleoside scavenging enzymes results in a loss of ability to scavenge DMB when the ring precursor is limited, but it does not prevent synthesis of  $\alpha$ -R. We then proposed that perhaps this effect was due to disruptions in DMB biosynthesis. To begin probing DMB biosynthesis, riboflavin, based on the results of earlier tracing studies, was fed to of a  $\Delta cobT \Delta cobB / pGkCbITS^+$  strain under conditions auxotrophic for DMB, but riboflavin was unable to resolve a DMB auxotrophy, even when provided at 100-fold the concentration provided in the tracing studies. We next attempted to feed intermediates of the anaerobic biosynthetic pathway, 5-hydroxybenzimidazole and 5-methoxybenzimidazole, and found that while they allowed growth, the cell appears to be incorporating DMB in their place. Strangely, however, blocks in purine synthesis did not stop growth in a strain producing CblS instead of CobT, but it did disrupt DMB scavenging. Our results indicate a possible connection to DMB scavenging at N<sup>5</sup>- carboxyaminoimidazole ribonucleotide, the carboxylated form of

AIR. These results indicate strong ties between purine metabolism and DMB/ $\alpha$ -R synthesis in *S. enterica* and offer avenues for further exploration of those questions.

## REFERENCES

1. Mattes TA, Deery E, Warren MJ, Escalante-Semerena JC. 2017. Cobalamin Biosynthesis and Insertion, p 1-24. In Scott RA (ed), Encyclopedia of Inorganic and Bioinorganic Chemistry doi:10.1002/9781119951438.eibc2489. John Wiley & Sons, Ltd, Chichester, UK.
2. Fonseca MV, Escalante-Semerena JC. 2000. Reduction of cob(III)alamin to cob(II)alamin in *Salmonella enterica* Serovar Typhimurium LT2. J Bacteriol 182:4304-4309.
3. Blanche F, Debussche L, Famechon A, Thibaut D, Cameron B, Crouzet J. 1991. A bifunctional protein from *Pseudomonas denitrificans* carries cobinamide kinase and cobinamide phosphate guanylyltransferase activities. J Bacteriol 173:6052-6057.
4. Friedmann HC, Harris DL. 1965. The Formation of alpha-glycosidic 5'-nucleotides by a single displacement trans-*N*-glycosidase. J Biol Chem 240:406-412.
5. Cameron B, Blanche F, Rouyez MC, Bisch D, Famechon A, Couder M, Cauchois L, Thibaut D, Debussche L, Crouzet J. 1991. Genetic analysis, nucleotide sequence, and products of two *Pseudomonas denitrificans* cob genes encoding nicotinate-nucleotide: dimethylbenzimidazole phosphoribosyltransferase and cobalamin (5'-phosphate) synthase. J Bacteriol 173:6066-6073.
6. Zayas CL, Escalante-Semerena JC. 2007. Reassessment of the late steps of coenzyme B<sub>12</sub> synthesis in *Salmonella enterica*: Evidence that dephosphorylation of

- adenosylcobalamin-5'-phosphate by the CobC phosphatase is the last step of the pathway. J Bacteriol 189:2210-2218.
7. Jeter RM, Olivera BM, Roth JR. 1984. *Salmonella typhimurium* synthesizes cobalamin (vitamin B12) de novo under anaerobic growth conditions. J Bacteriol 159:206-213.
  8. Woodson JD, Escalante-Semerena JC. 2004. CbiZ, an amidohydrolase enzyme required for salvaging the coenzyme B<sub>12</sub> precursor cobinamide in archaea. Proc Natl Acad Sci USA 101:3591-3596.
  9. Trzebiatowski JR, O'Toole GA, Escalante-Semerena JC. 1994. The *cobT* gene of *Salmonella typhimurium* encodes the NaMN: 5,6-dimethylbenzimidazole phosphoribosyltransferase responsible for the synthesis of *N*<sup>1</sup>-(5-phospho-alpha-D-ribose)-5,6-dimethylbenzimidazole, an intermediate in the synthesis of the nucleotide loop of cobalamin. J Bacteriol 176:3568-3575.
  10. Gray MJ, Escalante-Semerena JC. 2010. A new pathway for the synthesis of alpha-ribazole-phosphate in *Listeria innocua*. Mol Microbiol 77:1429-1438.
  11. Johnson WM, Kido Soule MC, Kujawinski EB. 2016. Evidence for quorum sensing and differential metabolite production by a marine bacterium in response to DMSP. ISME J 10:2304-2316.
  12. Gray MJ, Escalante-Semerena JC. 2007. Single-enzyme conversion of FMNH<sub>2</sub> to 5,6-dimethylbenzimidazole, the lower ligand of B<sub>12</sub>. Proc Natl Acad Sci U S A 104:2921-2926.
  13. Taga ME, Larsen NA, Howard-Jones AR, Walsh CT, Walker GC. 2007. BluB cannibalizes flavin to form the lower ligand of vitamin B12. Nature 446:449-453.

14. Campbell GR, Taga ME, Mistry K, Lloret J, Anderson PJ, Roth JR, Walker GC. 2006. *Sinorhizobium meliloti bluB* is necessary for production of 5,6-dimethylbenzimidazole, the lower ligand of B12. *Proc Natl Acad Sci U S A* 103:4634-4369.
15. Mehta AP, Abdelwahed SH, Fenwick MK, Hazra AB, Taga ME, Zhang Y, Ealick SE, Begley TP. 2015. Anaerobic 5-Hydroxybenzimidazole formation from aminoimidazole ribotide: an unanticipated intersection of thiamin and vitamin B12 biosynthesis. *J Am Chem Soc* doi:10.1021/jacs.5b03576.
16. Hazra AB, Han AW, Mehta AP, Mok KC, Osadchiy V, Begley TP, Taga ME. 2015. Anaerobic biosynthesis of the lower ligand of vitamin B12. *Proc Natl Acad Sci U S A* 112:10792-10797.
17. Cheong CG, Escalante-Semerena JC, Rayment I. 2001. Structural investigation of the biosynthesis of alternative lower ligands for cobamides by nicotinate mononucleotide: 5,6-dimethylbenzimidazole phosphoribosyltransferase from *Salmonella enterica*. *J Biol Chem* 276:37612-37620.
18. Crofts TS, Seth EC, Hazra AB, Taga ME. 2013. Cobamide structure depends on both lower ligand availability and CobT substrate specificity. *Chem Biol* doi:10.1016/j.chembiol.2013.08.006.
19. Hazra AB, Tran JL, Crofts TS, Taga ME. 2013. Analysis of substrate specificity in CobT homologs reveals widespread preference for DMB, the lower axial ligand of vitamin B(12). *Chem Biol* 20:1275-1285.
20. Pakin C, Bergaentzle M, Aoude-Werner D, Hasselmann C. 2005.  $\alpha$ -Ribazole, a fluorescent marker for the liquid chromatographic determination of vitamin B<sub>12</sub> in foodstuffs. *J Chromatogr A* 1081:182-189.

CHAPTER 2  
LITERATURE REVIEW:  
COBALAMIN BIOSYNTHESIS AND INSERTION<sup>1</sup>

---

<sup>1</sup> Mattes, T. A., Deery, E., Warren, M. J. and J. C Escalante-Semerena. 2017. *Encyclopedia of Inorganic and Bioinorganic Chemistry*. Accepted.  
Reprinted here with permission of publisher.

## ABSTRACT

Metal-containing cyclic tetrapyrroles are widely distributed in nature, and together comprise the family of compounds frequently referred to as ‘the pigments of life’, namely cobamides (Cba, contain cobalt), chlorophylls (contain magnesium), hemes (contain iron), and factor F<sub>430</sub> (contains nickel). In comparison to these other modified tetrapyrroles, the B<sub>12</sub> architecture is slightly different. The chemistry of the cobalt ion is key to the function of the molecule as either a coenzyme or cofactor. Other differences include a contraction of the tetrapyrrole mainframe, which allows for tighter binding of the metal, and the presence of a lower nucleotide loop that provides an extra ligand for the metal. The biosynthesis of adenosylcobalamin requires the concerted effort of around thirty enzyme-mediated steps tethered with the cellular provision of a range of cofactors and cobalt. The biosynthesis can be divided into two major sections, the first being the synthesis of the tetrapyrrole-derived corrin ring and the second involving the synthesis and attachment of the lower nucleotide loop. In the last decade, much has been learned about how the vitamin form is converted to its biologically active coenzymic form, providing mechanistic answers into the events that overcome steep thermodynamic barriers in the formation of the covalent, organometallic bond between the cobalt ion of the ring and the 5'-deoxyadenosyl upper ligand. Exciting recent discoveries regarding the biosynthesis of the lower ligand base 5,6-dimethylbenzimidazole in aerobes and anaerobes have filled long-standing gaps of knowledge, providing a solid platform for the analysis of what is likely to be a membrane-anchored multienzyme complex.

## INTRODUCTION

**Which organisms synthesize, and which use cobamides?** *The makers:* To date, Cba biosynthesis is a metabolic capability found only in some bacteria and archaea, but not in eukarya (1). Some microorganisms cannot synthesize the entire molecule *de novo* but, if provided with the complete tetrapyrrole macrocycle, they can attach the upper ligand, synthesize the lower ligand base, and assemble the nucleotide loop. All the enzymes needed for the assembly of the entire molecule have been identified through studies performed in different microorganisms. However, the complete set of genes encoding AdoCba biosynthetic functions has not been identified in any one microorganism. *The users:* Animals, including humans, require the Cba known as cobalamin (Cbl; contains 5,6-dimethylbenzimidazole as its lower ligand base). In humans, mal-absorption of Cbl causes megaloblastic anemia (a.k.a. pernicious anemia) (2, 3), while a Cbl-deficient diet can cause severe nervous system disorders (4-6). Animals do not synthesize Cbl, but they do convert vitamin B<sub>12</sub> (CNCbl) to AdoCbl, the biologically active form of Cbl (a.k.a. coenzyme B<sub>12</sub>). (7-9) Failure to convert the vitamin to the coenzyme results in inborn errors of metabolism associated with severe mental retardation and high infant mortality (5, 10, 11). Although higher plants do not use or synthesize Cbl, microalgae are known Cbl auxotrophs (12-14).

### ***De novo* Corrin Ring Biosynthesis.**

Bacteria and archaea make the corrin ring component of Cbas *de novo* by one of two routes, which are referred to as the aerobic or anaerobic routes. The aerobic route is so-called because the pathway requires molecular oxygen to assist in the ring contraction process. In contrast, the anaerobic route does not require oxygen and can operate under either anoxic or normoxic conditions. Overall, the transformation of uroporphyrinogen III into cobyrinic acid involves the addition of eight *S*-adenosylmethionine (SAM) derived methyl groups, cobalt insertion,

decarboxylation, six amidations and ring contraction. During the biosynthesis of the corrin ring the intermediates are termed precorrin-n, where n refers to the number of methyl groups that have been added to the uroporphyrinogen III template. The two pathways proceed with the same order of methyl group addition but they differ in the timing of cobalt insertion. As the anaerobic pathway involves the early chelation of cobalt, the intermediates along the anaerobic pathway are generally therefore cobalt-precorrins. The two pathways diverge at the level of precorrin-2 but re-join at the level of cobyrinic acid *a,c*-diamide. An overview of the two pathways, the intermediates and the enzymes involved is shown in Figure 2-1.

As with all modified tetrapyrroles the corrin component of B<sub>12</sub> is derived from uroporphyrinogen III. This molecule undergoes *bis*-methylation, with the addition of two SAM-derived methyl groups to positions C2 and C7 of the macrocycle in a reaction catalyzed by the enzyme uroporphyrinogen methyltransferase to yield the product precorrin-2 (Figure 2-2). This enzyme was first identified in *Pseudomonas denitrificans* and was designated CobA (15, 16). In some organisms the uroporphyrinogen methyltransferase is fused with other enzymes to generate multifunctional enzymes. For instance, in *Desulfovibrio vulgaris* it is fused to a uroporphyrinogen III synthase, thereby coupling the synthesis of uroporphyrinogen III and precorrin-2 (17). In *E. coli* and *S. enterica*, the uroporphyrinogen III methyltransferase is fused with a precorrin-2 dehydrogenase/sirohydrochlorin ferrochelatase called CysG, which is able to convert uroporphyrinogen III into siroheme (18, 19). The structures of both the CobA and CysG have been determined with the reaction product *S*-adenosylhomocysteine (SAH) (20, 21). The structure of another uroporphyrinogen methyltransferase, NirE, has also been determined but in the presence of uroporphyrinogen III (22). All the methyltransferases are homodimers, with each subunit composed of two a/b domains, with the active site located at the juncture. Thus each dimer has

two active sites. The uroporphyrinogen III binds in close proximity to the SAM-binding area to allow methylation initially at C2, which generates precorrin-1. The SAH dissociates away and is replaced by SAM and the precorrin-1 has to rebind in such a position so as to allow the second methylation at C7. It has been suggested that a catalytic arginine residue acts as a general base to enhance the reaction mechanism (22). A number of substitutions have also been reported that enhance the production of precorrin-1 over precorrin-2, presumably through favoring binding of uroporphyrinogen III over precorrin-1. It is at this stage that the two pathways for cobalamin production divide. In this article we will look at the anaerobic pathway first before describing the aerobic route.

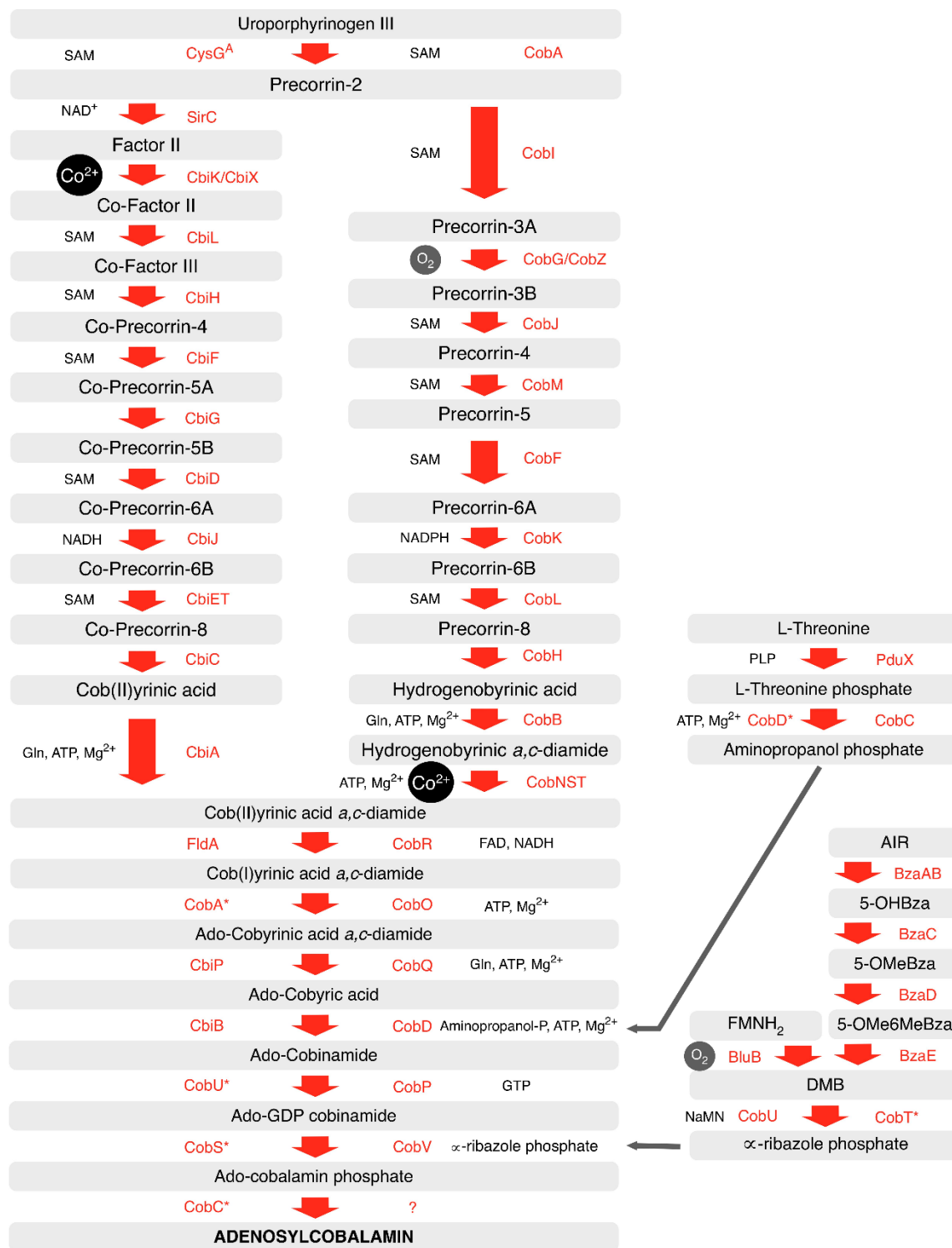


**Figure 2-1. Flow diagram outlining the intermediates en route from uroporphyrinogen III to adenosylcobalamin.** The diagram shows not only the pathways for corrin ring synthesis but also the sources of the aminopropanol and dimethylbenzimidazole.

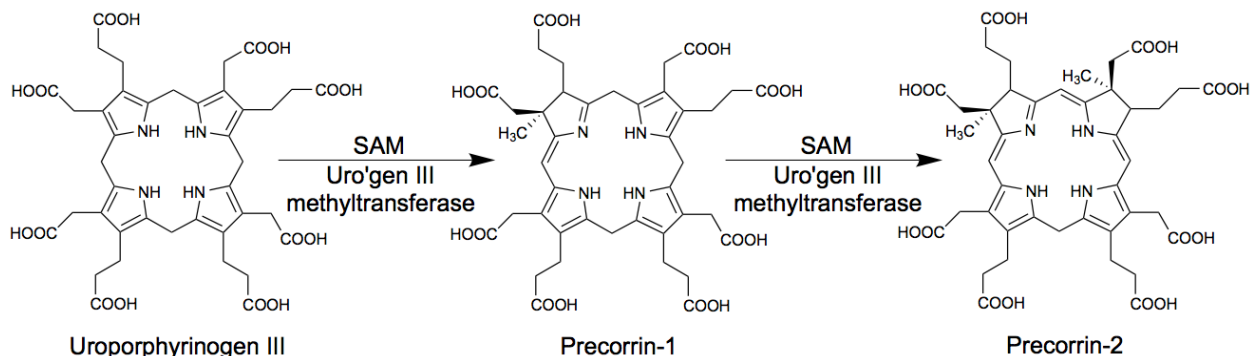


**Figure 2-2. The transformation of uroporphyrinogen III into precorrin-2.** The reaction is catalysed by the uroporphyrinogen III methyltransferase and methylates uroporphyrinogen III at positions 2 and 7 in an *S*-adenosylmethionine-dependent manner. The first methylation generates precorrin-1 prior to the second methylation event.

### The anaerobic route.

The anaerobic route between precorrin-2 and cobyrinic acid *a,c*-diamide is shown in Figure 2-3. The genes for the anaerobic route for cobalamin synthesis were initially identified in *S. enterica* (23, 24), and subsequently in *Bacillus megaterium* (25, 26). The genes formerly known as *cobI* were then re-named as *cbi* to reflect their involvement in *de novo* cobinamide biosynthesis. The genes for the conversion of cobinamide into cobalamin were termed *cob*. This nomenclature has caused a certain level of confusion as the genes in the aerobic pathway were all termed *cob*, which means that, for instance, the *cobA* gene refers to two quite separate encoded functions depending whether it relates to the aerobic or anaerobic pathway (Figure 2-1). On the anaerobic route precorrin-2 is oxidized to give sirohydrochlorin (sometimes referred to as factor II) (Figure 2-3). A number of enzymes capable of catalysing the dehydrogenation of precorrin-2 have been described, including CysG and SirC (20, 27, 28). These enzymes utilize  $\text{NADP}^+$  as a cofactor to assist in the removal of two protons and two electrons, thereby introducing another double bond, to give sirohydrochlorin. The structures of SirC and the relevant portion of CysG reveal a

homodimer with each monomer containing a Rossmann fold into which binds the NADP<sup>+</sup>. The synthesis of sirohydrochlorin provides a more stable framework into which the cobalt ion is chelated. Indeed, the cobaltochelataase is the next step in the pathway and converts sirohydrochlorin into cobalt-sirohydrochlorin (Figure 2-3). The first cobaltochelataase to be identified was CbiK from *S. enterica* (29) and the enzyme belongs to the type II chelataase family (30). Type II chelataases are generally either monomeric or homodimeric enzymes that insert a divalent metal ion without any requirement for ATP. CbiK was shown to insert cobalt into sirohydrochlorin although in the absence of cobalt it will insert iron to generate siroheme (29). The structure of CbiK has been solved and its overall topology is similar to the ferrochelataases associated with heme biosynthesis (*see "Heme Biosynthesis and Insertion"*) (31) despite a very low sequence similarity (32, 33). The enzyme catalyzes the removal of two protons from the pyrrole nitrogens to allow for metal insertion. A further specific cobaltochelataase was also discovered in *Bacillus megaterium*, and termed CbiX<sup>L</sup> (34). This protein shares some similarity to CbiK but sequence analysis also revealed that the *N*-terminal half of the protein shared sequence similarity with the *C*-terminal half. This suggested that the protein may have arisen as a result of a gene duplication and fusion event.

Moreover, the very *C*-terminal region of the protein contains an MXCXXC motif that is followed by a histidine-rich region. Subsequently, it was shown that the MXCXXC motif is involved in the formation of an Fe-S center and that the histidine rich region is able to bind divalent metal ions such as cobalt or nickel (34). The role of the Fe-S center remains unknown but it is interesting to note that a number of different chelataases appear to house these redox centers (35).

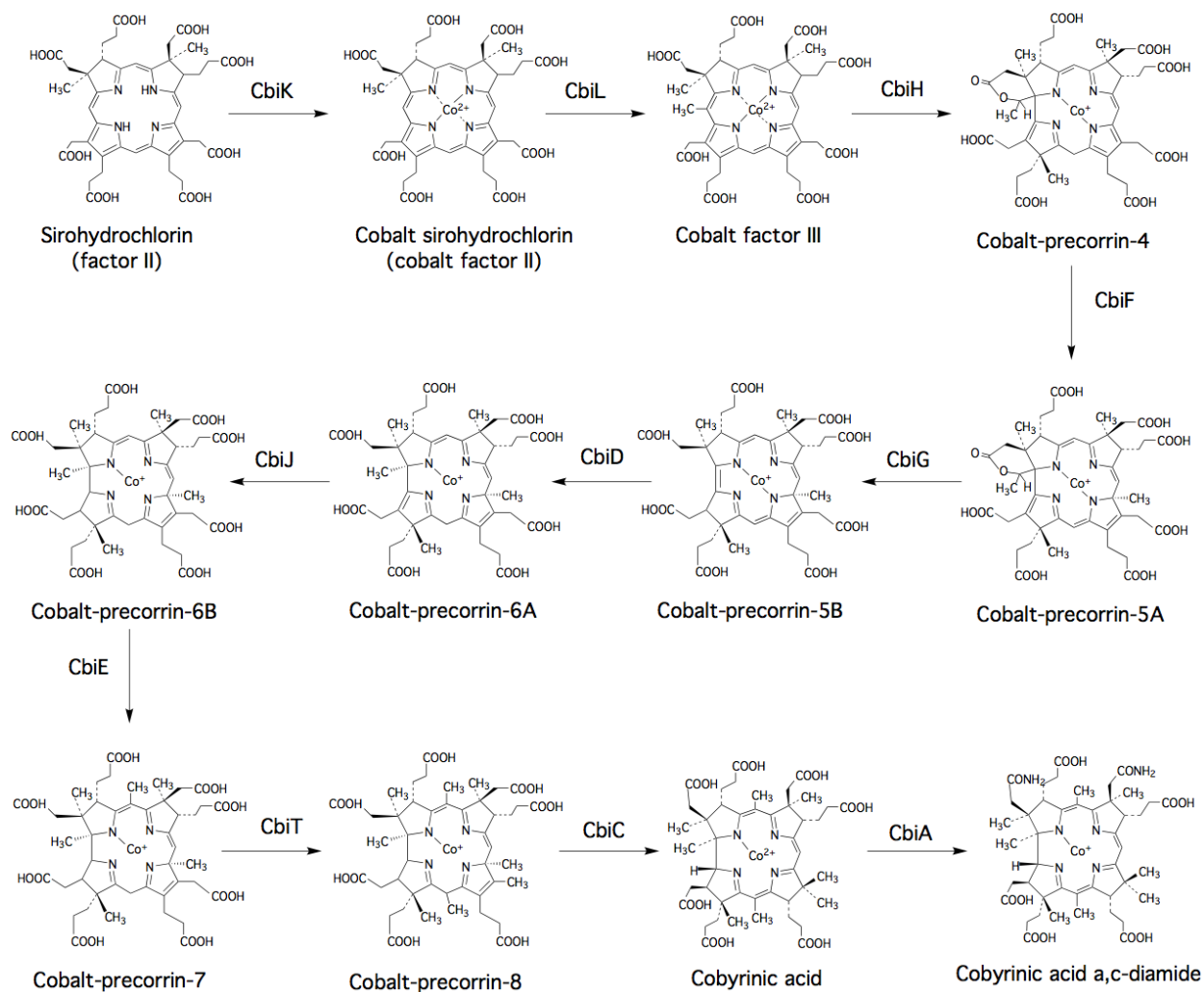


**Figure 2-3. The anaerobic pathway for corrin ring synthesis.** The steps involved in the transformation of sirohydrochlorin (factor II) and cobyric acid *a,c*-diamide are shown.

It is presumed that the histidine-rich sequence allows for binding of metal ion so that the protein can acquire the metal and store it in close proximity to the active site of the enzyme. The *N*-terminal protein sequence of CbiX<sup>L</sup> was used to search the protein databases for smaller versions of the chelatase. This revealed that such smaller proteins, of around 100 amino acids, are found in the Archaea (30). The genes encoding these proteins were cloned and the recombinant proteins were subsequently shown to act as cobaltochelataes. These smaller CbiX proteins were therefore termed CbiX<sup>S</sup>. The proteins dimerize to generate structures that have an overall topology that is

similar to CbiK (32, 36). Significantly, though, they have symmetrical active sites. All of these chelatasases have a number of histidine residues at the active site, which appear to be important for either proton abstraction or metal binding.

Cobalt sirohydrochlorin acts as the substrate for the C20 methyltransferase, which converts the substrate into cobalt-factor III in a reaction catalysed by CbiL (37-39). As with the majority of methyltransferases in the cobalamin biosynthetic pathway the C20 methyltransferase is a class III methyltransferase and therefore has a high degree of structural similarity to the other enzymes (40). Methylation at C20 appears initially as a futile process since the C20 position is extruded and lost during the ring contraction process. However, methylation is necessary to derivatize the C20 position into a tertiary alcohol, which studies have shown is required to promote the contraction reaction (41).

The ring contraction step is itself catalyzed by CbiH, a methyltransferase that adds a methyl group to C17 but in so doing initiates the formation of a direct bond between C1 and C19. The enzyme requires dithiothreitol (DTT), which is required to reduce the substrate, cobalt-factor III, to generate cobalt-precorrin-4 (42-44). In *B. megaterium* CbiH contains an Fe-S center and this redox center may be involved in the reduction of the macrocycle. Other CbiH enzymes do not appear to have an Fe-S center. Thus, CbiH is a multifunctional methyltransferase in that it promotes both methylation and ring contraction and in so doing generates a delta-lactone ring attached to ring A of the macrocycle (42-45).

Cobalt-precorrin-4 acts as the substrate for the C11 methyltransferase, CbiF, which generates cobalt-precorrin-5A (38, 42, 43, 46-49). This methyl group ultimately ends up in the C12 position after a subsequent rearrangement reaction. However, before that happens the delta-lactone ring is broken down, liberating acetaldehyde (44, 50), and generating cobalt-precorrin-5B in a reaction

catalyzed by CbiG (43, 45, 46). A further methylation at C1 by CbiD gives rise to cobalt-precorrin-6A (45, 51) before the removal of one of the double bonds in the macrocycle by CbiJ, which requires NADH as a cofactor, produces cobalt-precorrin-6B (45).

The next step sees the decarboxylation of the acetate side chain attached to ring C and the methylation of the C15 position in a reaction catalyzed by CbiT that gives rise to cobalt-precorrin-7 (45). The two processes are probably linked as neither a decarboxylated cobalt-precorrin-6B or a carboxylated cobalt-precorrin-7 has been isolated. The final methylation sees the addition of a methyl group to C5 in a reaction catalyzed by CbiE, which gives rise to cobalt-precorrin-8 (45). In some organisms the two individual enzymes, CbiE and CbiT, are found as a protein fusion, CbiET (26).

With the decarboxylation of the acetate on ring C having taken place the following reaction then sees the movement of the methyl group from C11 to C12. This comparatively unusual methyl rearrangement reaction generates cobyrinic acid in a reaction that is mediated by CbiC (45). This completes the methylation pattern found in the final cobamide molecule. The first two amidation reactions, out of a total of six, are mediated by CbiA (52), which amidates the *a* and *c* side chains to give cobyrinic acid *a,c*-diamide. The synthesis of cobyrinic acid *a,c*-diamide represents the intermediate where the anaerobic and aerobic pathways re-join.

### **The aerobic route**

The aerobic route between precorrin-2 and cobyrinic acid *a,c*-diamide is shown in Figure 2-4. In temporal terms the aerobic route was the first of the two routes of cobalamin biosynthesis to be determined. The elucidation involved a combination of some outstanding microbiology coupled with pioneering chemical biology approaches employed to determine the structures of the various intermediates and in particular the use of NMR (53-56). The pathway was worked out for the

bacterium *Pseudomonas denitrificans*, as this was the main strain that was being used for the commercial production of vitamin B<sub>12</sub>. Many of the steps of the aerobic pathway are similar to those already described for the anaerobic route but there are significant differences especially with respect to the method for ring contraction and the timing and mechanism for cobalt insertion.

The aerobic pathway for cobalamin biosynthesis starts from precorrin-2, where methylation of the C20 position by CobL gives precorrin-3A (57). This trimethylpyrrocorphin acts as the substrate for a mono-oxygenase called CobG, which shares some sequence similarity with sulphite reductase. The enzyme catalyzes the hydroxylation at C20, generating a tertiary alcohol, and also forms a gamma lactone with the acetic acid side chain on ring A, giving rise to a molecule called precorrin-3B (58-60). The enzyme binds a non-heme iron that presumably is used as the site of oxygen activation (61). Some organisms that operate the aerobic pathway employ a different enzyme to CobG. For instance, in *Rhodobacter capsulatus*, CobG is replaced by CobZ, a much larger protein that has a membrane-binding region (62). In fact CobZ can be divided into two distinct regions, where the *N*-terminal portion of the protein contains a non-covalently-bound FAD. The *C*-terminal region contains sequence that suggests it has seven transmembrane helices and also houses a heme group. A flexible region that contains a number of cysteine residues and likely contains a couple of 4Fe-4S centers link the *N*- and *C*- terminal regions of the protein. Overall, CobZ displays sequence similarity with TcuA and TcuB, which are involved in tricarballoylate metabolism.(63, 64)CobZ performs an identical reaction to CobG, likely using the flavin cofactor for the oxygenation process (62).

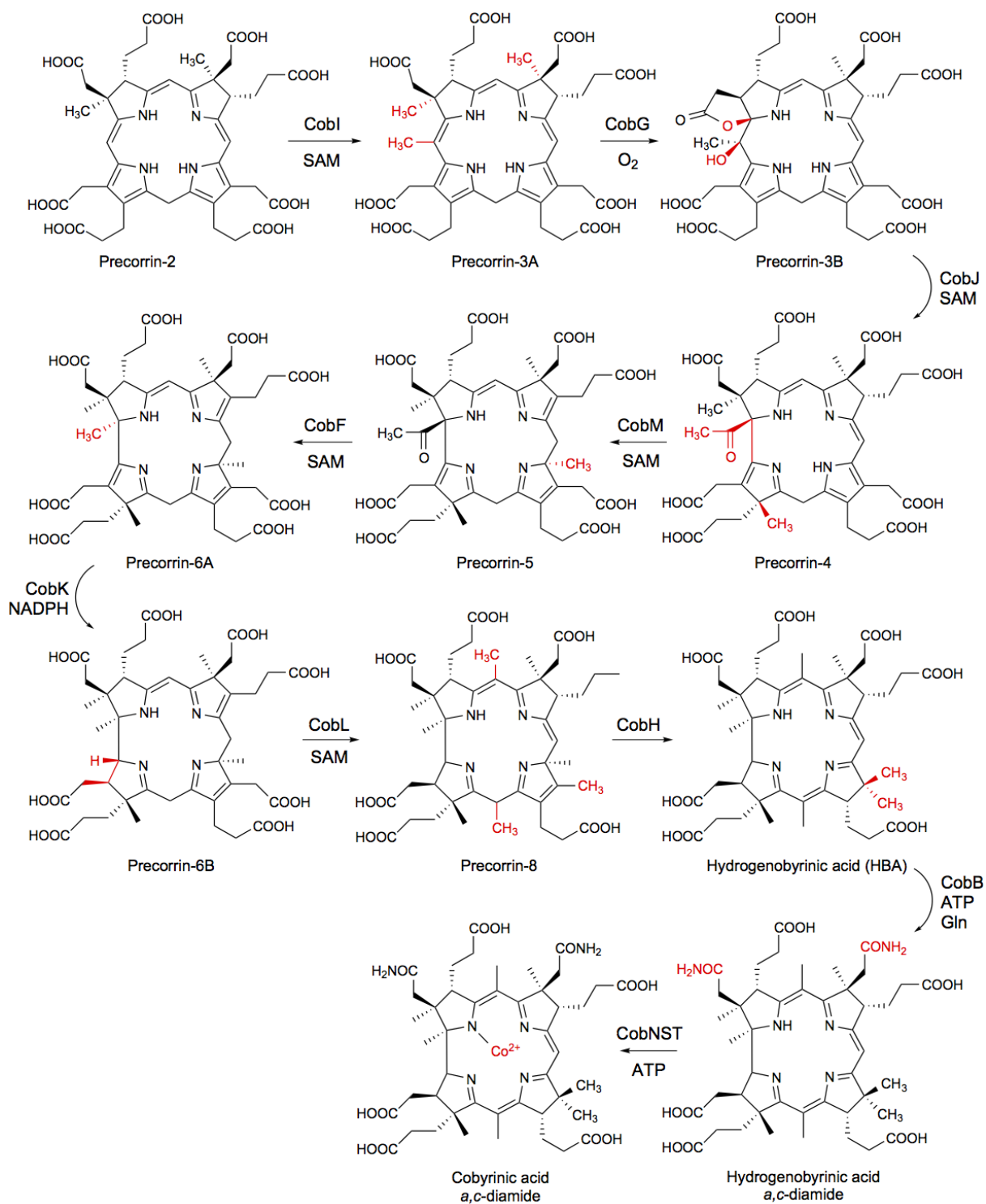


**Figure 2-4. The aerobic pathway for corrin ring synthesis.** The diagram highlights the intermediates and enzymes involved in the transformation of precorrin-2 into cobyrinic acid *a,c*-diamide.

Precorrin-3B acts as the substrate for the ring contraction enzyme CobJ, which not only methylates the C17 position but also contracts the macrocycle leaving the methylated C20 position extruded as an acetyl group attached to C1 (58, 60, 62). It is likely that the methylation and contraction represent a concerted process. The product of the ring contraction process is precorrin-4 (58, 65, 66). Methylation at C11 follows, and generates precorrin-5 in a reaction catalyzed by CobM (58, 67). Methylation at C1 then results in the loss of the extruded acetyl group as acetic acid in a reaction catalyzed by CobF and in so doing generates precorrin-6A (68, 69). The macrocycle is next reduced through the removal of a double bond in a reaction catalyzed by CobK which requires NADPH as a cofactor (70). Overall, the structure of the enzyme reveals how it is able to bind both the cofactor and substrate in the correct orientation so as to allow protonation of C18 and pro-R hydride transfer from NADPH to C19 (71). The product of the reaction is precorrin-6B.

The transformation of precorrin-6B to precorrin-8 is mediated by a single protein called CobL and involves methylation at C5 and C15, as well as decarboxylation of the acetic acid side chain attached to ring C (57). Sequence analysis suggested that CobL represented a fusion between two distinct methyltransferases and indeed this was subsequently shown to be the case after dissection of the main protein into two halves (72). The C-terminal portion of CobL was found to be responsible for the decarboxylation of the acetate side chain and methylation of C15, whereas the N-terminal region was shown to be responsible for the methylation at C5. In this respect the C-terminal region of CobL generates precorrin-7 whereas the N-terminal region transforms precorrin-7 into precorrin-8 (72). This is analogous to what happens with CbiT/E in the anaerobic pathway.

Precorrin-8 acts as the substrate for the methyl group rearrangement reaction, whereby the methyl group at C11 is moved to C12 (73). The effect of this enzyme is also to increase the conjugated system within the macrocycle, inducing a visible shift in the colour of the product, hydrogenobyric acid, which is bright orange in appearance (72, 73). The structure of the enzyme has also been solved and reveals the presence of a potential catalytic histidine residue in close proximity to ring C of the tetrapyrrole (74). It has been suggested that protonation of the pyrrole nitrogen on ring C may enhance the rearrangement reaction (74).

Hydrogenobyric acid is amidated on side chains *a* and *c* by CobB, in a reaction that requires glutamine and MgATP. The resulting hydrogenobyric acid *a,c*-diamide acts as the substrate for the cobaltochelatase. In contrast to the relatively simple cobaltochelatase system found in the anaerobic pathway, the aerobic cobaltochelatase is very complex. It requires three protein subunits for activity: CobN, -S and -T (75). For activity it also requires ATP and is analogous to the Mg-chelatase that is found associated with chlorophyll synthesis. Both CobS and T appear to form large hexameric ring structures (76), similar to the chaperone-like complexes that are characteristic of the AAA+ class of proteins. This oligomeric structure interacts with the main substrate binding-subunit CobN. Coupled with ATP hydrolysis this huge macromolecular complex is then able to chelate cobalt into hydrogenobyric acid *a,c*-diamide to generate cob(II)yrinic acid *a,c*-diamide.

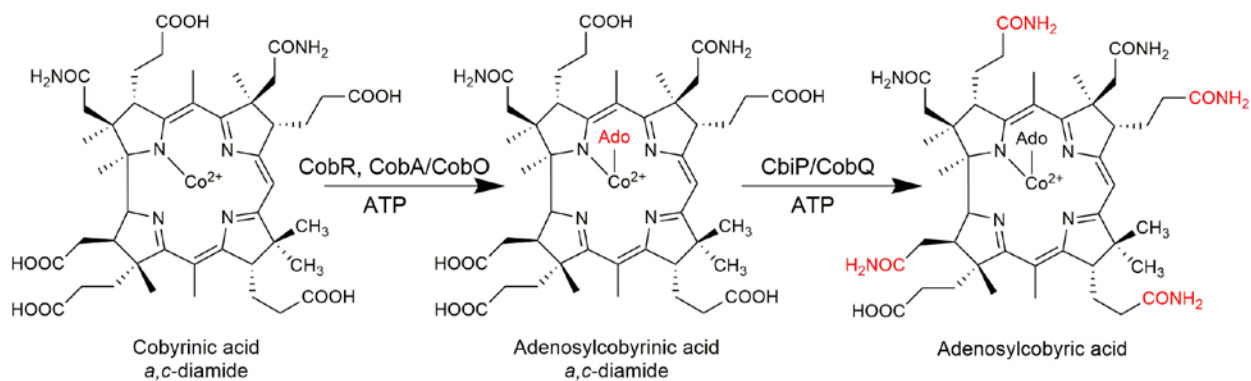


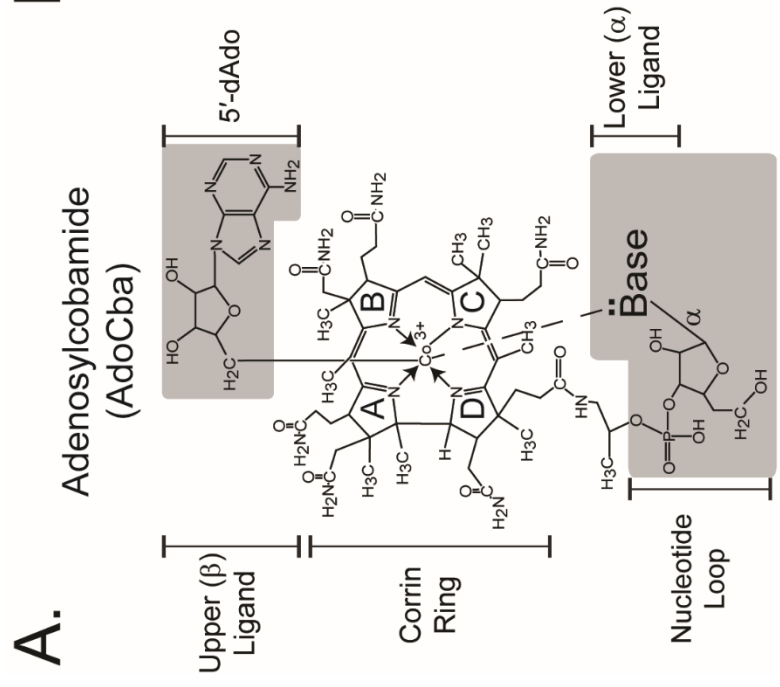
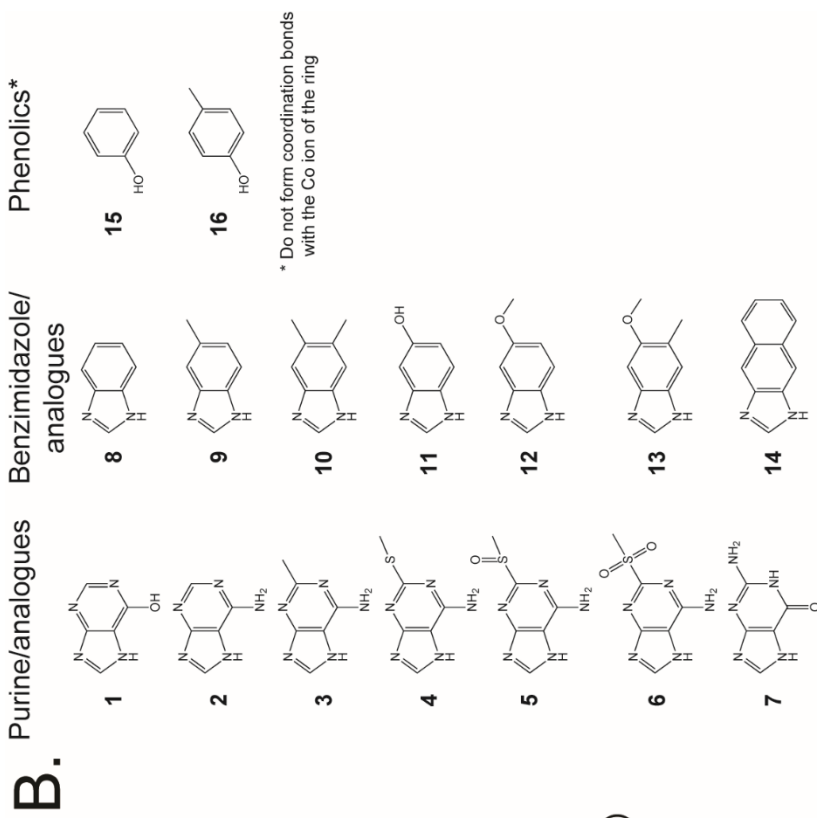
**Figure 2-5. The transformation of cobyric acid *a,c*-diamide into adenosylcobyric acid.** The diagram highlights the intermediates and enzymes involved in the transformation of cobyric acid *a,c*-diamide into adenosylcobyric acid. The first step shows the adenylation step, the second one yields adenosylcobyric acid after the indicated four sequential amidations.

### **From cobyric acid *a,c*-diamide to adenosylcobyric acid.**

The last section of the corrin ring synthesis is shared between the two main pathways for cobalamin synthesis and is shown in Figure 2-5. The completion of the corrin ring is afforded by both the adenylation of the cobalt and the amidations of the remaining side chains. Adenylation takes place in a reaction catalyzed by the adenylation transferase. This process is described in more detail as part of the cobalamin salvage and recycling system, but is catalyzed by CobA/CobO (77, 78), with the name differences reflecting the two different pathways. In some organisms there appears to be a specific reductase to help reduce the cobalt ion to the Co(I) state (79), but in other organisms this reduction would appear to be facilitated simply by a flavodoxin (80). The resulting adenosylcobyric acid *a,c*-diamide acts as the substrate for the final amidase CbiP/CobQ, which amidates the *b*, *d*, *e* and *f* side chains and in so doing generates adenosylcobyric acid (51, 81-83).

The remaining steps of cobalamin synthesis relate to conversion of the vitamin into the coenzyme form, the biosynthesis of the lower ligand base, the construction of the nucleotide loop and its attachment to the corrin macrocycle.

**Figure 2-6. AdoCba structure and lower ligand diversity.** A. Structure of AdoCba with a generalized base. A/B/C/D, pyrrole rings; 5'dAdo, 5' deoxyadenosine. B. Structures of observed lower ligand bases: **1**, Hypoxanthine; **2**, adenine; **3**, 2-methyladenine; **4**, 2-methylmercaptadenine; **5**, 2-methylsulfinyladenine; **6**, 2-methylsulfonyladenine; **7**, guanine. *Benzimidazole/analogs*: **8**, benzimidazole; **9**, 5-methylbenzimidazole; **10**, 5,6-dimethylbenzimidazole; **11**, 5-hydroxybenzimidazole; **12**, 5-methoxybenzimidazole; **13**, 5-methoxy-6-methylbenzimidazole; **14**, naphthimidazole; **15**, phenol; **16**, *p*-cresol.



## Upper ligand attachment

In addition to the aforementioned differences between cobamides and other cyclic tetrapyrroles, unlike the latter, cobamides (Cbas) have axial ligands (Figure 2-6A). The upper ligand of the coenzymic form of cobamides is 5'-deoxyadenosine. Typically, the base of the nucleotide loop forms a pH-dependent coordination bond with the cobalt ion of the ring, with the exception of the phenolic bases (Figure 2-6B).

There are two biologically active forms of cobamides. One form has a 5'-deoxyadenosyl (Ado) group covalently attached to the Co ion on the beta face of the corrin ring. The Ado group in adenosylated corrinoids is referred to as the upper or  $Co\beta$  axial ligand. AdoCbas are critical in reactions that proceed via radical chemistry, such as carbon skeleton rearrangements, dehydrations, and deaminations (84). The second biologically active form of Cbas is one where the Co ion is in the +1 state, and hence the Co ion does not have axial ligands. This active form of cobamides is critical for the function of Cba-dependent methyltransferases found in cells of all domains of life (85-87), and dehalogenases involved in organohalide respiration (88, 89).

Below we discuss the most recent findings regarding the enzymes that catalyze the synthesis of the unique Co-C bond found in AdoCbas. The enzymes responsible for the attachment of Ado groups to corrinoids are known as ATP:Co(I)rrinoid adenosyltransferases (*i.e.*, ACATs). The Co-C bond is labile to light, acidity, and reducing agents (90).

## Cobalt ion reduction

Results of studies in bacteria support the possibility that, upon entry into a cell, Co(III)rrinoids are likely non-enzymatically reduced to their Co(II) state, at the expense of dihydroflavins (91). At pH 7, the redox potentials of the FMN/FMNH<sub>2</sub> and FAD/FADH<sub>2</sub> couples ( $E'' = -190$  mV,  $E'' = -220$  mV, respectively) (92) are low enough to drive the reduction of Co(III) to Co(II) (91).

Reduction of Co(III) to Co(II) results in the removal of the upper ligand of the incoming corrinoid. Before the cell can replace that ligand, Co(II) corrinoids must be reduced to the Co(I) oxidation state to generate the “supernucleophile” that attacks ATP (93). In solution, the redox potential of the Co(II)/Co(I) couple is very low ( $E^{\circ} = -610$  mV) (94), which is substantially lower than the redox potential of biological reductants such as ferredoxin ( $E^{\circ} = -432$  mV), NADH ( $E^{\circ} = -320$  mV), and FADH<sub>2</sub> ( $E^{\circ} = -220$  mV) (92). The question of how cells overcome such a thermodynamic barrier remained unanswered until the last decade or so, when in-depth biochemical, spectroscopic, mutational and physiological analyses of ACATs were performed. There are three evolutionarily distinct classes of ACATs, all of which got their names because the genes encoding them were all found in the enterobacterium *Salmonella enterica* sv Typhimurium strain LT2 (hereafter *S. enterica*). The three classes are CobA, PduO and EutT. ACATs do not share homology at the nucleotide nor amino acid sequence level. The best-studied ACATs are CobA and PduO, but recent work has focused on the analysis of the EutT class. Our current understanding of how ACATs adenosylate corrinoids is discussed below.

### **The CobA class of ACATs**

The most extensively studied representative of this class of ACATs is the CobA enzyme (EC 2.5.1.17) from *S. enterica* (95). Homologues of *SeCobA* have been described in *E. coli* (known as BtuR) (96-98) and *P. denitrificans* (CobO) (78), and one archaeal enzyme of this class has also been studied (99). In *S. enterica*, CobA function is needed for the *de novo* synthesis of AdoCba, given that *cobA* mutant strains of this bacterium fail to assimilate non-adenosylated cobinamide, but can assimilate adenosylated cobinamide (95). CobA function is also needed to adenosylate cobamides, given that AdoCba is needed for the activation of expression of the *eut* operon, which encodes functions needed for the catabolism of ethanolamine (100-103). In a *S. enterica cobA*

mutant strain, expression of the *eut* operon is substantially reduced, but exogenous AdoCba restores expression of this operon (104). The ability of CobA to adenosylate complete and incomplete corrinoids has been confirmed *in vitro* (77, 105). Initial work with CobA required the chemical reduction of Co(III) to Co(I) (105), but biological reduction systems have been identified. As mentioned above, dihydroflavins serve to mediate the reduction of Co(III) to Co(II) in solution (91). After CobA binds its Co(II)rrinoid co-substrate, the lower ligand of the coenzyme is displaced by bulky hydrophobic side chains of the *N*-terminal helix of the opposite subunit, converting the 5-coordinate Co(II)rrinoid to a four-coordinate Co(II)rrinoid (106). Removal of the coordination bond between the lower ligand base and the cobalt ion results in the stabilization of the  $3d_z^2$  orbital of the cobalt ion with the concomitant rise in the redox potential of the Co(II)/Co(I) redox couple by ~250 mV (107). This stabilization facilitates the transfer of an electron from the flavin cofactor of flavodoxin A (FldA) to further reduce Co(II) to Co(I), generating the Co(I) state necessary for adenosylation (80). FldA itself is reduced by the NADP<sup>+</sup>:ferredoxin (flavodoxin) reductase (Fpr; EC 1.18.1.2) (80, 108). Disruption of the expected FldA-CobA binding interface restricts the reduction activity by 97.4% but not the adenosylation activity, as chemically reduced corrinoids were still adenosylated (108).

Investigations into the Co(II)/Co(I) reduction by CobA and its counterparts have been enabled by a combination of spectroscopic methods (107). Magnetic circular dichroism (MCD) spectroscopy (109) combined with electron paramagnetic resonance (EPR) (110) and density functional theory (DFT) (111) calculations, revealed the binding of 4-coordinate as opposed to 5-coordinate cobalamin by CobA (107). A qualitative difference in the MCD signals allows for differentiation between 4- and 5-coordinate cobalamin (112). The switch from 5-coordinate to 4-coordinate can be quantified and combined with biochemical assays to assess the ability of ACAT

variants to generate the necessary 4-coordinate substrate for adenosylation and has been used in several studies (113-123) to understand the mechanism by which these unique enzymes operate. Structural studies of CobA in complex with 4- and 5-coordinate Co(II)balamin have revealed conformational changes of the protein which allow for the formation of the 4-coordinate state (Figure 2-7) (106). The active site of CobA is hydrophobic and orients the ring below the Mg-ATP molecule. The hydrophobicity also serves to exclude water molecules which may prevent formation of the Co(II) state. Movement of residues Phe91 (7.1 Å by the  $\alpha$ -carbon) and Trp93 (5.1 Å) and the N-terminal helix of the opposite subunit, displace the lower ligand base and place Phe91 and Trp93 in an approximately perpendicular position to the ring, suggesting that it is through  $\pi$ - $\sigma$  interactions rather than  $\pi$ - $\pi$  stacking that the displacement of the lower ligand is achieved. It was also shown that Phe91 and Trp93 were not critical if replaced by similarly bulky aromatic residues, although replacements did reduce enzyme activity. Changes to Phe91 were more likely to result in decreased activity, possibly a result of its proximity to the central cobalt. Replacement of Phe91 with a His residue reduced activity by 95%, possibly as the result of coordination of an imidazole nitrogen to the central cobalt. In contrast, replacement of Trp93 with a Tyr residue improved the activity of the enzyme by 10 fold. While such a substitution has been observed in CobA homologues (*e.g.*, *Ralstonia solanacearum*) it is not currently understood why this substitution results in a better enzyme nor why it is not more frequently found in other CobA homologues. Upon reduction, Co(I) attacks the C5' of the ribose moiety of ATP releasing triphosphate.(124) ATP binds CobA as MgATP and is found within 3.1 Å of the central cobalt ion of the bound corrinoid (106). A hydrogen bond interaction between the  $\gamma$ -phosphate of ATP and the 2' OH of the ribose is critical to exposing the C5' for that attack (124).

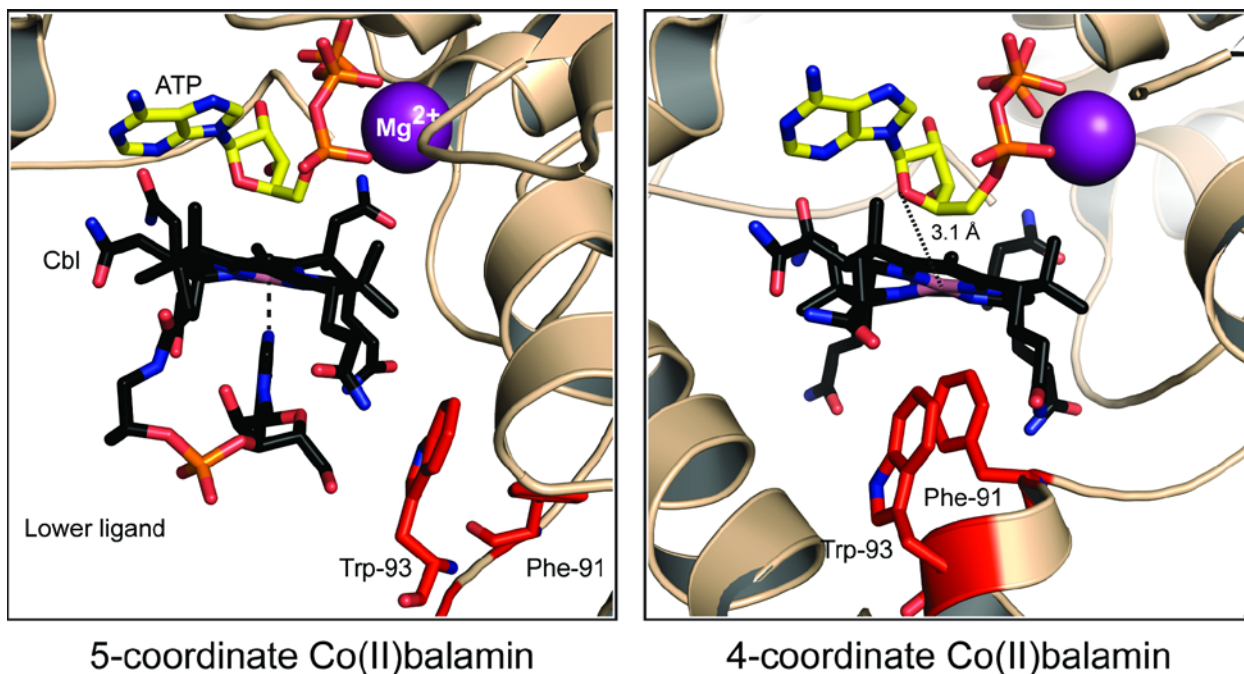


**Figure 2-7. Four- and five-coordinate Co(II)balamin in the active site of a CobA class ACAT.** Movement of Phe91 and Trp93 in *SeCobA* (PDB ID 4HUT) displaces the lower ligand of Co(II)balamin, preparing the central cobalt for reduction to the Co(I) state. Left panel: 5-coordinate Co(II)balamin. The *N1* of DMB of the lower ligand coordinates the central cobalt. Right panel. The movement of Phe91/Trp93 displaces the lower ligand, resulting in the formation of 4-coordinate Co(II)balamin. Neither Phe91 nor Trp93 coordinate the central cobalt. ATP is positioned 3.1 Å away from the ring, setting up the nucleophilic attack following the reduction of Co(II) to Co(I). ATP, yellow; Mg(II), purple; Co(II)balamin (Cbl), black; Phe91 and Trp93, red.

The P-loop of CobA is unique, as it only has seven residues, rather than the eight to nine normally found in consensus P-loops (Figure 2-9) (125). In addition, rather than burying the nucleoside in the loop, the ribose is exposed as the orientation of the entire nucleotide is inverted allowing the transfer of the adenosyl moiety rather than the transfer of the  $\gamma$ -phosphate (125).

### **The PduO class of ACATs**

The second class of ACATs is represented by *S. enterica* PduO (126). Despite its specialized role in *S. enterica*, PduO is the most widely distributed class of ACATs (127), with representatives found in archaea (99, 128) and humans (ATP:cobalamin adenosyltransferase, hATR) (7, 129). As part of the *pdu* operon of *S. enterica* (130, 131), PduO enables the adenylation of Cbas for the utilization of 1,2-propanediol (1,2-PDL). The catabolism of 1,2-PDL requires the function of diol dehydratase (EC 4.2.1.28), an AdoCba-dependent enzyme that catalyzes the first step of the conversion of 1,2-PDL to propionate (130-134). The catabolism of 1,2-PDL occurs within a metabolosome (or bacterial microcompartment), a proteinaceous organelle that isolates the enzymes of the pathway from the cytosolic environment to contain the toxic acetaldehyde intermediate (135-137). This isolation, combined with the need for AdoCbas for diol dehydratase activity (138), explains the presence of the ACAT PduO in the Pdu metabolosome. There are differences among PduO proteins. For example, the C-terminal domain of *S. enterica* PduO (145 residues) does not contribute directly to the adenylation activity and is absent in other PduO-like proteins, like the PduO protein in *Lactobacillus reuteri* (127, 133). The three-dimensional crystal structure of the C-terminal domain of *Se*PduO was recently reported, and was shown to bind heme and aquacobalamin (139). While the affinity for heme appeared to be stronger, the weak binding of aquacobalamin may better reflect the purpose of this domain. We speculate that the C-terminal domain of the *Se*PduO protein is to facilitate the ACAT role by loosely binding

non-adenosylated cobamides. The weak affinity for the latter would help transfer the cofactor from the C-terminal domain into the active site of the enzyme for reduction and adenosylation. This may explain why the loss of the C-terminal domain in *S. enterica* results in a decreased growth rate on 1,2-PDL (139).

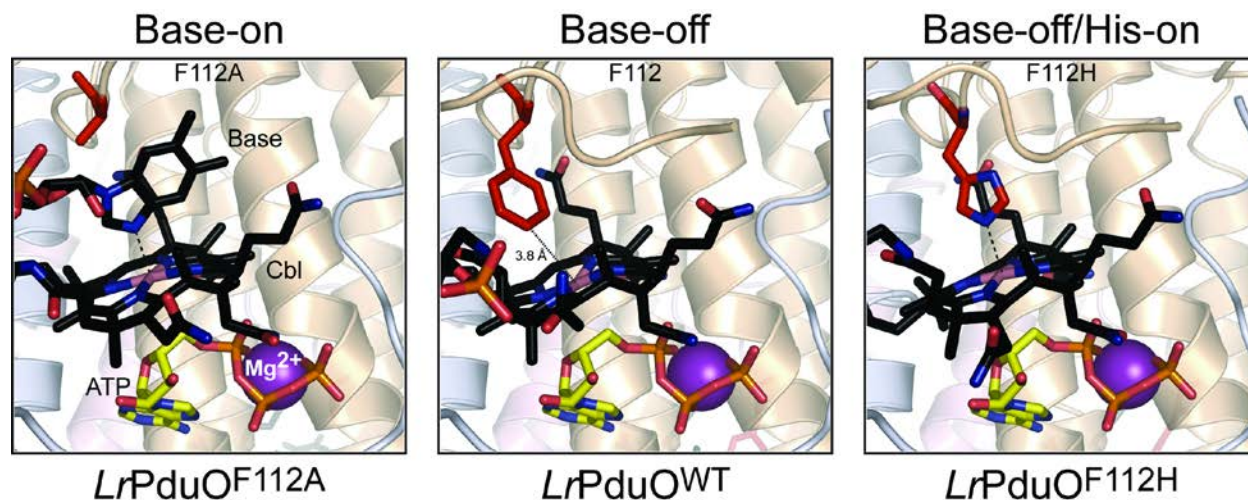


**Figure 2-8. Four- and five-coordinate Co(II)balamin in the active site of a PduO class ACAT.**

The Phe112 residue of *L. reuteri* PduO serves to displace the lower ligand of Co(II)balamin prior to reduction of the central cobalt to Co(I). Left panel: Replacement of Phe112 with an alanine (PDB ID 3GAI) permits the binding of Cbl in the base-on state as the lower ligand base coordinates cobalt. Center panel: Phe112 displaces the lower ligand (PDB ID 3CI1) to the base-off state but does not coordinate the central cobalt. Right panel: Replacement of Phe112 with histidine (PDB ID 3GAH) generates the base-off/His-on state, with the imidazolyl moiety of histidine coordinating the central cobalt. Legend: Ala112/Phe112/His112, red; Cbl/base, black; ATP, yellow; Mg(II) ion, purple.

Structural studies of the human hATR (9) and *Lactobacillus reuteri* PduO (121), as well as spectroscopic studies of the latter (119) indicate that, like CobA, *LrPduO* uses hydrophobic residues to crowd out the lower ligand (123, 140), raising the redox potential through the generation of a 4-coordinate Co(II)trinnoid species. Structural studies of *LrPduO* revealed that displacement of the lower ligand is enacted by the movement of a Phe residue (141) while the ring is maintained in a hydrophobic pocket (127). The non-coordinating Phe112 is found 3.8 Å from the central cobalt ion (PDB 3CI1) and, as seen in 4-coordinate Co(II)balamin in *SeCobA*, the lower ligand is disordered in the solved structure (Figure 2-8, central panel) as the bulky residue pushes the lower ligand away from the lower face of Cbl (127). Replacement of Phe112 with an Ala residue (PDB 3GAI) restores order to the lower ligand as the *N1* of DMB coordinates the central cobalt (Figure 2-8, left panel) (141). A Phe112A variant is active if provided Co(II)balamin, but cannot generate the Co(II) state (119, 141). If Phe112 is replaced by histidine (PDB 3GAH), the imidazole of His forms a coordination with the central cobalt (Figure 2-8, right panel) (141). While this enzyme is still active *in vitro*, it requires the displacement of the His residue before the Co(II)balamin can be reduced to the Co(I) state (119, 141). *LrPduO* is catalytically active as a trimer (142), a result that is consistent with results obtained with archaeal and human PduO-type enzymes (9, 128). The crystal structure of the *LrPduO* enzyme in complex with ATP revealed a novel ATP-binding site (TK/RXGDXGXT/S) at the *N*-terminus of each subunit (Figure 2-9), with the ATP-binding site formed at the subunit interface (127, 142). As with other ACATs, the by-product of the adenosylation reaction by *LrPduO* is triphosphate (133). In terms of substrate specificity, *SePduO* is specific for Cbl, while the *L. reuteri* homologue can also adenosylate Cbi (119).

Reduction of the cobalt ion from its Co(II) to its Co(I) oxidation state is critical to the formation of the Co-C bond needed for function of the coenzyme. Even though great strides have been made towards a better understanding of this reductive step, many questions remain unanswered. In *S. enterica*, The PduS protein was shown to mediate the reduction of Co(III) to Co(II) and Co(II) to Co(I) (143, 144). However, as discussed above, from work performed with *LrPduO*, it is clear that the Co(II)rrinoid 4-coordinate species needed to raise the redox potential of the Co(II)/Co(I) couple is generated only upon binding to the active site. To date, a Co(II)Cbl 4-coordinate species bound to PduS has not been detected (145). If indeed PduS were a reductase that could reduce Co(III)Cbl and Co(II)Cbl, then the transfer of Co(I)Cbl from the PduS active site to the PduO active site would have to be very efficient to avoid oxidation of the Co(I) ion, a mechanism that would likely imply strong protein-protein interactions between PduS and PduO.

### **The EutT class of ACATs**

The third class of ACATs is represented by *S. enterica* EutT (*SeEutT*) (104, 146, 147). *SeEutT*, like *SePduO*, is a specialized ACAT that synthesizes AdoCbas needed for ethanolamine utilization (104, 146). Ethanolamine utilization occurs inside a metabolosome, which, as in the case of 1,2-propanediol catabolism, is needed to contain reactive aldehyde to avoid damaging proteins, nucleic acids and other molecules (100, 101, 103, 135). At present, the cellular location of *SeEutT* is unclear. Knowledge of the location of *SeEutT* is of interest given its role as provider of the cofactor needed for the AdoCba-dependent ethanolamine ammonia-lyase (*SeEutBC*; EC 4.3.1.7) required for conversion of ethanolamine to acetaldehyde and ammonia. It has been proposed that the *SeEutBC* protein is not located inside the metabolosome, but instead it may be attached to the cytosolic side of the shell (148). Ultimately, the location of *SeEutBC* will determine the location of its reactivase (*SeEutA*) (149) and that of *SeEutT*. Logistically, this idea makes sense since the

synthesis and delivery of AdoCba to *SeEutBC* would be greatly facilitated if *SeEutT*, *SeEutA* and *SeEutBC* were in close proximity or even comprised a specialized complex that synthesizes and delivers AdoCba to *SeEutBC*. Access to AdoCba is not a concern since it is clear that AdoCbas enter the metabolosome, as *S. enterica eutT* mutant strains with a functional *SeCobA* enzyme can grow on ethanolamine when provided with exogenous non-adenosylated cobamides (104).

Early work on *SeEutT* showed that the activity of the enzyme was sensitive to oxygen and to the iron chelator bathophenanthroline (104). Subsequent work showed that the enzyme was a ferroprotein whose Fe(II) ions could be readily substituted by Zn(II) ions with limited loss of activity (150). Unsurprisingly, Zn(II)-*SeEutT* was not oxygen sensitive since Zn(II) is not a redox active metal, and was no longer sensitive to bathophenanthroline inactivation (150). Unlike *SePduO* and *SeCobA* ACATs, *SeEutT* cannot adenosylate incomplete corrinoids such as cobinamide (Cbi) because the enzyme cannot remove the axial solvent ligand (116). It has been proposed that the inability of *SeEutT* to adenosylate Cbi avoids AdoCbi in the active site of *SeEutBC*, thus generating an inactive enzyme (116). Results from spectroscopic analyses showed that 60% of Co(II)Cbi present was in the base-off form as a result of active site interaction with the ring (114). No P-loop-like ATP-binding domain has been identified in *SeEutT*, but a putative cytochrome oxidase/4Fe-4S cluster-like  ${}^{64}\text{HX}_7\text{HX}_3\text{CCX}_2\text{C}^{83}$  motif (Figure 2-9) has been shown to be essential for activity (147), but not for proper folding or protein stability (150). It has been proposed that the metal cofactor may play a role in the formation of the base-off form (114). Binding of ATP by *SeEutT* displaces water, and reduction of Co(II) to Co(I) triggers the attack on the C5' of adenosine (114). There are other notable differences between *SeEutT* and *LrPduO* and *SeCobA*. For example, unlike *LrPduO* and *SeCobA*, *SeEutT* uses dATP and ADP as substrates, and the by-products of the *SeEutT* reaction are pyrophosphate and orthophosphate instead of

triphosphate (147). Like *LrPduO*, but unlike *SeCobA*, dihydroflavins can reduce the Co(II)Cbl 4-coordinate species in the active site of *SeEutT* triggering the adenosylation reaction (150). To date, the three-dimensional structure of EutT-class ACATs has not been reported.

<b>SeCobA</b> PDB 1G5T	32 IVFT <b>G</b> NGK <b>GKT</b> TAAF 46
<b>LrPduO</b> PDB 2NT8	1 MKIY <b>TR</b> NGD <b>KGT</b> RIIG 17
<b>SeEutT</b> No Structure	64 QPV <b>H</b> GLTSSD <b>TH</b> PQA <b>CC</b> EL <b>CR</b> QPV 87

---

P-Loop ATP-binding motif (CobA)	<b>G</b> X <sub>4</sub> <b>GK</b> ( <b>T/S</b> )
PduO ATP-binding motif	<b>T</b> ( <b>K/R</b> ) X <b>GD</b> X <b>GX</b> ( <b>T/S</b> )
EutT metal-binding motif	<b>H</b> X <sub>7</sub> <b>H</b> X <sub>3</sub> <b>CC</b> X <sub>2</sub> <b>C</b>

**Figure 2-9. Binding motifs and sequences unique to the ACATs.** A. The ATP-binding sequences for *S. enterica* CobA and *L. reuteri* PduO and the metal-binding motif of *S. enterica* EutT. B. The consensus motifs found in the ACATs. The P-loop of *S. enterica* CobA has only 3 residues separating the first and second Gly residues, while most nucleotide-binding proteins have 4-5. Residues in red are highly conserved among members of these motif families.

## **The Nucleotide Loop Assembly (NLA) Pathway**

The nucleotide loop is unique because of an  $\alpha$ -*N*-glycosidic bond between the ribose and the base, and a phosphodiester bond involving the 3' hydroxyl group of the ribosyl moiety of the nucleotide. Cobamides, methanopterins and factor F<sub>420</sub> are the only coenzymes known to contain a phosphodiester bond. (151-153) Briefly, the NLA pathway consists of two branches. One branch activates the corrinoid and the other branch activates the base. The penultimate enzyme joins the two activated precursors, and the final step removes a residual phosphate group from the molecule to yield AdoCba (Figure 2-10). The reader should refer to Figure 2-10 for the remainder of this article.

## **Synthesis and attachment of aminopropanol-phosphate (AP-P) to the corrin ring**

Once cobyrinic acid (Cby) is converted to adenosylcobyrinic acid (AdoCby) by *SeCobA*, it is used as substrate by the adenosylcobinamide-phosphate (AdoCbi-P) synthase. In bacteria and archaea, the AdoCbi-P synthase (EC 6.3.1.10) condenses 1-amino-propanol-*O*-2-phosphate (AP-P) and AdoCby to generate AdoCbi-P (154, 155) via the attachment of AP-P to the carboxylate group of a propionyl substituent of pyrrole D of AdoCby. The attachment of AP-P to AdoCby is the last step in the *de novo* synthesis of the corrin ring biosynthesis pathway (154), and has been described *in vivo* in both the bacterial (154, 156-159) and archaeal pathways (155). How AP-P is attached to the corrin ring remains unknown. It is noteworthy that the AdoCbi synthase CbiB enzyme is an integral membrane protein found in the inner membrane of all AdoCba producers whose genome has been sequenced. The initial mutational and functional analysis of CbiB revealed residues exposed to the cytoplasm and the periplasm as critical for activity (154). Insights into the catalytic mechanism of CbiB have been hampered by difficulties in the isolation of wild type and variant proteins.

**Figure 2-10. The nucleotide loop assembly pathway for AdoCba biosynthesis in bacteria and archaea.** CbiZ, AdoCbi amidohydrolase; PduX, L-Thr kinase; CobD, L-Thr-P decarboxylase; CbiB, AdoCbi-P synthase; CobU, NTP:AdoCbi kinase and NTP:AdoCbi-P guanylyltransferase; YfcN, thiamine kinase; CobY, NTP:Ado-Cbi-P guanylyltransferase; BluB, O<sub>2</sub>-dependent DMB synthase; CobT, NaMN:DMB phosphoribosyltransferase; ArsAB, NaMN:DMB phosphoribosyltransferase; BzaAB/BzaF, ThiC-like proteins; BzaC, methyltransferase; BzaD, methyltransferase; BzaE, penultimate enzyme in anaerobic DMB biosynthesis; CblT,  $\alpha$ -R transporter; CblS,  $\alpha$ -R kinase; CobS, AdoCba-5'-phosphate synthase; CobC, AdoCba-P phosphatase; AdopseudoCbl, adenosyl-pseudocobalamin; AdoCby, adenosyl-cobyric acid; AP, aminopropanol; AP-P, aminopropanol-phosphate; AdoCbi, adenosylcobinamide; AdoCbi-P, adenosylcobinamide-phosphate; L-Thr, L-threonine; L-Thr-P, L-threonine-phosphate;  $\alpha$ -R,  $\alpha$ -ribazole;  $\alpha$ -RP,  $\alpha$ -ribazole-5'-phosphate; DMB, 5,6-dimethylbenzimidazole; FMNH<sub>2</sub>, dihydroflavin mononucleotide; 5-CH<sub>3</sub>O-, 6-Me, Bnz, 5-methoxy-6-methylbenzimidazole; 5-CH<sub>3</sub>O-Bnz, 5-methoxybenzimidazole; 5-OH-Bnz, 5-hydroxybenzimidazole; AIR, 5-aminoimidazole ribotide; AdoCbi-GDP, adenosylcobinamide-GDP; AdoCbl-P, adenosylcobalamin-phosphate; AdoCbl, adenosylcobalamin



### **Aminopropanol-phosphate (AP-P) synthesis**

AP-P is synthesized from L-threonine (L-Thr) by a two-step pathway. In the first step, the L-Thr kinase (PduX; EC 2.7.1.77) uses ATP to convert L-Thr to L-Thr-P (160). Homologues encoding this enzyme are found clustered with AdoCba biosynthetic genes (161). However, in *S. enterica*, *pduX* is the last gene of the 1,2-propanediol utilization (*pdu*) operon (136). Kinetic analysis of the PduX reaction suggests that ATP binds first, followed by L-Thr (162). A Mg(II) ion is needed for activity and may be important to correctly position the substrate in the active site and to labilize the  $\gamma$ -phosphate bond of ATP increasing the rate of transfer of the  $\gamma$ -phosphate of ATP to L-Thr (162). *In vivo* evidence supports the *in vitro* results that associate L-Thr kinase activity with PduX. That is, exogenous L-Thr-P bypasses the need for PduX activity and restores AdoCba biosynthesis in a *pduX* mutant strain (160). The absence of PduX results in an 89% reduction of AdoCba biosynthesis in *S. enterica* under anoxic conditions, while the loss of CbiB function completely arrests AdoCba production (160). Collectively, these data suggest the existence of PduX-like activities in *S. enterica*, probably a non-specific L-Thr kinase. Once L-Thr-P is synthesized, it is decarboxylated by the pyridoxal 5'-phosphate (PLP)-dependent L-Thr-P decarboxylase (CobD; EC 4.1.1.81) generating AP-P (163). The three-dimensional crystal structure of *SeCobD* has been solved (PDB 1LC5, 1LC7, 1LC8, 1LKC). Comparisons with other proteins in the database unveil the striking similarity of *SeCobD* (a decarboxylase) to those of PLP-dependent amino acid aminotransferases (164). *Readers interested in this enzyme should be aware of misannotations of CobD homologues as histidinol-phosphate aminotransferases.* The similarities among CobD and other PLP-dependent aminotransferases suggests that there was a gene duplication event at some point (165). *SeCobD* similarities to PLP-dependent aminotransferases extend to their oligomeric state. That is, active *SeCobD* is a dimer. Each *SeCobD* subunit has a large and a small domain,

with both domains contributing to the formation of the active site (164). The small domain contains *N*-terminal residues that extend over the active site to act as a cap, which coordinates L-Thr-P (164). The enzyme positions the carboxylate moiety of L-Thr-P out of the plane of the pyridoxal ring to prevent the formation of an internal aldimine as a result of shifting the position of the  $\alpha$ -hydrogen of L-Thr-P away from the catalytic lysine in the active site. This position of L-Thr-P results in its decarboxylation (165).

### **Attachment of AP-P to the corrin ring**

The *S. enterica* AdoCbi-P synthase *SeCbiB* can use ethanamine-phosphate (EA-P) in lieu of AP-P, but not L-Thr-P (154, 163). This suggests that the active site of *SeCbiB* cannot accommodate the carboxylate of L-Thr-P (154), the immediate precursor of AP-P (163, 166). Incorporation of EA-P as the linker moiety generates a different class of Cbas known as the nor-Cbas (167), which are the preferred Cba for some enzymes (*e.g.*, dehalogenases). For example, the epsilonproteobacterium *Sulfurospirillum multivorans* uses nor-pseudocobalamin (nor-pseudoCbl) to dechlorinate tetrachloroethene (PCE) (167). Not surprisingly, the *S. multivorans* CobD enzyme (encoded by SMUL\_1544) uses L-Ser-P to generate EA-P. L-Ser-P originates as an intermediate of serine biosynthesis, and the lack of a PduX homologue in *S. multivorans* may explain the preference for L-Ser-P. (157) When the SMUL\_1544 protein was produced in a *S. enterica*  $\Delta cobD$  strain, nor-pseudoCbl was exclusively formed, indicating that L-Ser-P was the preferred substrate of the *SmCobD* enzyme (157). Notably, when *S. multivorans* grows in medium supplemented with an excess of L-Thr-P, the cells synthesize pseudoCbl that cannot be reversed by an equal or greater addition of L-Ser-P. The same finding was observed when using the *S. enterica* heterologous system (157).

### Synthesis of adenosylcobinamide-GDP (AdoCbi-GDP)

The first step of the nucleotide loop assembly pathway (a.k.a. the late steps) is the conversion of AdoCbi-P to adenosylcobinamide-GDP (AdoCbi-GDP). Different enzymes capable of catalyzing this conversion have evolved in bacteria and archaea. In the bacterial lineage, this step is catalyzed by a bifunctional NTP:AdoCbi kinase/GTP:AdoCbi-P guanylyltransferase (EC 2.7.1.156/EC 2.7.7.62), which was first described in cell-free extracts of propionic acid bacteria(168) and later studied in more depth in *P. dentrificans* (169) and *S. enterica* (170). Labeling and structural studies of this class of enzymes showed that the phosphate of AdoCbi-P and the  $\alpha$ -phosphate of GTP are retained in AdoCbi-GDP, while the  $\gamma$ - and  $\beta$ -phosphates of GTP are released as pyrophosphate (169-171). The phosphate moiety of AdoCbi-P initiates the attack on the  $\alpha$ -phosphate of an enzyme-bound GMP intermediate (170), while the P-loop of the enzyme coordinates the  $\gamma$ -phosphate of GTP (171).

The same P-loop that coordinates pyrophosphate (171, 172) enables the AdoCbi kinase activity of the enzyme, which allows bacteria to use AdoCbi salvaged from the environment by phosphorylation of the hydroxyl group of the AP linker moiety. The enzyme then guanylylates AP-P, yielding AdoCbi-GDP (24, 169-171, 173). Notably, GTP enhances the activity of the AdoCbi kinase, suggesting that ATP may not be involved in AdoCbi salvaging (169, 170, 174). The picture of the catalytic mechanism of this complex enzyme is incomplete. From structural and biochemical studies performed on *SeCobU* we learned that the protein guanylylates itself at a histidinyl residue (His46) prior to the phosphorylation of AdoCbi (171, 174). Self guanylylation induces a 30-degree rotation that brings the  $C\alpha$  of His46  $\sim 10\text{\AA}$  closer to the P-loop bringing the phosphate ion in the P-loop into close proximity ( $6\text{\AA}$ ) with the  $\alpha$ -phosphate of GMP (171). When ATP is present in the reaction mixture, *SeCobU* adenylylates itself forming CobU~AMP, a more

stable intermediate than CobU~GMP. CobU adenylation greatly reduces the transferase activity of the enzyme, but CobU~AMP can still phosphorylate AdoCbi (174).

In contrast to bacteria, archaea have an AdoCbi-P guanylyltransferase (known as CobY) that lacks AdoCbi kinase activity. The absence of the kinase activity should not be interpreted to mean that archaea do not salvage cobinamide. CobY function was first described in the methanogenic archaeum *Methanobacterium thermoautotrophicum* strain  $\Delta$ H (175), and subsequently in *Halobacterium* sp. Strain NRC-1 (176) and *Methanocaldococcus jannaschii* (177, 178). All CobYs described thus far act as the AdoCbi-P guanylyltransferase that converts AdoCbi-P to AdoCbi-GDP. The CobY reaction does not proceed via an enzyme~GMP intermediate as is the case for CobU (171), but CobY likely binds GTP first before it transfers GMP to AdoCbi-P (178, 179). *MjCobY* also requires the corrinoid substrate to be adenosylated (178). Evolutionary differences between CobU and CobY can be gleaned from the similarities of CobU to RecA-like kinases (171), while CobY has more in common with sugar 1-phosphate nucleotidyltransferases (180) like GlmU (175).

### **Activation and attachment of the lower (Coc $\alpha$ ) ligand**

The identity of the lower ligand base in cobamides varies based on species and environment (181-183). This base is converted to its ribotide form prior to its attachment to the corrin ring (184-186). The direct activation of the base to its ribotide form is performed by the nicotinate mononucleotide:5,6-dimethylbenzimidazole phosphoribosyltransferase (NaMN:DMB PRTase; EC 2.4.2.21) (185, 187-189). The enzyme catalyzes the transfer of the phosphoribosyl moiety of NaMN (190) to the base, generating a unique  $\alpha$ -ribose (187, 191). This  $\alpha$ -ribose is known as  $\alpha$ -ribose-5'-phosphate ( $\alpha$ -RP) when the base is 5,6-dimethylbenzimidazole (DMB). Initial studies of NaMN:DMB PRTase were performed in *Propionibacterium freudenreichii* ssp.

*shermanii* (183, 184), but more recent studies examined other bacterial NaMN:DMB PRTases, including CobT from *S. enterica* (181, 185, 192) and CobU in *Pseudomonas dentrificans* (186). To date, no NaMN:DMB PRTase from an archaeal source has been characterized, though crystal structures of putative NaMN:DMB PRTases have been deposited for *Pyrococcus horikoshii* (PDB 3U4G) and *M. jannaschii* DSM 2661 (PDB 3L0Z).

Structural studies with the *S. enterica* CobT (*SeCobT* PDBs: 4KQF, 4KQG, 4KQH, 4KQI, 4KQJ, 4KQK, 1L4B, 1L4E, 1L4F, 1L4G, 1L4H, 1L4K, 1L4L, 1L4M, 1L4N, 1L5F, 1L5K, 1L5L, 1L5M, 1L5N, 1L5O, 1JHM, 1JHO, 1JHP, 1JHQ, 1JHR, 1JHU, 1JHV, 1JHX, 1JHY, 1JH8, 1JHA, 1D0S, 1D0V) revealed unique features of these NaMN:DMB PRTases not found in other PRTases. *SeCobT* is a dimer, with each subunit possessing two domains, one large and one small (193). The small domains of each protein serve to cap the large cavity of the large domain of the opposite protein, creating a hydrophobic pocket where DMB binds (193). The large domains resemble canonical Rossmann folds (194) found in other PRTases and nucleotide-binding proteins, but as seen with the inverted P-loop of CobA, the orientation of the substrates and their products is opposite of that found elsewhere (193). To enable the formation of the  $\alpha$ -*N*-glycosidic bond, the base of the nucleotides is found at the center of the parallel  $\beta$ -sheets that make up the Rossmann fold (191, 193). The base is typically found oriented towards the periphery. The catalytic glutamate then abstracts a proton from the *N3* of DMB, allowing *N1* to serve as the nucleophile that attacks from below the *C1'* of ribose, releasing nicotinic acid and inverting the  $\beta$ -*N*-glycosidic bond to form the product  $\alpha$ -RP (191). The base is bound first, to avoid premature hydrolysis of NaMN (191).

In *S. enterica*, it was determined that the CobB protein could compensate for the loss of CobT if a *S. enterica*  $\Delta$ *cobT* strain was provided with higher DMB concentrations, a result that suggested

that *SeCobB* had a higher  $K_m$  for DMB (195). Of note, the *SeCobB* protein does not play any role in AdoCba biosynthesis in this bacterium. In fact, *SeCobB* is a member of the Sir2 family of eukaryotic regulatory proteins (a.k.a. sirtuins) involved in gene silencing and cell ageing (195-198). Sirtuins have NAD<sup>+</sup>-dependent protein deacetylases (199-202) and NAD<sup>+</sup>-dependent ADP-ribosyltransferases (203, 204). Subsequent work showed that *SeCobT* could use NAD<sup>+</sup> as a substrate in lieu of NaMN. Under such conditions, *SeCobT* generated  $\alpha$ -DMB, adenine dinucleotide ( $\alpha$ -DAD) (205), which is currently thought to be cleaved by some, as-yet unknown hydrolase or pyrophosphatase to generate  $\alpha$ -RP and AMP. Whether the use of NAD<sup>+</sup> by *SeCobT* is physiologically relevant must await *in vivo* validation. Noteworthy is the fact that the  $K_m$  of *SeCobT* for NAD<sup>+</sup> is 18-fold higher than that of NaMN (205), but as intracellular levels of NAD<sup>+</sup> are approximately 790  $\mu$ M in *S. enterica* versus undetectable for NaMN (206), NAD<sup>+</sup> levels would be high enough to compensate for the difference in affinity. Regardless, the ability for *SeCobT*, and presumably its homologues, to use NAD<sup>+</sup>, NaMN, nicotinamide mononucleotide (NMN) or nicotinate adenine dinucleotide (NaAD) provides flexibility to the cell and allows the organism to activate DMB for the synthesis of AdoCbl (205).

### **Activation of other bases**

While most work has focused on the ability of these enzymes to activate DMB, the latter is not always the lower base found in the final product of the pathway, despite being the preferred substrate for NaMN:PRTases (207). In fact, a wide variety of purines and purine analogues are activated by CobT homologues (Figure 2-6B) (183, 189, 208). In *S. enterica*, the predominant cobamide synthesized is the adenine-containing AdopseudoCbl (209, 210), although synthesis of AdoCbl can be stimulated by the presence of DMB in the culture medium (210). It is hypothesized that both availability (182) and metabolic requirements (211, 212) can specialize the NaMN:base

PRTase of a specific organism. For example, the incorporation of DMB by *S. multivorans* disrupts its ability to dehalogenate tetrachloroethene as the PCE reductive dehalogenase selectively uses nor-pseudoCbl (25-fold reduction in the presence of nor-cobalamin versus nor-pseudoCbl) (212). Modifications to the active site of NaMN:DMB PRTase have been shown to change its response to specific bases (181, 192), even in the selection of certain asymmetric bases like 5-methoxybenzimidazole (213). A single modification of the active site of *SeCobT* allows the attachment of the ribose to either the *N1* or *N3* atom of the imidazole moiety and the subsequent generation of near equal proportions of both  $\alpha$ -5-methoxybenzimidazole-ribotide and  $\alpha$ -6-methoxybenzimidazole-ribotide where the native protein selectively phosphoribosylates at the *N1* atom to generate  $\alpha$ -5-methoxybenzimidazole-ribotide (213). The diversity has led microbes to evolve selective transport systems for specific cobamides and precursors to survive in the human gut (214, 215).

As mentioned above, the diversity of bases found in cobamides is broad (Figure 2-6B) (216). The NaMN:DMB PRTase-like enzyme from *S. ovata*, *ArsAB*, activates purines and purine analogues, but it can also phosphoribosylate phenolics (*e.g.*, phenol, *p*-cresol), generating  $\alpha$ -*O*-glycosidic bonds to the *C1* of ribose (217). The above-mentioned findings explain why in *S. ovata* the synthesis of benzimidazolylcobamides like AdoCbl inhibits specific phenoylCba-dependent acetogenic metabolisms such as those involved in the utilization of methanol or 3,4-dimethoxybenzoate (211). A structural comparison of *SoArsAB* (PDB 4HDM) and *SeCobT* (PDB 1JHU) in complex with *p*-cresol has revealed a set of three residue changes that allow *SeCobT* to activate phenolics, albeit poorly (181). These changes shift the catalytic residue of *SeCobT* (*i.e.*, Glu-317; residue 319 in *SoArsAB*) out of the way, allowing a water molecule in the active site,

which appears to help re-orient the hydroxyl moiety of *p*-cresol towards NaMN, enabling the transfer of the ribose-5'-phosphate (181, 218).

### **An alternative route to alpha-ribazole ( $\alpha$ -R)**

The genomes of some *Firmicutes* lack a gene encoding a NaMN:DMB PRTase homologue (161) including human pathogens such as *Listeria monocytogenes* and *Clostridium perfringens*. Instead, these organisms possess a pair of proteins, CblT and CblS, whose activities translocate  $\alpha$ -ribazole ( $\alpha$ -R) into the cell (CblT activity) and phosphorylate it to  $\alpha$ -R-5'-P ( $\alpha$ -RP; CblS kinase activity) (219). Some organisms possess both the CblT/CblS system and a NaMN:DMB PRTase homologue, *e.g.*, *Geobacillus kaustophilus*. In *G. kaustophilus*, the genes encoding CblS and CblT are found among the rest of the AdoCba biosynthetic genes (219), while its NaMN:DMB PRTase is elsewhere in the chromosome. Similarly, *cblS* is found clustered with the AdoCba biosynthetic genes of *L. innocua* (219), suggesting that CblS may be the preferred route to  $\alpha$ -RP in these organisms rather than through the NaMN:DMB PRTase. The source of  $\alpha$ -R in the environment is not known. It was recently reported that when the marine alphaproteobacterium *Ruegeria pomeroyi* strain DSS-3 is grown in the presence of dimethylsulfoniopropionate (DMSP),  $\alpha$ -R is released into the medium (220). *R. pomeroyi* has been shown to over-produce Cbl in exchange for fixed carbon (221), hence it is possible that a similar relationship exists in exchange for the riboside. *R. pomeroyi* lacks a CblS homologue, but it does have a NaMN:DMB PRTase and a DMB synthase known as BluB (discussed below) which allows the cell to synthesize  $\alpha$ -RP. The synthesized ribotide could be dephosphorylated and exported into the environment in exchange for other metabolites. A similar model could apply to other environments.

## Condensation of AdoCbi-GDP and $\alpha$ -RP

The penultimate step of the synthesis of coenzyme B<sub>12</sub> is catalyzed by AdoCbl-5'-phosphate (AdoCbl-5'-P) synthase (EC 2.7.8.26), encoded by *cobS* in *S. enterica* (222, 223), *cobV* in *P. denitrificans* (186). There is high sequence similarity (particularly in hydrophobicity) among CobS homologues, including in the archaea, indicating that strong selective pressures maintain AdoCba synthesis anchored to the cell membrane (222). In *S. enterica*, CobS condenses the product of CobU/CobY (AdoCbi-GDP) and the product of CobT ( $\alpha$ -ribotide) to form AdoCba-5'-phosphate (AdoCba-P) (224). The 3' hydroxyl of the  $\alpha$ -ribotide displaces GMP from AdoCbi-GDP, forming a phosphodiester bond. The  $\alpha$ -ribotide is the preferred substrate of CobS. Under the same reaction conditions CobS consumed 2500 pmol of  $\alpha$ -RP and only 20 pmol  $\alpha$ -R in 30 s (224). *S. enterica* CobS is an integral membrane protein (222). CobS topology was determined using LacZ and PhoA fusions at various positions of the enzyme, revealing two transmembrane domains and two embedded loops (222). Reasons for why AdoCba-P synthase (CobS in *S. enterica*) and AdoCbi-P synthase (CbiB in *S. enterica*) are universally located to the cell membrane remains unclear (154). This association with the membrane suggests that a multi-protein complex nucleated by CobS and CbiB exists in all AdoCba producers whose genome has been sequenced. Future studies are needed to investigate this possibility.

Not surprisingly, the overproduction and isolation of *SeCbiB* and *SeCobS* is difficult. When the wild-type allele of *S. enterica cobS* is induced in *E. coli* for the purpose of overproducing *SeCobS*, phage shock protein A (*EcPspA*) is also overproduced (222). PspA has been linked to membrane stress(225-228), which may explain why AdoCba synthesis in *S. enterica* is limited (222). Purification of *P. denitrificans* CobV (the homologue of *SeCobS*) yielded soluble protein with a 55-fold increase in activity, but the final protein remained in association with a high molecular

weight complex. The identity of the proteins putatively interacting with CobV was not established (186). A 20-AA truncation of the N-terminus of *PdCobV* ameliorates this problem, amplifying activity 200-fold in *E. coli* BL21  $\lambda$ DE3 (186). Based on the topology data (222), a similar truncation of CobS could improve the yield of *SeCobS* if it blocked its insertion in the membrane, decreasing the membrane stress that results in PspA production. It is also possible that due to the high amount of AdoCbl synthesis that occurs naturally in *P. denitrificans* (214 mg/L on sucrose, betaine, and DMB) (229), either the organism itself, or *PdCobV* specifically, has evolved some effective mechanism to control the stress of higher copies of the AdoCbl-5'-P synthase.

### **Removal of 5' phosphate from AdoCba-P completes the synthesis of AdoCba**

In *S. enterica*, the AdoCba-P phosphatase (CobC; EC 3.1.3.73) enzyme catalyzes the final step of AdoCba biosynthesis (224). The gene encoding *SeCobC* was identified over two decades ago (230), though the activity had been observed earlier in *Propionibacterium shermanii* (183, 190, 231) and *Clostridium stricklandii* (183). While it was originally proposed that the AdoCbl-5'-P synthase *SeCobS* was the final step of AdoCba biosynthesis (222), we now know that the final step is the removal of the 5' phosphate from the newly attached  $\alpha$ -RP in AdoCbl-5'-P (224). This is evident from the two orders of magnitude improvement in *SeCobS* activity in the presence of  $\alpha$ -RP versus  $\alpha$ -R (224). It is also possible to increase the rate of synthesis of AdoCba-5'-P by providing additional DMB or (CN)<sub>2</sub>Cbi to a *S. enterica*  $\Delta$ *cobC* strain (224). If *SeCobC* acted before *SeCobS*, the expectation would be that no matter how much  $\alpha$ -RP was generated, CobS would not synthesize AdoCba until  $\alpha$ -R was available. It is possible to bypass the need for *SeCobC*, but for that to happen the intracellular levels of AdoCba-P must be appreciably higher for non-specific phosphatase activity (224). The mechanism of *SeCobC* catalysis has not yet been reported, though a three-dimensional crystal structure of a homologue of the apo-enzyme from *Vibrio*

*parahaemolyticus* has been solved (PDB 3HJG). While no orthologues of *SeCobC* have been found in most archaeal genomes, a non-orthologous replacement, *CobZ* (Mm2058), has been described in the methanogenic archaeon *Methanosarcina mazei* Gö1 (232). *In vitro* and *in vivo* data confirmed that *MmCobZ* was a functional replacement for *CobC* (232).

### **Salvaging Complete and Incomplete Corrinoids**

The lack of AdoCbi kinase activity in *CobY* raises the possibility that archaea either do not salvage incomplete corrinoids or they use a kinase that is not homologous to *SeCobU*. In *S. enterica*, there is precedent for such a scenario. In that case the *YcfN* protein (thiamine kinase; EC 2.7.1.89) has been shown to phosphorylate AdoCbi, albeit poorly (233). To date, no AdoCbi kinase has been reported in archaea. Instead, archaea have evolved an enzyme that cleaves the amide bond that attaches AP to the nucleotide loop releasing cobyrinic acid (234), which enters the biosynthetic pathway as a substrate of the AdoCbi-P synthase (*CbiB*) (155). The alluded AdoCbi amidohydrolase is encoded by the *cbiZ* gene (*CbiZ*, EC 3.5.1.90). Evidence of the existence of *CbiZ* was obtained genetically in *Halobacterium* sp. strain NRC-1 (155) and biochemically in *Methanosarcina mazei* (234). *CbiZ* cleaves the AP linker from the carboxylic acid of pyrrole ring D of the corrin ring, generating AdoCby, which is then converted to AdoCbi-P by *CbiB* (234).

Although the evolutionary origin of *CbiZ* is archaeal, it has also been reported in some bacteria (235). Such a finding was intriguing because some bacteria that carried the *cbiZ* gene also carried *cobU* (e.g., *Rhodobacter sphaeroides*) (235). The existence of two ‘cobinamide salvaging pathways’ was unexpected, and prompted further analysis to uncover the reasons why some bacteria would have these seemingly redundant approaches for cobinamide salvaging (235). The *Rhodobacter sphaeroides* *CbiZ* enzyme requires the corrinoid substrate to be adenosylated (236), suggesting that the upper ligand may play some role in positioning the substrate. The *R.*

*sphaeroides* CbiZ enzyme cleaves AdopseudoCbl but not AdoCbl, which is the cofactor for ethylmalonyl- and methylmalonyl-CoA mutases involved in acetate catabolism in this bacterium (237). Unsurprisingly, when a *R. sphaeroides*  $\Delta$ *cbiZ* strain is provided with AdopseudoCbl, growth on acetate is substantially impaired (236), indicating that for some organisms, recycling the expensive ring is critical to its own ability to synthesize the cobamides they need. Notably, some bacteria of the genus *Dehalococcoides* have multiple copies of *cbiZ* gene in their chromosomes, but the function of these putative CbiZ enzymes has not been experimentally validated.

### **Biosynthesis of DMB and other benzimidazoles**

There are two distinct DMB biosynthetic routes known in bacteria and archaea, one that requires molecular oxygen, one that does not (238). The O<sub>2</sub>-dependent pathway involves the transformation of reduced flavin mononucleotide (FMNH<sub>2</sub>) (239) by a single enzyme (240, 241). DMB auxotrophs of *Sinorhizobium meliloti* led to the identification of *bluB* (242), whose gene product was directly involved in the conversion of FMNH<sub>2</sub> to DMB in an O<sub>2</sub>-dependent reaction (240, 241). Previous to the discovery of BluB, it was reported that incubation of 4,5-dimethylphenylene-1,2-diamine (DMPDA) and ribose-5-P at pH 7, 37°C and in the absence of enzymes would yield DMB in an O<sub>2</sub>-dependent manner (243). These findings were in agreement with labeling studies performed using the organisms *P. shermanii* (239, 244-246) and *S. enterica* serovar Typhimurium LT2 (247), which showed that FMN was the immediate precursor to DMB, and that the C1' of the ribose moiety of FMNH<sub>2</sub> served as the C2 of DMB (244). Structural studies (241) showed that molecular oxygen is positioned just above the isoalloxazine ring of FMNH<sub>2</sub> in the active site of BluB. Computational studies suggest that this allows the oxygen to attack the 4a carbon of the isoalloxazine ring, forming a flavin C4a-peroxide (248). The peroxide acts as a nucleophile, attacking C10a of the isoalloxazine and generating a transient dioxetane state, which then

decomposes into dimethylphenylenediimine ribose (DMPDI) and alloxan (248). It is proposed that alloxan serves as a proton donor and acceptor and a hydride acceptor as DMPDI reorganizes into DMB and erythrose-4-phosphate.(248)

It should be noted that no BluB-like activity has been identified in *S. enterica* despite suggestions that *S. enterica* uses FMNH<sub>2</sub> to generate its DMB (247). The ability of NaMN:DMB PRTase to activate adenine precludes the use of *in vivo* genetic approaches for the isolation of *bona fide* DMB auxotrophs in *S. enterica*. While it is possible that DMB synthesis in *S. enterica* proceeds non-enzymatically (243), the formation of the flavin C4a-hydroperoxide *in vitro* requires the use of high heat at an alkaline pH (249). It is therefore more likely that opening of the ring is enzymatically catalyzed. DMB production in *S. enterica* is thought to be low, as the organism can activate and use other bases such as adenine in the place of DMB (209, 210).

The anaerobic route to DMB has been described in *Eubacterium limosum*. Labeling studies identified glycine (250), glutamine (251), and formate (252) as donors to the final molecule, suggesting that the synthesis branches out from the purine biosynthetic pathway. Recently, 5-aminoimidazole ribotide (AIR) was described as the branch point between the synthesis of purines, thiamin, and DMB (253). While labeling studies identified erythrose-4-phosphate as a precursor to anaerobically synthesized DMB (252, 254), recent studies suggest that the ribityl moiety of AIR is sufficient to provide those four carbons (255), suggesting that erythrose-4-phosphate feeds in through ribose metabolism. In *E. limosum* and other anaerobes, DMB synthesis proceeds from AIR to 5-hydroxybenzimidazole (5-OH-Bza) via a pair of ThiC-like proteins, BzaA and BzaB. Some anaerobes only have a single ThiC homologue, BzaF, but it has also been shown to generate 5-OH-benzimidazole from AIR (255). Next, two methyltransferase reactions catalyzed by BzaC and BzaD generate 5-methoxy-benzimidazole and 5-methoxy-6-methylbenzimidazole,

respectively (255). The final step is putatively catalyzed by BzaE, which converts 5-methoxyl moiety to a methyl moiety, finishing the DMB molecule (255). Methionine, in the form of *S*-adenosyl-methionine (SAM), provides the methyl groups on the final DMB molecule (255, 256). Interestingly, some anaerobes lack BzaC, BzaD, or BzaE, resulting in the formation of cobamides containing the precursor at each step (255). This ultimately contributes to some of the diversity of cobamides observed in the environment (181, 182, 207, 257, 258).

### **CONCLUDING REMARKS**

The field of AdoCba biosynthesis has been the focus of multidisciplinary approaches, all of which have made profound contributions to our understanding of the complexities of the assembly of this magnificent molecule. Even after so many decades of work by so many investigators, critical gaps of knowledge remain regarding the function, regulation, and integration of this major biosynthetic pathway into the metabolic network and regulatory systems of the cells producing it.

### **ACKNOWLEDGEMENTS**

The authors declare no conflict of interest. This work was supported by USPHS grant R37 GM040313 to JCE-S. Funding to MJW and ED from the Biotechnology and Biological Sciences Research Council is acknowledged.

## REFERENCES.

1. Escalante-Semerena JC, Warren MJ. 2008. Biosynthesis and Use of Cobalamin (B<sub>12</sub>). *In* Böck A, Curtiss III R, Kaper JB, Karp PD, Neidhardt FC, Nyström T, Slauch JM, Squires CL (ed), *EcoSal - Escherichia coli and Salmonella: cellular and molecular biology*. ASM Press, Washington, D. C.
2. Folkers K. 1982. History of vitamin B<sub>12</sub>: pernicious anemia to crystalline cyanocobalamin, p 1-17. *In* Dolphin D (ed), B<sub>12</sub>, vol 1. John Wiley and Sons., New York, NY.
3. Pruthi RK, Tefferi A. 1994. Pernicious anemia revisited. *Mayo Clin Proc* 69:144-150.
4. Gherasim C, Lofgren M, Banerjee R. 2013. Navigating the B<sub>12</sub> road: assimilation, delivery and disorders of cobalamin. *J Biol Chem* 288:13186-13193.
5. Graham SM, Arvela OM, Wise GA. 1992. Long-term neurologic consequences of nutritional vitamin-B<sub>12</sub> deficiency in infants. *J Pediat* 121:710-714.
6. Saintieau O, Berigaud S, Kaltenbach G, Bouchon JP. 1990. Regressive dementia-like syndrome due to vitamin B<sub>12</sub> deficiency without hematological abnormalities in a 92-year old subject. *Presse Med* 19:1683.
7. Leal NA, Park SD, Kima PE, Bobik TA. 2003. Identification of the human and bovine ATP: cob(I)alamin adenosyltransferase cDNAs based on complementation of a bacterial mutant. *J Biol Chem* 278:9227-9234.
8. Leal NA, Olteanu H, Banerjee R, Bobik TA. 2004. Human ATP:Cob(I)alamin adenosyltransferase and its interaction with methionine synthase reductase. *J Biol Chem* 279:47536-47542.

9. Schubert HL, Hill CP. 2006. Structure of ATP-bound human ATP:cobalamin adenosyltransferase. *Biochemistry* 45:15188-15196.
10. Dillon MJ, England JM, Gompertz D, Goodey PA, Grant DB, Hussein HA, Linnell JC, Matthews DM, Mudd SH, Newns GH, Seakins JW, Uhlenendorf BW, Wise IJ. 1974. Mental retardation, megaloblastic anaemia, methylmalonic aciduria and abnormal homocysteine metabolism due to an error in vitamin B12 metabolism. *Clin Sci Mol Med* 47:43-61.
11. Selhub J, Morris MS, Jacques PF. 2007. In vitamin B12 deficiency, higher serum folate is associated with increased total homocysteine and methylmalonic acid concentrations. *Proc Natl Acad Sci U S A* 104:19995-20000.
12. Helliwell KE, Lawrence AD, Holzer A, Kudahl UJ, Sasso S, Krautler B, Scanlan DJ, Warren MJ, Smith AG. 2016. Cyanobacteria and eukaryotic algae use different chemical variants of vitamin B12. *Curr Biol* doi:10.1016/j.cub.2016.02.041.
13. Croft MT, Lawrence AD, Raux-Deery E, Warren MJ, Smith AG. 2005. Algae acquire vitamin B12 through a symbiotic relationship with bacteria. *Nature* 438:90-93.
14. Croft MT, Warren MJ, Smith AG. 2006. Algae need their vitamins. *Eukaryot Cell* 5:1175-1183.
15. Blanche F, Debussche L, Thibaut D, Crouzet J, Cameron B. 1989. Purification and characterization of S-adenosyl-L-methionine: uroporphyrinogen III methyltransferase from *Pseudomonas denitrificans*. *J Bacteriol* 171:4222-4231.
16. Crouzet J, Cauchois L, Blanche F, Debussche L, Thibaut D, Rouyez MC, Rigault S, Mayaux JF, Cameron B. 1990. Nucleotide sequence of a *Pseudomonas denitrificans* 5.4-kilobase DNA fragment containing five *cob* genes and identification of structural genes

- encoding S-adenosyl-L-methionine: uroporphyrinogen III methyltransferase and cobyrinic acid a,c-diamide synthase. *J Bacteriol* 172:5968-5979.
17. Lobo SA, Brindley A, Warren MJ, Saraiva LM. 2009. Functional characterization of the early steps of tetrapyrrole biosynthesis and modification in *Desulfovibrio vulgaris* Hildenborough. *Biochem J* 420:317-325.
  18. Spencer JB, Stolowich NJ, Roessner CA, Scott AI. 1993. The *Escherichia coli cysG* gene encodes the multifunctional protein, siroheme synthase. *FEBS Lett* 335:57-60.
  19. Warren MJ, Bolt EL, Roessner CA, Scott AI, Spencer JB, Woodcock SC. 1994. Gene dissection demonstrates that the *Escherichia coli cysG* gene encodes a multifunctional protein. *Biochem J* 302:837-844.
  20. Stroupe ME, Leech HK, Daniels DS, Warren MJ, Getzoff ED. 2003. CysG structure reveals tetrapyrrole-binding features and novel regulation of siroheme biosynthesis. *Nat Struct Biol* 10:1064-1073.
  21. Vevodova J, Graham RM, Raux E, Schubert HL, Roper DI, Brindley AA, Ian Scott A, Roessner CA, Stamford NP, Elizabeth Stroupe M, Getzoff ED, Warren MJ, Wilson KS. 2004. Structure/function studies on a S-adenosyl-L-methionine-dependent uroporphyrinogen III C methyltransferase (SUMT), a key regulatory enzyme of tetrapyrrole biosynthesis. *J Mol Biol* 344:419-433.
  22. Storbeck S, Saha S, Krausze J, Klink BU, Heinz DW, Layer G. 2011. Crystal structure of the heme d1 biosynthesis enzyme NirE in complex with its substrate reveals new insights into the catalytic mechanism of S-adenosyl-L-methionine-dependent uroporphyrinogen III methyltransferases. *J Biol Chem* 286:26754-26767.

23. Roth JR, Lawrence JG, Bobik TA. 1996. Cobalamin (coenzyme B12): synthesis and biological significance. *Annu Rev Microbiol* 50:137-181.
24. Roth JR, Lawrence JG, Rubenfield M, Kieffer-Higgins S, Church GM. 1993. Characterization of the cobalamin (vitamin B<sub>12</sub>) biosynthetic genes of *Salmonella typhimurium*. *J Bacteriol* 175:3303-3316.
25. Raux E, Lanois A, Rambach A, Warren MJ, Thermes C. 1998. Cobalamin (vitamin B-12) biosynthesis: functional characterization of the *Bacillus megaterium* *cbi* genes required to convert uroporphyrinogen III into cobyrinic acid *a,c*-diamide. *Biochem J* 335:167-173.
26. Raux E, Lanois A, Warren MJ, Rambach A, Thermes C. 1998. Cobalamin (vitamin B<sub>12</sub>) biosynthesis: identification and characterization of a *Bacillus megaterium* *cobI* operon. *Biochem J* 335:159-166.
27. Leech HK, Raux-Deery E, Heathcote P, Warren MJ. 2002. Production of cobalamin and sirohaem in *Bacillus megaterium*: an investigation into the role of the branchpoint chelataases sirohydrochlorin ferrochelataase (SirB) and sirohydrochlorin cobalt chelataase (CbiX). *Biochem Soc Trans* 30:610-613.
28. Raux E, Leech HK, Beck R, Schubert HL, Santander PJ, Roessner CA, Scott AI, Martens JH, Jahn D, Thermes C, Rambach A, Warren MJ. 2003. Identification and functional analysis of enzymes required for precorrin-2 dehydrogenation and metal ion insertion in the biosynthesis of sirohaem and cobalamin in *Bacillus megaterium*. *Biochem J* 370:505-516.
29. Raux E, Thermes C, Heathcote P, Rambach A, Warren MJ. 1997. A role for *Salmonella typhimurium* *cbiK* in cobalamin (vitamin B12) and siroheme biosynthesis. *J Bacteriol* 179:3202-3212.

30. Brindley AA, Raux E, Leech HK, Schubert HL, Warren MJ. 2003. A story of chelatase evolution: identification and characterization of a small 13-15-kDa "ancestral" cobaltochelatase (CbiXS) in the archaea. *J Biol Chem* 278:22388-22395.
31. Medlock AE, Dailey HA. 2017. Heme Biosynthesis and Insertion, p 1-14. *In* Scott RA (ed), *Encyclopedia of Inorganic and Bioinorganic Chemistry* doi:doi:10.1002/9781119951438.eibc2486. John Wiley & Sons, Ltd, Chichester, UK.
32. Romao CV, Ladakis D, Lobo SA, Carrondo MA, Brindley AA, Deery E, Matias PM, Pickersgill RW, Saraiva LM, Warren MJ. 2011. Evolution in a family of chelatases facilitated by the introduction of active site asymmetry and protein oligomerization. *Proc Natl Acad Sci U S A* 108:97-102.
33. Schubert HL, Raux E, Wilson KS, Warren MJ. 1999. Common chelatase design in the branched tetrapyrrole pathways of heme and anaerobic cobalamin synthesis. *Biochemistry* 38:10660-10669.
34. Leech HK, Raux E, McLean KJ, Munro AW, Robinson NJ, Borrelly GP, Malten M, Jahn D, Rigby SE, Heathcote P, Warren MJ. 2003. Characterization of the cobaltochelatase CbiXL: evidence for a 4Fe-4S center housed within an MXCXXC motif. *J Biol Chem* 278:41900-4197.
35. Dailey HA, Finnegan MG, Johnson MK. 1994. Human ferrochelatase is an iron-sulfur protein. *Biochemistry* 33:403-407.
36. Yin J, Xu LX, Cherney MM, Raux-Deery E, Bindley AA, Savchenko A, Walker JR, Cuff ME, Warren MJ, James MN. 2006. Crystal structure of the vitamin B<sub>12</sub> biosynthetic cobaltochelatase, CbiX (S), from *Archaeoglobus fulgidus*. *J Struct Funct Genomics* 7:37-50.

37. Frank S, Deery E, Brindley AA, Leech HK, Lawrence A, Heathcote P, Schubert HL, Brocklehurst K, Rigby SE, Warren MJ, Pickersgill RW. 2007. Elucidation of substrate specificity in the cobalamin (vitamin B12) biosynthetic methyltransferases. Structure and function of the C20 methyltransferase (CbiL) from *Methanothermobacter thermautotrophicus*. J Biol Chem 282:23957-23969.
38. Roessner CA, Warren MJ, Santander PJ, Atshaves BP, Ozaki S, Stolowich NJ, Iida K, Scott AI. 1992. Expression of 9 *Salmonella typhimurium* enzymes for cobinamide synthesis. Identification of the 11-methyl and 20-methyl transferases of corrin biosynthesis. FEBS Lett 301:73-78.
39. Wada K, Harada J, Yaeda Y, Tamiaki H, Oh-Oka H, Fukuyama K. 2007. Crystal structures of CbiL, a methyltransferase involved in anaerobic vitamin B biosynthesis, and CbiL in complex with S-adenosylhomocysteine - implications for the reaction mechanism. FEBS J 274:563-573.
40. Schubert HL, Blumenthal RM, Cheng X. 2003. Many paths to methyltransfer: a chronicle of convergence. Trends Biochem Sci 28:329-335.
41. Eschenmoser A. 1988. Vitamin B12: experiments concerning the origin of its molecular structure. Angew Chem Int Ed Engl 27:5-40.
42. Moore SJ, Biedendieck R, Lawrence AD, Deery E, Howard MJ, Rigby SE, Warren MJ. 2013. Characterization of the enzyme CbiH60 involved in anaerobic ring contraction of the cobalamin (vitamin B12) biosynthetic pathway. J Biol Chem 288:297-305.
43. Santander PJ, Kajiwara Y, Williams HJ, Scott AI. 2006. Structural characterization of novel cobalt corrinoids synthesized by enzymes of the vitamin B<sub>12</sub> anaerobic pathway. Bioorg Med Chem 14:724-731.

44. Santander PJ, Roessner CA, Stolowich NJ, Holderman MT, Scott AI. 1997. How corrinoids are synthesized without oxygen: nature's first pathway to vitamin B<sub>12</sub>. *Chem Biol* 4:659-666.
45. Moore SJ, Lawrence AD, Biedendieck R, Deery E, Frank S, Howard MJ, Rigby SE, Warren MJ. 2013. Elucidation of the anaerobic pathway for the corrin component of cobalamin (vitamin B<sub>12</sub>). *Proc Natl Acad Sci U S A* 110:14906-14911.
46. Kajiwara Y, Santander PJ, Roessner CA, Perez LM, Scott AI. 2006. Genetically engineered synthesis and structural characterization of cobalt-precorrin 5A and -5B, two new intermediates on the anaerobic pathway to vitamin B<sub>12</sub>: definition of the roles of the CbiF and CbiG enzymes. *J Am Chem Soc* 128:9971-9978.
47. Ozaki SI, Roessner CA, Stolowich NJ, Atshaves BP, Hertle R, Muller G, Scott AI. 1993. Multienzyme synthesis and structure of Factor-S3. *J Am Chem Soc* 115:7935-7938.
48. Santander PJ, Stolowich NJ, Scott AI. 1999. Chemoenzymatic synthesis of an unnatural tetramethyl cobalt corphinoid. *Bioorg Med Chem* 7:789-794.
49. Schubert HL, Wilson KS, Raux E, Woodcock SC, Warren MJ. 1998. The X-ray structure of a cobalamin biosynthetic enzyme, cobalt-precorrin-4 methyltransferase. *Nat Struct Biol* 5:585-592.
50. Wang J, Stolowich NJ, Santander PJ, Park JH, Scott AI. 1996. Biosynthesis of vitamin B<sub>12</sub>: concerning the identity of the two-carbon fragment eliminated during anaerobic formation of cobyrinic acid. *Proc Natl Acad Sci U S A* 93:14320-14322.
51. Roessner CA, Williams HJ, Scott AI. 2005. Genetically engineered production of 1-desmethylcobyrinic acid, 1-desmethylcobyrinic acid *a,c*-diamide, and cobyrinic acid *a,c*-

- diamide in *E. coli* implies a role for CbiD in C-1 methylation in the anaerobic pathway to cobalamin. *J Biol Chem* 280:16748-16753.
52. Fresquet V, Williams L, Raushel FM. 2004. Mechanism of cobyrinic acid *a,c*-diamide synthetase from *Salmonella typhimurium* LT2. *Biochemistry* 43:10619-10627.
  53. Battersby AR. 1994. How nature builds the pigments of life: the conquest of vitamin B<sub>12</sub>. *Science* 264:1551-1557.
  54. Blanche F, Cameron B, Crouzet J, Debussche L, Thibaut D, Vuilhorgne M, Leeper FJ, Battersby AR. 1995. Vitamin-B<sub>12</sub> - How the problem of its biosynthesis was solved. *Angewand Chem Intern Ed* 34:383-411.
  55. Scott AI. 1996. Travels of an organic chemist along nature's pathways. *Bioorg Med Chem* 4:965-985.
  56. Iggo JA, Liu J, Khimyak YZ. 2011. Nuclear Magnetic Resonance (NMR) Spectroscopy of Inorganic/Organometallic Molecules. *In* Scott RA (ed), *Encyclopedia of Inorganic and Bioinorganic Chemistry* doi:10.1002/9781119951438.eibc0295.
  57. Blanche F, Famechon A, Thibaut D, Debussche L, Cameron B, Crouzet J. 1992. Biosynthesis of vitamin B<sub>12</sub> in *Pseudomonas denitrificans*: the biosynthetic sequence from precorrin-6y to precorrin-8x is catalyzed by the *cobL* gene product. *J Bacteriol* 174:1050-1052.
  58. Debussche L, Thibaut D, Cameron B, Crouzet J, Blanche F. 1993. Biosynthesis of the corrin macrocycle of coenzyme B<sub>12</sub> in *Pseudomonas denitrificans*. *J Bacteriol* 175:7430-7440.
  59. Debussche L, Thibaut D, Danzer M, Debu F, Frechet D, Herman F, Blanche F, Vuilhorgne M. 1993. Biosynthesis of Vitamin-B(12) - Structure of precorrin-3b, the

- trimethylated substrate of the enzyme catalyzing ring contraction. *J Chem Soc Chem Comm*:1100-1103.
60. Scott AI, Roessner CA, Stolowich NJ, Spencer JB, Min C, Ozaki SI. 1993. Biosynthesis of vitamin B<sub>12</sub>. Discovery of the enzymes for oxidative ring contraction and insertion of the fourth methyl group. *FEBS Lett* 331:105-108.
  61. Schroeder S, Lawrence AD, Biedendieck R, Rose RS, Deery E, Graham RM, McLean KJ, Munro AW, Rigby SE, Warren MJ. 2009. Demonstration that CobG, the monooxygenase associated with the ring contraction process of the aerobic cobalamin (vitamin B<sub>12</sub>) biosynthetic pathway, contains a Fe-S center and a mononuclear non-heme iron center. *J Biol Chem* 284:4796-4805.
  62. McGoldrick HM, Roessner CA, Raux E, Lawrence AD, McLean KJ, Munro AW, Santabarbara S, Rigby SE, Heathcote P, Scott AI, Warren MJ. 2005. Identification and characterization of a novel vitamin B<sub>12</sub> (cobalamin) biosynthetic enzyme (CobZ) from *Rhodobacter capsulatus*, containing flavin, heme, and Fe-S cofactors. *J Biol Chem* 280:1086-1094.
  63. Lewis JA, Escalante-Semerena JC. 2006. The FAD-dependent tricarballylate dehydrogenase (TcuA) enzyme of *Salmonella enterica* converts tricarballylate into *cis*-aconitate. *J Bacteriol* 188:5479-5486.
  64. Lewis JA, Escalante-Semerena JC. 2007. Tricarballylate catabolism in *Salmonella enterica*. The TcuB protein uses 4Fe-4S clusters and heme to transfer electrons from FADH<sub>2</sub> in the tricarballylate dehydrogenase (TcuA) enzyme to electron acceptors in the cell membrane. *Biochemistry* 46:9107-9115.

65. Alanine AID, Ichinose K, Thibaut D, Debussche L, Stamford NPJ, Leeper FJ, Blanche F, Battersby AR. 1994. Biosynthesis of Vitamin-B12 - Use of Specific C-13-labeling for structural studies on Factor Iv. *J Chem Soc Chem Comm*:193-196.
66. Thibaut D, Debussche L, Frechet D, Herman F, Vuilhorgne M, Blanche F. 1993. Biosynthesis of Vitamin-B12 - the structure of factor-Iv, the oxidized form of precorrin-4. *J Chem Soc Chem Comm*:513-515.
67. Min C, Atshaves BP, Roessner CA, Stolowich NJ, Spencer JB, Scott AI. 1993. Isolation, structure, and genetically engineered synthesis of precorrin-5, the pentamethylated intermediate of vitamin B12 biosynthesis. *J Amer Chem Soc* 115:10380-10381.
68. Thibaut D, Blanche F, Debussche L, Leeper FJ, Battersby AR. 1990. Biosynthesis of vitamin B12: structure of precorrin-6x octamethyl ester. *Proc Natl Acad Sci U S A* 87:8800-8804.
69. Thibaut D, Debussche L, Blanche F. 1990. Biosynthesis of vitamin B12: isolation of precorrin-6x, a metal-free precursor of the corrin macrocycle retaining five S-adenosylmethionine-derived peripheral methyl groups. *Proc Natl Acad Sci U S A* 87:8795-8799.
70. Blanche F, Thibaut D, Famechon A, Debussche L, Cameron B, Crouzet J. 1992. Precorrin-6x reductase from *Pseudomonas denitrificans*: purification and characterization of the enzyme and identification of the structural gene. *J Bacteriol* 174:1036-1042.
71. Gu S, Sushko O, Deery E, Warren MJ, Pickersgill RW. 2015. Crystal structure of CobK reveals strand-swapping between Rossmann-fold domains and molecular basis of the reduced precorrin product trap. *Sci Rep* 5:16943.

72. Deery E, Schroeder S, Lawrence AD, Taylor SL, Seyedarabi A, Waterman J, Wilson KS, Brown D, Geeves MA, Howard MJ, Pickersgill RW, Warren MJ. 2012. An enzyme-trap approach allows isolation of intermediates in cobalamin biosynthesis. *Nature Chem Biol* 8:933-940.
73. Thibaut D, Couder M, Famechon A, Debussche L, Cameron B, Crouzet J, Blanche F. 1992. The final step in the biosynthesis of hydrogenobyric acid is catalyzed by the *cobH* gene product with precorrin-8x as the substrate. *J Bacteriol* 174:1043-1049.
74. Shipman LW, Li D, Roessner CA, Scott AI, Sacchettini JC. 2001. Crystal structure of precorrin-8x methyl mutase. *Structure* 9:587-596.
75. Debussche L, Couder M, Thibaut D, Cameron B, Crouzet J, Blanche F. 1992. Assay, purification, and characterization of cobaltochelatase, a unique complex enzyme catalyzing cobalt insertion in hydrogenobyric acid a,c-diamide during coenzyme B<sub>12</sub> biosynthesis in *Pseudomonas denitrificans*. *J Bacteriol* 174:7445-7451.
76. Lundqvist J, Elmlund D, Heldt D, Deery E, Soderberg CA, Hansson M, Warren M, Al-Karadaghi S. 2009. The AAA(+) motor complex of subunits CobS and CobT of cobaltochelatase visualized by single particle electron microscopy. *J Struct Biol* 167:227-234.
77. Suh SJ, Escalante-Semerena JC. 1993. Cloning, sequencing and overexpression of *cobA* which encodes ATP:corrinoid adenosyltransferase in *Salmonella typhimurium*. *Gene* 129:93-97.
78. Debussche L, Couder M, Thibaut D, Cameron B, Crouzet J, Blanche F. 1991. Purification and partial characterization of cob(I)alamin adenosyltransferase from *Pseudomonas denitrificans*. *J Bacteriol* 173:6300-6302.

79. Lawrence AD, Deery E, McLean KJ, Munro AW, Pickersgill RW, Rigby SE, Warren MJ. 2008. Identification, characterization, and structure/function analysis of a corrin reductase involved in adenosylcobalamin biosynthesis. *J Biol Chem* 283:10813-10821.
80. Fonseca MV, Escalante-Semerena JC. 2001. An in vitro reducing system for the enzymic conversion of cobalamin to adenosylcobalamin. *J Biol Chem* 276:32101-32108.
81. Crouzet J, Levy-Schil S, Cameron B, Cauchois L, Rigault S, Rouyez MC, Blanche F, Debussche L, Thibaut D. 1991. Nucleotide sequence and genetic analysis of a 13.1-kilobase-pair *Pseudomonas denitrificans* DNA fragment containing five *cob* genes and identification of structural genes encoding Cob(D)alamin adenosyltransferase, cobyrinic acid synthase, and bifunctional cobinamide kinase-cobinamide phosphate guanylyltransferase. *J Bacteriol* 173:6074-6087.
82. Fresquet V, Williams L, Raushel FM. 2007. Partial randomization of the four sequential amidation reactions catalyzed by cobyrinic acid synthetase with a single point mutation. *Biochemistry* 46:13983-13993.
83. Williams L, Fresquet V, Santander PJ, Raushel FM. 2007. The multiple amidation reactions catalyzed by cobyrinic acid synthetase from *Salmonella typhimurium* are sequential and dissociative. *J Am Chem Soc* 129:294-295.
84. Halpern J. 1985. Mechanisms of coenzyme B<sub>12</sub>-dependent rearrangements. *Science* 227:869-875.
85. Can M, Armstrong FA, Ragsdale SW. 2014. Structure, function, and mechanism of the nickel metalloenzymes, CO dehydrogenase, and acetyl-CoA synthase. *Chem Rev* 114:4149-7414.

86. Krzycki JA. 2004. Function of genetically encoded pyrrolysine in corrinoid-dependent methylamine methyltransferases. *Curr Opin Chem Biol* 8:484-491.
87. Koutmos M, Datta S, Patridge KA, Smith JL, Matthews RG. 2009. Insights into the reactivation of cobalamin-dependent methionine synthase. *Proc Natl Acad Sci U S A* 106:18527-18532.
88. Wohlfarth G, Diekert G. 1999. Reductive dehalogenases., p 871-893. *In* Banerjee R (ed), *Chemistry and Biochemistry of B12*. John Wiley & Sons, Inc., New York.
89. Payne KA, Quezada CP, Fisher K, Dunstan MS, Collins FA, Sjuts H, Levy C, Hay S, Rigby SE, Leys D. 2015. Reductive dehalogenase structure suggests a mechanism for B12-dependent dehalogenation. *Nature* 517:513-6.
90. Weissbach H, Ladd JN, Volcani BE, Smyth RD, Barker HA. 1960. Structure of the adenylobamide coenzyme: degradation by cyanide, acid, and light. *J Biol Chem* 235:1462-1473.
91. Fonseca MV, Escalante-Semerena JC. 2000. Reduction of cob(III)alamin to cob(II)alamin in *Salmonella enterica* Serovar Typhimurium LT2. *J Bacteriol* 182:4304-4309.
92. Hoover DM, Jarrett JT, Sands RH, Dunham WR, Ludwig ML, Matthews RG. 1997. Interaction of *Escherichia coli* cobalamin-dependent methionine synthase and its physiological partner flavodoxin: binding of flavodoxin leads to axial ligand dissociation from the cobalamin cofactor. *Biochemistry* 36:127-138.
93. Vitols E, Walker GA, Huennekens FM. 1966. Enzymatic conversion of vitamin B-12s to a cobamide coenzyme, alpha-(5,6-dimethylbenzimidazolyl)deoxyadenosylcobamide (adenosyl-B-12). *J Biol Chem* 241:1455-1461.

94. Lexa D, Saveant J-M. 1983. The electrochemistry of vitamin B12. *Acc Chem Res* 16:235-243.
95. Escalante-Semerena JC, Suh SJ, Roth JR. 1990. *cobA* function is required for both de novo cobalamin biosynthesis and assimilation of exogenous corrinoids in *Salmonella typhimurium*. *J Bacteriol* 172:273-280.
96. Lundrigan MD, Kadner RJ. 1989. Altered cobalamin metabolism in *Escherichia coli* *btuR* mutants affects *btuB* gene regulation. *J Bacteriol* 171:154-161.
97. Lundrigan MD, De Veaux LC, Mann BJ, Kadner RJ. 1987. Separate regulatory systems for the repression of *metE* and *btuB* by vitamin B<sub>12</sub> in *Escherichia coli*. *Mol Gen Genet* 206:401-407.
98. Lundrigan MD, Koster W, Kadner RJ. 1991. Transcribed sequences of the *Escherichia coli* *btuB* gene control its expression and regulation by vitamin B12. *Proc Natl Acad Sci U S A* 88:1479-1483.
99. Buan NR, Rehfeld K, Escalante-Semerena JC. 2006. Studies of the CobA-type ATP:Co(I)rrinoid adenosyltransferase enzyme of *Methanosarcina mazei* strain Gö1. *J Bacteriol* 188:3543-3550.
100. Roof DM, Roth JR. 1988. Ethanolamine utilization in *Salmonella typhimurium*. *J Bacteriol* 170:3855-3863.
101. Roof DM, Roth JR. 1989. Functions required for vitamin B12-dependent ethanolamine utilization in *Salmonella typhimurium*. *J Bacteriol* 171:3316-3323.
102. Roof DM, Roth JR. 1992. Autogenous regulation of ethanolamine utilization by a transcriptional activator of the *eut* operon in *Salmonella typhimurium*. *J Bacteriol* 174:6634-6643.

103. Kofoed E, Rappleye C, Stojiljkovic I, Roth J. 1999. The 17-gene ethanolamine (*eut*) operon of *Salmonella typhimurium* encodes five homologues of carboxysome shell proteins. *J Bacteriol* 181:5317-5329.
104. Buan NR, Suh SJ, Escalante-Semerena JC. 2004. The *eutT* gene of *Salmonella enterica* encodes an oxygen-labile, metal-containing ATP:corrinoid adenosyltransferase enzyme. *J Bacteriol* 186:5708-5714.
105. Suh S, Escalante-Semerena JC. 1995. Purification and initial characterization of the ATP:corrinoid adenosyltransferase encoded by the *cobA* gene of *Salmonella typhimurium*. *J Bacteriol* 177:921-925.
106. Moore TC, Newmister SA, Rayment I, Escalante-Semerena JC. 2012. Structural insights into the mechanism of four-coordinate cob(II)alamin formation in the active site of the *Salmonella enterica* ATP:co(I)rrinoid adenosyltransferase (CobA) enzyme: Critical role of residues Phe91 and Trp93. *Biochemistry* 51:9647-9657.
107. Stich TA, Buan NR, Escalante-Semerena JC, Brunold TC. 2005. Spectroscopic and computational studies of the ATP:Corrinoid adenosyltransferase (CobA) from *Salmonella enterica*: Insights into the mechanism of adenosylcobalamin biosynthesis. *J Am Chem Soc* 127:8710-8719.
108. Buan NR, Escalante-Semerena JC. 2005. Computer-assisted docking of flavodoxin with the ATP:Co(I)rrinoid adenosyltransferase (CobA) enzyme reveals residues critical for protein-protein interactions but not for catalysis. *J Biol Chem* 280:40948-40956.
109. Mack J, Stillman MJ. 2011. Magnetic Circular Dichroism (MCD) Spectroscopy. *In* Scott RA (ed), *Encyclopedia of Inorganic and Bioinorganic Chemistry* doi:10.1002/9781119951438.eibc0289.

110. Hales BJ. 2011. Electron Paramagnetic Resonance (EPR) Spectroscopy. *In* Scott RA (ed), Encyclopedia of Inorganic and Bioinorganic Chemistry doi:10.1002/9781119951438.eibc0310.
111. Rappoport D, Crawford NRM, Furche F, Burke K. 2011. Approximate Density Functionals: Which Should I Choose? *In* Scott RA (ed), Encyclopedia of Inorganic and Bioinorganic Chemistry doi:10.1002/9781119951438.eibc0380.
112. Stich TA, Buan NR, Brunold TC. 2004. Spectroscopic and computational studies of Co(2+)corrinoids: spectral and electronic properties of the biologically relevant base-on and base-off forms of Co(2+)cobalamin. *J Am Chem Soc* 126:9735-9749.
113. Stich TA, Yamanishi M, Banerjee R, Brunold TC. 2005. Spectroscopic evidence for the formation of a four-coordinate Co(2+)cobalamin species upon binding to the human ATP:Cobalamin adenosyltransferase. *J Am Chem Soc* 127:7660-7661.
114. Pallares IG, Moore TC, Escalante-Semerena JC, Brunold TC. 2016. Spectroscopic studies of the EutT adenosyltransferase from *Salmonella enterica*: Mechanism of four-coordinate Co(II)Cbl formation. *J Am Chem Soc* 138:3694-3704.
115. Conrad KS, Jordan CD, Brown KL, Brunold TC. 2015. Spectroscopic and Computational Studies of Cobalamin Species with Variable Lower Axial Ligation: Implications for the Mechanism of Co-C Bond Activation by Class I Cobalamin-Dependent Isomerases. *Inorg Chem* doi:10.1021/ic502665x.
116. Park K, Mera PE, Moore TC, Escalante-Semerena JC, Brunold TC. 2015. Unprecedented mechanism employed by the *Salmonella enterica* EutT ATP:Co(I) corrinoid adenosyltransferase precludes adenylation of incomplete Co(II)corrinoids. *Angew Chem Int Ed Engl* 54:7158-7161.

117. Pallares IG, Moore TC, Escalante-Semerena JC, Brunold TC. 2014. Spectroscopic studies of the *Salmonella enterica* adenosyltransferase enzyme *SeCobA*: Molecular-level insight into the mechanism of substrate cob(II)alamin activation. *Biochemistry* 53:7969-7982.
118. Park K, Brunold TC. 2013. Combined spectroscopic and computational analysis of the vibrational properties of Vitamin B12 in its Co<sup>3+</sup>, Co<sup>2+</sup>, and Co<sup>1+</sup> oxidation states. *J Phys Chem B* doi:10.1021/jp309392u.
119. Park K, Mera PE, Escalante-Semerena JC, Brunold TC. 2012. Spectroscopic characterization of active-site variants of the PduO-type ATP:Corrinoid adenosyltransferase from *Lactobacillus reuteri*: Insights into the mechanism of four-coordinate Co(II)corrinoid formation. *Inorg Chem* 51:4482-4494.
120. Liptak MD, Fleischhacker AS, Matthews RG, Telser J, Brunold TC. 2009. Spectroscopic and computational characterization of the base-off forms of cob(II)alamin. *J Phys Chem B* 113:5245-5254.
121. St Maurice M, Mera P, Park K, Brunold TC, Escalante-Semerena JC, Rayment I. 2008. Structural characterization of a human-type corrinoid adenosyltransferase confirms that coenzyme B<sub>12</sub> is synthesized through a four-coordinate intermediate. *Biochemistry* 47:5755-66.
122. Liptak MD, Datta S, Matthews RG, Brunold TC. 2008. Spectroscopic study of the cobalamin-dependent methionine synthase in the activation conformation: effects of the Y1139 residue and S-adenosylmethionine on the B12 cofactor. *J Am Chem Soc* 130:16374-16381.

123. Park K, Mera PE, Escalante-Semerena JC, Brunold TC. 2008. Kinetic and spectroscopic studies of the ATP:corrinoic adenosyltransferase PduO from *Lactobacillus reuteri*: substrate specificity and insights into the mechanism of Co(II)corrinoic reduction. *Biochemistry* 47:9007-9015.
124. Fonseca MV, Buan NR, Horswill AR, Rayment I, Escalante-Semerena JC. 2002. The ATP:co(I)rrinoic adenosyltransferase (CobA) enzyme of *Salmonella enterica* requires the 2'-OH Group of ATP for function and yields inorganic triphosphate as its reaction byproduct. *J Biol Chem* 277:33127-33131.
125. Bauer CB, Fonseca MV, Holden HM, Thoden JB, Thompson TB, Escalante-Semerena JC, Rayment I. 2001. Three-dimensional structure of ATP:corrinoic adenosyltransferase from *Salmonella typhimurium* in its free state, complexed with MgATP, or complexed with hydroxycobalamin and MgATP. *Biochemistry* 40:361-374.
126. Johnson CL, Pechonick E, Park SD, Havemann GD, Leal NA, Bobik TA. 2001. Functional genomic, biochemical, and genetic characterization of the *Salmonella pduO* gene, an ATP:cob(I)alamin adenosyltransferase gene. *J Bacteriol* 183:1577-1584.
127. St Maurice M, Mera PE, Taranto MP, Sesma F, Escalante-Semerena JC, Rayment I. 2007. Structural characterization of the active site of the PduO-type ATP:Co(I)rrinoic adenosyltransferase from *Lactobacillus reuteri*. *J Biol Chem* 282:2596-2605.
128. Saridakis V, Yakunin A, Xu X, Anandakumar P, Pennycooke M, Gu J, Cheung F, Lew JM, Sanishvili R, Joachimiak A, Arrowsmith CH, Christendat D, Edwards AM. 2004. The structural basis for methylmalonic aciduria. The crystal structure of archaeal ATP:cobalamin adenosyltransferase. *J Biol Chem* 279:23646-23653.

129. Dobson CM, Wai T, Leclerc D, Kadir H, Narang M, Lerner-Ellis JP, Hudson TJ, Rosenblatt DS, Gravel RA. 2002. Identification of the gene responsible for the *cblB* complementation group of vitamin B12-dependent methylmalonic aciduria. *Hum Mol Genet* 11:3361-3369.
130. Walter D, Ailion M, Roth J. 1997. Genetic characterization of the *pdu* operon: use of 1,2-propanediol in *Salmonella typhimurium*. *J Bacteriol* 179:1013-1022.
131. Jeter RM. 1990. Cobalamin-dependent 1,2-propanediol utilization by *Salmonella typhimurium*. *J Gen Microbiol* 136:887-896.
132. Tobimatsu T, Sakai T, Hashida Y, Mizoguchi N, Miyoshi S, Toraya T. 1997. Heterologous expression, purification, and properties of diol dehydratase, an adenosylcobalamin-dependent enzyme of *Klebsiella oxytoca*. *Arch Biochem Biophys* 347:132-40.
133. Johnson CL, Buszko ML, Bobik TA. 2004. Purification and initial characterization of the *Salmonella enterica* PduO ATP:Cob(I)alamin adenosyltransferase. *J Bacteriol* 186:7881-7887.
134. Parsons JB, Frank S, Bhella D, Liang M, Prentice MB, Mulvihill DP, Warren MJ. 2010. Synthesis of empty bacterial microcompartments, directed organelle protein incorporation, and evidence of filament-associated organelle movement. *Mol Cell* 38:305-315.
135. Rondon MR, Kazmierczak R, Escalante-Semerena JC. 1995. Glutathione is required for maximal transcription of the cobalamin biosynthetic and 1,2-propanediol utilization (*cob/pdu*) regulon and for the catabolism of ethanolamine, 1,2-propanediol, and propionate in *Salmonella typhimurium* LT2. *J Bacteriol* 177:5434-5439.

136. Bobik TA, Havemann GD, Busch RJ, Williams DS, Aldrich HC. 1999. The propanediol utilization (*pdu*) operon of *Salmonella enterica* serovar Typhimurium LT2 includes genes necessary for formation of polyhedral organelles involved in coenzyme B<sub>12</sub>-dependent 1, 2-propanediol degradation. *J Bacteriol* 181:5967-5975.
137. Yeates TO, Jorda J, Bobik TA. 2013. The shells of BMC-type microcompartment organelles in bacteria. *J Mol Microbiol Biotechnol* 23:290-299.
138. Toraya T. 2000. Radical catalysis of B<sub>12</sub> enzymes: structure, mechanism, inactivation, and reactivation of diol and glycerol dehydratases. *Cell Mol Life Sci* 57:106-127.
139. Ortiz de Orue Lucana D, Hickey N, Hensel M, Klare JP, Geremia S, Tiufiakova T, Torda AE. 2016. The crystal structure of the C-terminal domain of the *Salmonella enterica* PduO protein: An old fold with a new heme-binding mode. *Front Microbiol* 7:1010.
140. Park K, Mera PE, Escalante-Semerena JC, Brunold TC. 2016. Resonance Raman spectroscopic study of the interaction between Co(II)corrinoids and the ATP:corrinoid adenosyltransferase PduO from *Lactobacillus reuteri*. *J Biol Inorg Chem* 21:669-681.
141. Mera PE, St Maurice M, Rayment I, Escalante-Semerena JC. 2009. Residue Phe112 of the human-type corrinoid adenosyltransferase (PduO) enzyme of *Lactobacillus reuteri* is critical to the formation of the four-coordinate Co(II) corrinoid substrate and to the activity of the enzyme. *Biochemistry* 48:3138-3145.
142. Mera PE, Maurice MS, Rayment I, Escalante-Semerena JC. 2007. Structural and functional analyses of the human-type corrinoid adenosyltransferase (PduO) from *Lactobacillus reuteri*. *Biochemistry* 46:13829-13836.
143. Cheng S, Bobik TA. 2010. Characterization of the PduS cobalamin reductase of *Salmonella* and its role in the Pdu microcompartment. *J Bacteriol* 192:5071-5080.

144. Sampson EM, Johnson CL, Bobik TA. 2005. Biochemical evidence that the *pduS* gene encodes a bifunctional cobalamin reductase. *Microbiology* 151:1169-1177.
145. Parsons JB, Lawrence AD, McLean KJ, Munro AW, Rigby SE, Warren MJ. 2010. Characterisation of PduS, the *pdu* metabolosome corrin reductase, and evidence of substructural organisation within the bacterial microcompartment. *PLoS One* 5:e14009.
146. Sheppard DE, Penrod JT, Bobik T, Kofoed E, Roth JR. 2004. Evidence that a B12-adenosyl transferase is encoded within the ethanolamine operon of *Salmonella enterica*. *J Bacteriol* 186:7635-7644.
147. Buan NR, Escalante-Semerena JC. 2006. Purification and initial biochemical characterization of ATP:Cob(I)alamin adenosyltransferase (EutT) enzyme of *Salmonella enterica*. *J Biol Chem* 281:16971-16977.
148. Huseby DL, Roth JR. 2013. Evidence that a metabolic microcompartment contains and recycles private cofactor pools. *J Bacteriol* 195:2864-2879.
149. Mori K, Bando R, Hieda N, Toraya T. 2004. Identification of a reactivating factor for adenosylcobalamin-dependent ethanolamine ammonia lyase. *J Bacteriol* 186:6845-6854.
150. Moore TC, Mera PE, Escalante-Semerena JC. 2014. the EutT enzyme of *Salmonella enterica* is a unique ATP:Cob(I)alamin adenosyltransferase metalloprotein that requires ferrous ions for maximal activity. *J Bacteriol* 196:903-910.
151. Hodgkin DC, Kamper J, Lindsey J, MacKay M, Pickworth J, Robertson JH, Shoemaker CB, White JG, Prosen RJ, Trueblood KN. 1957. The structure of vitamin B12. I. An outline of the crystallographic investigation of vitamin B12. *Proc Roy Soc A* 242:228-263.

152. van Beelen P, Stassen AP, Bosch JW, Vogels GD, Guijt W, Haasnoot CA. 1984. Elucidation of the structure of methanopterin, a coenzyme from *Methanobacterium thermoautotrophicum*, using two-dimensional nuclear-magnetic-resonance techniques. Eur J Biochem 138:563-571.
153. Eirich LD, Vogels GD, Wolfe RS. 1978. Proposed structure for coenzyme F420 from Methanobacterium. Biochemistry 17:4583-4593.
154. Zayas CL, Claas K, Escalante-Semerena JC. 2007. The CbiB protein of *Salmonella enterica* is an integral membrane protein involved in the last step of the de novo corrin ring biosynthetic pathway. J Bacteriol 189:7697-7708.
155. Woodson JD, Zayas CL, Escalante-Semerena JC. 2003. A new pathway for salvaging the coenzyme B<sub>12</sub> precursor cobinamide in archaea requires cobinamide-phosphate synthase (CbiB) enzyme activity. J Bacteriol 185:7193-7201.
156. Raux E, Lanois A, Levillayer F, Warren MJ, Brody E, Rambach A, Thermes C. 1996. *Salmonella typhimurium* cobalamin (vitamin B<sub>12</sub>) biosynthetic genes: functional studies in *S. typhimurium* and *Escherichia coli*. J Bacteriol 178:753-767.
157. Keller S, Treder A, SH VR, Escalante-Semerena JC, Schubert T. 2016. The SMUL\_1544 gene product governs norcobamide biosynthesis in the tetrachloroethene-respiring bacterium *Sulfurospirillum multivorans*. J Bacteriol 198:2236-2243.
158. Gray MJ, Escalante-Semerena JC. 2009. In vivo analysis of cobinamide salvaging in *Rhodobacter sphaeroides* strain 2.4.1. J Bacteriol 191:3842-3851.
159. Rémy E, Debussche L, Thibaut D. How is aminopropanol biosynthesized in B<sub>12</sub> producing bacteria?, p P-46. In (ed),

160. Fan C, Bobik TA. 2008. The PDUX enzyme of *Salmonella enterica* is an L-threonine kinase used for coenzyme B<sub>12</sub> synthesis. *J Biol Chem* 283:11322-11329.
161. Rodionov DA, Vitreschak AG, Mironov AA, Gelfand MS. 2003. Comparative genomics of the vitamin B<sub>12</sub> metabolism and regulation in prokaryotes. *J Biol Chem* 278:41148-41159.
162. Fan C, Fromm HJ, Bobik TA. 2009. Kinetic and functional analysis of L-threonine kinase, the PduX enzyme of *Salmonella enterica*. *J Biol Chem* 284:20240-20248.
163. Brushaber KR, O'Toole GA, Escalante-Semerena JC. 1998. CobD, a novel enzyme with L-threonine-*O*-3-phosphate decarboxylase activity, is responsible for the synthesis of (*R*)-1-amino-2-propanol *O*-2-phosphate, a proposed new intermediate in cobalamin biosynthesis in *Salmonella typhimurium* LT2. *J Biol Chem* 273:2684-2691.
164. Cheong CG, Bauer CB, Brushaber KR, Escalante-Semerena JC, Rayment I. 2002. Three-dimensional structure of the L-threonine-*O*-3-phosphate decarboxylase (CobD) enzyme from *Salmonella enterica*. *Biochemistry* 41:4798-4808.
165. Cheong CG, Escalante-Semerena JC, Rayment I. 2002. Structural studies of the L-threonine-*O*-3-phosphate decarboxylase (CobD) enzyme from *Salmonella enterica*: the apo, substrate, and product-aldimine complexes. *Biochemistry* 41:9079-9089.
166. Grabau C, Roth JR. 1992. A *Salmonella typhimurium* cobalamin-deficient mutant blocked in 1-amino-2-propanol synthesis. *J Bacteriol* 174:2138-2144.
167. Kräutler B, Fieber W, Osterman S, Fasching M, Ongania K-H, Gruber K, Kratky C, Mikl C, Siebert A, Diekert G. 2003. The cofactor of tetrachloroethene reductive dehalogenase of *Dehalospirillum multivorans* is Norpseudob<sub>12</sub>, a new type of natural corrinoid. *Helv Chim Acta* 86:3698-3716.

168. Ronzio RA, Barker HA. 1967. Enzymic synthesis of guanosine diphosphate cobinamide by extracts of propionic acid bacteria. *Biochemistry* 6:2344-2354.
169. Blanche F, Debussche L, Famechon A, Thibaut D, Cameron B, Crouzet J. 1991. A bifunctional protein from *Pseudomonas denitrificans* carries cobinamide kinase and cobinamide phosphate guanylyltransferase activities. *J Bacteriol* 173:6052-6057.
170. O'Toole GA, Escalante-Semerena JC. 1995. Purification and characterization of the bifunctional CobU enzyme of *Salmonella typhimurium* LT2. Evidence for a CobU-GMP intermediate. *J Biol Chem* 270:23560-23569.
171. Thompson TB, Thomas MG, Escalante-Semerena JC, Rayment I. 1999. Three-dimensional structure of adenosylcobinamide kinase/adenosylcobinamide phosphate guanylyltransferase (CobU) complexed with GMP: evidence for a substrate-induced transferase active site. *Biochemistry* 38:12995-3005.
172. Thompson TB, Thomas MG, Escalante-Semerena JC, Rayment I. 1998. Three-dimensional structure of adenosylcobinamide kinase/adenosylcobinamide phosphate guanylyltransferase from *Salmonella typhimurium* determined to 2.3 Å resolution. *Biochemistry* 37:7686-95.
173. O'Toole GA, Escalante-Semerena JC. 1993. *cobU*-dependent assimilation of nonadenosylated cobinamide in *cobA* mutants of *Salmonella typhimurium*. *J Bacteriol* 175:6328-6336.
174. Thomas MG, Thompson TB, Rayment I, Escalante-Semerena JC. 2000. Analysis of the adenosylcobinamide kinase/adenosylcobinamide-phosphate guanylyltransferase (CobU) enzyme of *Salmonella typhimurium* LT2. Identification of residue His-46 as the site of guanylylation. *J Biol Chem* 275:27576-27586.

175. Thomas MG, Escalante-Semerena JC. 2000. Identification of an alternative nucleoside triphosphate: 5'- deoxyadenosylcobinamide phosphate nucleotidyltransferase in *Methanobacterium thermoautotrophicum* ΔH. J Bacteriol 182:4227-4233.
176. Woodson JD, Peck RF, Krebs MP, Escalante-Semerena JC. 2003. The *cobY* gene of the archaeon *Halobacterium* sp. strain NRC-1 is required for de novo cobamide synthesis. J Bacteriol 185:311-316.
177. Newmister SA, Otte MM, Escalante-Semerena JC, Rayment I. 2011. Structure and mutational analysis of the archaeal GTP:AdoCbi-P guanylyltransferase (CobY) from *Methanocaldococcus jannaschii*: Insights into GTP binding and dimerization. Biochemistry 50:5301-5313.
178. Otte MM, Escalante-Semerena JC. 2009. Biochemical characterization of the GTP:adenosylcobinamide-phosphate guanylyltransferase (CobY) enzyme of the hyperthermophilic archaeon *Methanocaldococcus jannaschii*. Biochemistry 48:5882-5889.
179. Singarapu KK, Otte MM, Tonelli M, Westler WM, Escalante-Semerena JC, Markley JL. 2015. Solution structural studies of GTP:Adenosylcobinamide-phosphate guanylyltransferase (CobY) from *Methanocaldococcus jannaschii*. PLoS One 10:e0141297.
180. Brown K, Pompeo F, Dixon S, Mengin-Lecreulx D, Cambillau C, Bourne Y. 1999. Crystal structure of the bifunctional N-acetylglucosamine 1-phosphate uridyltransferase from *Escherichia coli*: a paradigm for the related pyrophosphorylase superfamily. EMBO J 18:4096-4107.

181. Chan CH, Newmister SA, Talyor K, Claas KR, Rayment I, Escalante-Semerena JC. 2014. Dissecting cobamide diversity through structural and functional analyses of the base-activating CobT enzyme of *Salmonella enterica*. *Biochim Biophys Acta* 1840:464-475.
182. Crofts TS, Seth EC, Hazra AB, Taga ME. 2013. Cobamide structure depends on both lower ligand availability and CobT substrate specificity. *Chem Biol* doi:10.1016/j.chembiol.2013.08.006.
183. Friedmann HC. 1965. Partial purification and properties of a single displacement trans-*N*-glycosidase. *J Biol Chem* 240:413-418.
184. Friedmann HC, Harris DL. 1965. The Formation of alpha-glycosidic 5'-nucleotides by a single displacement trans-*N*-glycosidase. *J Biol Chem* 240:406-412.
185. Trzebiatowski JR, O'Toole GA, Escalante-Semerena JC. 1994. The *cobT* gene of *Salmonella typhimurium* encodes the NaMN: 5,6-dimethylbenzimidazole phosphoribosyltransferase responsible for the synthesis of *N*<sup>1</sup>-(5-phospho-alpha-D-ribose)-5,6-dimethylbenzimidazole, an intermediate in the synthesis of the nucleotide loop of cobalamin. *J Bacteriol* 176:3568-3575.
186. Cameron B, Blanche F, Rouyez MC, Bisch D, Famechon A, Couder M, Cauchois L, Thibaut D, Debussche L, Crouzet J. 1991. Genetic analysis, nucleotide sequence, and products of two *Pseudomonas denitrificans* cob genes encoding nicotinate-nucleotide: dimethylbenzimidazole phosphoribosyltransferase and cobalamin (5'-phosphate) synthase. *J Bacteriol* 173:6066-6073.
187. Friedmann HC, Cagen LM. 1970. Microbial biosynthesis of B12-like compounds. *Annu Rev Microbiol* 24:159-208.

188. Trzebiatowski JR, Escalante-Semerena JC. 1997. Purification and characterization of CobT, the nicotinate-mononucleotide:5,6-dimethylbenzimidazole phosphoribosyltransferase enzyme from *Salmonella typhimurium* LT2. *J Biol Chem* 272:17662-17667.
189. Cheong CG, Escalante-Semerena JC, Rayment I. 2001. Structural investigation of the biosynthesis of alternative lower ligands for cobamides by nicotinate mononucleotide:5,6-dimethylbenzimidazole phosphoribosyltransferase from *Salmonella enterica*. *J Biol Chem* 276:37612-37620.
190. Fyfe JA, Friedmann HC. 1969. Vitamin B<sub>12</sub> biosynthesis. Enzyme studies on the formation of the alpha-glycosidic nucleotide precursor. *J Biol Chem* 244:1659-1666.
191. Cheong CG, Escalante-Semerena JC, Rayment I. 2002. Capture of a labile substrate by expulsion of water molecules from the active site of nicotinate mononucleotide:5,6-dimethylbenzimidazole phosphoribosyltransferase (CobT) from *Salmonella enterica*. *J Biol Chem* 277:41120-7.
192. Claas KR, Parrish JR, Maggio-Hall LA, Escalante-Semerena JC. 2010. Functional analysis of the nicotinate mononucleotide:5,6-dimethylbenzimidazole phosphoribosyltransferase (CobT) enzyme, involved in the late steps of coenzyme B<sub>12</sub> biosynthesis in *Salmonella enterica*. *J Bacteriol* 192:145-154.
193. Cheong CG, Escalante-Semerena JC, Rayment I. 1999. The three-dimensional structures of nicotinate mononucleotide:5,6-dimethylbenzimidazole phosphoribosyltransferase (CobT) from *Salmonella typhimurium* complexed with 5,6-dimethylbenzimidazole and its reaction products determined to 1.9Å resolution. *Biochemistry* 38:16125-16135.

194. Rossmann MG, Argos P. 1975. A comparison of the heme binding pocket in globins and cytochrome b5. *J Biol Chem* 250:7525-7532.
195. Tsang AW, Escalante-Semerena JC. 1998. CobB, a new member of the SIR2 family of eucaryotic regulatory proteins, is required to compensate for the lack of nicotinate mononucleotide:5,6-dimethylbenzimidazole phosphoribosyltransferase activity in *cobT* mutants during cobalamin biosynthesis in *Salmonella typhimurium* LT2. *J Biol Chem* 273:31788-31794.
196. Brachmann CB, Sherman JM, Devine SE, Cameron EE, Pillus L, Boeke JD. 1995. The SIR2 gene family, conserved from bacteria to humans, functions in silencing, cell cycle progression, and chromosome stability. *Genes Dev* 9:2888-2902.
197. Lin SJ, Defossez PA, Guarente L. 2000. Requirement of NAD and SIR2 for life-span extension by calorie restriction in *Saccharomyces cerevisiae*. *Science* 289:2126-2128.
198. Rine J, Herskowitz I. 1987. Four genes responsible for a position effect on expression from HML and HMR in *Saccharomyces cerevisiae*. *Genetics* 116:9-22.
199. Imai S, Johnson FB, Marciniak RA, McVey M, Park PU, Guarente L. 2000. Sir2: an NAD-dependent histone deacetylase that connects chromatin silencing, metabolism, and aging. *Cold Spring Harb Symp Quant Biol*, 65:297-302.
200. Smith JS, Brachmann CB, Celic I, Kenna MA, Muhammad S, Starai VJ, Avalos JL, Escalante-Semerena JC, Grubmeyer C, Wolberger C, Boeke JD. 2000. A phylogenetically conserved NAD(+)-dependent protein deacetylase activity in the Sir2 protein family. *Proc Natl Acad Sci U S A* 97:6658-6663.

201. Starai VJ, Celic I, Cole RN, Boeke JD, Escalante-Semerena JC. 2002. Sir2-dependent activation of acetyl-CoA synthetase by deacetylation of active lysine. *Science* 298:2390-2392.
202. Tanner KG, Landry J, Sternglanz R, Denu JM. 2000. Silent information regulator family of NAD-dependent histone/protein deacetylases generates a unique product, 1-*O*-acetyl-ADP-ribose. *Proc Natl Acad Sci U S A* 97:14178-14182.
203. Frye RA. 1999. Characterization of five human cDNAs with homology to the yeast SIR2 gene: Sir2-like proteins (sirtuins) metabolize NAD and may have protein ADP-ribosyltransferase activity. *Biochem Biophys Res Commun* 260:273-279.
204. Tanny JC, Dowd GJ, Huang J, Hilz H, Moazed D. 1999. An enzymatic activity in the yeast Sir2 protein that is essential for gene silencing. *Cell* 99:735-745.
205. Maggio-Hall LA, Escalante-Semerena JC. 2003. Alpha-5,6-Dimethylbenzimidazole adenine dinucleotide (alpha-DAD), a putative new intermediate of coenzyme B12 biosynthesis in *Salmonella typhimurium*. *Microbiology* 149:983-990.
206. Bochner BR, Ames BN. 1982. Complete analysis of cellular nucleotides by two-dimensional thin layer chromatography. *J Biol Chem* 257:9759-9769.
207. Hazra AB, Tran JL, Crofts TS, Taga ME. 2013. Analysis of substrate specificity in CobT homologs reveals widespread preference for DMB, the Lower axial ligand of vitamin B12. *Chem Biol* doi:10.1016/j.chembiol.2013.08.007.
208. Friedmann HC, Fyfe JA. 1969. Pseudovitamin B<sub>12</sub> biosynthesis. Enzymatic formation of a new adenylic acid, 7- $\alpha$ -D-ribofuranosyladenine 5'-phosphate. *J Biol Chem* 244:1667-1671.

209. Anderson PJ, Lango J, Carkeet C, Britten A, Kräutler B, Hammock BD, Roth JR. 2008. One pathway can incorporate either adenine or dimethylbenzimidazole as an alpha-axial ligand of B<sub>12</sub> cofactors in *Salmonella enterica*. *J Bacteriol* 190:1160-1171.
210. Keck B, Renz P. 2000. *Salmonella typhimurium* forms adenylobamide and 2-methyladenylobamide, but no detectable cobalamin during strictly anaerobic growth. *Arch Microbiol* 173:76-77.
211. Mok KC, Taga ME. 2013. Growth inhibition of *Sporomusa ovata* by incorporation of benzimidazole bases into cobamides. *J Bacteriol* 195:1902-1911.
212. Keller S, Ruetz M, Kunze C, Krautler B, Diekert G, Schubert T. 2014. Exogenous 5,6-dimethylbenzimidazole caused production of a non-functional tetrachloroethene reductive dehalogenase in *Sulfurospirillum multivorans*. *Environ Microbiol* 16:3361-3369.
213. Crofts TS, Hazra AB, Tran JL, Sokolovskaya OM, Osadchiy V, Ad O, Pelton J, Bauer S, Taga ME. 2014. Regiospecific formation of cobamide isomers is directed by CobT. *Biochemistry* 53:7805-7815.
214. Degnan PH, Barry NA, Mok KC, Taga ME, Goodman AL. 2014. Human gut microbes use multiple transporters to distinguish vitamin B12 analogs and compete in the gut. *Cell Host Microbe* 15:47-57.
215. Seth EC, Taga ME. 2014. Nutrient cross-feeding in the microbial world. *Front Microbiol* 5:350.
216. Renz P. 1999. Biosynthesis of the 5,6-dimethylbenzimidazole moiety of cobalamin and of other bases found in natural corrinoids, p 557-575. *In* Banerjee R (ed), *Chemistry and Biochemistry of B12*. John Wiley & Sons, Inc., New York.

217. Chan CH, Escalante-Semerena JC. 2011. ArsAB, a novel enzyme from *Sporomusa ovata* activates phenolic bases for adenosylcobamide biosynthesis. *Mol Microbiol* 81:952-967.
218. Newmister SA, Chan CH, Escalante-Semerena JC, Rayment I. 2012. Structural insights into the function of the nicotinate mononucleotide:phenol/p-cresol phosphoribosyltransferase (ArsAB) enzyme from *Sporomusa ovata*. *Biochemistry* 51:8571-8582.
219. Gray MJ, Escalante-Semerena JC. 2010. A new pathway for the synthesis of alpha-ribazole-phosphate in *Listeria innocua*. *Mol Microbiol* 77:1429-1438.
220. Johnson WM, Kido Soule MC, Kujawinski EB. 2016. Evidence for quorum sensing and differential metabolite production by a marine bacterium in response to DMSP. *ISME J* doi:10.1038/ismej.2016.6.
221. Durham BP, Sharma S, Luo H, Smith CB, Amin SA, Bender SJ, Dearth SP, Van Mooy BA, Campagna SR, Kujawinski EB, Armbrust EV, Moran MA. 2015. Cryptic carbon and sulfur cycling between surface ocean plankton. *Proc Natl Acad Sci U S A* 112:453-457.
222. Maggio-Hall LA, Claas KR, Escalante-Semerena JC. 2004. The last step in coenzyme B(12) synthesis is localized to the cell membrane in bacteria and archaea. *Microbiology* 150:1385-1395.
223. Maggio-Hall LA, Escalante-Semerena JC. 1999. In vitro synthesis of the nucleotide loop of cobalamin by *Salmonella typhimurium* enzymes. *Proc Natl Acad Sci U S A* 96:11798-11803.
224. Zayas CL, Escalante-Semerena JC. 2007. Reassessment of the late steps of coenzyme B<sub>12</sub> synthesis in *Salmonella enterica*: Evidence that dephosphorylation of

- adenosylcobalamin-5'-phosphate by the CobC phosphatase is the last step of the pathway. J Bacteriol 189:2210-2218.
225. Kobayashi R, Suzuki T, Yoshida M. 2007. *Escherichia coli* phage-shock protein A (PspA) binds to membrane phospholipids and repairs proton leakage of the damaged membranes. Mol Microbiol 66:100-109.
226. Jovanovic G, Lloyd LJ, Stumpf MP, Mayhew AJ, Buck M. 2006. Induction and function of the phage shock protein extracytoplasmic stress response in *Escherichia coli*. J Biol Chem 281:21147-21161.
227. Darwin AJ. 2005. The phage-shock-protein response. Mol Microbiol 57:621-628.
228. Model P, Jovanovic G, Dworkin J. 1997. The *Escherichia coli* phage-shock-protein (psp) operon. Mol Microbiol 24:255-261.
229. Kang Z, Zhang J, Zhou J, Qi Q, Du G, Chen J. 2012. Recent advances in microbial production of delta-aminolevulinic acid and vitamin B12. Biotechnol Adv 30:1533-1542.
230. O'Toole GA, Trzebiatowski JR, Escalante-Semerena JC. 1994. The *cobC* gene of *Salmonella typhimurium* codes for a novel phosphatase involved in the assembly of the nucleotide loop of cobalamin. J Biol Chem 269:26503-26511.
231. Schneider Z, Friedmann HC. 1972. Studies on the enzymatic dephosphorylation of vitamin B12 5'-phosphate. Arch Biochem Biophys 152:488-495.
232. Zayas CL, Woodson JD, Escalante-Semerena JC. 2006. The *cobZ* gene of *Methanosarcina mazei* Gö1 encodes the nonorthologous replacement of the  $\alpha$ -ribazole-5'-phosphate phosphatase (CobC) enzyme of *Salmonella enterica*. J Bacteriol 188:2740-2743.

233. Otte MM, Woodson JD, Escalante-Semerena JC. 2007. The thiamine kinase (YcfN) enzyme plays a minor but significant role in cobinamide salvaging in *Salmonella enterica*. *J Bacteriol* 189:7310-7315.
234. Woodson JD, Escalante-Semerena JC. 2004. CbiZ, an amidohydrolase enzyme required for salvaging the coenzyme B<sub>12</sub> precursor cobinamide in archaea. *Proc Natl Acad Sci USA* 101:3591-3596.
235. Gray MJ, Tavares NK, Escalante-Semerena JC. 2008. The genome of *Rhodobacter sphaeroides* strain 2.4.1 encodes functional cobinamide salvaging systems of archaeal and bacterial origins. *Mol Microbiol* 70:824-836.
236. Gray MJ, Escalante-Semerena JC. 2009. The cobinamide amidohydrolase (cobyric acid-forming) CbiZ enzyme: a critical activity of the cobamide remodelling system of *Rhodobacter sphaeroides*. *Mol Microbiol* 74:1198-1210.
237. Alber BE, Spanheimer R, Ebenau-Jehle C, Fuchs G. 2006. Study of an alternate glyoxylate cycle for acetate assimilation by *Rhodobacter sphaeroides*. *Mol Microbiol* 61:297-309.
238. Hollriegel V, Lamm L, Rowold J, Horig J, Renz P. 1982. Biosynthesis of vitamin B<sub>12</sub>. Different pathways in some aerobic and anaerobic microorganisms. *Arch Microbiol* 132:155-158.
239. Renz P. 1970. Riboflavin as precursor in the biosynthesis of 5,6-dimethylbenzimidazole moiety of vitamin B<sub>12</sub>. *FEBS Lett* 6:187-189.
240. Gray MJ, Escalante-Semerena JC. 2007. Single-enzyme conversion of FMNH<sub>2</sub> to 5,6-dimethylbenzimidazole, the lower ligand of B<sub>12</sub>. *Proc Natl Acad Sci U S A* 104:2921-2926.

241. Taga ME, Larsen NA, Howard-Jones AR, Walsh CT, Walker GC. 2007. BluB cannibalizes flavin to form the lower ligand of vitamin B12. *Nature* 446:449-453.
242. Campbell GR, Taga ME, Mistry K, Lloret J, Anderson PJ, Roth JR, Walker GC. 2006. *Sinorhizobium meliloti bluB* is necessary for production of 5,6-dimethylbenzimidazole, the lower ligand of B12. *Proc Natl Acad Sci U S A* 103:4634-4369.
243. Maggio-Hall LA, Dorrestein PC, Escalante-Semerena JC, Begley TP. 2003. Formation of the dimethylbenzimidazole ligand of coenzyme B12 under physiological conditions by a facile oxidative cascade. *Org Lett* 5:2211-2213.
244. Renz P, Weyhenmeyer R. 1972. Biosynthesis of the 5,6-dimethylbenzimidazole from riboflavin. Transformation of C-1' of riboflavin into C-2 of 5,6-dimethylbenzimidazole. *FEBS Lett* 22:124-126.
245. Horig JA, Renz P, Heckmann G. 1978. [5-15N]Riboflavin as precursor in the biosynthesis of the 5,6- dimethylbenzimidazole moiety of vitamin B12. A study by 1H and 15N magnetic resonance spectroscopy. *J Biol Chem* 253:7410-7414.
246. Horig JA, Renz P. 1980. Biosynthesis of vitamin B12. Some properties of the 5,6-dimethylbenzimidazole-forming system of *Propionibacterium freudenreichii* and *Propionibacterium shermanii*. *Eur J Biochem* 105:587-592.
247. Keck B, Munder M, Renz P. 1998. Biosynthesis of cobalamin in *Salmonella typhimurium*: transformation of riboflavin into the 5,6-dimethylbenzimidazole moiety. *Arch Microbiol* 171:66-68.
248. Wang XL, Quan JM. 2011. Intermediate-assisted multifunctional catalysis in the conversion of flavin to 5,6-dimethylbenzimidazole by BluB: A density functional theory study. *J Am Chem Soc* 133:4079-4091.

249. Renz P, Wurm R, Horig J. 1977. Nonenzymatic transformation of riboflavin into 5,6-dimethylbenzimidazole. *Z Naturforsch C* 32:523-527.
250. Lamm L, Heckmann G, Renz P. 1982. Biosynthesis of vitamin B12 in anaerobic bacteria. Mode of incorporation of glycine into the 5,6-dimethylbenzimidazole moiety in *Eubacterium limosum*. *Eur J Biochem* 122:569-571.
251. Vogt JRA, Renz P. 1988. Biosynthesis of vitamin B-12 in anaerobic bacteria. Experiments with *Eubacterium limosum* on the origin of the amide groups of the corrin ring and of N-3 of the 5,6-dimethylbenzimidazole part. *Eur J Biochem* 171:655-659.
252. Munder M, Vogt JR, Vogler B, Renz P. 1992. Biosynthesis of vitamin B12 in anaerobic bacteria. Experiments with *Eubacterium limosum* on the incorporation of D-[1-<sup>13</sup>C]erythrose and [<sup>13</sup>C]formate into the 5,6-dimethylbenzimidazole moiety. *Eur J Biochem* 204:679-683.
253. Mehta AP, Abdelwahed SH, Fenwick MK, Hazra AB, Taga ME, Zhang Y, Ealick SE, Begley TP. 2015. Anaerobic 5-Hydroxybenzimidazole formation from aminoimidazole ribotide: an unanticipated intersection of thiamin and vitamin B12 biosynthesis. *J Am Chem Soc* doi:10.1021/jacs.5b03576.
254. Vogt JR, Lamm-Kolonko L, Renz P. 1988. Biosynthesis of vitamin B-12 in anaerobic bacteria. Experiments with *Eubacterium limosum* and D-erythrose <sup>14</sup>C-labeled in different positions. *Eur J Biochem* 174:637-640.
255. Hazra AB, Han AW, Mehta AP, Mok KC, Osadchiy V, Begley TP, Taga ME. 2015. Anaerobic biosynthesis of the lower ligand of vitamin B12. *Proc Natl Acad Sci U S A* 112:10792-10797.

256. Lamm L, Horig JA, Renz P, Heckmann G. 1980. Biosynthesis of vitamin B12. Experiments with the anaerobe *Eubacterium limosum* and some labelled substrates. *Eur J Biochem* 109:115-118.
257. Kräutler B, Kohler HP, Stupperich E. 1988. 5'-Methylbenzimidazolyl-cobamides are the corrinoids from some sulfate-reducing and sulfur-metabolizing bacteria. *Eur J Biochem* 176:461-469.
258. Stupperich E, Eisinger HJ, Kräutler B. 1988. Diversity of corrinoids in acetogenic bacteria. *p*-Cresolylcobamide from *Sporomusa ovata*, 5-methoxy-6-methylbenzimidazolylcobamide from *Clostridium formicoaceticum* and vitamin B12 from *Acetobacterium woodii*. *Eur J Biochem* 172:459-464.

## CHAPTER 3

*SALMONELLA ENTERICA* SYNTHESIZES 5,6-DIMETHYLBENZIMIDAZOYL-(DMB)- $\alpha$ -  
RIBOSIDE. WHY SOME *FIRMICUTES* DO NOT REQUIRE THE CANONICAL DMB  
ACTIVATION SYSTEM TO SYNTHESIZE ADENOSYLCOBALAMIN<sup>2</sup>

---

<sup>2</sup> Mattes, T.A. and J. C. Escalante-Semerena. 2016. *Molecular Microbiology*. Accepted.  
Reprinted with permission from the publisher.

## ABSTRACT

5,6-Dimethylbenzimidazolyl-(DMB)- $\alpha$ -ribose, a.k.a.  $\alpha$ -ribazole-5'-phosphate ( $\alpha$ -RP) is an intermediate in the biosynthesis of adenosylcobalamin (AdoCbl) in many prokaryotes. In such microbes,  $\alpha$ -RP is synthesized by nicotinate mononucleotide (NaMN):DMB phosphoribosyltransferases (CobT in *S. enterica*), in a reaction that is considered to be the canonical step for the activation of the base of the nucleotide present in adenosylcobamides. Some *Firmicutes* lack CobT-type enzymes, but have a two-protein system comprised of a transporter (*i.e.*, CblT) and a kinase (*i.e.*, CblS) that can salvage exogenous  $\alpha$ -ribazole ( $\alpha$ -R) from the environment using CblT to take up  $\alpha$ -R, followed by  $\alpha$ -R phosphorylation by CblS. We report that the CblT and CblS proteins from *Geobacillus kaustophilus* restore  $\alpha$ -RP synthesis in *S. enterica* lacking the DMB-activating CobT enzyme. We also show that a *S. enterica cobT* strain that synthesizes *GkCblS* ectopically makes only AdoCbl, even under growth conditions where the synthesis of pseudoCbl is favored. Our results indicate that *S. enterica* synthesizes  $\alpha$ -R, a metabolite that had not been detected in this bacterium, and that *GkCblS* has a strong preference for DMB-ribose over adenine-ribose as substrate. We propose that in some *Firmicutes* DMB is activated to  $\alpha$ -RP via  $\alpha$ -R using an as-yet-unknown route to convert DMB to  $\alpha$ -R, and CblS to convert  $\alpha$ -R to  $\alpha$ -RP.

## INTRODUCTION

Cobamides (Cbas) are cobalt containing cyclic tetrapyrroles. In these structurally complex molecules the pyrrolic N atoms of the ring (a.k.a. the corrin ring) chelate the cobalt ion. In addition to these equatorial ligands, the cobalt ion interacts with two axial ligands (a.k.a. upper, lower ligands). The lower ligand of cobamides is tethered to the ring through a structure known as the nucleotide loop (Figure 3-1A). Cobamides differ from each other by the nature of the base of the nucleotide loop, which can range from purines, purine analogues, or phenolics (1). The best-studied cobamide is cobalamin (Cbl), which contains 5,6-dimethylbenzimidazole (DMB) as its lower ligand base. In its coenzymic form, the upper ligand of Cbl is 5-'deoxyadenosine (AdoCbl, Figure 3-1A).

*Salmonella enterica* sv Typhimurium strain LT2 (hereafter *S. enterica*) synthesizes the corrin ring *de novo* only under anoxic conditions (2, 3); for a review see (4). This bacterium incorporates different ligand bases as a function of oxygen in the environment. Under microaerophilic conditions, *S. enterica* synthesizes AdoCbl, but under anoxic conditions *S. enterica* incorporates adenine or 2-methyladenine into the final product of the pathway (5). The cobamide containing adenine as the lower ligand base is known as pseudoCbl (6).

Notably, under normoxic conditions and in the presence of precursors including a complete corrin ring *S. enterica* can assemble the nucleotide loop *de novo* via a branch of the pathway known as the nucleotide loop assembly (NLA) pathway. (7). Four enzymes catalyze the NLA pathway (Figure 3-1): CobU activates the incomplete corrinoid at the expense of GTP; CobT activates the lower ligand base at the expense of nicotinate mononucleotide (NaMN); CobS joins the activated ring and base; and the last enzyme, CobC, dephosphorylates the molecule yielding the final product. When *S. enterica* uses exogenous incomplete corrinoids such as cobinamide to make

AdoCbl, the latter needs to be adenosylated before CobU can use it. CobA, the housekeeping adenosyltransferase, adenosylates cobinamide.

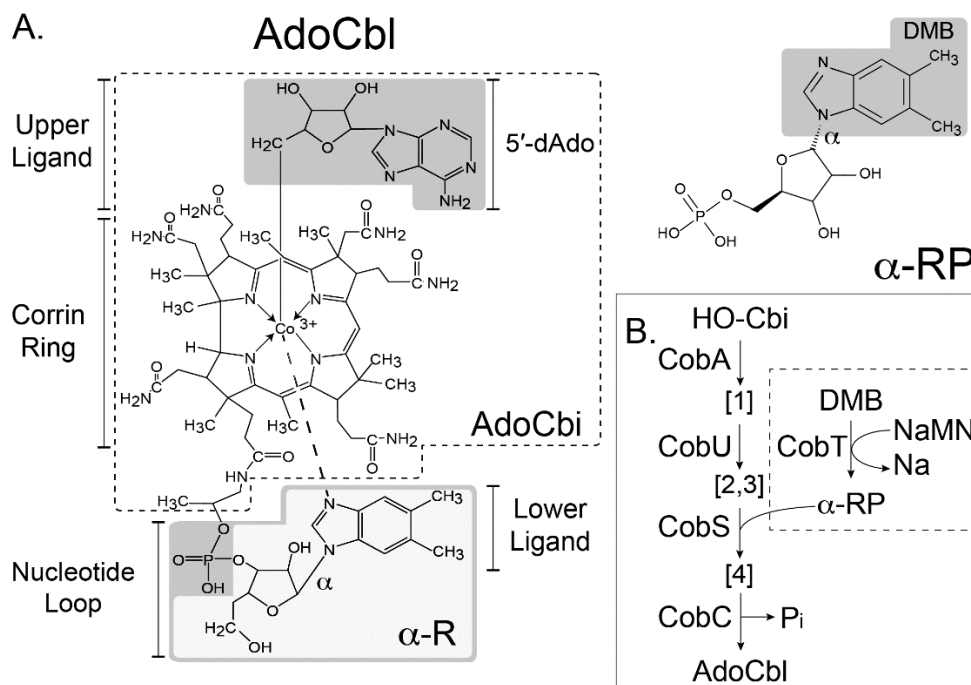


**Figure 3-1. Late steps in AdoCbl biosynthesis.** A. Structures relevant to this study. Adenosylcobalamin, AdoCbl; 5,6-dimethylbenzimidazole, DMB;  $\alpha$ -ribazole-5'-phosphate,  $\alpha$ -RP. B. Activation of DMB in *S. enterica* and its incorporation into AdoCbl. In *S. enterica*, DMB and other purines and purine analogues, are activated to the corresponding  $\alpha$ -ribotide by the NaMN:DMB phosphoribosyltransferase CobT. Abbreviations: NaMN, nicotinate mononucleotide; Na, nicotinate; HO-Cbi, hydroxocobinamide; CobA, ATP:Co(I)rrinoid adenosyltransferase; CobU, NTP:Ado-cobinamide kinase / NTP:Ado-cobinamide-phosphate guanylyltransferase; CobS, AdoCbl-5' phosphate synthase; CobC, Ado-Cba-P phosphatase. Biosynthetic intermediates are generated in the following order: [1], AdoCbi; [2], AdoCbi-P; [3], AdoCbi-GDP; [4], AdoCbl-5'-P.

We are interested in the synthesis and activation of DMB in this bacterium (Figure 3-1A, shaded, upper right). The biosynthesis of DMB has been described in other organisms. For example, in *Eubacterium limosum*, DMB synthesis proceeds through a five-enzyme pathway starting from 5'-aminoimidazole ribotide (AIR), the central branch point of thiamine and purine biosynthesis (8) by an enzyme homologous to the HMP-P synthase (ThiC) (9, 10). In *Rhodobacter sphaeroides* and other organisms, DMB synthesis proceeds through a single-enzyme conversion of reduced flavin mononucleotide (11-13). To date, neither mechanism has been identified in *S. enterica*, although a report in the literature suggests that riboflavin may be a precursor to DMB in this bacterium (14).

In *S. enterica*, DMB is activated in one step to its ribotide form (Figure 3-1B). This reaction is catalyzed by the nicotinate mononucleotide (NaMN):DMB phosphoribosyltransferase CobT enzyme (15), which transfers the ribosyl-5'-phosphate moiety from NaMN to DMB, releasing the activated  $\alpha$ -ribotide,  $\alpha$ -ribazole-phosphate (hereafter  $\alpha$ -RP) and nicotinate (Figure 3-1A). CobT-like enzymes are wide spread amongst AdoCba producers (16).

The *S. enterica* CobT enzyme can activate a wide variety of substrates including adenine (17). Homologues of the *SeCobT* enzyme in the acetogenic bacterium *Sporomusa ovata* can also activate phenolic bases such as *p*-cresol and phenol (1, 18).

The lack of substrate specificity of the *S. enterica* CobT enzyme poses a problem for the studies of DMB biosynthesis in this bacterium. Notably, to date true DMB auxotrophs of *S. enterica* have not been isolated. *S. enterica*  $\Delta cobT$  strains require exogenous DMB to grow, but this requirement is not due to a block in DMB biosynthesis but to the presence of an alternative enzyme (15). The NAD<sup>+</sup>-dependent CobB sirtuin can substitute for CobT in the activation of DMB (19), further complicating the analysis of DMB biosynthesis in this bacterium.

In *Listeria innocua*, we identified a pair of proteins that are responsible for the transport and conversion of the DMB riboside ( $\alpha$ -R) to its  $\alpha$ -ribotide ( $\alpha$ -RP) (20). The above-mentioned *L. innocua* proteins are known as *LinCblT* (a transporter), and *LinCblS* (a kinase). Notably, the *LinCblTS* proteins showed specificity for  $\alpha$ -R, but it required  $\alpha$ -R to be provided exogenously (20). Here, we report the identification of homologues of *LinCblT* and *LinCblS* in *Geobacillus kaustophilus*, which support Cbl-dependent growth of a *S. enterica*  $\Delta cobT$  strain without the addition of  $\alpha$ -R, opening the doors for the use of genetic approaches for the analysis of DMB synthesis, and its activation to  $\alpha$ -R.

## RESULTS

### ***Geobacillus kaustophilus* CblT and CblS restore cobamide-dependent methionine synthesis in *S. enterica* in the absence of exogenous $\alpha$ -R**

Efforts aimed at validating the function of CblS and CblT homologues in *Firmicutes* led us to a pair of proteins from the deep-sea thermophile *Geobacillus kaustophilus*, namely GK2255 (hereafter *GkCblS*) and GK2256 (hereafter *GkCblT*). We used Clustal Omega (21) to compare the sequence of these proteins. Using this approach we determined that the *GkCblT* and *GkCblS* proteins were 45% and 51% similar, respectively, to the *L. innocua* counterparts (Figure A-1B and A-1C). In *G. kaustophilus*, the *cblS* and *cblT* genes are located within the *cob* operon of *G. kaustophilus* (Figure A-1A), suggesting that in this bacterium, the CblS and CblT proteins participate in AdoCbl biosynthesis.

### **Assessing the functionality of *G. kaustophilus* CblTS proteins in *S. enterica***

To determine whether or not *GkCblS* and *GkCblT* were functional, the *G. kaustophilus* *cblT*<sup>+</sup> and *cblS*<sup>+</sup> alleles were placed under the control of the arabinose-inducible *P<sub>araBAD</sub>* promoter of plasmid pBAD24 (22). The resulting plasmid (p*GkCblTS2*) was transformed into JE12939 (*cobT*

*cobB*), which lacked the two enzymes (CobT, CobB) known to activate lower ligand bases into their corresponding  $\alpha$ -ribotides (15, 19). Strain JE12939 also lacked the cobamide-independent methionine synthase MetE enzyme, resulting in a methionine auxotrophy that, under normoxic conditions, could be corrected by cobamides or methionine (23). In the absence of methionine, the strain uses the cobamide-dependent methionine synthase MetH enzyme to methylate homocysteine yielding methionine (23); the *metE cobT cobB* / pGkCbITS2 strain is hereafter referred to as JE17830. A negative control strain (JE17827) had the same genetic background but carried the empty cloning vector pBAD24. A positive control strain (JE17828) harboring a plasmid encoding the wild-type CobT protein was also constructed.

The above-mentioned strains were used in experiments aimed at assessing  $\alpha$ -RP synthesis *in vivo* and whether *GkCbIT*, *GkCbIS* or both were needed. For this purpose, strains were grown under normoxic conditions at 37°C. In all experiments described below, minimal NCE medium was supplemented with (CN)<sub>2</sub>Cbi as a precursor of AdoCbl. We supplemented the culture medium with (CN)<sub>2</sub>Cbi because under normoxic conditions *S. enterica* does not synthesize the corrin ring (2, 23), due to the lack of activation of the adenosylcobinamide-phosphate (AdoCbi-P) biosynthetic genes (3). In *S. enterica*, the conversion of (CN)<sub>2</sub>Cbi into AdoCbl requires the synthesis of  $\alpha$ -RP by *SeCobT*.

*i) GkCbITS compensate for the absence of CobT in the presence of high concentrations of cobinamide and the absence of exogenous  $\alpha$ -R.*

In the first experiment, the medium was supplemented with (CN)<sub>2</sub>Cbi (5 nM) but not with  $\alpha$ -R. Under these conditions strain JE17827 carrying the cloning vector failed to grow (Figure 3-2A, triangles) and required the addition of CNCbl to grow (Figure 3-2A, diamonds), the strain

carrying plasmids encoding  $\text{cobT}^+$  (Figure 3-2A, squares) or  $\text{cblTS}^+$  (Figure 3-2A, circles) exhibited robust growth.

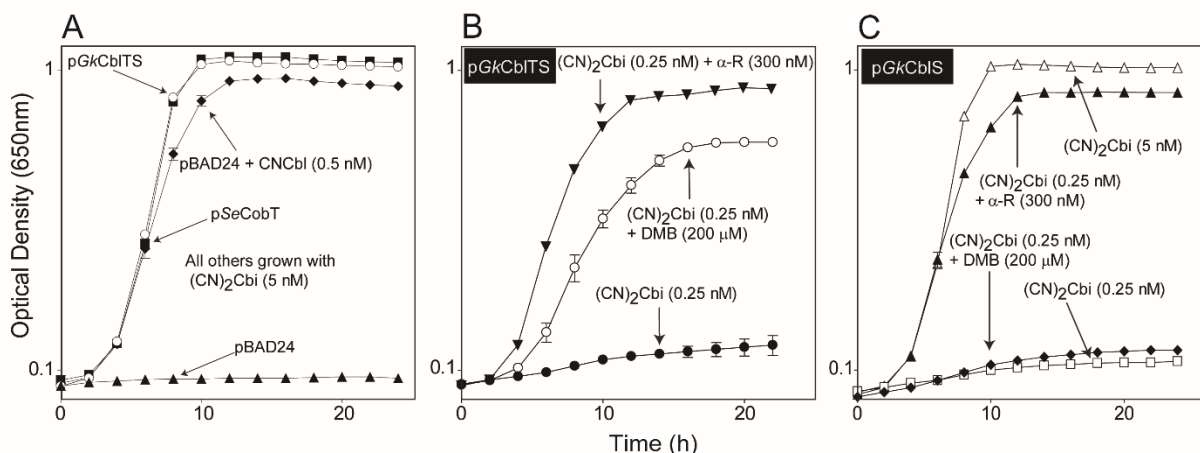
ii) *At low concentrations of cobinamide GkCblTS compensate for the absence of CobT only if DMB or  $\alpha$ -RP is provided.*

It has been reported that the activity of the AdoCbl-5'-P synthase CobS enzyme of *S. enterica* increases when the enzyme is saturated with either AdoCbi-GDP or  $\alpha$ -RP (24). With this in mind, we decreased the concentration of  $(\text{CN})_2\text{Cbi}$  to determine whether the addition of DMB would stimulate  $\alpha$ -R synthesis, hence growth. Strain JE17830 was grown as above, except that the concentration of cobinamide in the medium was reduced to 0.25 nM. (a 200-fold reduction). At this cobinamide concentration, strain JE17830 failed to grow (Figure 3-2B, solid circles). In contrast, the addition of DMB (200  $\mu\text{M}$ ) or  $\alpha$ -R (300 nM) restored growth (Figure 3-2B, open circles, black triangles, respectively). These data suggested that DMB synthesis or scavenging was the limiting factor in the synthesis of  $\alpha$ -RP in strain JE17830 under the conditions tested.

iii) *GkCblT is not required for the conversion of DMB to  $\alpha$ -R.*

These of the experiments described in section ii) above did not inform on whether or not CblT function ( $\alpha$ -R transporter) was needed for the conversion of DMB to  $\alpha$ -R. To address the latter question, a strain carrying a plasmid encoding *GkCblS* under  $P_{\text{araBAD}}$  control was constructed and grown under limited concentration of cobinamide (0.25 nM) with or without  $\alpha$ -R or DMB supplementation, or with excess cobinamide (5nM). As shown in figure 2C, when the concentration of cobinamide was limiting and neither DMB nor  $\alpha$ -R was present in the medium, strain JE21364 ( $\Delta\text{metE ara-9 } \Delta\text{cobT } \Delta\text{cobB} / \text{pGkCblS}$ ) did not grow (Figure 3-2C, squares). Strain JE21364 failed to respond to the presence of DMB (Figure 3-2C, diamonds), but did respond to the presence of  $\alpha$ -R (Figure 3-2C, solid triangles). In addition, when the concentration of

cobinamide was increased 200 fold (to 5 nM) without  $\alpha$ -R supplementation, the strain grew fast and to high density with a minimal lag time (Figure 3-2C, open triangles). Our interpretation of these is discussed below.



(Author's Note: Figure re-formatted for this work.)

**Figure 3-2. *GkCbIS* is necessary and sufficient for incorporation of endogenously generated  $\alpha$ -R into AdoCba.** Four strains were used in these experiments, all of which had the following chromosomal mutations:  $\Delta metE$   $ara-9$   $\Delta cobT$   $\Delta cobB$ . The difference among strains was the plasmid they harbored. JE17827 (pBAD24), JE17828 (pSeCobT), JE17830 (pGkCbITS), and JE21364 (pGkCbIS). A. Growth behavior of strains JE17827, JE17828, and JE17830 under conditions of excess cobinamide (5 nM) in the medium. B. Growth behavior of strain JE17830 under conditions of limiting cobinamide in the medium (0.25 nM). When added to the medium DMB and  $\alpha$ -R were present at the indicated concentrations. C. Growth behavior of strain JE21364 under limiting cobinamide conditions (0.25 nM). When added to the medium, DMB and  $\alpha$ -R were present at the indicated concentrations. These results are representative of six biological replicates each one of which was performed in technical duplicates.

### ***G. kaustophilus* CblS is an $\alpha$ -ribazole kinase**

The similarity of *GkCblS* to *L. innocua* CblS (Figure A-1) suggested that *GkCblS* had  $\alpha$ -R kinase activity. To investigate this possibility, *G. kaustophilus cblS*<sup>+</sup> was cloned into vector pTEV5 (25) and over-produced as a hexahistidine-tagged fusion protein in strain JE13607 (*E. coli* BL21( $\lambda$ DE3) *cobT762::kan*<sup>+</sup>). The protein was purified by nickel-affinity chromatography; the His<sub>6</sub> tag was not removed. Elution of the tagged protein from the column resulted in highly enriched His<sub>6</sub>-*GkCblS* around approximately 28.5 kDa (Figure 3-3, lane 6), consistent with the expected molecular mass of *GkCblS* (25.5 kDa).

The purified protein was tested for  $\alpha$ -R kinase and NaMN::DMB phosphoribosyltransferase (CobT) activity. To test for  $\alpha$ -R kinase activity, protein (3  $\mu$ g) was added to a reaction mixture containing HEPES (50 mM, pH 7.4), MgCl<sub>2</sub> (5 mM), KCl (750 mM), TCEP (5 mM), ATP (0.5 mM), and  $\alpha$ -R (0.25 mM). The reaction was incubated for 3 h at 37 °C. As a negative control, a reaction mixture devoid of protein was incubated under the same conditions. The products of the reactions were separated by RP-HPLC on a C18 column as described under *Experimental procedures*. The addition of *GkCblS* resulted in the loss of the  $\alpha$ -R peak (Figure 3-4A, 10.2 min) and formation of a new peak (Figure 3-4B, 8.9 min). To verify the identity of this peak, DMB and NaMN were incubated with purified *SeCobT* to generate  $\alpha$ -RP, and the reaction products were separated by RP-HPLC using the same conditions. Addition of *SeCobT* resulted in the loss of the DMB peak (Figure 3-4C, 11 min) and the formation of the expected product  $\alpha$ -RP peak (Figure 3-4D, 8.5 min). The UV-spectra and retention times were similar to those observed in Figure 3-4B, indicating that the product of *GkCblS* was  $\alpha$ -RP. An observed shift in the retention time for  $\alpha$ -RP (8.5 min to 8.9 min) between the *SeCobT* and the  $\alpha$ -R kinase results was likely due to a difference in the pH of the CobT reaction mixture (10 vs 7.4). The UV-vis spectrum of the compound eluting

8.5 min post injection was similar to the spectrum of the compound eluting 8.9 min post injection. In a parallel experiment, DMB and NaMN were incubated with *GkCbIS*, but no  $\alpha$ -RP formation was detected (data not shown).

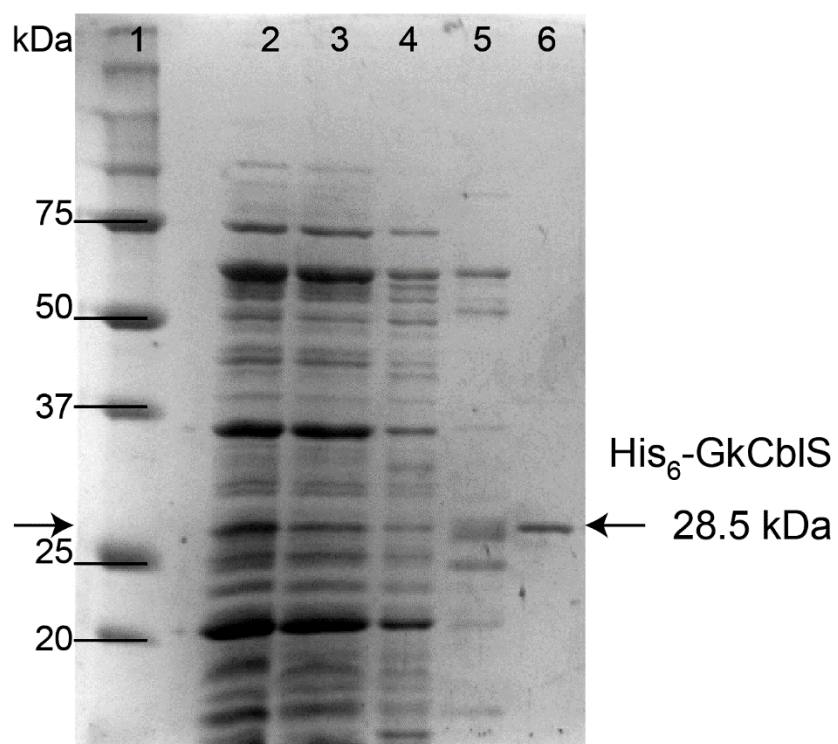
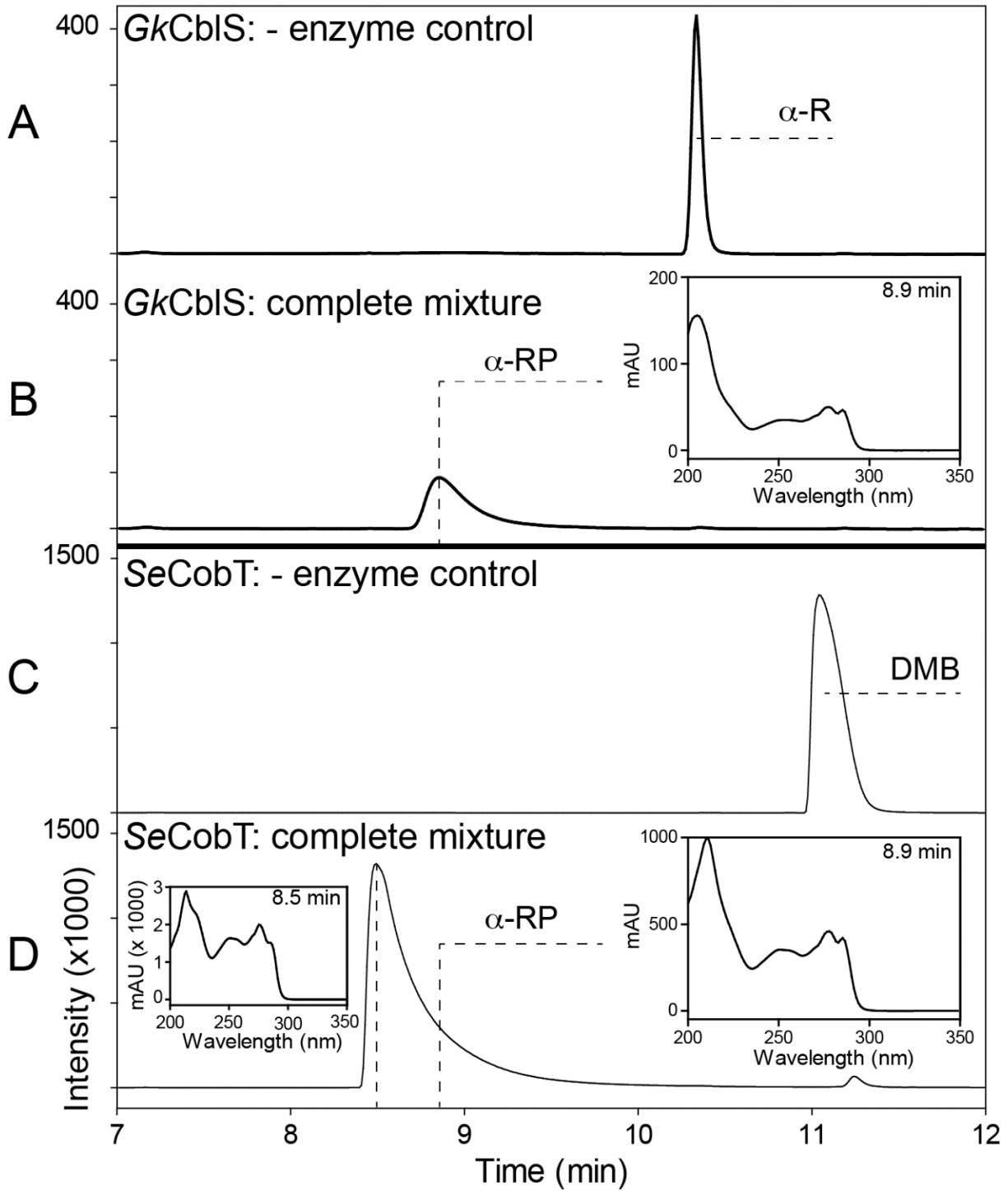


**Figure 3-3. Purified His<sub>6</sub>-GkCbIS.** Lanes, left to right: 1, Molecular mass markers; 2, crude cell-free extract; 3, column flow through; 4, bind buffer eluate (10 mM imidazole); 5, wash buffer eluate (150 mM imidazole); 6, elution buffer eluate [imidazole (750 mM), TCEP (5 mM), glycerol (5%, v/v)]. Molecular mass of His<sub>6</sub>-GkCbIS (28.5 kDa) calculated from its primary sequence.

**Figure 3-4. *GkCblS* converts  $\alpha$ -R to  $\alpha$ -RP at the expense of ATP.** *In vitro* assay conditions and the RP-HPLC protocol are described in the *Experimental procedures* section. The addition of purified *GkCblS* to a reaction mixture containing  $\alpha$ -R (A) and ATP gave rise to a peak at 8.9 min (B). The UV-spectrum of the compound generating the signal is shown in the inset. The identity of this peak was confirmed to be  $\alpha$ -RP by using the *SeCobT* phosphoribosyltransferase reaction as a control. *SeCobT* synthesizes  $\alpha$ -RP from DMB and NaMN (15, 26, 39). The retention time of *SeCobT*-derived  $\alpha$ -RP (panel D) was the same as that of the *GkCblS* reaction product (B). The UV-spectra of each product are shown in the insets. Compound elution was monitored at 287 nm. Chromatograms do not show the peaks for donor nucleotides, which eluted between 2 and 3 min post injection.



### ***S. enterica* does not produce pseudoCbl in the presence of GkCbITS**

To determine what lower ligand *GkCbITS* activated when produced in *S. enterica*, corrinoids were extracted from cells grown under different conditions. Deproteinated extracts obtained as described under *Experimental procedures* were resolved by RP-HPLC and fractionated. Two indicator strains were used to establish the presence of cobamides in deproteinated extracts of strains of interest. The first indicator strain was JE8214 (*metE cobS*), a strain lacking the Cbl-independent methionine synthase (MetE) and the AdoCbl-5'-P synthase (CobS) enzymes. The absence of MetE demanded that the methylation homocysteine to methionine occurred via the Cba-dependent MetH enzyme; the absence of CobS in strain JE8214 blocked adenosylcobamide biosynthesis. The presence of *metE* and *cobS* null alleles in strain JE8214 rendered the strain auxotrophic for cobamides or methionine. To determine whether methionine or cobamides were present in deproteinated extracts, we used a second indicator strain, namely strain JE12403. In addition to the *metE* and *cobS* null alleles, strain JE12403 also carried a *btuB* null allele. The BtuB protein is responsible for the transport of corrinoids (including cobamides) across the *S. enterica* outer membrane. Unlike strain JE8214, strain JE12403 grew only if methionine was present in the deproteinated extract being tested. A soft agar layer seeded with one of these strains was poured over a minimal medium plate lacking corrinoids. Samples of fractions obtained after RP-HPLC analysis of deproteinated extracts were spotted onto the hardened soft agar layer. A fraction was determined to contain a complete cobamide if it supported growth of strain JE8214 but not JE12403. The presence of cobamides in a fraction of interest was confirmed by UV-vis spectroscopy and mass spectrometry.

As a control, a mixture of authentic pseudoCbl, (CN)<sub>2</sub>Cbi, and CNCbl at a known concentration was resolved, fractionated, and assayed (Figure 3-5A). Bioassay of the fractions collected

indicated the presence of complete cobamides in fractions eluting between 11.5 min and 18.5 min post injection. The strongest signals were detected at 12 and 17 min. UV-vis spectra and mass spectrometry confirmed the presence of pseudoCbl and Cbl, respectively. The peak observed at 14 min in the HPLC trace was cobinamide (denoted by (CN)<sub>2</sub>Cbi in Figure 3-5).

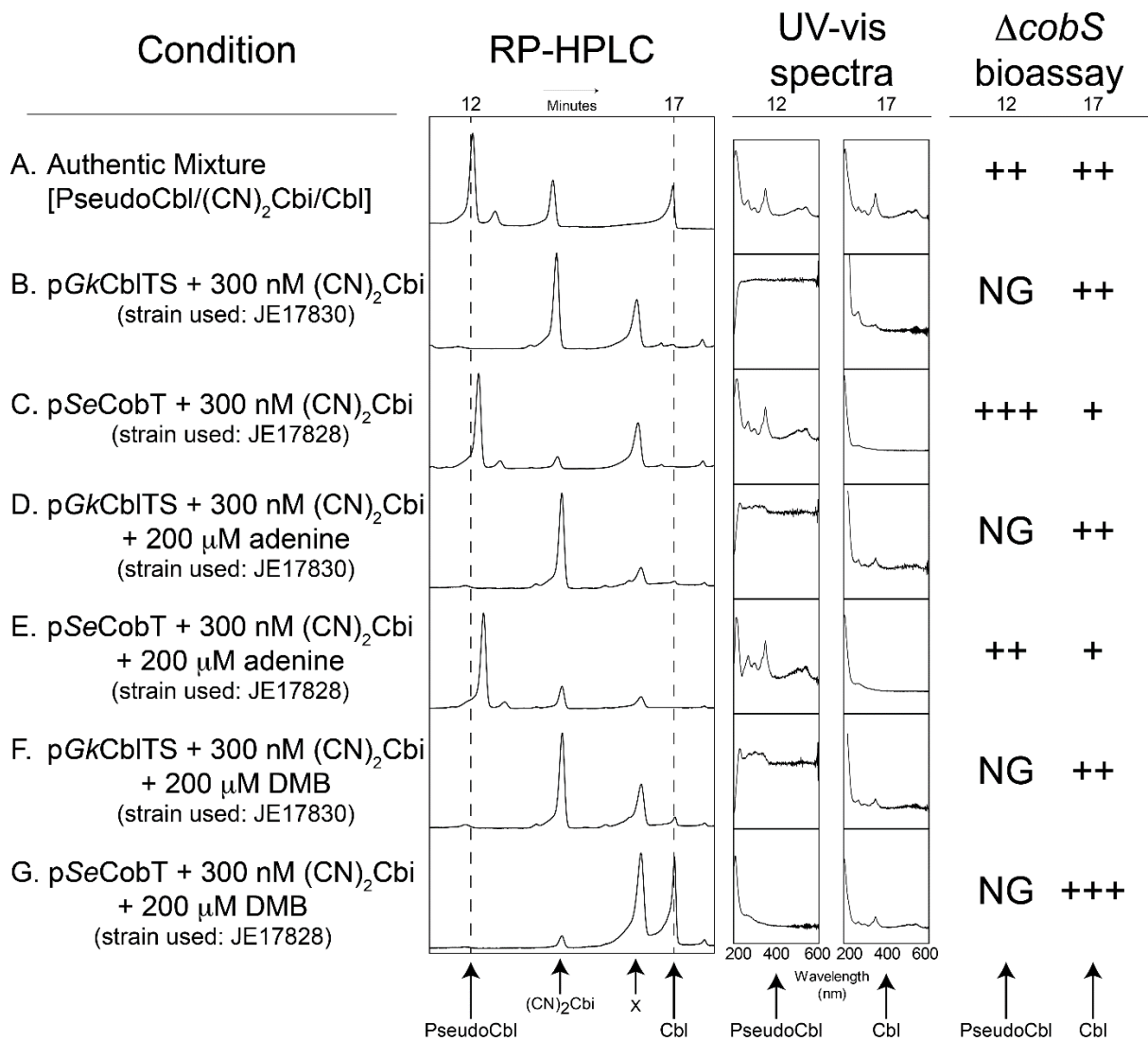
RP-HPLC analysis of deproteinated extracts of strain JE17828 (p*SeCobT*<sup>WT</sup>) grown on minimal medium supplemented with (CN)<sub>2</sub>Cbi (300 nM) but no DMB, showed the presence of complete cobamides in fractions collected between 11.5 min and 13 min as well as between fractions collected between 16 min and 17.5 min (Figure 3-5C). The strongest signal was observed with compounds eluting 12 min post injection. When strain JE17830 (p*GkCblITS*<sup>WT</sup>) was grown under similar conditions, complete cobamides were detected in fractions collected between 14.5 and 18 min, with the strongest signal obtained with compounds eluting 17 min post injection (Figure 3-5B). These data suggested that strain JE17830 did not synthesize pseudoCbl, an idea that was supported by the lack of signal in the UV-vis spectra (Figure 3-5B) or the mass spectrometry data (data not shown).

To try and guide cobamide biosynthesis towards pseudoCbl, adenine (200 μM) was added to the culture medium already containing (CN)<sub>2</sub>Cbi (300 nM). Deproteinated extracts of strain JE17828 contained complete cobamides with the strongest signal observed at 12.5 min post injection (Figure 3-5E). Extracts of strain JE17830 grown under the same conditions contained complete cobamides between 14.5 min and 18 min, with the strongest signal observed at 17 min (Figure 3-5D). These data supported the conclusion that JE17830 did not produce pseudoCbl under the growth conditions used. For comparison, a strain with the same genetic background but carrying a plasmid encoding *SeCobT*<sup>WT</sup> made pseudoCbl (Figure 3-5E).

To determine whether or not the addition of DMB would change the cobamide made by strains JE17828 (*pSeCobT*) and JE17830 (*pGkCbITS*), DMB (200  $\mu$ M) was added to medium containing (CN)<sub>2</sub>Cbi (300 nM). RP-HPLC analysis of deproteinated extracts of strain JE17828 showed a shift, with cobamides detected between 12.5 min and 18.5 min, with the largest peak at 17 min (Figure 3-5G). That is, strain JE17828 made Cbl only, with no detectable evidence of pseudoCbl production. In contrast, extracts of strain JE17830 contained complete cobamides that were detected between 14.5 min and 18 min post injection, with the strongest growth response observed when material eluted at 17 min was tested (Figure 3-5F). Notably, no detectable increase was observed in the bioassay of any of the fractions of extracts of strain JE17830. Close analysis of the chromatogram at 17 min revealed a signal in extracts of the strain grown in DMB-supplemented medium, but not in extracts of the same strain grown in adenine-supplemented medium or in extracts of the strain grown in medium devoid of base supplements. We note that a signal detected in all prepared samples around 16 min (denoted by X in Figure 3-5) was not a cobamide on the basis of the UV-vis spectrum and bioassay results (Figure A-2), did not support growth (data not shown) and was not further identified.

### Figure 3-5. RP-HPLC Analysis of corrinoid extracts.

*RP-HPLC.* Corrinoid extracts from JE12939 derivatives were separated by RP-HPLC as described in the *Experimental procedures* section; their elution was monitored at 367 nm. DMB or adenine was added as indicated to determine whether biosynthesis could be directed. Traces were normalized for comparison purposes. Normalization was achieved by considering the peak with the highest absorbance as 100%. Dashed lines indicate fractions at 12 and 17 min post injection. Expected retention times for pseudoCbl, CNCbl, and (CN)<sub>2</sub>Cbi are indicated below the traces. Peak indicated by “X” is not a corrinoid as indicated by its UV-vis spectrum and bioassay results (Figure A-2); its identity was not established. As a control, a 0.5 μM solution of authentic pseudoCbl, (CN)<sub>2</sub>Cbi, and CNCbl was analyzed under the same conditions (Figure 3-5A). *UV-vis spectra.* Spectra were obtained from the RP-HPLC chromatogram at the elution time identified by the dashed line. UV-vis spectra shown in row A were obtained with authentic compounds. The first column reflects the UV-vis spectrum collected at 12 min and the second column reflects the spectrum at 17 min. Peaks at 367 nm and 525 nm were indicative of a corrinoid. *ΔcobS bioassay.* Bioassays were performed as described in the *Experimental procedures* section. These fractions are representative of the highest peak for pseudoCbl and CNCbl elution, respectively, as confirmed by mass spectrometry. Growth indicates the presence of a complete cobamide. Abbreviations: NG, no growth; +, halo diameter < 5 mm; ++, diameter between 5 mm and 10 mm; +++, halo diameter > 10 mm. The following strains were used: Panel A, none; panels B, D, F, JE17830; panels C, G, E, JE17828.



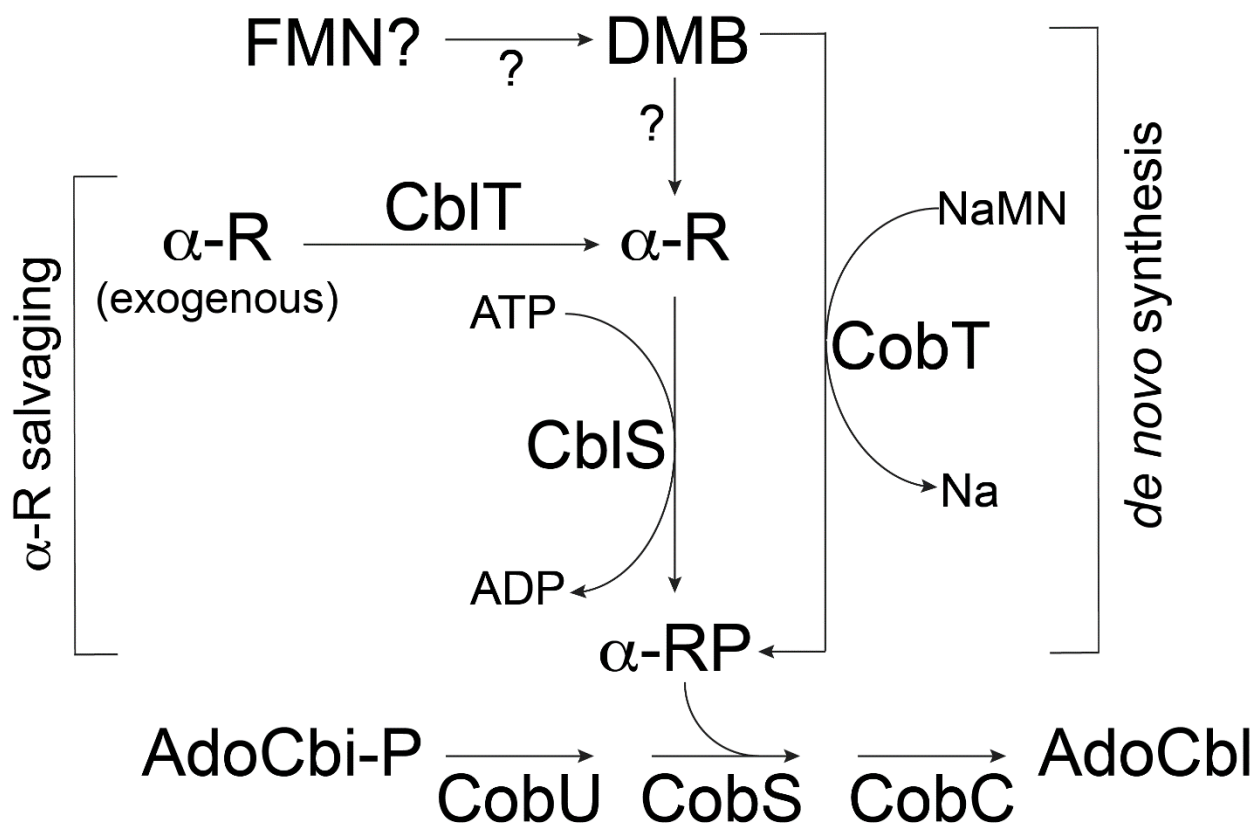


**Figure 3-6. Expanded view of  $\alpha$ -RP biosynthesis via direct DMB activation or  $\alpha$ -R scavenging.** The presence of both the CobT-dependent synthesis of  $\alpha$ -RP and the CbITS proteins in a single organism (*e.g.*, *G. kaustophilus*) may be an indicator of the presence of  $\alpha$ -R in the environment. As shown in this study, *S. enterica* can convert DMB to  $\alpha$ -R via an unknown mechanism. Other bacteria, like *G. kaustophilus* may also be able to convert DMB to  $\alpha$ -R, thus expanding the role of the CbITS system from salvaging to *de novo* synthesis. In *S. enterica*, it has been proposed that DMB is derived from FMN, but the enzymes involved have not been identified. Abbreviations: FMN, flavin mononucleotide; CobU, NTP:Ado-cobinamide kinase and NTP:Ado-cobinamide-phosphate guanylyltransferase; CobS, AdoCbl-phosphate synthase; CobC, Ado-Cbi-P phosphatase.

## DISCUSSION

Here we report that the CblS and CblT proteins from the Firmicute *G. kaustophilus* can substitute for the CobT enzyme in the synthesis of the intermediate  $\alpha$ -RP of the AdoCbl biosynthetic pathway in *S. enterica*. Below we discuss our interpretation of the results and the implications of the findings.

### **What is the physiological role of the *GkCblTS* proteins in *Firmicutes*?**

Prior to this work, it was accepted that in cobamide producers DMB activation to  $\alpha$ -RP was catalyzed by a DMB:NaMN phosphoribosyltransferase, *e.g.*, the CobT enzyme of *S. enterica* (26). From previous work we learned that some *Firmicutes* (*e.g.*, *L. innocua*) possessed what appeared to be an  $\alpha$ -R salvaging system comprised of an  $\alpha$ -R transporter (CblT) and an  $\alpha$ -R kinase (CblS) (20). The identification of the CblTS system in *L. innocua* left one question unanswered. Since the *L. innocua* genome does not encode a CobT homologue, is *L. innocua* an obligate  $\alpha$ -R salvaging bacterium? If the answer were yes, then one wonders how this bacterium survives in an environment where it needs to synthesize AdoCbl, but the environment is devoid of  $\alpha$ -R. The results reported herein recapitulate the *L. innocua* conundrum in a *S. enterica*  $\Delta$ *cobT* strain that can synthesize CblTS. Growth analyses of such a strain showed that *S. enterica* has an as-yet-unknown mechanism to synthesize  $\alpha$ -R. We propose that *Firmicutes* also synthesize  $\alpha$ -R endogenously, and that the CblTS proteins serve the dual purpose of being a system that generates  $\alpha$ -RP from exogenous or endogenously synthesized  $\alpha$ -R.

### ***S. enterica* synthesizes $\alpha$ -R, a previously unknown capability of this bacterium**

The *in vivo* analyses of *GkCblTS* functions revealed an unexpected metabolic capability of *S. enterica*, which is that *S. enterica* can convert DMB into its riboside,  $\alpha$ -R. Results shown in figure 2, support the following conclusions: i) In the presence of high amounts of cobinamide, an AdoCba

precursor, *GkCblTS* can compensate for the lack of *SeCobT* during the synthesis of AdoCba without any addition to the medium, meaning that the  $\alpha$ -R needed by the *GkCblS* kinase to make  $\alpha$ -RP must be endogenously synthesized (Figure 3-2A); ii) under the same growth conditions (*i.e.*, high exogenous cobinamide levels), the *GkCblT* protein is dispensable (Figure 3-2C, open triangles), supporting the idea that *GkCblS* is necessary and sufficient for the phosphorylation of  $\alpha$ -R; iii) that *GkCblT* may be able to transport DMB (compare open circles in Figure 3-2B to diamonds in Figure 3-2C); iv) that *S. enterica* can acquire  $\alpha$ -R in the absence of *GkCblT* (Figure 3-2C, solid triangles). Since *S. enterica* does not make a CblT homologue, these results suggest that  $\alpha$ -R is transported into *S. enterica* via non-specific means. Although it is unclear whether DMB was endogenously synthesized or salvaged in the experiments performed in these studies, the results strongly support the conclusion that *S. enterica* can convert DMB to  $\alpha$ -R. To the best of our knowledge, this is the first example of such a conversion in any organism.

### ***GkCblS* has kinase activity, and appears to prefer $\alpha$ -R over $\alpha$ -adenosine as substrate**

Given the primary sequence similarity between *GkCblS* and *LinCblS* (Figure A-1), it was not unexpected to find that *GkCblS* had  $\alpha$ -R kinase activity. What was surprising, however, was the strong preference of the enzyme for  $\alpha$ -R over  $\alpha$ -adenosine. Results of guided biosynthesis experiments with *GkCblS* as the sole means to activate DMB or adenine failed to yield pseudoCbl, even though the cultures were grown in the presence of excess adenine and no exogenous DMB. These results suggest that *GkCblS* had a strong preference for  $\alpha$ -R over  $\alpha$ -adenosine (Figure 3-5D). When the control experiment was performed with *SeCobT*, the cell made mostly pseudoCbl (Figure 3-5E), consistent with our knowledge that the *SeCobT* enzyme can use either DMB or adenine as substrate. The conclusion that *GkCblS* prefers  $\alpha$ -R over  $\alpha$ -adenosine as substrate is further supported by results of *in vivo* (Figure 3-2) and *in vitro* experiments (Figure 3-4).

**An opportunity to identify the *S. enterica* enzyme that converts DMB to  $\alpha$ -R, and to investigate the putative DMB biosynthetic pathway in this bacterium**

An understanding of if and how *S. enterica* makes DMB has remained an enigma since the discovery of cobamide biosynthesis in this bacterium was reported over three decades ago (23). The lack of a system that would use  $\alpha$ -R but not  $\alpha$ -adenosine as substrate made it difficult to isolate *bona fide* DMB auxotrophs of *S. enterica*. Because strain JE21634 ( $\Delta met$  *ara-9*  $\Delta cobT$   $\Delta cobB$  / *pGkCblS*) only makes AdoCbl, this genetic background offers valuable opportunities for the use of *in vivo* genetic approaches to investigate the putative DMB biosynthetic pathway in this bacterium, and the conversion of DMB to  $\alpha$ -R. To our knowledge, the existence of these enzymes has not been reported in *S. enterica* or any other cobamide producer.

At present, it is unclear whether *S. enterica* synthesizes DMB *de novo*. The claim that this bacterium synthesizes DMB is weakened by the fact that genes encoding enzymes responsible for its synthesis have not been identified. It is possible that *S. enterica* and other organisms synthesize DMB via an as-yet uncharacterized pathway distinct from the five-enzyme, anoxic pathway found in *Eubacterium limosum* (8) and the single enzyme, oxygen-dependent pathway identified in *Rhodobacter sphaeroides* and *Sinorhizobium meliloti* (11-13). The absence of *bona fide* *S. enterica* DMB auxotrophs suggests that either that this bacterium does not have a dedicated pathway for DMB synthesis, that the pathway is also needed for other metabolic purposes, or that one or more of the functions involved in the putative pathway is essential. The isolation of DMB auxotrophs probably has been complicated by the broad distribution of DMB in the environment and culture media commonly used in our laboratories (27).

### **An expanded model for the synthesis of $\alpha$ -RP in bacteria**

Collectively, our data support the conclusion that *S. enterica* can synthesize  $\alpha$ -R but cannot phosphorylate it to  $\alpha$ -RP (Figs. 2, 5). It appears, however, that some *Firmicutes* have evolved an  $\alpha$ -R kinase that can phosphorylate  $\alpha$ -R. It is unclear what the selective pressure for the evolution of such a kinase may have been in *G. kaustophilus*, since the genome of this bacterium also encodes a homologue of the *SeCobT* enzyme (locus tag *gk1793*). It is possible that this bacterium is exposed to  $\alpha$ -R in the marine environment it inhabits, which is not unlikely since the presence of  $\alpha$ -R in marine environments was recently reported (28). If that were the case, then the *GkCbITS* proteins would likely be the  $\alpha$ -R scavenging system, while the *GkCobT* enzyme would play a role in *de novo* synthesis in this bacterium. Figure 6 shows a model for the synthesis and activation of DMB in bacteria that either have the canonical DMB activation system (e.g., *CobT*) or the *CbIS*-dependent pathway to convert  $\alpha$ -R, to  $\alpha$ -RP. We suggest that *G. kaustophilus* uses *GkCbITS* and *GkCobT* for different purposes.

## EXPERIMENTAL PROCEDURES

### Chemicals

Unless otherwise indicated, chemicals were obtained from Sigma-Aldrich. Pseudocobalamin was extracted from laboratory strains by growing *S. enterica* in medium containing 1,2-propanediol as the sole source of carbon and energy. Under such conditions, this bacterium produces only pseudoCbl (29). Corrinoids were extracted from cultures grown on 1,2-propanediol using procedures described below. Alpha-ribazole ( $\alpha$ -R) was obtained by the method described in (30) with the modifications described in (20).

### Bacterial strain construction

All strains and plasmids used are listed in Table 3-1. Transformations were performed as described (31) with no modifications.

### Plasmid construction

All primers used in this study are listed in Table 3-2. DNA amplification and restriction digestions were performed according to manufacturer's protocols. All restriction enzymes used were purchased from Thermo Fisher Scientific Inc., unless otherwise stated.

pGkCblTS1. The adjacent *Geobacillus kaustophilus* *cblT*<sup>+</sup> and *cblS*<sup>+</sup> coding sequences (locus tags *gk2256* and *gk2255*, respectively) were amplified from *G. kaustophilus* HTA426 genomic DNA using primers Gk\_cblTS\_EcoRI\_5' and Gk\_cblTS\_HindIII\_3' and the resulting PCR product was inserted into plasmid pGEM-T Easy (Promega) using the cloning strategy described by the manufacturer; the resulting plasmid was named pGkCblTS1.

**Table 3-1. Strains and plasmids used in this study.** Unless otherwise stated, strains and plasmids were constructed during the course of this work.

Strains	Antibiotic resistance	Relevant genotype	Reference or source
<b><i>E. coli</i> strains<sup>1</sup></b>			
DH5 $\alpha$ /F'			
JE13607	Km <sup>R</sup>	BL21 ( $\lambda$ DE3) <i>cobT762::kan<sup>+</sup></i>	(1)
<b><i>S. enterica</i> strains<sup>2</sup></b>			
TR6583		<i>metE205 ara-9</i>	K. Sanderson via J. Roth
JE7088		$\Delta$ <i>metE2702 ara-9</i>	Lab collection
JE8214	Cm <sup>R</sup>	<i>metE205 ara-9 cobS1312::cat</i>	Lab collection
JE12403	Km <sup>R</sup>	<i>metE205 ara-9 <math>\Delta</math>cobS1313 btuB7::MudJ<sup>3</sup></i>	Lab collection
JE12939		$\Delta$ <i>metE2702 ara-9 <math>\Delta</math>cobT1380 <math>\Delta</math>cobB1375</i>	Lab collection
JE17827	Ap <sup>R</sup>	$\Delta$ <i>metE2702 ara-9 <math>\Delta</math>cobT1380 <math>\Delta</math>cobB1375</i> / pBAD24	
JE17828	Ap <sup>R</sup>	$\Delta$ <i>metE2702 ara-9 <math>\Delta</math>cobT1380 <math>\Delta</math>cobB1375</i> / pCOBT140	
JE17830	Ap <sup>R</sup>	$\Delta$ <i>metE2702 ara-9 <math>\Delta</math>cobT1380 <math>\Delta</math>cobB1375</i> / pGkCbITS2	
JE21364	Ap <sup>R</sup>	$\Delta$ <i>metE2702 ara-9 <math>\Delta</math>cobT1380 <math>\Delta</math>cobB1375</i> / pGkCbIS3	
<b>Plasmids</b>			
pGEM-T Easy	Ap <sup>R</sup>	TA cloning vector	Promega
pT7-5	Ap <sup>R</sup>	Overexpression vector	(40)
pBAD24	Ap <sup>R</sup>	Cloning vector with P <sub>araBAD</sub> arabinose-inducible promoter	(22)
pBAD33	Cm <sup>R</sup>	Cloning vector with P <sub>araBAD</sub> arabinose-inducible promoter	(22)
pTEV5	Ap <sup>R</sup>	TEV protease-cleavable His <sub>6</sub> tag overexpression vector	(25)
pJO27	Ap <sup>R</sup>	<i>S. enterica cobT<sup>+</sup></i> in pT7-5	(15)
pGkCbITS1	Ap <sup>R</sup>	<i>G. kaustophilus cblT<sup>+</sup> cblS<sup>+</sup></i> in pGEM-T Easy	
pGkCbITS2	Ap <sup>R</sup>	<i>G. kaustophilus cblT<sup>+</sup> cblS<sup>+</sup></i> in pBAD24	
pGkCbIS1	Cm <sup>R</sup>	<i>G. kaustophilus cblS<sup>+</sup></i> in pBAD33	
pGkCbIS2	Ap <sup>R</sup>	<i>G. kaustophilus cblS<sup>+</sup></i> translational fusion to His <sub>6</sub> tag for protein purification in pTEV5	
pGkCbIS3	Ap <sup>R</sup>	<i>G. kaustophilus cblS<sup>+</sup></i> in pBAD24	
pCOBT81	Cm <sup>R</sup>	<i>S. enterica cobT<sup>+</sup></i> in pBAD33	
pCOBT140	Ap <sup>R</sup>	<i>S. enterica cobT<sup>+</sup></i> in pBAD24	

<sup>1</sup> All *E. coli* strains used in this study were derivatives of *E. coli* K-12

<sup>2</sup> All *S. enterica* strains used in this study were derivatives of *S. enterica* sv Typhimurium strain LT2

<sup>3</sup> MudJ is an abbreviation of MudII1734 (Castilho *et al.*, 1984)

Ap<sup>R</sup>, Ampicillin resistance; Cm<sup>R</sup>, chloramphenicol resistance; Km<sup>R</sup>, kanamycin resistance

**Table 3-2. Oligonucleotides used in this study.**

Primer	Sequence (5' → 3')*
Gk_cblTS_EcoRI_5'	<u>AGAATTCC</u> ACCATGAACCGCCGCTTGGCTT
Gk_cblTS_HindIII_3'	ATGAAGCTTTT <u>ACC</u> ACTCGACGTGCAGTG
Gk_cblS_XbaI_RBS_5'	GAGGCGTCTAG <u>A</u> AGGAGGCACCATGCGTGATGTGCTTTTCC
pTEV5_PIPE_gkCblS_5'	AACCTGTATTTTCAGGGGCATGCGTGATGTGCTTTTCC
pTEV5_PIPE_gkCblS_3'	AGCTCGAGAATTCATGGTTACC <u>ACTCG</u> ACGTGCAG
pTEV5_PIPE_NheI_5'	GCCCTGAAAATACAGGTTTTTCACTAGTTG
pTEV5_PIPE_XhoI_3'	CCATGGAATTCTCGAGCTCCCG
Gk_CblS_EcoRI_5'	GAGGCGGAATTC <u>C</u> ACCATGCGTGATGTGCTTTTCC
Sal_CobT_BAD24_EcoRI_5'	CAGGAATTC <u>C</u> GAGACATCTTATGCAGACACTACACGC
Sal_CobT_BAD24_XbaI_3'	CAGTCTAGACGATGGGTCGGGTTATGTTGC

\*Restriction sites introduced for cloning are underlined.

### Plasmid construction (Cont'd.)

pGkCblTS2. The *G. kaustophilus* *cblT*<sup>+</sup> and *cblS*<sup>+</sup> coding sequences were excised from pGkCblTS1 and subcloned into the EcoRI and HindIII sites of pBAD24 to yield plasmid pGkCblTS2. The plasmid pGkCblTS2 was used for complementation assays and corrinoid analyses.

pGkCblS1. The *G. kaustophilus* *cblS*<sup>+</sup> coding sequence was amplified off pGkCBLTS2 using primers Gk\_cblS\_XbaI\_RBS\_5' and Gk\_cblTS\_HindIII\_3'. The DNA fragment was cut and inserted between the XbaI and HindIII sites of pBAD33. The resulting plasmid was named pGkCblS1

pGkCblS2. This vector was constructed using the polymerase incomplete primer extension (PIPE) method (32). The *G. kaustophilus* *cblS*<sup>+</sup> coding sequence was amplified off pGkCBLTS1 using the primers pTEV5\_PIPE\_gkCblS\_5' and pTEV5\_PIPE\_gkCblS\_3'. The vector backbone pTEV5 was amplified using the primers pTEV5\_PIPE\_NheI\_5' and pTEV5\_PIPE\_XhoI\_3'. Following overnight cutting with DpnI, the fragments were mixed in equal volumes and transformed into chemically competent *E. coli* DH5α cells (31). The constructed plasmid results

in the *cbIS* coding sequence being inserted between the *NheI* and *XhoI* sites of pTEV5. The plasmid pGkCbIS2 was used for protein overproduction.

pGkCbIS3. The *G. kaustophilus cbIS*<sup>+</sup> coding sequence was amplified off pGkCBLS1 using primers Gk\_cbIS\_EcoRI\_5' and Gk\_cbITS\_HindIII\_3'. The DNA fragment was cut and inserted between the *EcoRI* and *HindIII* sites of pBAD24. The plasmid pGkCbIS3 was used for complementation assays.

pCOBT81. The *Salmonella enterica cobT*<sup>+</sup> coding sequence was excised from pJO27 (33) and subcloned into the *SacI* and *HindIII* sites of pBAD33 to yield plasmid pCOBT81. The plasmid pCOBT81 was used for constructing pCOBT140.

pCOBT140. The *Salmonella enterica cobT*<sup>+</sup> coding sequence was amplified off pCOBT81 using primers Sal\_CobT\_BAD24\_EcoRI\_5' and Sal\_CobT\_BAD24\_XbaI\_3'. The DNA fragment was inserted between the *EcoRI* and *XbaI* sites of pBAD24. The plasmid pCOBT140 was used for complementation assays and corrinoid analyses.

### **Growth analyses**

Strains were grown at 37 °C in no-carbon essential (NCE) minimal medium (34) supplemented with ribose (22 mM) as a carbon and energy source. Minimal medium also contained trace minerals, magnesium sulfate (1 mM), ampicillin (100 µg mL<sup>-1</sup>), and L(+)-arabinose (500 µM). Where indicated, 5,6-dimethylbenzimidazole (DMB, 200 µM), α-ribazole (α-R, 300 nM), dicyanocobinamide [(CN)<sub>2</sub>Cbi] (0.25 nM or 5 nM), and cyanocobalamin (CNCbl, 0.5 nM) were added. α-Ribazole was synthesized as reported (20). Growth analyses were performed in 96-well microtiter dishes, with each strain grown under indicated conditions in duplicate. Each well contained 200 µL of medium inoculated with 1% (v/v) of an overnight starter culture grown for at least 20 h on nutrient broth (Difco) to lower the level of residual nutrients in the medium. Cell

density was monitored at 650 nm using a computer-controlled BioTek ELx808 absorbance plate reader (BioTek Instruments). Readings were acquired every 30 min with continuous shaking. Data were analyzed using the GraphPad Prism v4 software package (GraphPad Software).

### **Corrinoid extraction and analysis**

Production. Strains were grown at 37 °C in NCE minimal medium supplemented with ribose (22 mM) as a carbon and energy source. Minimal medium also contained trace minerals, magnesium sulfate (1 mM), ampicillin (100 µg mL<sup>-1</sup>), (CN)<sub>2</sub>Cbi (300 nM), and L(+)-arabinose (500 µM). Where indicated, DMB or adenine (200 µM) was added. Culture medium (100 mL) was prepared in 500-mL baffled flasks and inoculated by the addition of 1% (v/v) of an overnight culture grown for at least 20 h in nutrient broth (NB, Difco). Cultures were grown for >20 h at 37 °C with shaking (150 rpm) (New Brunswick Innova 44R refrigerated incubator shaker). The cells were then harvested by centrifugation at 5,500 x g for 15 min (Beckman/Coulter Avanti J25-I centrifuge, equipped with a JLA-16.250 rotor). Cell pellets were resuspended in 5 mL of 100 mM ammonium acetate solution containing potassium cyanide (10 mM) at pH 4, and frozen at -20 °C until processed.

Extraction protocol. Cobamide extraction and isolation was performed using a modification of procedures reported elsewhere (35, 36). Briefly, frozen cell suspensions were thawed and incubated at 70 °C with constant shaking (100 rpm) for 2.5 h using a ThermoScientific MaxQ 4000 shaker. Cell debris was removed by centrifugation at 43,000 x g for 1 h (Beckman/Coulter Avanti J25-I centrifuge, equipped with a JA-25.25 rotor). The supernatant was passed over a 0.45-µm polyethersulfone syringe filter (VWR). Amberlite XAD4 resin (Rohm and Haas) was cleaned of impurities by washing with methanol, followed by extensive washing with water prior to use. Amberlite XAD4 resin (250 mg) was used per ml of extract, and allowed to incubate overnight at

37 °C with shaking to bind corrinoids. The unbound material was removed separated from the resin by suction, and the resin was washed with 10 volumes of MilliQ water (EMD Millipore). Two volumes of methanol were added to the resin and incubated overnight to desorb corrinoids. The methanol layer was pulled off, dispensed into a tube, and concentrated under vacuum (Eppendorf Vacufuge Plus) at 60 °C for 5.5 h at max speed (1400 rpm). The pellets were resuspended in 400 µL of a 1:4 ratio of buffer B (KH<sub>2</sub>PO<sub>4</sub> (100 mM), KCN (10 mM), pH 8 + 50% (v/v) acetonitrile) and buffer C (KH<sub>2</sub>PO<sub>4</sub> (100 mM), KCN (10 mM), pH 6.5). Resuspended samples were passed over a Costar<sup>®</sup> Spin-X<sup>®</sup> Centrifuge Tube Filter (Corning; 0.45 µM cellulose acetate) and incubated overnight at 4 °C.

Isolation. Ten-fold dilutions of the extracts were prepared and passed over a Costar<sup>®</sup> Spin-X<sup>®</sup> centrifuge tube filter (Corning; 0.45 µM cellulose acetate). The filtrates were dispensed into Prominence 12x32mm MT-IT autosampler vials (Shimadzu) and capped with 9-mm screw caps fitted with PTFE/Silicone septa (VWR). Cobamides were resolved by RP-HPLC using a Shimadzu Prominence UFLC equipped with a Phenomenex Synergi Hydro-RP (150 x 4.6 mm) as described (1, 37), with some modifications. The column was equilibrated at 20 % buffer B (see above) for 2.5 min at a flow rate of 1.0 mL min<sup>-1</sup> and developed on a linear gradient to 35% buffer B over 9 min, further developed to 100% buffer B over 7 min, and operated for 5 min at 100% buffer B. Corrinoids were detected at 367 nm on a computer-controlled Shimadzu Nexera X2 SPD-30A diode array detector. Fractions (0.5 mL ea.) were collected on a computer-controlled Shimadzu FRC-10 fraction collector between 7 and 20 min post injection.

Bioassay. Fractions were tested for the presence of complete corrinoids by bioassay. Agar plates containing NCE medium were supplemented with trace minerals, ribose (22 mM), and magnesium sulfate (1 mM) and antibiotic (chloramphenicol, 5 µg/mL; or kanamycin, 25 µg/mL). A 4-mL soft

agar (0.7%, w/v) overlay was seeded with 100  $\mu$ L of an overnight starter culture of indicator strains JE8214 (*cobS*) or JE12403 (*cobS btuB*) and poured over the minimal plates. Samples (2  $\mu$ L ea.) of the fractions were spotted on the overlay and plates were incubated overnight at 37 °C. A halo of growth in the soft agar layer seeded with JE8214 (*cobS*) but not in the layer seeded with JE12403 (*cobS btuB*) indicated the presence of a cobamide. The diameter of the halo was recorded and compared to the HPLC trace. Cobamide identity was analyzed by MALDI-TOF mass spectrometry.

### **Purification of His<sub>6</sub>-tagged *GkCblS* protein**

His<sub>6</sub>-tagged *GkCblS* was overproduced in JE13607 (BL21 ( $\lambda$ DE3) *cobT762::kan<sup>+</sup>*) (1) using plasmid p*GkCblS2* (*cblS<sup>+</sup>*). Cells were grown in 50 mL of Terrific Broth (Cold Spring Harbor Laboratory Protocols, <http://cshprotocols.cshlp.org/content/2006/1/pdb.rec8620>) overnight at 37 °C in a 250-mL flask. The cells were harvested by centrifugation at 6,000 x *g* using an Avanti J-20 XPI floor centrifuge equipped with a JLA-8.1000 rotor (Beckman Coulter). Eight grams of cell paste were frozen at -80 °C until use. Cell paste was resuspended in binding buffer containing HEPES (4-(2-hydroxyethyl)piperazine-1-ethanesulfonic acid, 50 mM), NaCl (500 mM), imidazole (10 mM), pH 7.3 @ 24 °C). The cell paste (g): buffer (ml) ratio used was 1:5. To ensure cell lysis, 15 mg of lysozyme was added to the suspension and the cell was allowed to incubate for 30 min at room temperature. The serine protease inhibitor phenylmethanesulfonyl fluoride (PMSF; Acros Organics) was added at a concentration of 200  $\mu$ M. Cells were broken by sonication (3 cycles, 50% duty, 1.2-min cycle, 2 s on, 8 s off) with a 550 Sonic Dismembrator (Fisher Scientific). A salted ice bath was used to prevent enzyme inactivation due to heat. Cell debris was removed by centrifugation at 39,000 x *g* using an Avanti J-25I floor centrifuge with a JA-25.25 rotor

(Beckman Coulter). The supernatant was passed over a 0.45- $\mu$ m polyethersulfone syringe filter (VWR) to remove any remaining debris.

The filtered cell-free extract was loaded onto 5 mL of Ni-NTA affinity resin (HisPur; ThermoFisher Scientific) column. After loading, the column was washed with four column volumes using the following buffers: binding buffer (described above); washing buffer [HEPES (50 mM, pH 7.3), NaCl (500 mM), imidazole (150 mM)]; and elution buffer [HEPES (50 mM, pH 7.3), NaCl (500 mM), imidazole (750 mM), *tris*(2-carboxyethyl)phosphine (TCEP, 5 mM), glycerol (5%, v/v)]. The final elutant was concentrated using an Amicon-15 concentrator (MWCO 10 kDa; Millipore) for 13 min at 3,220 x *g* (Eppendorf 5810). The concentrate was dialyzed against decreasing salt concentrations down to 250 mM NaCl. The first dialysis also included EDTA (0.5 mM) for nickel chelation. The final protein concentration was quantified using a microtiter plate protocol for the Bradford protein assay (38) using a commercially available kit (BioRad). Purified protein was flash frozen in liquid nitrogen and stored at -80 °C until used.

### **Assessment of $\alpha$ -ribazole kinase activity**

*In vitro* activity assay. The enzymatic activity of purified His<sub>6</sub>-GkCb1S protein was assayed using a modification of the  $\alpha$ -R kinase assay (20). Reaction mixtures (100  $\mu$ L) contained HEPES buffer (50 mM, pH 7.4), MgCl<sub>2</sub> (5 mM), KCl (750 mM), TCEP (5 mM), ATP (0.5 mM),  $\alpha$ -ribazole (0.25 mM) and protein (3  $\mu$ g);  $\alpha$ -R was obtained as described (20). Reactions were incubated for 3 h at 37 °C in a BioRad DNA Engine Dyad ThermoCycler, and stopped by heating for 10 min at 80 °C. A sample (120  $\mu$ L) of ammonium acetate (20 mM) at pH 4.5 was added to the reactions, which were then passed over a Costar<sup>®</sup> Spin-X<sup>®</sup> Centrifuge Tube Filter (Corning; 0.45  $\mu$ M cellulose acetate). The filtrates were dispensed into Prominence 12x32mm MT-IT autosampler vials (Shimadzu) and capped with 9-mm screw caps fitted with PTFE/Silicone septa (VWR).

HPLC analysis. The product of the kinase assay was resolved by RP-HPLC using a modification of the described separation protocol for  $\alpha$ -RP (20). A Shimadzu Prominence UFLC equipped with a Kinetex 5 $\mu$  C18 column (150 x 4.6 mm; Phenomenex) and a SecurityGuard ULTRA guard column (C18 cartridge; Phenomenex) was equilibrated at a flow rate of 0.8 mL min<sup>-1</sup> with 3% (v/v) acetonitrile / 97% (v/v) of ammonium acetate (20 mM, pH 4.5). After injection, the column was developed for 12 min to 40% (v/v) acetonitrile and then 5 min to 80% (v/v) acetonitrile. Compounds were detected at 287 nm using a computer-controlled Shimadzu Nexera X2 SPD-30A diode array detector. As a reference for the formation of  $\alpha$ -ribazole-5'-phosphate ( $\alpha$ -RP), retention time and spectra of the product peak were compared to the product formed as a result of the described *SeCobT* activity assay (1, 39) for the formation of  $\alpha$ -RP from DMB and NaMN. Data were analyzed using the GraphPad Prism v4 software package (GraphPad Software).

## **ACKNOWLEDGEMENTS**

The authors do not have a conflict of interest. This work was supported by USPHS grant R37 GM40313 from the National Institutes of General Medical Sciences to J. C. E.-S. The authors thank Dr. Dennis Phillips and the University of Georgia Proteomics and Mass Spectrometry Core Facility for technical assistance.

## **REFERENCES**

1. Chan CH, Escalante-Semerena JC. 2011. ArsAB, a novel enzyme from *Sporomusa ovata* activates phenolic bases for adenosylcobamide biosynthesis. *Mol Microbiol* 81:952-967.
2. Jeter RM, Roth JR. 1987. Cobalamin (vitamin B<sub>12</sub>) biosynthetic genes of *Salmonella typhimurium*. *J Bacteriol* 169:3189-3198.
3. Escalante-Semerena JC, Roth JR. 1987. Regulation of cobalamin biosynthetic operons in *Salmonella typhimurium*. *J Bacteriol* 169:2251-2258.

4. Escalante-Semerena JC, Warren MJ. 2008. Biosynthesis and Use of Cobalamin (B<sub>12</sub>). In Böck A, Curtiss III R, Kaper JB, Karp PD, Neidhardt FC, Nyström T, Slauch JM, Squires CL (ed), *EcoSal - Escherichia coli and Salmonella: cellular and molecular biology*. ASM Press, Washington, D. C.
5. Keck B, Renz P. 2000. *Salmonella typhimurium* forms adenylobamide and 2-methylobamide, but no detectable cobalamin during strictly anaerobic growth. *Arch Microbiol* 173:76-77.
6. Friedmann HC, Fyfe JA. 1969. Pseudovitamin B<sub>12</sub> biosynthesis. Enzymatic formation of a new adenylic acid, 7- $\alpha$ -D-ribofuranosyladenine 5'-phosphate. *J Biol Chem* 244:1667-1671.
7. Escalante-Semerena JC. 2007. Conversion of cobinamide into adenylobamide in bacteria and archaea. *J Bacteriol* 189:4555-4560.
8. Hazra AB, Han AW, Mehta AP, Mok KC, Osadchiy V, Begley TP, Taga ME. 2015. Anaerobic biosynthesis of the lower ligand of vitamin B<sub>12</sub>. *Proc Natl Acad Sci U S A* 112:10792-10797.
9. Martinez-Gomez NC, Downs DM. 2008. ThiC is an [Fe-S] cluster protein that requires AdoMet to generate the 4-amino-5-hydroxymethyl-2-methylpyrimidine moiety in thiamin synthesis. *Biochemistry* 47:9054-9056.
10. Martinez-Gomez NC, Poyner RR, Mansoorabadi SO, Reed GH, Downs DM. 2009. Reaction of AdoMet with ThiC generates a backbone free radical. *Biochemistry* 48:217-219.

11. Gray MJ, Escalante-Semerena JC. 2007. Single-enzyme conversion of FMNH<sub>2</sub> to 5,6-dimethylbenzimidazole, the lower ligand of B<sub>12</sub>. *Proc Natl Acad Sci U S A* 104:2921-2926.
12. Taga ME, Larsen NA, Howard-Jones AR, Walsh CT, Walker GC. 2007. BluB cannibalizes flavin to form the lower ligand of vitamin B<sub>12</sub>. *Nature* 446:449-453.
13. Campbell GR, Taga ME, Mistry K, Lloret J, Anderson PJ, Roth JR, Walker GC. 2006. *Sinorhizobium meliloti bluB* is necessary for production of 5,6-dimethylbenzimidazole, the lower ligand of B<sub>12</sub>. *Proc Natl Acad Sci U S A* 103:4634-4369.
14. Keck B, Munder M, Renz P. 1998. Biosynthesis of cobalamin in *Salmonella typhimurium*: transformation of riboflavin into the 5,6-dimethylbenzimidazole moiety. *Arch Microbiol* 171:66-68.
15. Trzebiatowski JR, O'Toole GA, Escalante-Semerena JC. 1994. The *cobT* gene of *Salmonella typhimurium* encodes the NaMN: 5,6-dimethylbenzimidazole phosphoribosyltransferase responsible for the synthesis of N<sup>1</sup>-(5-phospho-alpha-D-ribose)-5,6-dimethylbenzimidazole, an intermediate in the synthesis of the nucleotide loop of cobalamin. *J Bacteriol* 176:3568-3575.
16. Rodionov DA, Vitreschak AG, Mironov AA, Gelfand MS. 2003. Comparative genomics of the vitamin B<sub>12</sub> metabolism and regulation in prokaryotes. *J Biol Chem* 278:41148-41159.
17. Cheong CG, Escalante-Semerena JC, Rayment I. 2001. Structural investigation of the biosynthesis of alternative lower ligands for cobamides by nicotinate mononucleotide: 5,6-dimethylbenzimidazole phosphoribosyltransferase from *Salmonella enterica*. *J Biol Chem* 276:37612-37620.

18. Chan CH, Newmister SA, Talyor K, Claas KR, Rayment I, Escalante-Semerena JC. 2014. Dissecting cobamide diversity through structural and functional analyses of the base-activating CobT enzyme of *Salmonella enterica*. *Biochim Biophys Acta* 1840:464-475.
19. Tsang AW, Escalante-Semerena JC. 1998. CobB, a new member of the SIR2 family of eucaryotic regulatory proteins, is required to compensate for the lack of nicotinate mononucleotide:5,6-dimethylbenzimidazole phosphoribosyltransferase activity in *cobT* mutants during cobalamin biosynthesis in *Salmonella typhimurium* LT2. *J Biol Chem* 273:31788-31794.
20. Gray MJ, Escalante-Semerena JC. 2010. A new pathway for the synthesis of alpha-ribazole-phosphate in *Listeria innocua*. *Mol Microbiol* 77:1429-1438.
21. Sievers F, Wilm A, Dineen D, Gibson TJ, Karplus K, Li W, Lopez R, McWilliam H, Remmert M, Soding J, Thompson JD, Higgins DG. 2011. Fast, scalable generation of high-quality protein multiple sequence alignments using Clustal Omega. *Mol Syst Biol* 7:539.
22. Guzman LM, Belin D, Carson MJ, Beckwith J. 1995. Tight regulation, modulation, and high-level expression by vectors containing the arabinose PBAD promoter. *J Bacteriol* 177:4121-30.
23. Jeter RM, Olivera BM, Roth JR. 1984. *Salmonella typhimurium* synthesizes cobalamin (vitamin B<sub>12</sub>) de novo under anaerobic growth conditions. *J Bacteriol* 159:206-213.
24. Zayas CL, Escalante-Semerena JC. 2007. Reassessment of the late steps of coenzyme B<sub>12</sub> synthesis in *Salmonella enterica*: Evidence that dephosphorylation of

- adenosylcobalamin-5'-phosphate by the CobC phosphatase is the last step of the pathway. J Bacteriol 189:2210-2218.
25. Rocco CJ, Dennison KL, Klenchin VA, Rayment I, Escalante-Semerena JC. 2008. Construction and use of new cloning vectors for the rapid isolation of recombinant proteins from *Escherichia coli*. Plasmid 59:231-237.
  26. Trzebiatowski JR, Escalante-Semerena JC. 1997. Purification and characterization of CobT, the nicotinate-mononucleotide:5,6-dimethylbenzimidazole phosphoribosyltransferase enzyme from *Salmonella typhimurium* LT2. J Biol Chem 272:17662-17667.
  27. Crofts TS, Men Y, Alvarez-Cohen L, Taga ME. 2014. A bioassay for the detection of benzimidazoles reveals their presence in a range of environmental samples. Front Microbiol 5:592.
  28. Johnson WM, Kido Soule MC, Kujawinski EB. 2016. Evidence for quorum sensing and differential metabolite production by a marine bacterium in response to DMSP. ISME J doi:10.1038/ismej.2016.6.
  29. Anderson PJ, Lango J, Carkeet C, Britten A, Kräutler B, Hammock BD, Roth JR. 2008. One pathway can incorporate either adenine or dimethylbenzimidazole as an alpha-axial ligand of B<sub>12</sub> cofactors in *Salmonella enterica*. J Bacteriol 190:1160-1171.
  30. Pakin C, Bergaentzle M, Aoude-Werner D, Hasselmann C. 2005.  $\alpha$ -Ribazole, a fluorescent marker for the liquid chromatographic determination of vitamin B<sub>12</sub> in foodstuffs. J Chromatogr A 1081:182-189.
  31. Maniatis T, Fritsch EF, Sambrook J. 1982. Introduction of plasmid and bacteriophage lambda into *Escherichia coli*, p 250-251. In Maniatis T, Fritsch EF, Sambrook J (ed),

- Molecular cloning: a laboratory manual. Cold Spring Harbor Laboratory, Cold Spring Harbor, New York.
32. Klock HE, Koesema EJ, Knuth MW, Lesley SA. 2008. Combining the polymerase incomplete primer extension method for cloning and mutagenesis with microscreening to accelerate structural genomics efforts. *Prot-Struct Funct Bioinformat* 71:982-994.
  33. O'Toole GA, Rondon MR, Escalante-Semerena JC. 1993. Analysis of mutants of defective in the synthesis of the nucleotide loop of cobalamin. *J Bacteriol* 175:3317-3326.
  34. Berkowitz D, Hushon JM, Whitfield HJ, Jr., Roth J, Ames BN. 1968. Procedure for identifying nonsense mutations. *J Bacteriol* 96:215-220.
  35. Keller S, Ruetz M, Kunze C, Krautler B, Diekert G, Schubert T. 2014. Exogenous 5,6-dimethylbenzimidazole caused production of a non-functional tetrachloroethene reductive dehalogenase in *Sulfurospirillum multivorans*. *Environmental Microbiology* 16:3361-3369.
  36. Kittaka-Katsura H, Fujita T, Watanabe F, Nakano Y. 2002. Purification and characterization of a corrinoid compound from *Chlorella* tablets as an algal health food. *J Agric Food Chem* 50:4994-4997.
  37. Blanche F, Thibaut D, Couder M, Muller JC. 1990. Identification and quantitation of corrinoid precursors of cobalamin from *Pseudomonas denitrificans* by high-performance liquid chromatography. *Anal Biochem* 189:24-29.
  38. Bradford MM. 1976. A rapid and sensitive method for the quantitation of microgram quantities of protein utilizing the principle of protein-dye binding. *Anal Biochem* 72:248-254.

39. Claas KR, Parrish JR, Maggio-Hall LA, Escalante-Semerena JC. 2010. Functional analysis of the nicotinate mononucleotide:5,6-dimethylbenzimidazole phosphoribosyltransferase (CobT) enzyme, involved in the late steps of coenzyme B<sub>12</sub> biosynthesis in *Salmonella enterica*. *J Bacteriol* 192:145-154.
40. Tabor S, Richardson CC. 1992. A bacteriophage T7 RNA polymerase/promoter system for controlled exclusive expression of specific genes. . *Biotechnology* 24:280-284.
41. Castilho BA, Olfson P, Casadaban MJ. 1984. Plasmid insertion mutagenesis and *lac* gene fusion with mini-Mu bacteriophage transposons. *J Bacteriol* 158:488-495.

## CHAPTER 4

# FACILE ISOLATION OF $\alpha$ -RIBAZOLE FROM VITAMIN B<sub>12</sub> HYDROLYSATES USING BORONATE AFFINITY CHROMATOGRAPHY<sup>3</sup>

---

<sup>3</sup> Mattes, T.A. and J. C. Escalante-Semerena. 2018. *Journal of Chromatography-B*. Accepted.  
This chapter is reprinted with permission from the publisher.

## ABSTRACT

Alpha-ribazole ( $\alpha$ -R) is a unique riboside found in the nucleotide loop of coenzyme B<sub>12</sub> (CoB<sub>12</sub>).  $\alpha$ -R is not an intermediate of the *de novo* biosynthetic pathway of coenzyme B<sub>12</sub>, but some bacteria of the phylum *Firmicutes* have evolved a two-protein system (transporter, kinase) that scavenges  $\alpha$ -R from the environment and converts it to the pathway intermediate  $\alpha$ -RP. Since  $\alpha$ -R is not commercially available, one must either synthesize  $\alpha$ -R, or isolate it from hydrolysates of vitamin B<sub>12</sub> (cyano-B<sub>12</sub>, CNB<sub>12</sub>), so the function of the above-mentioned proteins can be studied. Here we report a facile protocol for the isolation of  $\alpha$ -R from CNB<sub>12</sub> hydrolysates. CNB<sub>12</sub> dissolved in NaOH (5 M) was heated to 85°C for 75 min, then cooled to 4°C for 30 min. The solution was neutralized with HCl (5 M), and the hydrolysate was diluted with an equal volume of ammonium acetate (0.3 M, pH 8.8). Alkaline phosphatase was added and the mixture was incubated at 37°C for 16 h. After incubation, the sample was loaded onto a boronate affinity resin column, washed with ammonium sulfate (0.3 M, pH 8.8), water (to remove residual corrinoids) and finally with formic acid (0.1 M) to release ( $\alpha$ -R). Formic acid was removed by lyophilization, and the final yield of  $\alpha$ -R was 85% from the theoretically recoverable amount. Methods for quantifying the concentration of  $\alpha$ -R are reported.

### *Highlights*

- $\alpha$ -R is not commercially available and is needed for the analysis of a recently discovered  $\alpha$ -R scavenging pathway
- A facile procedure is described for the production of  $\alpha$ -R
- The procedure yields 85% of the theoretically recoverable amount of  $\alpha$ -R from vitamin B<sub>12</sub>
- The procedure reduces 90% of the waste generated by alternative methods

## INTRODUCTION

Coenzyme B<sub>12</sub> (CoB<sub>12</sub>, Figure 4-1A) is the largest coenzyme known, only some microbes synthesize it, and its synthesis requires ~30 enzymes [reviewed in (1)]. The enzyme that catalyzes the penultimate step of the pathway attaches two activated intermediates, one is alpha-ribazole-5'-phosphate ( $\alpha$ -R-5'P,  $\alpha$ -RP; Figure 4-1A, bottom right), the other one is adenosyl-cobinamide-GDP (structure not shown); the product of this reaction is CoB<sub>12</sub>-P. The last enzyme of the pathway removes the 5'-phosphate group of  $\alpha$ -RP yielding the biologically active coenzyme (Figure 4-1A).

Most CoB<sub>12</sub>-synthesizing organisms synthesize  $\alpha$ -RP from 5,6-dimethylbenzimidazole (DMB) (Figure 4-1B). Notably, some *Firmicutes* lack the NaMN:DMB phosphoribosyltransferase (CobT) enzyme, and instead have evolved a DMB-riboside ( $\alpha$ -R, bottom left, Figure 4-1A; UV-Visible spectrum, Figure 4-1C) transporter (*i.e.*, CblT), and a kinase (*i.e.*, CblS) to convert  $\alpha$ -R into  $\alpha$ -RP (2, 3). At present, in-depth biochemical studies of the CblT and CblS enzymes are limited by the fact that  $\alpha$ -R is not commercially available.

Protocols for the chemical synthesis of  $\alpha$ -R and the alkaline release of  $\alpha$ -R from vitamin B<sub>12</sub> have been reported (4, 5). For our initial studies of CblT and CblS enzymes (2) we followed a protocol that hydrolyzed CNB<sub>12</sub> under alkaline conditions to release  $\alpha$ -R, and used reverse-phase liquid chromatography to resolve  $\alpha$ -R from the mixture. The low yield of  $\alpha$ -R generated by this method was likely due to the hydrophilic nature of  $\alpha$ -R and corrinoids, a property that makes it difficult to separate these compounds by reverse-phase chromatography. Hence, we developed a protocol for the isolation of mg amounts of  $\alpha$ -R from hydrolysates of CNB<sub>12</sub> using boronate affinity chromatography (BAC). We took advantage of the rapid and reversible formation of cyclic esters between boronic acids and *cis*-diol containing biomolecules to improve the yield of  $\alpha$ -R. Under alkaline conditions, boronic acids and *cis*-diols form cyclic esters, and these interactions

can be reversed by medium acidification. BAC has been extensively used for the analysis of complex mixtures containing saccharides, ribosylated metabolites, nucleosides and nucleotides (6-9). On average, the protocol described herein yielded 3.5 mg of  $\alpha$ -R per 25 mg of CNB<sub>12</sub> hydrolyzed.

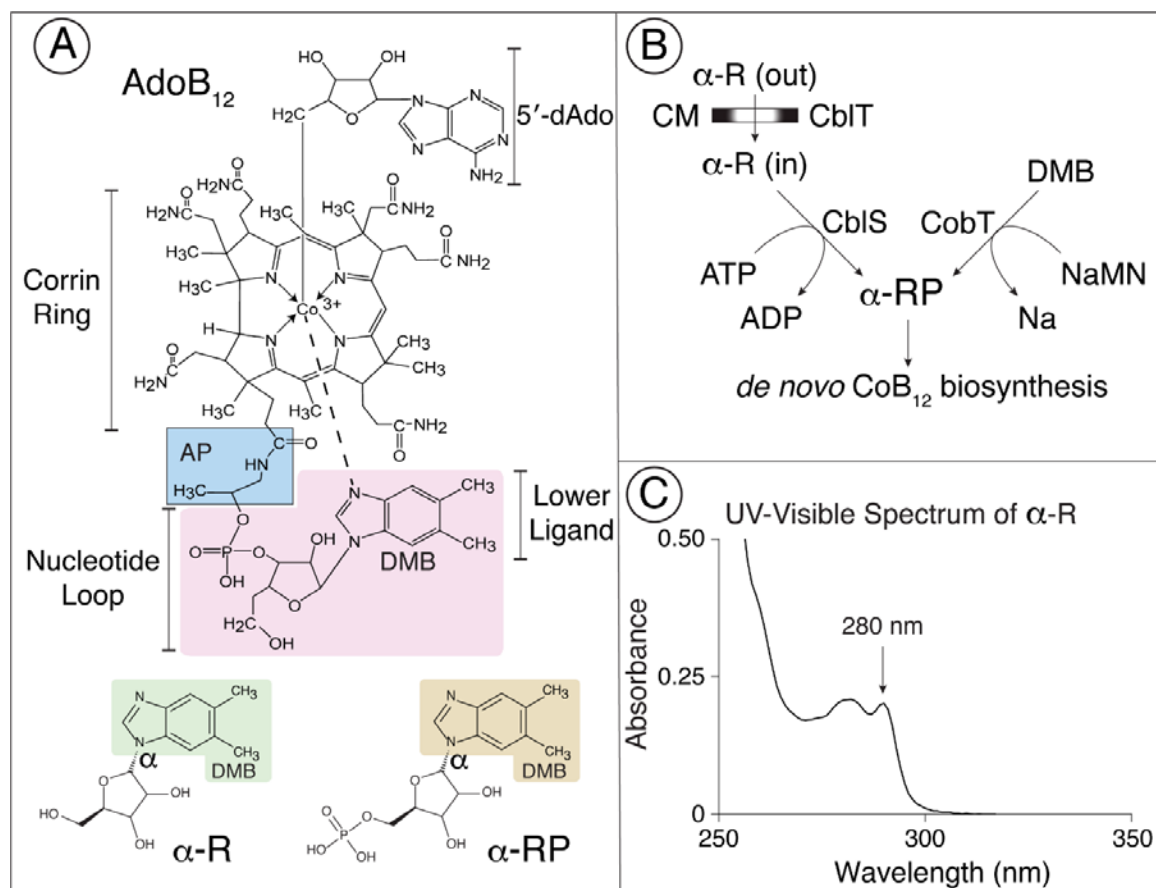


**Figure 4-1. Structure of coenzyme B<sub>12</sub> (CoB<sub>12</sub>), its precursors, and the known routes to  $\alpha$ -R-5'-P.** A (Top). Structure of CoB<sub>12</sub>. The nucleotide loop (pink) containing 5,6-dimethylbenzimidazole (DMB) is tethered to the corrin ring by the aminopropanol (AP; blue) substituent. A (bottom): the DMB riboside  $\alpha$ -R (bottom left) and ribotide  $\alpha$ -R-5'-phosphate ( $\alpha$ -RP; bottom right). B. The two known routes to  $\alpha$ -RP. Abbreviations: cell membrane, CM;  $\alpha$ -R transporter, CblT;  $\alpha$ -R kinase, CblS; DMB:NaMN PRTase, CobT; nicotinate mononucleotide, NaMN; nicotinic acid, Na. C. The UV-visible spectrum of  $\alpha$ -R dissolved in DMSO.

## **MATERIALS AND METHODS.**

### **Reagents**

Immobilized Boronic Acid Gel® (#20244) was obtained from Thermo Fisher Scientific. Unless otherwise indicated, chemicals were obtained from Millipore Sigma. Alkaline phosphatase (ALP) derived from bovine intestinal mucosa was obtained from Millipore Sigma and contains >10 diethanolamine (DEA) units per mg of solid.

### **Bacterial strains**

All bacterial strains and plasmids used in this study are listed in Table B-1 (Appendix B).

### **$\alpha$ -Ribazole synthesis**

#### 2.3.1 Vitamin B<sub>12</sub> preparation and hydrolysis

Vitamin B<sub>12</sub> (CNB<sub>12</sub>; 50 mg; 73.8  $\mu$ mol) was re-suspended in 5 mL of water that was deionized using a MilliQ Water Purification System (Millipore). After transferring the solution into a screw-capped 250-mL Erlenmeyer flask, either 5 mL of NaOH (5 M) or water was added to the mixture. The resulting solution was placed in a water bath (85-90°C) for 75 min. After cooling for 30 min at 4°C, the solution was neutralized with HCl (5 M) prior to dephosphorylation by alkaline phosphatase (ALP). To determine the amount of  $\alpha$ -R release, a 5- $\mu$ L sample was taken at each step; samples were diluted 100-fold prior to measuring fluorescence at 312 nm (Appendix B-1.2).

#### 2.3.2 De-phosphorylation of $\alpha$ -R-3'-P

To convert  $\alpha$ -R-3'-P to its riboside, ALP was added to the solution. Fifteen mL of a solution containing [(NH<sub>4</sub>)Ac (0.3 M), MgCl<sub>2</sub> (2 mM, pH 8.8) was added to the hydrolysate. ALP was added in excess (>1000 U; 1U = amount of enzyme that hydrolyses 1  $\mu$ mol of nitrophenyl-phosphate per minute at 37°C) and the solution was incubated at 37°C for at least 16 h. The

resulting solution was centrifuged at 3,220 x g for 20 min and the supernatant was filtered using a syringe filter (0.45  $\mu$ m polyethersulfone membrane; VWR).

### 2.3.3. Boronate affinity chromatography (BAC)

After ALP treatment,  $\alpha$ -R was isolated by passing the solution over a boronate column as described (10) with some modifications. Briefly, a 1.5-mL column of Immobilized Boronic Acid Gel® (Thermo Fisher Scientific; 110  $\mu$ mol AMP binding capacity/mL of resin) was equilibrated with (NH<sub>4</sub>)Ac (0.3 M, pH 8.8). The hydrolysate mixture was passed over the column, and the column was washed with (NH<sub>4</sub>)Ac (0.3 M, pH 8.8) until the eluate was clear. The column appeared slightly pink likely due to non-specific binding of a corrinoid. The column was washed with 1.5 mL of MilliQ water to remove (NH<sub>4</sub>)Ac. Bound  $\alpha$ -R was desorbed with formic acid (0.1 M; 6-mL). The column was regenerated between cycles with five column volumes of formic acid (0.1 M) and five column volumes of (NH<sub>4</sub>)Ac (0.3 M, pH 8.8). As per the manufacturer's instructions, the resin can be used for up to 10 cycles but should be discarded if it remains colored after regeneration.

### 2.3.4. Product concentration

The eluent (3 mL) was shell-frozen in a 50-mL conical tube (VWR) over a mixture of ethanol and dry ice. Parafilm was used to seal the end of the tube and punctured 5-6 times before lyophilization that resulted in a white crystalline powder. The dry product was re-suspended on 200  $\mu$ L dimethyl sulfoxide (DMSO), and the  $\alpha$ -R final concentration and yield were determined by measuring fluorescence (Appendix B-1.2) or absorbance (Appendix B-1.3.2). The final product was analyzed by MALDI-TOF mass spectrometry to confirm its identity. The biological activity of the product was assessed by bioassay (Appendix B-1.5).

## RESULTS AND DISCUSSION

### CNB<sub>12</sub> hydrolysis conditions

In other described protocols, alkaline hydrolysis of CNB<sub>12</sub> is performed at 100°C for 50 min (2). We tested whether heating at a lower (85°C) or higher temperature (121°C at 124.1 kPa) would make a difference in the yield of  $\alpha$ -R. Six samples of CNB<sub>12</sub> were prepared using ultrapure water (10 mg mL<sup>-1</sup>) in screw-capped 250-mL Erlenmeyer flasks (2.3.1). The initial CNB<sub>12</sub> concentration was needed to determine the theoretical  $\alpha$ -R yield (Appendix B-1.1). From 100 mg of CNB<sub>12</sub>, we calculated a maximum yield of ~21 mg of  $\alpha$ -R.

To assess the impact of NaOH on  $\alpha$ -R release, an equal volume (5 mL) of water or NaOH was added to each flask containing dissolved CNB<sub>12</sub> (50 mg; ~7.4 mM). Three sets of hydrolysis mixtures, each with two replicates, were incubated at different temperatures: i) room temperature (25°C, benchtop), ii) 85°C (water bath), and iii) 121°C (45-min autoclave cycle, 124.1 kPa). The samples that were not autoclaved were incubated for 75 min at the stated temperature, followed by a 30-min cooling time at 4°C. The period of incubation (75 min) was chosen to match the duration of a 45-min autoclave cycle. Using fluorescence and the calculated quantum yield for  $\alpha$ -R (Appendix B-1.2), the amount of  $\alpha$ -R released was compared to an expected yield of ~10 mg. In the absence of NaOH, the amount of  $\alpha$ -R released was negligible regardless of the method of heating used (data not shown).

The results for  $\alpha$ -R release under alkaline conditions under the different conditions are shown in Table 4-1. An average of 0.3 mg of  $\alpha$ -R (*i. e.*, 2.5% of the theoretical yield) was detected following treatment at room temperature (25°C). Growth was detected by the corrinoid scavenging assay (Appendix B-1.4), indicating incomplete CNB<sub>12</sub> hydrolysis.

**Table 4-1. Comparison of the estimated amount of  $\alpha$ -R released under different hydrolysis conditions.**

<b>Heating Treatment</b>	<b>Sample</b>	<b>Starting Material</b>	<b><math>\alpha</math>-R Expected (mg)</b>	<b><math>\alpha</math>-R Released (mg)</b>	<b>% Released</b>
Room temperature (25 °C)	#1	CNB <sub>12</sub> (50 mg)	10.4	0.3	2.7%
	#2	CNB <sub>12</sub> (50 mg)	10.4	0.2	2.3%
	<b>Average</b>		<b>10.4</b>	<b>0.3</b>	<b>2.5%</b>
Water Bath (85 °C)	#1	CNB <sub>12</sub> (50 mg)	10.4	8.4	80.8%
	#2	CNB <sub>12</sub> (50 mg)	10.4	8.0	77.2%
	<b>Average</b>		<b>10.4</b>	<b>8.2</b>	<b>79.0%</b>
Autoclave (121 °C)	#1	CNB <sub>12</sub> (50 mg)	10.4	8.5	82.1%
	#2	CNB <sub>12</sub> (50 mg)	10.4	8.4	81.4%
	<b>Average</b>		<b>10.4</b>	<b>8.5</b>	<b>81.8%</b>

At 85°C, 8.2 mg of  $\alpha$ -R (*i.e.*, 79% of the theoretical yield) was detected while 8.5 mg of  $\alpha$ -R (*i.e.*, 82% of the theoretical yield) was detected in the autoclaved samples. The B<sub>12</sub> indicator strain did not grow when a sample of the solution of CNB<sub>12</sub> that was heated at 85°C was added to the culture medium. We observed a similar response when a sample of the CNB<sub>12</sub> solution that was autoclaved was added to the culture medium (Appendix B-1.4). We interpreted these results to mean that the indicator strain could not repair the damage done to CNB<sub>12</sub> under the conditions used. Because autoclave hydrolysate products could not be removed from the boronate resin, autoclave treatment was discontinued for the remainder of the study.

### **3.2 No loss of $\alpha$ -R was detected in an ALP-treated CNB<sub>12</sub> solution.**

Alkaline hydrolysis of CNB<sub>12</sub> resulted in a mixture of the riboside  $\alpha$ -R and  $\alpha$ -R-3'-P (5). To increase the concentration of  $\alpha$ -R, ALP was used to dephosphorylate  $\alpha$ -R-3'-P (2.3.2). After overnight incubation at 37°C, samples were clarified by centrifugation (15 min, 3000 x *g*) and filtration. Quantification of free  $\alpha$ -R by fluorescence (Appendix B-1.2) indicated no change following ALP treatment.

#### **3.2.1. Resolving $\alpha$ -R from other hydrolysis products.**

A method previously used by our laboratory relied on reverse-phase chromatography (Lichroprep® RP-18, Merck) to resolve products using a methanol gradient (2). That procedure generated large volumes (0.5 L), with  $\alpha$ -R distributed in 20% of the fractions collected. In addition,  $\alpha$ -R eluted off the column together with an unidentified corrinoid. To expedite the resolution of  $\alpha$ -R from other hydrolysis products, we switched to boronate affinity chromatography (2.3.3). The specificity of boronate for *cis*-diol-containing compounds has been used for decades to separate nucleotides, nucleosides, catechols, carbohydrates, glycoproteins, etc (11-13). Interactive compounds (in our case  $\alpha$ -R) bind to the resin at alkaline pH and compounds are released from the column by acidification. Here, we used a described batch BAC method to rapidly decrease the pH from 8.8 to 3 (10).

#### **3.2.2. $\alpha$ -R concentration and yield quantification.**

Following elution from the resin, the  $\alpha$ -R-containing fraction (confirmed by bioassay) was concentrated by lyophilization (2.3.4) and re-suspended in dimethyl sulfoxide (DMSO). MALDI-TOF mass spectrometry of the isolated product revealed a mass of 279.2 Da (Figure B-4), consistent with the theoretical mass of  $\alpha$ -R (278.3 Da). We quantified the yield of  $\alpha$ -R by fluorescence (Appendix B-1.2).

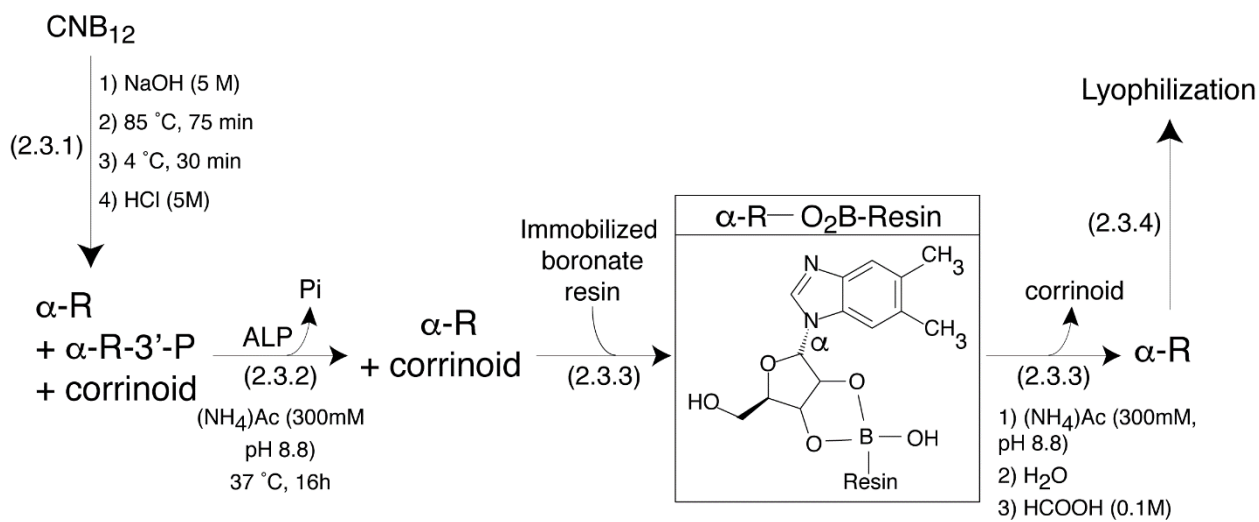


**Figure 4-2. Schematic of the process for the isolation of  $\alpha$ -R synthesis from CNB<sub>12</sub> hydrolysates.** The section corresponding to each step is found in parentheses. Corrinoid refers to the inactive CNB<sub>12</sub> derivative. Abbreviations: alkaline phosphatase, ALP; formic acid, HCOOH; ammonium acetate, (NH<sub>4</sub>)Ac;  $\alpha$ , refers to the configuration of the *N*-glycosidic bond.

**Table 4-2. A comparison to the previously published yield as determined by absorbance (Appendix B 1.3.2)**

<b>Comparison</b>	<b>Starting Material</b>	<b><math>\alpha</math>-R Expected (mg)</b>	<b>Yield (mg)</b>	<b>% Yield</b>	<b>% Yield, Adjusted<sup>1</sup></b>
Lichroprep® RP-C18/ solid phase extraction [2]	CNB <sub>12</sub> (100 mg)	20.5	8.0	39%	49%
Immobilized boronate/ lyophilization	CNB <sub>12</sub> (50 mg)	10.3	6.9	67%	85%

<sup>1</sup> Adjusted to the maximum release of  $\alpha$ -R from CNB<sub>12</sub> in a water bath (79%)

Assuming diol equivalency between AMP and  $\alpha$ -R, a 1.5-mL column of immobilized boronate was estimated to have an  $\alpha$ -R capacity of 46 mg. From a freshly-prepared column loaded with 8.2 mg of  $\alpha$ -R, we recovered 6.2 mg of  $\alpha$ -R, a recovery of 76%. The recovered  $\alpha$ -R was active in our bioassay (Appendix B-1.5), supporting similar growth rates to previously isolated, equimolar concentrations of  $\alpha$ -R (Figure B-5).

## **CONCLUSIONS.**

The boronate-affinity chromatography method for the isolation of  $\alpha$ -R described herein (Figure 4-2) is rapid, minimizes the amount of waste, and generates mg amounts of this coenzyme B<sub>12</sub> precursor. Two significant improvements of BAC over the reverse phase chromatography method described elsewhere (2) were a higher yield of  $\alpha$ -R (36% higher; Table 4-2), and a 10-fold reduction in sample volume.

We anticipate this method to be adaptable for the isolation of different  $\alpha$ -ribosides (other than  $\alpha$ -R) present in cobamides synthesized by different microbes (14, 15). This method could also be

adapted for the identification of lower ligands in a population sample (16), as an alternative to reverse phase chromatography for the separation of cobamides (3).

## ACKNOWLEDGEMENTS

We thank Vincent Starai for the use of fluorescence microplate reader. Technical assistance for mass spectrometry were provided by Dr. Dennis Phillips and the University of Georgia Proteomics and Mass Spectrometry Core Facility. This work was supported by National Institutes of Health grant R37 GM040313 to J.C.E.-S. Declaration of Interest: None.

## REFERENCES

1. Mattes TA, Deery E, Warren MJ, Escalante-Semerena JC. 2017. Cobalamin Biosynthesis and Insertion, p 1-24. *In* Scott RA (ed), Encyclopedia of Inorganic and Bioinorganic Chemistry doi:10.1002/9781119951438.eibc2489. John Wiley & Sons, Ltd, Chichester, UK.
2. Gray MJ, Escalante-Semerena JC. 2010. A new pathway for the synthesis of alpha-ribazole-phosphate in *Listeria innocua*. *Mol Microbiol* 77:1429-1438.
3. Mattes TA, Escalante-Semerena JC. 2017. *Salmonella enterica* synthesizes 5,6-dimethylbenzimidazolyl-(DMB)-alpha-riboside. Why some *Firmicutes* do not require the canonical DMB activation system to synthesize adenosylcobalamin. *Mol Microbiol* 103:269-281.
4. Brown KL, Zou X, Banka RR, Perry CB, Marques HM. 2004. Solution Structure and Thermolysis of Co $\beta$ -5'-Deoxyadenosylimidazolylcobamide, a Coenzyme B12 Analogue with an Imidazole Axial Nucleoside. *Inorg Chem* 43:8130-8142.

5. Pakin C, Bergaentzle M, Aoude-Werner D, Hasselmann C. 2005.  $\alpha$ -Ribazole, a fluorescent marker for the liquid chromatographic determination of vitamin B<sub>12</sub> in foodstuffs. *J Chromatogr A* 1081:182-189.
6. James TD, Sandanayake KRAS, Shinkai S. 1996. Saccharide sensing with molecular receptors based on boronic acid. *Angew Chem Int Ed* 35:1910-1922.
7. Li H, Wang H, Liu Y, Liu Z. 2012. A benzoboroxole-functionalized monolithic column for the selective enrichment and separation of cis-diol containing biomolecules. *Chem Commun (Camb)* 48:4115-4117.
8. Elstner M, Weisshart K, Mullen K, Schiller A. 2012. Molecular logic with a saccharide probe on the few-molecules level. *J Am Chem Soc* 134:8098-8100.
9. Jiang HP, Qi CB, Chu JM, Yuan BF, Feng YQ. 2015. Profiling of *cis*-diol-containing nucleosides and ribosylated metabolites by boronate-affinity organic-silica hybrid monolithic capillary liquid chromatography/mass spectrometry. *Sci Rep* 5:7785.
10. Pfadenhauer EH, Tong S-D. 1979. Determination of inosine and adenosine in human plasma using high-performance liquid chromatography and a boronate affinity gel. *J Chromatog B: Biomedl Sci Appl* 162:585-590.
11. Weith HL, Wiebers JL, Gilham PT. 1970. Synthesis of cellulose derivatives containing the dihydroxyboryl group and a study of their capacity to form specific complexes with sugars and nucleic acid components. *Biochemistry* 9:4396-401.
12. Soundararajan S, Badawi M, Kohlrust CM, Hageman JH. 1989. Boronic acids for affinity chromatography: spectral methods for determinations of ionization and diol-binding constants. *Anal Biochem* 178:125-134.

13. Bongartz D, Hesse A. 1995. Selective extraction of quercetrin in vegetable drugs and urine by off-line coupling of boronic acid affinity chromatography and high-performance liquid chromatography. *J Chromatogr B Biomed Appl* 673:223-230.
14. Hoffmann B, Oberhuber M, Stupperich E, Bothe H, Buckel W, Konrat R, Kräutler B. 2000. Native corrinoids from *Clostridium cochlearium* are adeninylcobamides: spectroscopic analysis and identification of pseudovitamin B(12) and factor A. *J Bacteriol* 182:4773-4782.
15. Stupperich E, Kräutler B. 1988. Pseudo vitamin B12 or 5-hydroxybenzimidazolylcobamide are the corrinoids found in methanogenic bacteria. *Arch Microbiol* 149:213-217.
16. Crofts TS, Men Y, Alvarez-Cohen L, Taga ME. 2014. A bioassay for the detection of benzimidazoles reveals their presence in a range of environmental samples. *Front Microbiol* 5:592.

## CHAPTER 5

FUNCTIONAL STUDIES OF  $\alpha$ -RIBOSIDE ACTIVATION BY THE  $\alpha$ -R KINASE CBL5  
FROM *GEOBACILLUS KAUSTOPHILUS* CONFIRM THE EXCLUSIVE SYNTHESIS OF  
5,6-DIMETHYLBENZIMIDAZOLYL- $\alpha$ -RIBOSIDE BY *SALMONELLA ENTERICA*<sup>4</sup>

---

<sup>4</sup> Mattes, T.A. and J. C. Escalante-Semerena. To be submitted to *Journal of Bacteriology*

## ABSTRACT.

Different forms of the coenzyme B<sub>12</sub> exist in nature, with variations in the identity of the lower ligand. This nucleotide contains an  $\alpha$ -N-glycosidic linkage between a base and ribose-5'-phosphate, a unique bond found *only* in coenzyme B<sub>12</sub>. In *Salmonella enterica*, the base is typically either the purine adenine (ADE) or the purine analog 5,6-dimethylbenzimidazole (DMB). The base must be activated to its ribotide form to synthesize the coenzyme, and typically proceeds via a direct activation in organisms like *S. enterica*. However, some *Firmicutes* have evolved a way to scavenge the  $\alpha$ -riboside form of the base from the environment, transporting it via the protein CblT and activating it to the ribotide via an ATP-utilizing kinase, CblS. Heterologous expression of the CblT/CblS system from *Geobacillus kaustophilus* in an *S. enterica* strain unable to directly activate the base revealed that *S. enterica* could synthesize the DMB-riboside  $\alpha$ -Ribazole ( $\alpha$ -R) endogenously. It is not known how this riboside is synthesized, or why *only*  $\alpha$ -R is synthesized in *S. enterica*.

Here, we report that *Gk* CblS can activate any riboside carrying an  $\alpha$ -N-glycosidic linkage, confirmed *in vivo*. No activation occurred when a DMB-riboside featuring a  $\beta$ -N-glycosidic bond was provided, indicating it is the N-glycosidic bond and not the base which dictates whether the kinase can phosphorylate the riboside. Curiously, an *S. enterica* strain expressing the kinase in place of the direct activation could utilize the ADE-containing  $\alpha$ -Ado, but it required nearly four orders of magnitude more riboside than other  $\alpha$ -ribosides.  $\alpha$ -Ado was activated by whole cell extract from these strains, with no detectable catabolism of the riboside, indicating a potential transport issue. These results confirm that *S. enterica* does not make  $\alpha$ -Ado. Alanine scanning of conserved residues to generate catalytic variants of the *Gk* CblS kinase yielded two potential variants for probing how *S. enterica* synthesizes DMB and  $\alpha$ -R.

## INTRODUCTION.

The final steps of coenzyme B<sub>12</sub> (adenosylcobalamin, AdoCbl) biosynthesis requires the condensation of two precursors: the activated ring precursor AdoCbi-GDP and an  $\alpha$ -N-linked ribotide, such as  $\alpha$ -ribazole-5'-phosphate ( $\alpha$ -RP) (1). In *Salmonella enterica*, synthesis of this  $\alpha$ -RP from its base, 5,6-dimethylbenzimidazole (DMB), is catalyzed by the DMB: nicotinate mononucleotide (NaMN) phosphoribosyltransferase (PRTase, CobT) (2, 3). Ribose-5'-phosphate (R5P) is transferred from nicotinate to DMB, inverting the N-glycosidic bond (4). CobT can activate a variety of bases, including adenine and DMB (5-7). However, some *Firmicutes* lack the DMB: NaMN PRTase enzyme. Instead, they appear to use a pair of proteins, CblT and CblS, as a transporter and kinase, to scavenge  $\alpha$ -ribazole ( $\alpha$ -R) from the environment (8). (See Figure 3-6, reproduced below.)

As reported (9), the  $\alpha$ -R kinase and transporter from *Geobacillus kaustophilus* can compensate for the loss of CobT in *S. enterica*. These results suggest that *S. enterica* makes  $\alpha$ -ribazole, which was unexpected. To better understand how *S. enterica* makes  $\alpha$ -R, it is necessary to understand the parameters by which the kinase CblS phosphorylates the  $\alpha$ -riboside. Of interest is why *Gk* CblS only appears to be activating the DMB-containing  $\alpha$ -R in *S. enterica*.

Considering the noted promiscuity of CobT, it seems strange that CblT/CblS would be limited to activation of only  $\alpha$ -R. For instance, *Lactobacillus coryniformis* CRL1001 synthesizes pseudocobalamin (pseudoCbl), the adenine-containing cobamide (10). Curiously, *L. coryniformis* does not have a functional CobT homolog as the gene encoding the PRTase is disrupted (ATO00\_12005). Instead, *L. coryniformis* carries *cbIS* (ATO00\_09620) and *cbIT* (ATO00\_09490). So presumably, in this organism, CblS can activate an  $\alpha$ -N-linked adenosine ( $\alpha$ -Ado) to the ribotide and condense that with AdoCbi-GDP to synthesize pseudoCbl.

So why not in *S. enterica*? It is possible that *S. enterica* does not have enough free adenine base in the cell to permit synthesis (11). Directly feeding the riboside  $\alpha$ -Ado could force *S. enterica* to synthesize pseudoCbl, assuming *Gk* CblS can phosphorylate  $\alpha$ -Ado.

Here, we report the *Gk* CblS kinase can activate only ribosides with an  $\alpha$ -N-glycosidic linkage *in vitro*. Curiously, possible transport issues may interfere with the ability of the CblS kinase to activate other  $\alpha$ -ribosides in *S. enterica*. We also report on some initial work to generate catalytic variants, and some variants may prove useful tools for understanding how *S. enterica* synthesizes  $\alpha$ -ribosides.

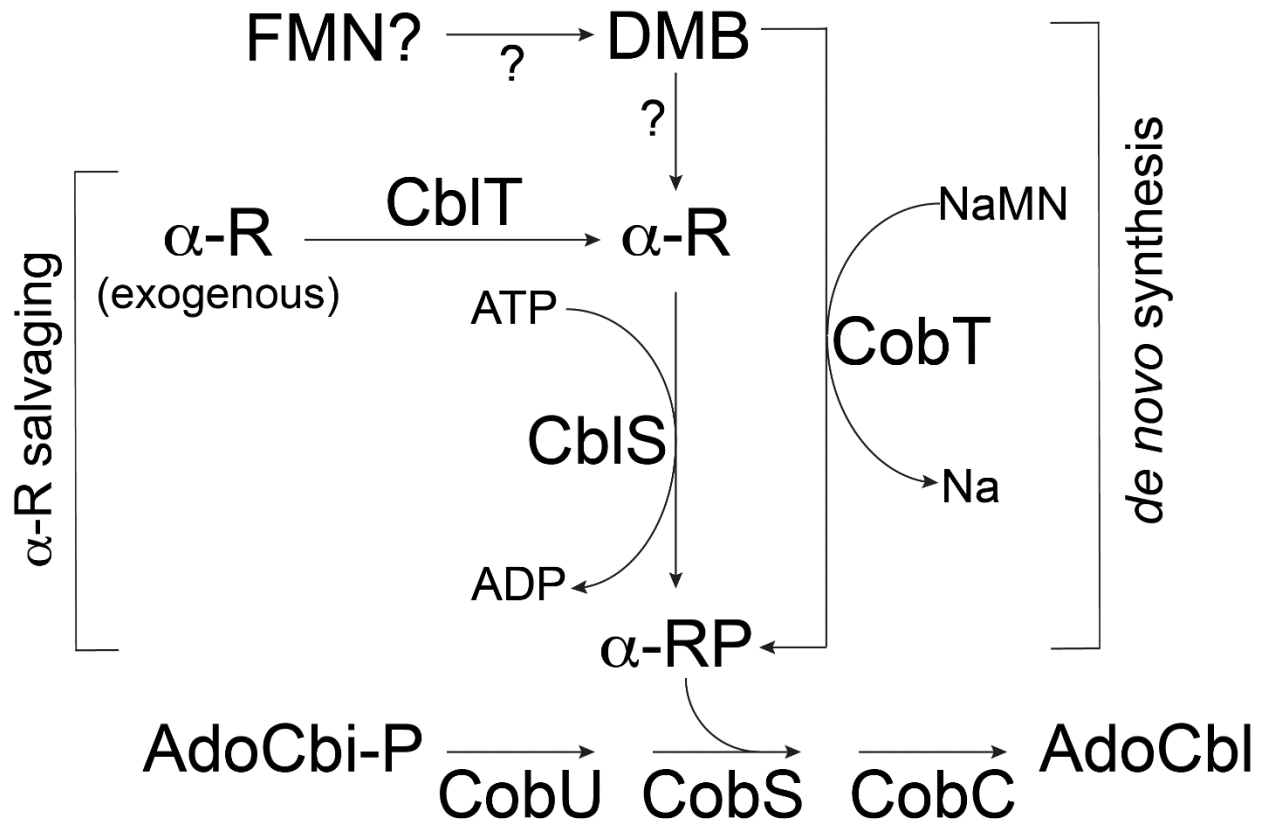


**Figure 3-6 (Reprinted).** Expanded view of  $\alpha$ -RP biosynthesis via direct DMB activation or  $\alpha$ -R scavenging. The presence of both the CobT-dependent synthesis of  $\alpha$ -RP and the CbITS proteins in a single organism (*e.g.*, *G. kaustophilus*) may be an indicator of the presence of  $\alpha$ -R in the environment. As shown in the prior study (9), *S. enterica* can convert DMB to  $\alpha$ -R via an unknown mechanism. Other bacteria, like *G. kaustophilus*, may also be able to convert DMB to  $\alpha$ -R, thus expanding the role of the CbITS system from salvaging to *de novo* synthesis. In *S. enterica*, it is proposed that DMB can be derived from FMN, but the enzymes involved have not been identified. Abbreviations: FMN, flavin mononucleotide; CobU, NTP:Ado-cobinamide kinase and NTP:Ado-cobinamide-phosphate guanylyltransferase; CobS, AdoCbl-phosphate synthase; CobC, Ado-Cba-P phosphatase.

## **MATERIALS AND METHODS.**

### **Reagents.**

Unless otherwise indicated, chemicals were obtained from Sigma Millipore. Authentic  $\alpha$ -ribazole was synthesized as reported (12).  $\alpha$ -Ribosides and  $\beta$ -ribazole were synthesized as described below. The alkaline phosphatase (ALP; from bovine intestinal mucosa; Millipore Sigma) used for dephosphorylating ribotides contains >10 diethanolamine (DEA) units per mg of solid. Immobilized Boronic Acid Gel® (#20244) for purifying ribosides was obtained from Thermo Fisher Scientific.

### **Bacterial strain construction.**

The bacterial strains and plasmids used in this work are found in Table 5-1. Transformations were performed as described (13).

### **Plasmid construction.**

The sequences of the primers used in this study are listed in Table 5-2. DNA amplification, restriction digestion, and ligation were performed according to manufacturer's instructions. Site-directed mutagenesis was performed using primers designed using PrimerX (available at <http://www.bioinformatics.org/primerx/>) to modify conserved residues predicted to be involved in ATP binding for *Gk CblS*<sup>WT</sup> (R46, V47, E51, T94, S96, E98, S174, and E180) to an alanine residue in both the over-expression (p*GkCblS*2) and complementation (p*GkCblS*3) vectors. The plasmids, which were successfully modified and are confirmed by sequencing, are reported in Table 5-1. The hexahistidine tag of *Gk CblS* and *Stm DeoD* adds the following protein sequence (~3 kDa) to the N-terminus of the protein: MSYYHHHHHDYDIPTSENLYFQG (14).

### **Preparation of $\alpha$ -adenosine and $\alpha$ -benzimidazolyl-ribosides.**

The CobT enzyme of *S. enterica* was purified as described (3). The reaction mixture (800  $\mu$ L) contained CHES buffer (pH 9.5, 100 mM), enzyme (30  $\mu$ g), base (4 mM), and nicotinate mononucleotide (NaMN; 2.5 mM). The reaction proceeded at 37 °C for 16+ h. 10 U of ALP was added to cleave the 5' phosphate, and the reaction was incubated at 37 °C for 16+ h. A shift to 100 °C for 15 min followed by centrifugation (15 min; 15k x g) terminated the reactions. The reaction was diluted with loading buffer (1.6 mL) containing ammonium acetate (300 mM, pH 8.8) and magnesium chloride (2 mM), and passed over a column containing equilibrated immobilized boronate resin (0.25 mL; Thermofisher Scientific). Following a wash with five column volumes of loading buffer, the ribosides were eluted with formic acid (1.5 mL). The eluate was lyophilized, resuspended in DMSO (100%), and quantified using absorbance as described (12), using the wavelengths and coefficients found in Table 5-3.

### **pStmDeoD1 construction.**

*S. enterica deoD* (*stm4570*) was amplified from genomic DNA by Phusion polymerase using the primers Stm\_DeoD\_BspQI\_5' and Stm\_DeoD\_BspQI\_3'. The resulting DNA product was cloned into the BspQI site of pTEV18 as described (15) and confirmed by sequencing.

### **Over-production and purification of hexahistidine-tagged *Stm* DeoD.**

pStmDeoD1 was transformed into JE13607 (*E. coli* BL21 *cobT::kan*) (16). Cells were grown in Terrific Broth (50 mL; 250-mL flask) for 16 h at 37 °C and harvested by centrifugation (20 min; 3000 x g) using an Eppendorf 5810 R benchtop centrifuge. The cell pellet was stored at -20 °C until needed.

A lysis buffer solution of BugBuster® reagent (Novagen) was prepared by diluting the concentrated solution (10x) in a binding buffer containing Tris (50 mM, pH 8), NaCl (500 mM),

and imidazole (4 mM). A 1:4 ratio (m/v) of the cell pellet to lysis buffer was used to resuspend the harvested cells. The cell suspension was incubated for 30 min (25 °C) in a Roto-Bot programmable rotator (Program F1, Speed 25; Benchmark). The suspension was centrifuged (2hr; 43,000 x g) using an Avanti J-25I floor centrifuge with a JA-25.25 rotor (Beckman Coulter).

The cell-free lysate was loaded on to Ni-NTA affinity resin (2.5 mL; HisPur; ThermoFisher Scientific). The column was washed with six column volumes of binding buffer (as described above) and washing buffer [Tris (50 mM, pH 8), NaCl (500 mM), and imidazole (60 mM)]. An elution buffer [Tris (50 mM, pH 8), NaCl (500 mM), and imidazole (400 mM)] was used to dislodge the H6-tagged *Stm* DeoD from the resin. The eluate was dialyzed against Tris-HCl (50 mM, pH 8) buffer three times. The first dialysis also contained EDTA (10 mM) for nickel chelation. The last dialysis contained glycerol (5% v/v). The final protein concentration was quantified using a microtiter plate protocol for the Bradford protein assay using a commercially available kit (BioRad). Purified protein was flash frozen in liquid nitrogen and stored at -80 °C.

### **Preparation of $\beta$ -ribazole.**

A reaction mixture (1-mL) containing potassium phosphate dibasic (50 mM, pH 7), *Stm* DeoD (10  $\mu$ g), guanosine (2.5 mM), and DMB (5 mM) was prepared and incubated at 37 °C for 16 h. The reaction mixture was diluted with loading buffer (1 mL) containing ammonium acetate (300 mM, pH 8.8) and magnesium chloride (2 mM), and passed over a column containing equilibrated immobilized boronate resin (0.25 mL; Thermofisher Scientific) and washed with five additional column volumes of loading buffer.  $\beta$ -R was eluted with formic acid (1.5 mL). The eluate was lyophilized and resuspended in DMSO (10%). The product was purified from any remaining guanosine by HPLC separation as described for the separation of ribotides in (9). Guanosine elutes at 3.7 min while  $\beta$ -R elutes at 18.5 min. Fractions containing  $\beta$ -R were pooled and desalted using

a SepPak C18 Plus (Waters). The  $\beta$ -R was eluted on methanol and dried under vacuum using an Eppendorf VacuFuge. The final product was resuspended in DMSO (100%) and quantified using absorbance spectroscopy as previously described (12) using the extinction coefficient of DMB on DMSO (Table 5-3).

### **Over-production and purification of hexahistidine-tagged *Gk* CblS.**

Cells containing over-produced *Gk* CblS were harvested as previously reported (9). Cell pellets were resuspended in binding buffer containing potassium phosphate dibasic (50 mM, pH 7.2), potassium chloride (350 mM), imidazole (10 mM), glycerol (5%), tris(2-carboxyethyl)phosphine (TCEP, 0.5 mM), and Triton X-100 (0.5%) at 25 °C. The cell paste to buffer ratio was 1:10 (m/v). The suspension was passed over a cell disruptor twice at 172,000 kPa. Cell debris was removed by centrifugation (1 hr; 15,000  $\times$  g) using an Avanti J-25I floor centrifuge with a JA-25.25 rotor (Beckman Coulter). The supernatant was passed over a polyethersulfone (PES) syringe filter (0.45- $\mu$ m; VWR) to remove any remaining debris. The cell pellet was resuspended in the binding buffer (5 mL) and centrifuged again. The supernatant was passed over a PES syringe filter (0.45  $\mu$ m; VWR) to remove any remaining debris and pooled with the first supernatant.

The cell-free lysate was loaded onto Ni-NTA affinity resin (5 mL; HisPur; ThermoFisher Scientific). The column was washed with three column volumes each of binding buffer [potassium phosphate dibasic (50 mM), potassium chloride (350 mM), imidazole (10 mM), glycerol (5%), TCEP (0.5 mM), pH 7.2 at 25 °C] and washing buffer [potassium phosphate dibasic (50 mM), potassium chloride (350 mM), imidazole (15 mM), glycerol (5%), TCEP (0.5 mM), pH 7.2 at 25 °C]. *Gk* CblS was eluted with four column volumes of elution buffer [potassium phosphate dibasic (50 mM), potassium chloride (350 mM), imidazole (750 mM), glycerol (5%), TCEP (0.5 mM), pH 7.2 at 25 °C]. The eluate was dialyzed against decreasing salt concentrations to 100 mM KCl.

The first dialysis also included EDTA (10 mM) for nickel chelation. The final protein concentration was quantified using a microtiter plate protocol for the Bradford protein assay using a commercially available kit (BioRad). Purified protein was flash frozen in liquid nitrogen and stored at -80 °C. The hexahistidine tag was not cleaved from H6-*GkCbIS* as it does not separate from the recombinant rTEV protease (14).

#### **Gel permeation FPLC analysis.**

H6-*GkCbIS* (125 µg) was injected onto a Superose 12 10/300 gel filtration column (GE Healthcare Life Sciences) connected to an ÄKTApurifier fast protein liquid chromatography (FPLC) system (GE Healthcare Life Sciences). The column was equilibrated with a buffer containing HEPES (4-(2-hydroxyethyl)piperazine-1-ethanesulfonic acid, 50 mM, pH 7.5), potassium chloride (250 mM), magnesium chloride (5 mM), *tris*(2-carboxyethyl)phosphine (TCEP, 2.5 mM). A flow rate of 0.5 mL min<sup>-1</sup> was used to develop the column, and a mixture of standards (BioRad) was applied to the column to generate a calibration curve. Elution was monitored at 280 nm, and the final analysis was performed using UNICORN 4.11 software (GE Healthcare Life Sciences).

**Table 5-1. Strains and plasmids used in this study.**

Strains	Antibiotic resistance	Relevant genotype	Reference or source
<i>E. coli</i> strains <sup>1</sup>			
DH5 $\alpha$ /F'			
JE13607	Km <sup>R</sup>	BL21 ( $\lambda$ DE3) <i>cobT762::kan<sup>+</sup></i>	(16)
<i>S. enterica</i> strains <sup>2</sup>			
TR6583		<i>metE205 ara-9</i>	K. Sanderson via J. Roth
JE7088		$\Delta$ <i>metE2702 ara-9</i>	Lab collection
JE12939		$\Delta$ <i>metE2702 ara-9</i> $\Delta$ <i>cobT1380</i> $\Delta$ <i>cobB1375</i>	Lab collection
JE17827	Ap <sup>R</sup>	$\Delta$ <i>metE2702 ara-9</i> $\Delta$ <i>cobT1380</i> $\Delta$ <i>cobB1375</i> / pBAD24	(9)
JE17830	Ap <sup>R</sup>	$\Delta$ <i>metE2702 ara-9</i> $\Delta$ <i>cobT1380</i> $\Delta$ <i>cobB1375</i> / pGkCblTS2	(9)
JE21364	Ap <sup>R</sup>	$\Delta$ <i>metE2702 ara-9</i> $\Delta$ <i>cobT1380</i> $\Delta$ <i>cobB1375</i> / pGkCblS3	(9)
Plasmids			
pBAD24	Ap <sup>R</sup>	Cloning vector with P <sub>araBAD</sub> arabinose-inducible promoter	(17)
pTEV18	Ap <sup>R</sup>	TEV protease-cleavable His <sub>6</sub> tag overexpression vector	(14, 15)
pGkCblTS2	Ap <sup>R</sup>	<i>G. kaustophilus cblT<sup>+</sup> cblS<sup>+</sup></i> in pBAD24	(9)
pGkCblS2	Ap <sup>R</sup>	<i>G. kaustophilus cblS<sup>WT</sup></i> translational fusion to His <sub>6</sub> tag for protein purification in pTEV5	(9)
pGkCblS2 T94A	Ap <sup>R</sup>	<i>G. kaustophilus cblS<sup>T94A</sup></i> translational fusion to His <sub>6</sub> tag for protein purification in pTEV5	
pGkCblS2 E98A	Ap <sup>R</sup>	<i>G. kaustophilus cblS<sup>E98A</sup></i> translational fusion to His <sub>6</sub> tag for protein purification in pTEV5	
pGkCblS3	Ap <sup>R</sup>	<i>G. kaustophilus cblS<sup>WT</sup></i> in pBAD24	(9)
pGkCblS3 R46A	Ap <sup>R</sup>	<i>G. kaustophilus cblS<sup>R46A</sup></i> in pBAD24	
pGkCblS3 E51A	Ap <sup>R</sup>	<i>G. kaustophilus cblS<sup>E51A</sup></i> in pBAD24	
pGkCblS3 S96A	Ap <sup>R</sup>	<i>G. kaustophilus cblS<sup>S96A</sup></i> in pBAD24	
pGkCblS3 E98A	Ap <sup>R</sup>	<i>G. kaustophilus cblS<sup>E98A</sup></i> in pBAD24	
pGkCblS3 S174A	Ap <sup>R</sup>	<i>G. kaustophilus cblS<sup>S174A</sup></i> in pBAD24	
pGkCblS3 E180A	Ap <sup>R</sup>	<i>G. kaustophilus cblS<sup>E180A</sup></i> in pBAD24	
pStmDeoD1	Ap <sup>R</sup>	<i>S. enterica deoD<sup>WT</sup></i> translational fusion to His <sub>6</sub> tag for protein purification in pTEV5	

<sup>1</sup> All *E. coli* strains used in this study were derivatives of *E. coli* K-12

<sup>2</sup> All *S. enterica* strains used in this study were derivatives of *S. enterica* sv Typhimurium strain LT2

Ap<sup>R</sup>, Ampicillin resistance; Km<sup>R</sup>, kanamycin resistance

**Table 5-2. Oligonucleotides used in this study.**

<i>Cloning Primers</i>	
Stm_deoD_BspQI_5'	NNGCTCTTCNTTTCATGGCAACTCCACATATTAATGC
Stm_deoD_BspQI_3'	NNGCTCTTCNTTATTACTCTTTATCGCCC
<i>Site-Directed Mutagenesis</i>	
GkCblS_sdm_R46A_F	CTCCATCAAGGCAACGGCGGGCGGAAAAATACGCA
GkCblS_sdm_R46A_R	TGCGTATTTTTCCGCCGCCGTTGCCTTGATGGAG
GkCblS_sdm_V47A_F	GCTCCATCAAGGCAGCGCGGGCGGAAAAA
GkCblS_sdm_V47A_R	TTTTTCCGCCCGCGCTGCCTTGATGGAGC
GkCblS_sdm_E51A_F	CGTTGCCTTGATGGCGCTGTTGAGCGTCCG
GkCblS_sdm_E51A_R	CGACGCTCAACAGCGCCATCAAGGCAACG
GkCblS_sdm_T94A_F	CCGTGCTGCCGCGGATCGGGAGATC
GkCblS_sdm_T94A_R	GATCTCCCGATCGCCGGCAGCACGG
GkCblS_sdm_S96A_F	GAAAATTCGATTCCGTGGCGCCGGTGATCGGGAGAT
GkCblS_sdm_S96A_R	ATCTCCCGATCACCGGCGCCACGGAATCGAATTTTC
GkCblS_sdm_E98A_F	GTGGGAAAATTCGATGCCGTGCTGCCGGTG
GkCblS_sdm_E98A_R	CACCGGCAGCACGGCATCGAATTTTCCCAC
GkCblS_sdm_S174A_F	TTCGTAATAAATACCTTTCGCGCCGATGGGAATCAATTCG
GkCblS_sdm_S174A_R	CGAATTGATTCCCATCGGCGCGAAAGGTATTTATTACGAA
GkCblS_sdm_E180A_F	CTAACAGCTGTGTCCATGCGTAATAAATACCTTTCGAGC
GkCblS_sdm_E180A_R	GCTCGAAAGGTATTTATTACGCATGGACACAGCTGTTAG

**Table 5-3. Wavelengths and extinction coefficients of bases dissolved in DMSO.**

Base	Abbrev.	Wavelength ( $\lambda$ ) nm	Ext. Coefficient ( $\epsilon$ ) $M^{-1} cm^{-1}$
Adenosine	ADE	265	12969
Benzimidazole	Bza	274	4326
Phenol		274	1783
Dimethylbenzimidazole	DMB	280	5091
<i>p</i> -cresol		282	2126
5'-methoxybenzimidazole	methoxyBza	288	4223
5-hydroxybenzimidazole	hydroxyBza	291	4398

### **Continuous spectrophotometric assay for measuring *Gk* CblS kinase activity.**

Kinetic parameters for the activation of ribosides by *Gk* CblS were determined using a continuous spectrophotometric assay that coupled the synthesis of ADP to the oxidation of reduced NADH using the enzymes pyruvate kinase (PK) and lactate dehydrogenase (LDH). Phosphoenolpyruvate (PEP) is dephosphorylated to pyruvate by PK and pyruvate is reduced to lactate by LDH, oxidizing NADH. The oxidation of NADH is monitored at 340 nm.

To assess *Gk* CblS activity, reaction mixtures (100  $\mu$ L) contained 4-(2-hydroxyethyl)piperazine-1-ethanesulfonic acid (HEPES, 50 mM, pH 7.5), KCl (800 mM), MgCl<sub>2</sub> (5 mM), TCEP (1.25 mM), ATP (1.75 mM), PEP (3 mM), NADH (3 mM), PK (40U), and LDH (100 U). The PK (from rabbit muscle, 350-600 U / mg protein) and LDH (from rabbit muscle, ~550 U / mg protein) solutions contain 3.2M ammonium sulfate solutions. Before use, the ammonium sulfate was removed by centrifugation at 4 °C (10 min; 15k x g) and resuspended on the reaction buffer. *Gk* CblS was added at 2  $\mu$ g unless otherwise indicated. The riboside substrates were added at the concentrations indicated. Reaction mixtures were loaded into a standard 96-well plate and incubated at 37°C for 3 min. The ribosides were added to initialize the reaction after 3 min. Reactions were monitored at 340 nm for 1.5 h in a computer-controlled Powerwave XS plate reader (37°C, Biotek Instruments). Maximum velocities ( $V_{max}$ ) were calculated using Gen 5 2.0 software (Biotek Instruments) after correcting the  $A_{340}$  values to a distance of 1 cm.

### ***Gk* CblS kinase activity HPLC assay.**

Purified *Gk* CblS (2  $\mu$ g) was added to a reaction mixture (50  $\mu$ L) containing HEPES buffer (pH 7.5, 50 mM), KCl (800 mM), MgCl<sub>2</sub> (5 mM), TCEP (1.25 mM), ATP (1.75 mM), and riboside (500  $\mu$ M). No enzyme controls were also set up. The reaction mixtures were incubated for 30 min at 37 °C and then heated to 95 °C for five min to terminate. An equal volume (50  $\mu$ L) of ammonium

acetate (20 mM; pH 4.5) was added to the reaction, and the product was centrifuged (15k x g for 10 min) to remove precipitates. The reaction products were then analyzed by HPLC separation as described (9).

### **Growth analyses.**

Strains were grown at 37 °C in no-carbon essential (NCE) minimal medium (18) supplemented with ribose (22 mM) as a carbon and energy source. Minimal medium also contained trace minerals, magnesium sulfate (1 mM), ampicillin (100 µg mL<sup>-1</sup>), L(+)-arabinose (500 µM) and dicyanocobinamide [(CN)<sub>2</sub>Cbi] (0.25 nM). Thiamine (50 µM) and ribosides were added as indicated. Growth analyses were performed in 96-well microtiter dishes, with each strain grown under indicated conditions in duplicate. Each well contained 200 µL of medium inoculated with 1% (v/v) of an overnight starter culture grown for at least 20 h on nutrient broth (Difco) to lower the level of residual nutrients in the medium. Cell density was monitored at 650 nm using a computer-controlled BioTek Powerwave XS absorbance plate reader (BioTek Instruments). Readings were acquired every 15 min for 24 h with continuous shaking. Data were analyzed using Microsoft Excel (Microsoft) and the GraphPad Prism v7 software package (GraphPad Software). The natural log of 2 was divided by the specific growth rate  $\mu$  (defined as the change in absorbance in natural log divided by time) to give the generation time in hours.

### **Corrinoid Extraction and Separation.**

Two flasks (baffled, 500-mL) containing minimal NCE medium (100-mL) were supplemented with trace minerals, magnesium sulfate (1 mM), D-ribose (22 mM), L-arabinose (500 µM), ampicillin (100 µg mL<sup>-1</sup>), (CN)<sub>2</sub>Cbi (1 µM), and  $\alpha$ -Ado (1 µM). The medium was inoculated by the addition of 1% (v/v) of an overnight culture of the *S. enterica* strain  $\Delta cobT \Delta cobB / pGkCbITS2^+$  (JE17830) grown for at least 20 h in nutrient broth (NB, Difco). Cultures were grown

for >20 h at 37 °C with shaking (150 rpm) (New Brunswick Innova 44R refrigerated incubator shaker). The cells were harvested by centrifugation (15 min; 5,500 × g) using an Avanti J25-I centrifuge (Beckman Coulter), equipped with a JLA-16.250 rotor. Cell pellets were resuspended in an ammonium acetate (100 mM, pH 4) solution (5 mL) containing potassium cyanide (10 mM), and frozen at -20 °C until processed. Corrinoid extraction and isolation proceeded as described (9), with the modifications that samples were resuspended in 100-μL of buffer C [KH<sub>2</sub>PO<sub>4</sub> (100 mM), KCN (10 mM), pH 6.5] before separation by HPLC and no bioassay was conducted.

### **α-Riboside activation by *S. enterica* cell extract.**

#### Cultivation.

Minimal NCE was supplemented with trace minerals, magnesium sulfate (1 mM), D-ribose (22 mM), L-arabinose (500 μM), ampicillin (100 mg mL<sup>-1</sup>), (CN)<sub>2</sub>Cbi (0.25 nM), and DMB (50 μM). An overnight of the *S. enterica* strain Δ*cobT* Δ*cobB* / p*GkCblTS2*<sup>+</sup> (JE17830) grown for 16+ h on nutrient broth (NB) was subcultured at 1% (v/v) in 50-mL of the prepared medium. The inoculation was grown at 37C for 16+ h. Cells were harvested by centrifugation (20 min; 3000 x g) using an Eppendorf 5810 R benchtop centrifuge. The pellet was frozen at -20 °C until needed.

#### Cell lysis.

A lysis buffer solution of BugBuster® reagent (Novagen) was prepared by diluting the concentrated solution (10x) in a binding buffer containing Tris (50mM, pH 8), NaCl (500 mM), and imidazole (4 mM). The thawed cell pellet was resuspended in the lysis buffer (1:4 m/v). The suspension was incubated for 30 min at 25 °C in a Roto-Bot programmable rotator (Program F1, Speed 25; Benchmark), yielding a whole cell extract. The membrane and insoluble portions of the whole cell extract were removed by centrifuging a portion of the whole cell extract (30 min; 39 k x g) and passing the supernatant over a PES syringe filter (0.45-μm; VWR), resulting in a soluble

cell extract. The cell extracts were dialyzed against a buffer containing Tris (50 mM) and NaCl (500 mM) twice, with the second dialysis including glycerol (5% v/v) as well. The total protein concentration was estimated using a NanoDrop 2000 spectrophotometer (Thermo Fisher Scientific).

#### HPLC assay.

Dialyzed *S. enterica* cell extract (10 µg) or no enzyme were added to a reaction mixture (50 µL) containing HEPES buffer (50 mM, pH 7.5), KCl (800 mM), MgCl<sub>2</sub> (5 mM), TCEP (1.25 mM), ATP (1.75 mM), and riboside (500 µM). The reactions were incubated for 12 h at 37 °C and then heated at 95 °C for 5 min to stop the reaction. Ammonium acetate (50 µL; 20 mM; pH 4.5) was added to the reaction, and the products were centrifuged (10 min; 15k x g) to remove precipitates. The reaction products were then analyzed by HPLC separation as described (9).

## RESULTS.

As mentioned earlier, the *Firmicute L. cornyformis*, which lacks a functional DMB: NaMN PRTase but does have a homolog of the kinase CblS, synthesizes pseudoCbl, which uses adenine instead of DMB as the lower ligand base (10). We have shown that CblS homologs from *Listeria innocua* (8) and *G. kaustophilus* (9) can activate the DMB-riboside  $\alpha$ -R. To assess whether or not *Gk* CblS can modify ribosides *other* than  $\alpha$ -R, such as  $\alpha$ -Ado, *Gk* CblS was purified to homogeneity. The purified protein was then used to develop a continuous spectrophotometric assay (Figure 5-1A) using pyruvate kinase (PK) and lactate dehydrogenase (LDH) (19). Briefly, the kinase transfers the  $\gamma$ -phosphate from ATP to the riboside, generating ADP. PK transfers a phosphate from phosphoenolpyruvate, generating ATP and pyruvate. LDH reduces pyruvate to lactate while oxidizing NADH. This oxidation results in a decrease in absorbance at 340 nm, which can be measured. Using the extinction coefficient of NADH ( $6220 \text{ M}^{-1} \text{ cm}^{-1}$ ), the turnover rate for NADH to  $\text{NAD}^+$  can be determined, which is assumed to be equal to the transfer mediated by the kinase.

**Figure 5-1. Optimizing the coupled kinase assay for use with *Gk* CblS.**

A. Schematic diagram of the reaction. Abbreviations: Pyruvate Kinase, PK; Phosphoenolpyruvate, PEP; Lactate dehydrogenase, LDH.

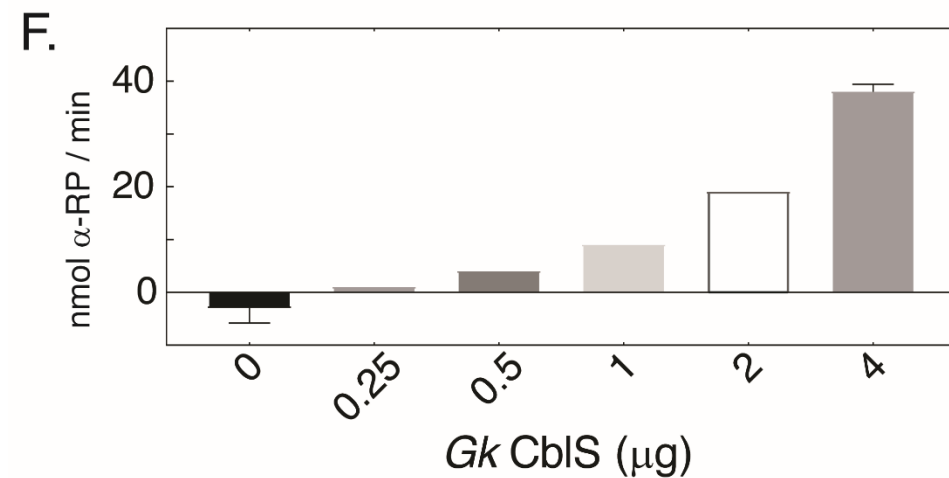
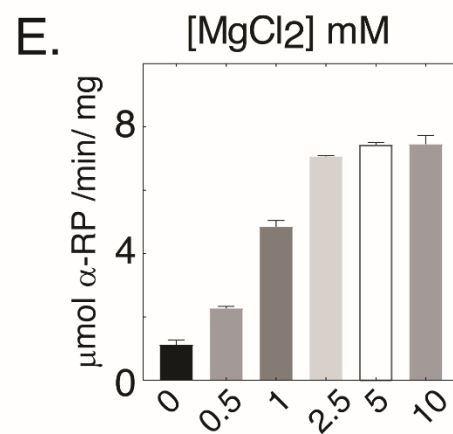
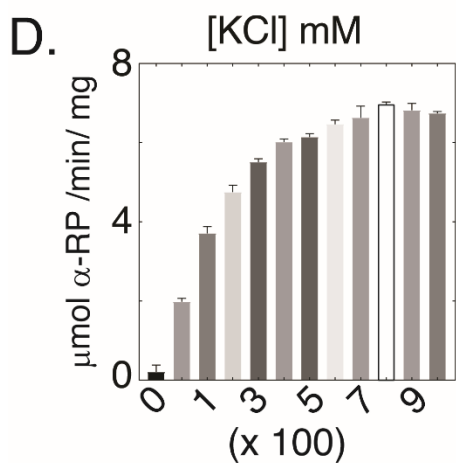
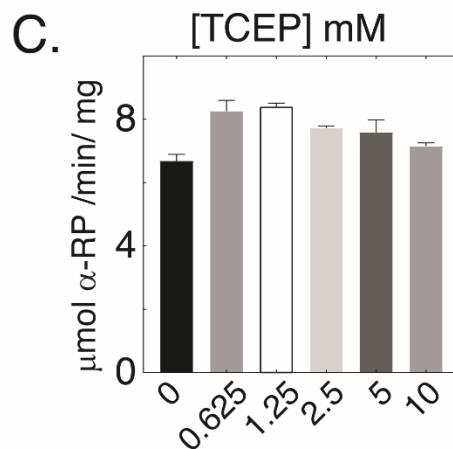
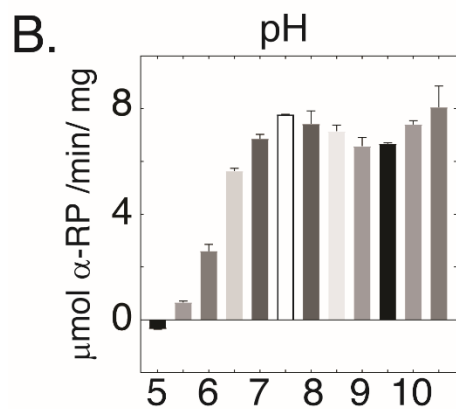
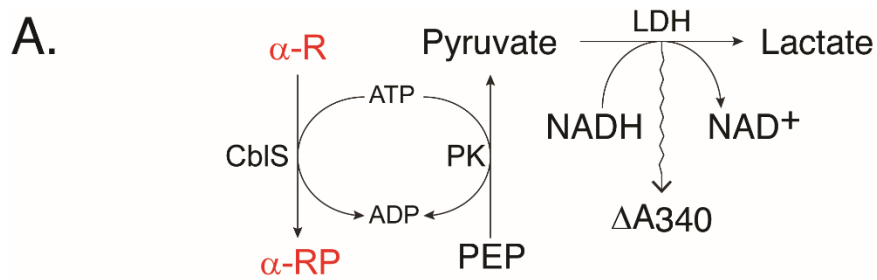
B. Specific activity of *Gk* CblS at various pH values. Buffers of various pH values were tested in 0.5 unit increments from pH 5 to 10.5. The reaction mixture contained buffer (50mM), KCl (750 mM), MgCl<sub>2</sub> (5 mM), TCEP (5 mM), ATP (1 mM),  $\alpha$ -R (1 mM), PEP (3 mM), NADH (3 mM), *Gk* CblS (2  $\mu$ g), PK (40 U), and LDH (100 U).

C. Specific activity of *Gk* CblS at various TCEP concentrations. The reaction mixture contained HEPES (pH 7.5, 50mM), KCl (750 mM), MgCl<sub>2</sub> (5 mM), ATP (1 mM),  $\alpha$ -R (1 mM), PEP (3 mM), NADH (3 mM), *Gk* CblS (2  $\mu$ g), PK (40 U), and LDH (100 U).

D. Specific activity of *Gk* CblS at various KCl concentrations. KCl was added from 50 mM to 1M. The reaction mixture contained HEPES (pH 7.5, 50mM), MgCl<sub>2</sub> (5 mM), TCEP (1.25 mM), ATP (1 mM),  $\alpha$ -R (1 mM), PEP (3 mM), NADH (3 mM), *Gk* CblS (2  $\mu$ g), PK (40 U), and LDH (100 U).

E. Specific activity of *Gk* CblS at various MgCl<sub>2</sub> concentrations. The reaction mixture contained HEPES (pH 7.5, 50mM), KCl (800 mM), TCEP (1.25 mM), ATP (1 mM),  $\alpha$ -R (1 mM), PEP (3 mM), NADH (3 mM), *Gk* CblS (2  $\mu$ g), PK (40 U), and LDH (100 U).

F. Effect of *Gk* CblS quantity (by mass) on the rate under optimized conditions. The reaction mixture contained HEPES (pH 7.5), KCl (800 mM), MgCl<sub>2</sub> (5 mM), TCEP (1.25 mM), ATP (1 mM),  $\alpha$ -R (1 mM) PEP (3 mM), NADH (3 mM), PK (40 U), and LDH (100 U).



### **Determining optimal conditions for the *Gk* CblS-PK/LDH coupled assay.**

The coupled reaction conditions were optimized starting from the initial conditions reported previously [HEPES (pH 7.5, 50 mM), KCl (750 mM), MgCl<sub>2</sub> (5 mM), and TCEP (5 mM)] (9). Testing proceeded in the following order: pH, [TCEP], [KCl], and [MgCl<sub>2</sub>]. Each subsequent step represented an additional round of optimization (i.e., the optimized pH value was used to determine the optimal concentration of TCEP required).

pH. *Gk CblS* was screened against a range of pH values from 5 to 10.5 (Figure 5-1B). Specific activity increased from pH 5 to 7.5, decreased from pH 7.5 to 9, and then increased again from pH 9.5 to 10.5. Specific activity was maximized at 8 μmol α-RP min<sup>-1</sup> mg<sup>-1</sup> at pH 7.5 (HEPES, 50 mM).

TCEP. TCEP is a chemical reductant that reduces surface cysteines and prevents aggregation and precipitation during the purification of the CblS kinase (the kinase has 4 Cys residues). The concentration of TCEP was varied (0 to 10 mM) and the specific activity of the kinase was determined (Figure 5-1C). Activity was detected even in the absence of TCEP, but the specific activity (7 μmol α-RP min<sup>-1</sup> mg<sup>-1</sup>) was maximized at 1.25 mM TCEP.

Potassium chloride. KCl has been associated with enhancing protein stability. The specific activity of the kinase was screened against a range of KCl concentrations from 0 to 1 M (Figure 5-1D). No activity was detected when KCl was absent, but the specific activity increased with the concentration of KCl until maximizing at 800 mM (specific activity = 7 μmol min<sup>-1</sup> mg<sup>-1</sup>).

MgCl<sub>2</sub>. Both PK and *Gk* CblS interact with ATP and thus require Mg<sup>2+</sup>. The specific activity of the CblS kinase at 1 mM ATP was determined for a range of MgCl<sub>2</sub> concentrations from 0 to 10 mM (Figure 5-1E). Activity was minimal (> 1 μmol α-RP min<sup>-1</sup> mg<sup>-1</sup>) when no MgCl<sub>2</sub> was

provided but increased as [MgCl<sub>2</sub>] increased. The specific activity was maximized when the MgCl<sub>2</sub>: ATP ratio was 5:1 (5 mM MgCl<sub>2</sub>).

**Optimal conditions.** To summarize, the optimal activity (in  $\mu\text{mol } \alpha\text{-RP min}^{-1} \text{ mg}^{-1}$ ) for *Gk* CblS (2  $\mu\text{g}$ ) was determined to occur when the buffer contains HEPES (pH 7.5; 50 mM), KCl (800 mM), Mg<sub>2</sub>Cl (5 mM), and TCEP (1.25 mM). The linearity of the reaction was demonstrated from 0.5  $\mu\text{g}$  to 4  $\mu\text{g}$  of *Gk* CblS (Figure 5-1F) as doubling of enzyme resulted in a doubling of the rate (i.e., from 9 nmol  $\alpha\text{-RP min}^{-1}$  at 1  $\mu\text{g}$  to 19 nmol  $\alpha\text{-RP min}^{-1}$  at 2  $\mu\text{g}$ ).

#### **Active *Gk* CblS is a monomer.**

The CblS kinases share a conserved region with the PurM-like Superfamily (cl10019). This superfamily's members include the dimers PurM and SelD and monomers PurL, ThiL, and HypE. The protein was analyzed by gel permeation using fast protein liquid chromatography (FPLC) to determine the oligomeric state of hexahistidine-tagged (H6) *Gk* CblS. A calibration curve plotting molecular mass (kDa) as a function of retention time was determined using commercially available standards (BioRad). When tested on a buffer containing HEPES (50 mM, pH 7.5), KCl (250 mM), MgCl<sub>2</sub> (5 mM), and TCEP (2.5 mM), H6-*Gk* CblS had a retention time consistent with a ~27 kDa protein (Figure 5-2). The hypothetical mass of an H6-*Gk* CblS is 28.5 kDa, indicating that the kinase is a monomer.

#### ***Gk* CblS kinetic parameters for $\alpha\text{-R}$ and ATP.**

The Michaelis-Menten kinetic parameters for the substrates  $\alpha\text{-R}$  (Figure 5-3A) and ATP (Figure 5-3B) were determined using the optimized assay. One substrate was provided in excess (1 mM) while the other substrate was varied. Those values are reported in Table 5-4. The apparent  $K_m$  for ATP is 300  $\mu\text{M}$ , and for  $\alpha\text{-R}$  is 360  $\mu\text{M}$ .

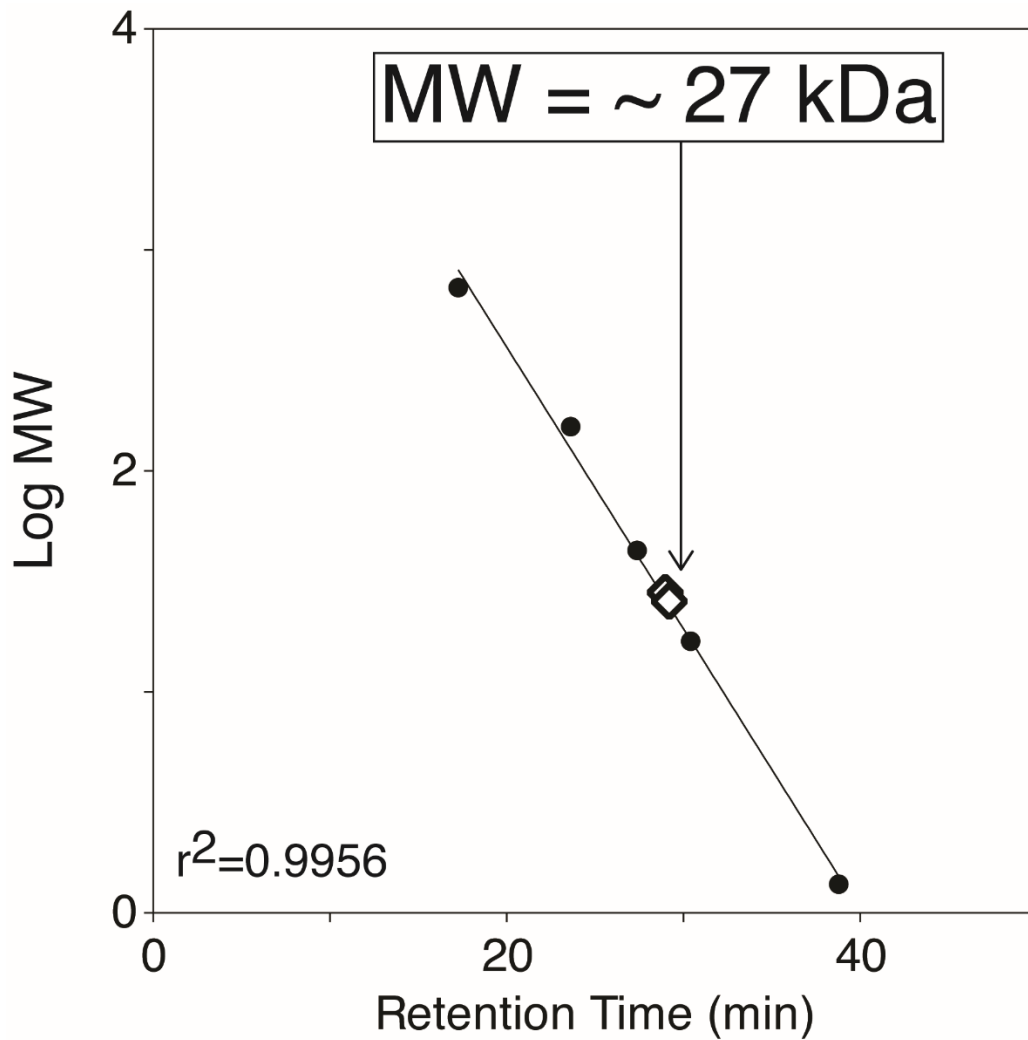


**Figure 5-2. H6-Gk CblS is a monomer in solution.** Following gel permeation analysis, the retention time of H6-Gk CblS was compared to times of a mixture of standards (Bio-Rad Laboratories) used to generate a calibration curve. The standards used were  $\gamma$ -globulin (158 kDa), ovalbumin (44 kDa), myoglobin (17 kDa), and vitamin B12 (1.35 kDa).

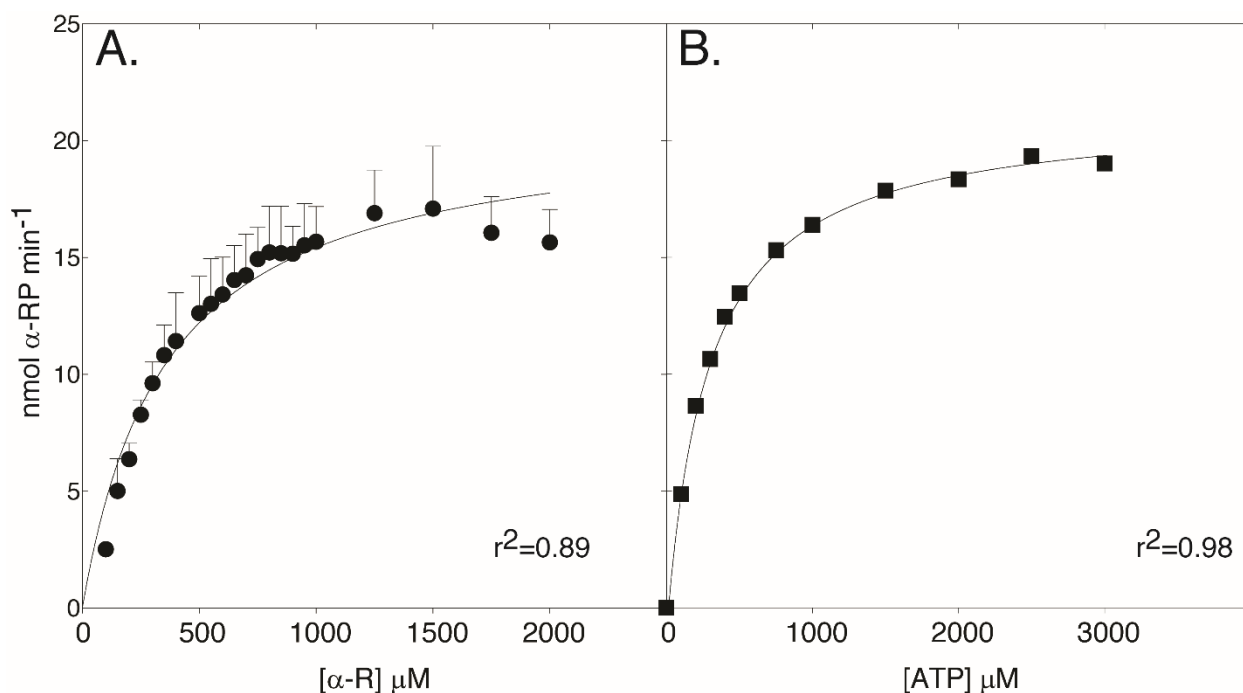


**Figure 5-3. Determining the Michaelis-Menten kinetic parameters for *Gk* CblS on  $\alpha$ -R and ATP.** The apparent  $K_m$  values for the substrates  $\alpha$ -R and ATP were determined using a reaction mixture containing HEPES (pH 7.5), KCl (800 mM), MgCl<sub>2</sub> (5 mM), TCEP (1.25 mM), PEP (3 mM), NADH (3 mM), *Gk* CblS (2  $\mu$ g), PK (40 U), and LDH (100 U). A. [ATP] constant at 1 mM, [ $\alpha$ -R] varied from 0 to 2mM. B. [ $\alpha$ -R] constant at 1 mM, [ATP] varied from 0 to 3 mM.

**Table 5-4. Michaelis-Menten kinetic parameters for *Gk* CblS on  $\alpha$ -R and ATP.**

	$K_m$ ( $\mu$ M)	$V_{max}$ (nmol/min)	$k_{cat}$ (s <sup>-1</sup> )	$k_{cat}/k_m$ (M <sup>-1</sup> s <sup>-1</sup> )
$\alpha$ -R	358	21	5	13914
ATP	297	21	5	17057

***Gk* CblS phosphorylates  $\alpha$ -Ado but not  $\beta$ -ribosides *in vitro*.**

The optimized assay was used to determine whether the identity of the base or the orientation of the N-glycosidic bond effect activation by the kinase.  $\alpha$ -Ribosides of adenine and the four purine analogs [benzimidazole (Bza), 5-hydroxybenzimidazole (hydroxyBza), 5-methoxybenzimidazole (methoxyBza), and DMB] were prepared using the DMB: NaMN PRTase CobT from *S. enterica* (see Materials and Methods). HydroxyBza and methoxyBza were identified as precursors to DMB in some organisms and represent possible benzimidazolyl- $\alpha$ -ribosides found in nature (20). Note that activation of hydroxyBza (and methoxyBza) to the  $\alpha$ -riboside may yield both an  $\alpha$ -5'hydroxyBza-riboside as well as an  $\alpha$ -6'hydroxyBza-riboside as the molecule is asymmetric and either N1 or N3 of the imidazole ring may be linked to the ribose (21).

The purine nucleoside phosphorylase DeoD (22) from *S. enterica* is used to synthesize  $\beta$ -ribazole (the  $\beta$ -N-glycosidic-linked epimer of the DMB-riboside). The synthesized molecules were cleaned up and quantified as described in the Materials and Methods. After confirmation by HPLC separation that the ribosides are pure, their identities were verified by mass spectrometry (see Figure C1). An attempt was made to synthesize the phenolic  $\alpha$ -ribosides using purified ArsAB and phenol or p-cresol (16), but they could not be purified using the boronate affinity resin method and were not tested.

A coupled assay reaction mixture was prepared using the optimized conditions with ATP at 1.75 mM. After a 3-minute pre-incubation, the ribosides were added at 360  $\mu$ M. The reactions were allowed to proceed for 1.5 h and absorbance was monitored at 340 nm every 45 sec. As these reactions were performed in a 96-well plate, the pathlengths were corrected to 1-cm using the software settings (Biotek Gen 2.0). Maximum velocity values were calculated across eight time-points with the corrected values, and the specific activity was calculated using the extinction

coefficient of NADH ( $6220 \text{ M}^{-1} \text{ cm}^{-1}$ ) by assuming a 1:1 ratio of NADH/NAD turnover to ATP/ADP.

No phosphorylation activity was detected when the kinase was reacted with any  $\beta$ -riboside, including  $\beta$ -R or Ado (Figure 5-4A). The specific activity of  $\alpha$ -R under these conditions was  $4 \mu\text{mol } \alpha\text{-RP min}^{-1} \text{ mg}^{-1}$ .

The kinase was active when provided the  $\alpha$ -ribosides  $\alpha$ -Bza-R ( $3 \mu\text{mol } \alpha\text{-RP min}^{-1} \text{ mg}^{-1}$ ),  $\alpha$ -hydroxyBza-R ( $3 \mu\text{mol } \alpha\text{-RP min}^{-1} \text{ mg}^{-1}$ ), and  $\alpha$ -methoxyBza-R ( $5 \mu\text{mol } \alpha\text{-RP min}^{-1} \text{ mg}^{-1}$ ) as well (Figure 5-4B). Incredibly, activity was also detected in the presence of  $\alpha$ -Ado ( $2 \mu\text{mol } \alpha\text{-RP min}^{-1} \text{ mg}^{-1}$ ). These results indicate the orientation of the N-glycosidic bond determines whether the kinase can activate a riboside, not the identity of the base. The variation in activity between ribosides is likely the result of affinity, and the presence of charges on the less active molecules could indicate a hydrophobic active site.

The reactions with  $\alpha$ -ribosides were repeated, minus the components of the coupled reaction (PK, LDH, PEP, and NADH), to confirm that the observed activity was the result of a phosphate transfer to the target riboside. These reactions were incubated at  $37 \text{ }^\circ\text{C}$  for 30 min and shifted to  $95 \text{ }^\circ\text{C}$  for 5 minutes to terminate. An equal volume of ammonium acetate (50mM, pH 4.5) was added, and the reactions were centrifuged to remove particles. The products were then separated by HPLC as described (9). HPLC traces and UV-Vis spectra for the reaction of *Gk CblS* with  $\alpha$ -R (A) and  $\alpha$ -Ado (B) are available in Figure 5-5. The traces for  $\alpha$ -Bza-R (A),  $\alpha$ -hydroxyBza-R (B), and  $\alpha$ -methoxyBza-R (C) can be found in Figure C2. The HPLC traces were normalized to the tallest peak of the trace (100% = maximum value). UV-visible spectra of the suspected riboside peaks were captured and normalized (100% = maximum value).

As expected, when the DMB-riboside  $\alpha$ -R was treated with *Gk* CblS + ATP (Figure 5-5A), a shift from  $\alpha$ -R (17.5 min, top) to  $\alpha$ -RP (15.2 min, bottom) can be observed.

In the absence of *Gk* CblS (Figure 5-5B, top),  $\alpha$ -Ado (500  $\mu$ M) elutes at 3.2 min. Treatment with *Gk* CblS (Figure 5-5B, bottom) and ATP yielded a shift to 2.4 min, indicating phosphorylation and synthesis of  $\alpha$ -Ado-P ( $\alpha$ -AMP). The UV-Vis spectra of the two peaks are similar (Figure 5-5B, bottom right). Similar shifts were observed (Figure C2) for  $\alpha$ -Bza-R,  $\alpha$ -hydroxyBza-R, and  $\alpha$ -methoxyBza-R, confirming that the specific activities observed are the result of phosphorylation. These data indicate that it is the orientation of the N-glycosidic bond that dictates the target of the kinase, not the base.

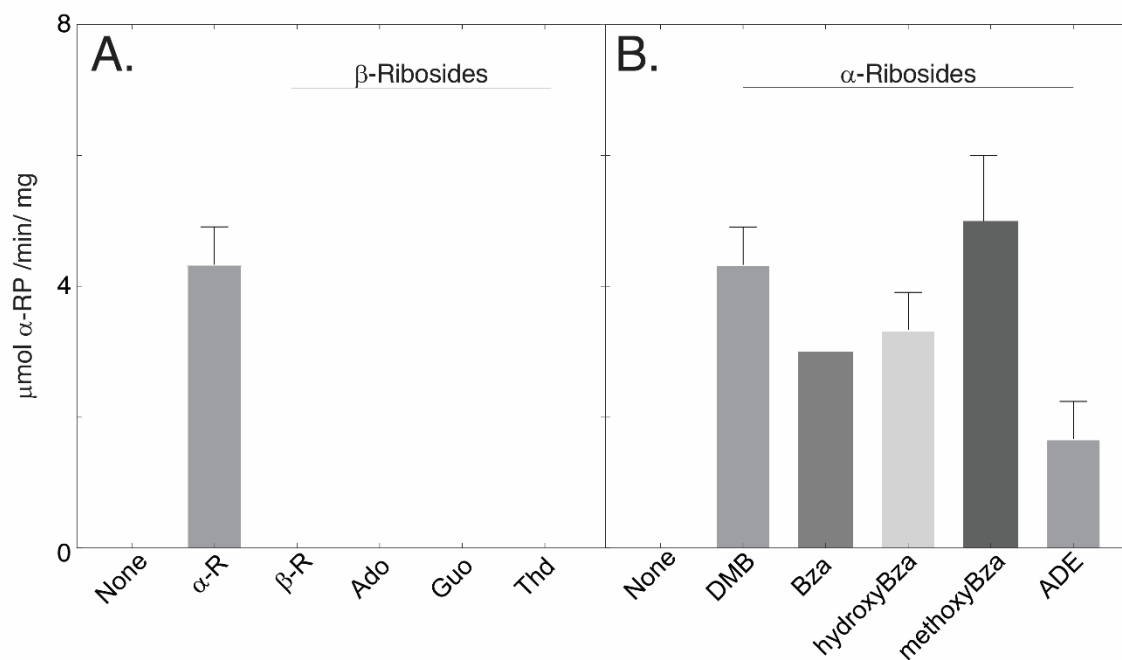


**Figure 5-4. Specific activity of *Gk* CblS for different ribosides at 1.75 mM ATP.** Reactions contained 2 μg *Gk* CblS in a reaction mixture containing HEPES (pH 7.5), KCl (800 mM), MgCl<sub>2</sub> (5 mM), TCEP (1.25 mM), ATP (1.75 mM), PEP (3 mM), NADH (3 mM), PK (40 U), and LDH (100 U). Ribosides were added at 360 μM. A. β-Ribosides. B. α-ribosides. Abbreviations: Negative control/no riboside, NEG; Adenosine, Ado; Guanosine, Guo; Thymidine, Thd; α-R, DMB; α-Bza-R, Bza; α-hydroxyBza-R, hydroxyBza; α-methoxyBza-R, methoxyBza; α-Ado, ADE

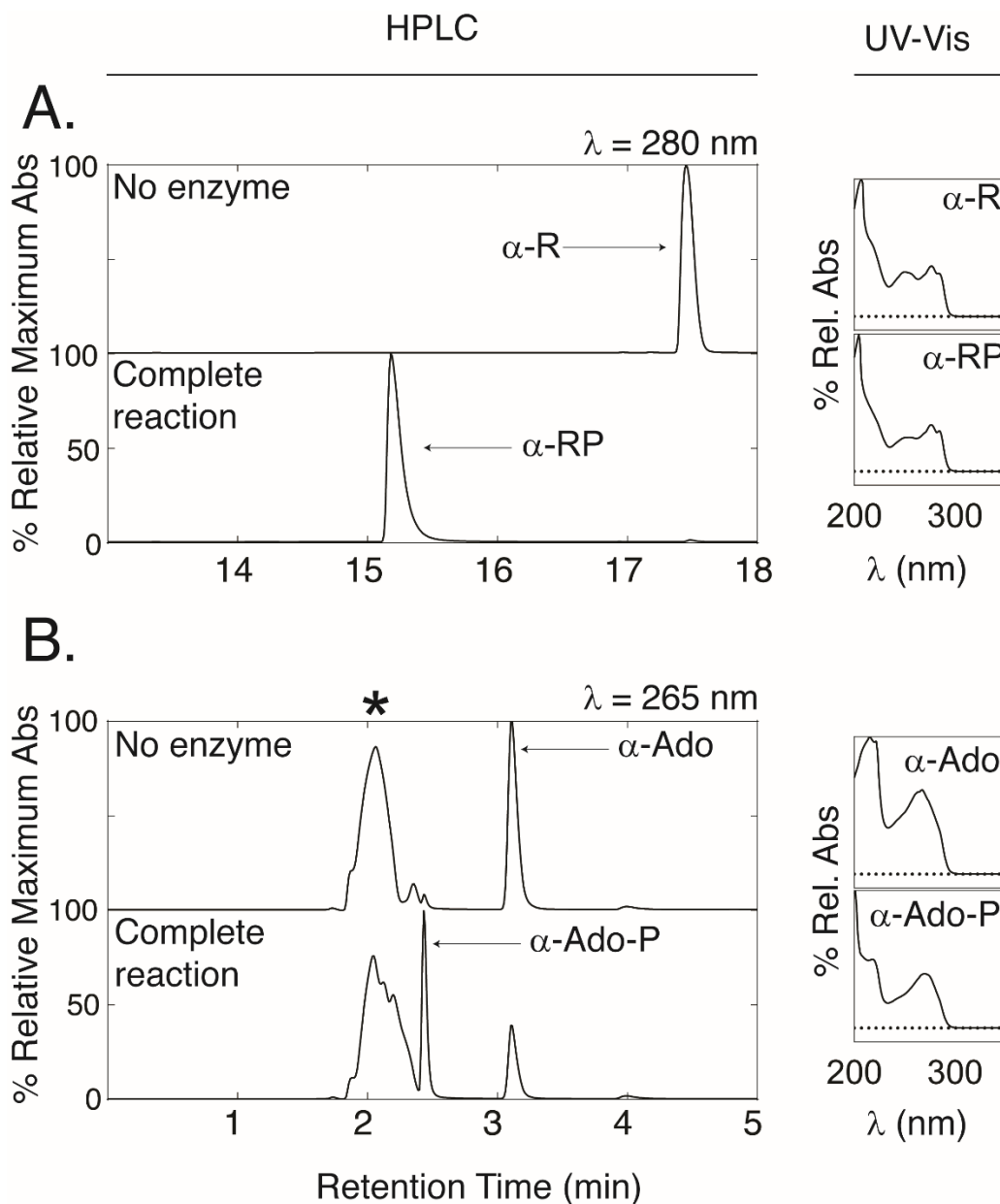


**Figure 5-5. *Gk* CblS phosphorylates  $\alpha\text{-Ado}$ .** A reaction mixture containing *Gk* CblS (2  $\mu\text{g}$ ), HEPES (pH 7.5), KCl (800 mM), MgCl<sub>2</sub> (5 mM), TCEP (1.25 mM), ATP (1.75 mM), and  $\alpha\text{-riboside}$  (500  $\mu\text{M}$ ) was incubated for 30 min at 37 °C before shifting to 95 °C. The products were then separated by HPLC (left) and analyzed. The UV-Visible spectra of the ribosides are presented to the right. A. Top: No enzyme + ATP +  $\alpha\text{-R}$ , Bottom: *Gk* CblS + ATP +  $\alpha\text{-R}$ . B. Top: No enzyme + ATP +  $\alpha\text{-Ado}$ , Bottom: *Gk* CblS + ATP +  $\alpha\text{-Ado}$ . ATP/ADP elute at 2 min (\*).

**An *S. enterica*  $\Delta cobT$   $\Delta cobB$  strain producing *Geobacillus kaustophilus* CblS can utilize other  $\alpha$ -ribosides to restore cobamide-dependent growth when the ring precursor is limited.**

When *S. enterica* uses *Gk* CblS and *Gk* CblT in place of CobT, only the DMB-containing Cbl is synthesized. The complete conversion of the ring precursor (CN)<sub>2</sub>Cbi into AdoCbl requires the synthesis of the  $\alpha$ -ribotide  $\alpha$ -RP. The condensation reaction of the ribotide with the prepared ring occurs at the AdoCbl-5'-P synthase (23), encoded by CobS in *S. enterica*. Saturation of CobS with either the ring or the lower ligand nucleotide increases efficiency (23). The ring (CN)<sub>2</sub>Cbi is necessary as a precursor of AdoCbl because, under normoxic conditions, *S. enterica* does not synthesize the corrin ring (24, 25) as the presence of oxygen causes the inactivation of the genes responsible for the biosynthesis of adenosylcobinamide-phosphate (AdoCbi-P) (26).

By limiting the amount of (CN)<sub>2</sub>Cbi provided, JE21364 becomes auxotrophic for  $\alpha$ -R (JE17830 becomes auxotrophic for either DMB or  $\alpha$ -R) (9). As the data above indicate, however, the kinase *can* activate other  $\alpha$ -ribosides, including  $\alpha$ -Ado. Whether *Gk CblS* can activate non-DMB  $\alpha$ -ribosides *in vivo*, particularly  $\alpha$ -Ado, will be assessed under (CN)<sub>2</sub>Cbi-limiting conditions at 37°C.

We will use the parental strain JE12939, which lacks the two enzymes (CobT, CobB) known to catalyze the direct activation of bases to their respective  $\alpha$ -ribotides (2, 27). This strain also lacks MetE, which catalyzes the final step in cobamide-independent methionine synthesis, resulting in a methionine auxotrophy. Under normoxic conditions, a *metE* strain requires either cobamides or methionine for growth (24). Cobamides are utilized by the cobamide-dependent methionine synthase MetH enzyme to methylate homocysteine, yielding methionine (24) and thus satisfying the auxotrophy.

To compensate for the loss of *S. enterica*  $\Delta cobT$  and  $\Delta cobB$ , the plasmids p*GkCblS3* (contains *G. kaustophilus cblS* under the control of the arabinose-inducible promoter P<sub>araBAD</sub>) and

pGkCblTS2 (contains *G. kaustophilus* *cblT* and *cblS* under the control of the P<sub>araBAD</sub> promoter) are inserted into JE12939, yielding JE21364 and JE17830, respectively (9). (As a control for kinase-independent growth, the empty cloning vector pBAD24 was inserted into JE12939 to yield JE17827.)

The effective concentration required to satisfy the  $\alpha$ -R requirement of JE21364 (*Gk CblS* only) was determined.  $\alpha$ -R was titrated from 0 to 500 pM (Figure 5-6). The cells were provided with only the ring precursor (CN)<sub>2</sub>Cbi at limiting levels (0.25 nM) to control for the impact of endogenous pools of  $\alpha$ -R (9). The addition of 100 pM  $\alpha$ -R yielded a 42% reduction in generation time (17 h to 10 h). At 300 pM, an 87% reduction was observed (17 h to 2 h). In the prior study (9),  $\alpha$ -R was added at 300 nM so, in the interest of comparison, the synthesized ribosides will be tested at both 300 pM and 300 nM.

The results of feeding the various synthesized ribosides are found in Figure 5-7, Table C1 (300 pM), and Table C2 (300 nM). In the absence of the kinase (JE17827), no significant reduction in generation time was detected, regardless of whether  $\alpha$ - or  $\beta$ -ribosides were provided. Similarly, there was no significant difference between the absence of riboside and supplementation with  $\beta$ -riboside ( $\beta$ -Ado or  $\beta$ -R) for either JE21364 or JE17830. These results confirm that the synthesis of an  $\alpha$ -ribotide is necessary for growth. They also indicate that no mutase exists in *S. enterica* for converting  $\beta$ -ribosides to  $\alpha$ -ribosides.

The generation time for JE21364 was reduced 89% (25 h to 3 h) when provided authentic  $\alpha$ -R. Similar results were observed for JE17830 (2 h at 300 pM). No significant change in those generation times was detected when  $\alpha$ -R was increased by 1000-fold. These results indicate that i) the synthesis of  $\alpha$ -RP by the kinase is maximized and ii) there is no detectable substrate or feedback inhibition by  $\alpha$ -R or  $\alpha$ -RP under these conditions.

The addition of  $\alpha$ -Bza-R and  $\alpha$ -methoxyBza-R showed significant reductions in generation time when fed at 300 pM to either JE21364 (3 h; 89%) or JE17830 (2 h; 93%), suggesting activation of these ribosides to their ribotide. No demonstrable substrate inhibition was observed when the riboside addition was increased to 300 nM (2h).

A less significant but still notable reduction (41%; 25 h to 15 h) was observed when  $\alpha$ -hydroxyBza-R was added to the medium in the presence of JE21364. The reduction improved to 93% (2 h) when  $\alpha$ -hydroxyBza-R was increased to 1000-fold. Similar responses were recorded for JE17830. *In vitro* data (Figure 5-4) did not indicate a significant difference in the activity of the kinase for the activation of  $\alpha$ -Bza-R and  $\alpha$ -hydroxyBza-R, so the *in vivo* data indicate a possible transport issue, likely due to the presence of the polar hydroxyl group.

Curiously, the addition of  $\alpha$ -Ado at even 300 nM failed to restore growth in either JE21364 or JE17830. As before, the *in vitro* data indicate that the kinase should be able to activate the riboside. The concentration was increased to 1  $\mu$ M (Table C3) to determine if a transportation barrier also exists for  $\alpha$ -Ado. In *S. enterica*, the AdoCbl-5'-P synthase CobS can incorporate the un-activated  $\alpha$ -R *in vitro*, albeit almost 100-fold less efficiently (23). At 1  $\mu$ M  $\alpha$ -R, kinase-independent growth can be observed.

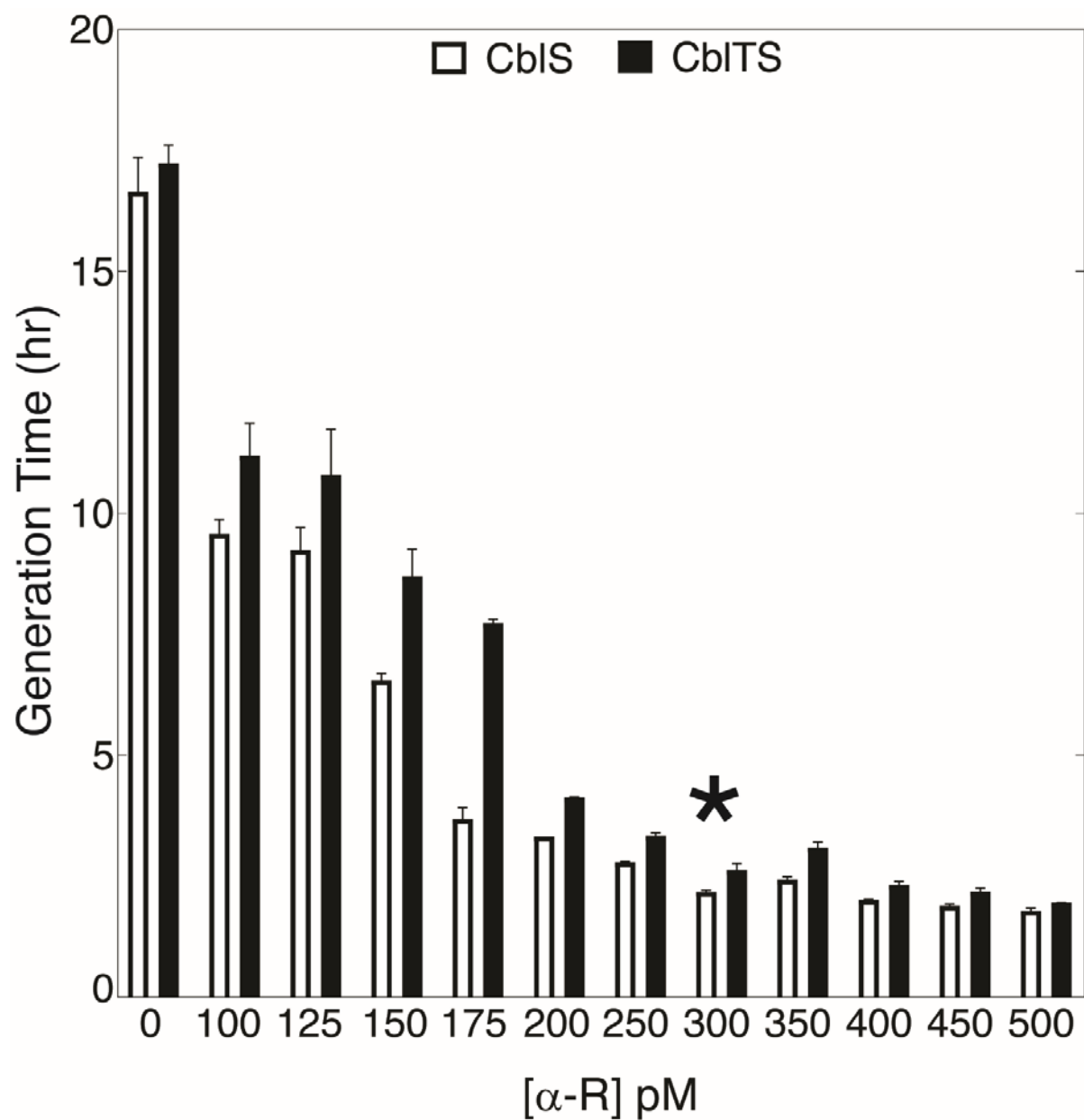


**Figure 5-6. The kinase requires picomolar amounts of  $\alpha$ -R to restore growth in a  $\Delta cobT$   $\Delta cobB$  strain.** JE21364 (CblS<sup>+</sup>, white bars) and JE17830 (CblT<sup>+</sup> CblS<sup>+</sup>, black bars) were grown on minimal NCE medium containing ribose (22 mM), trace minerals, magnesium sulfate (1 mM), L-arabinose (500 mM), ampicillin (100 mg mL<sup>-1</sup>) and (CN)<sub>2</sub>Cbi (0.25 nM).  $\alpha$ -R concentration was varied from 0 to 500 pM. The asterisk (\*) indicates the minimal amount of  $\alpha$ -R necessary to maximize the growth rate.

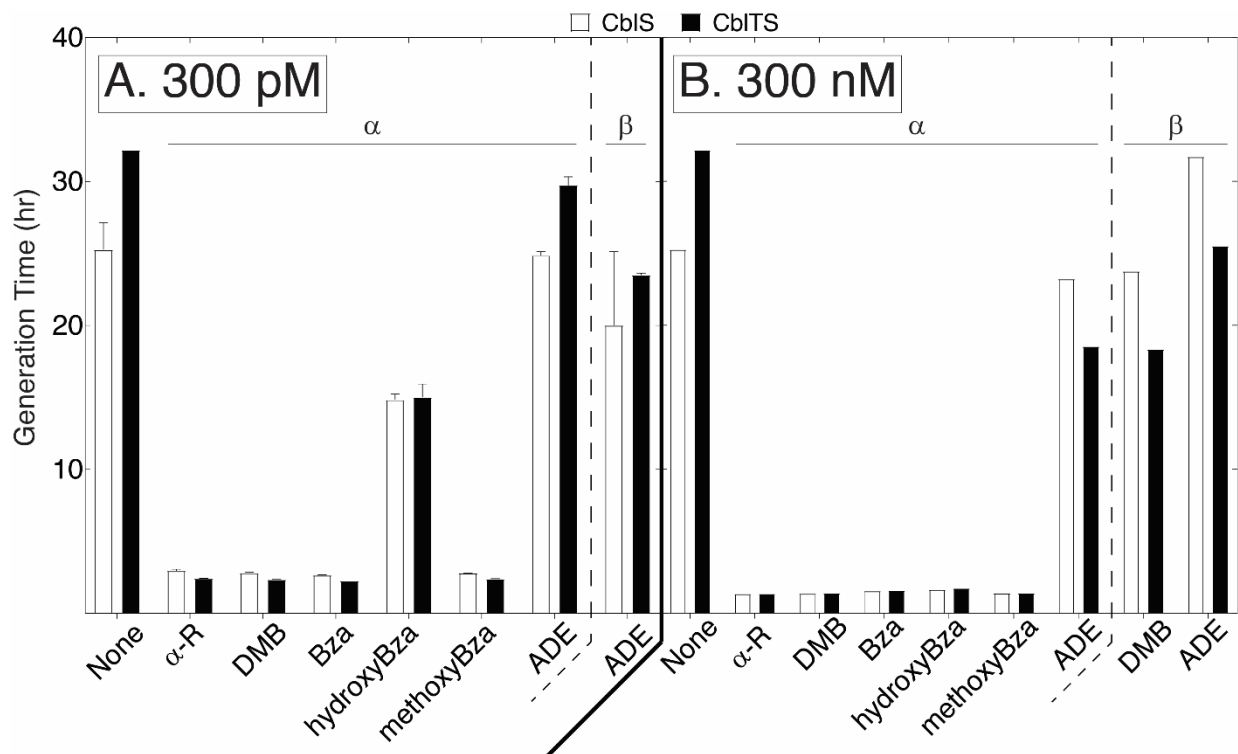


**Figure 5-7. The CblS kinase can activate a-ribosides in *S. enterica*.** JE21364 (CblS<sup>+</sup>, white bars) and JE17830 (CblT<sup>+</sup> CblS<sup>+</sup>, black bars) were grown on minimal NCE medium containing ribose (22 mM), trace minerals, magnesium sulfate (1 mM), L-arabinose (500 mM), ampicillin (100 mg mL<sup>-1</sup>) and (CN)<sub>2</sub>Cbi (0.25 nM). Ribosides were added at the concentrations indicated. A. Ribosides provided at 300 pM. B. Ribosides provided at 300 nM. Abbreviations: Negative control/no riboside, None; Postive control/authentic α-R, α-R; Ribazole, DMB; α-Bza-R, Bza; α-hydroxyBza-R, hydroxyBza; α-methoxyBza-R, methoxyBza; Adenosine, Ade; alpha-linked ribosides, α; beta-ribosides, β

Curiously, supplementation with 1  $\mu$ M  $\alpha$ -Ado does *not* restore kinase-independent growth (JE17827). When *Gk CblT* and *Gk CblS* are provided, there is a significant ( $p < 0.05$ ) reduction in the generation time (64%; 29 h to 10 h). At 300 nM, the reduction (38%; 29 h to 18 h) was found to be less significant ( $p = 0.1$ ). However, even at 1  $\mu$ M  $\alpha$ -Ado, JE17830 still fails to reach density unless DMB (2 h) or  $\alpha$ -R (1 h) are provided (Appendix C Table C2). These results could indicate that something is happening to  $\alpha$ -Ado in transport, but the kinase is still active.

**$\alpha$ -Ado is activated *in vitro* by *S. enterica*  $\Delta cobT \Delta cobB$  / p*GkCblTS*<sup>+</sup> (JE17830) cell extract.**

If the observed inability to activate is the result of possible interference from transport, phosphorylation of  $\alpha$ -Ado by *Gk CblS* should be detectable in the cell extract. A culture of JE17830 was grown under minimal conditions in which *Gk CblS* activity is necessary. After harvesting the cells, they were lysed using chemical lysis and then dialyzed into a buffer containing Tris (50 mM, pH 8) and NaCl (500 mM). The total protein content was estimated using a Nanodrop 2000 spectrophotometer (Thermo Fisher Scientific).

Using the reaction conditions from the purified enzyme assay earlier (Figure 5-5), 10  $\mu$ g of the whole cell extract was added, and the reaction was allowed to proceed for 12 h at 37 °C. The reactions were terminated by shifting the temperature to 95 °C before adding 50  $\mu$ L of ammonium acetate. After centrifugation at 15k x *g* for 15 minutes, the reaction was separated by HPLC as described (9). A peak was observed (Figure 5-8A) which shares a retention time (2.4 min) with the  $\alpha$ -AMP synthesized by the pure protein (Figure 5-5B) and is not present in the absence of the extract or the pure protein. These results suggest that the barrier to  $\alpha$ -Ado activation is the importation of the molecule rather than any catabolic activity of the cell. Interestingly, activity in the whole cell extract was five times that observed in the soluble portion, suggesting that the kinase *CblS* is membrane-associated.

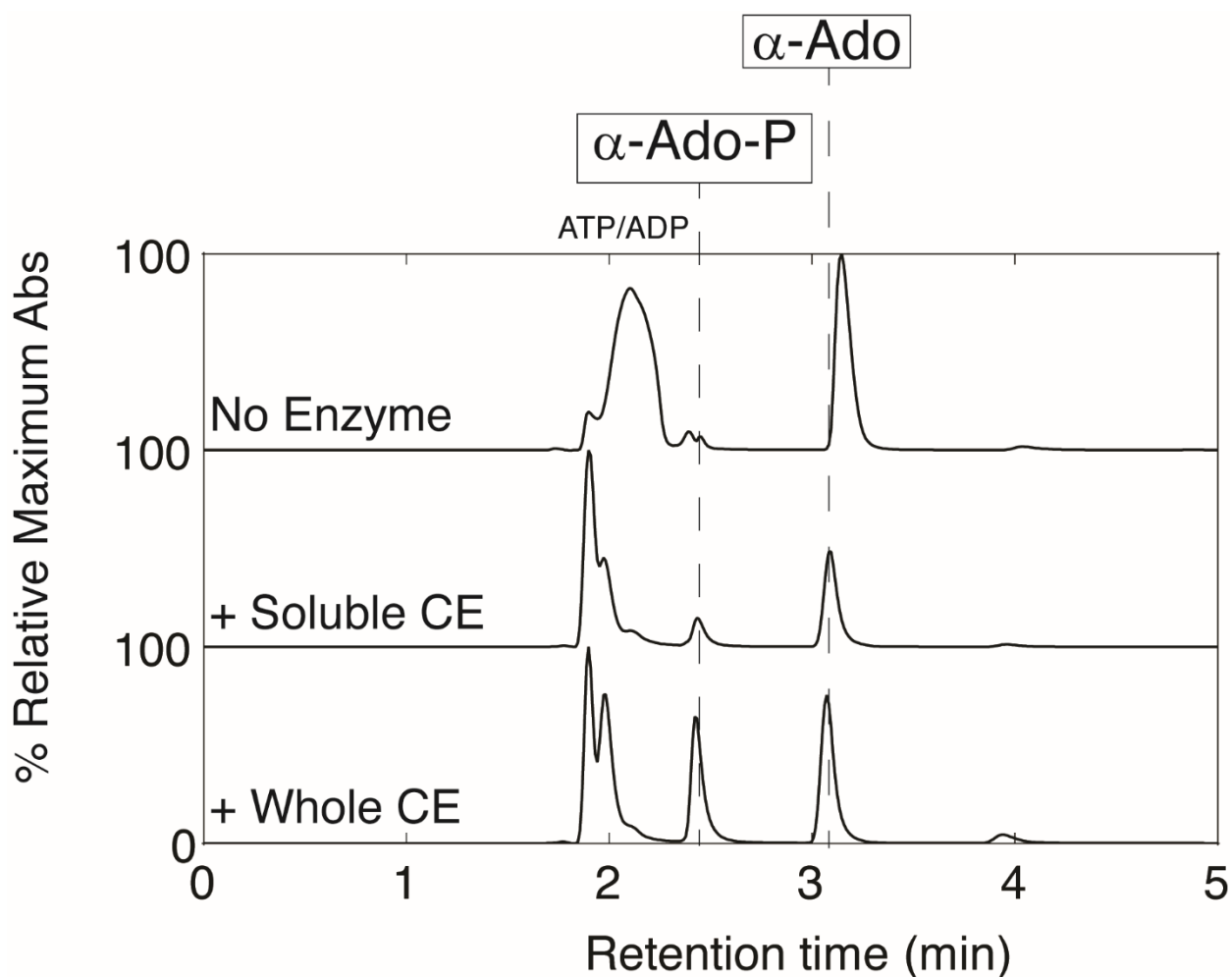


**Figure 5-8. Cell extracts of  $\Delta cobT \Delta cobB$  / pGkCbITS<sup>+</sup> (JE17830) can activate  $\alpha$ -Ado *in vitro*.**

Cell extracts were prepared as described in the *Materials and Methods*. A reaction mixture containing cell extract (10  $\mu$ g), HEPES (pH 7.5), KCl (800 mM), MgCl<sub>2</sub> (5 mM), TCEP (1.25 mM), ATP (1.75 mM), and  $\alpha$ -Ado (500  $\mu$ M) was incubated for 12 h at 37 °C before shifting to 95 °C. Reactions were separated by HPLC and peaks identified by retention times and confirmed by mass spectrometry. Retention times: ATP/ADP, ~2 min;  $\alpha$ -Ado-P (a-AMP), 2.4 min;  $\alpha$ -Ado, 3.2 min.

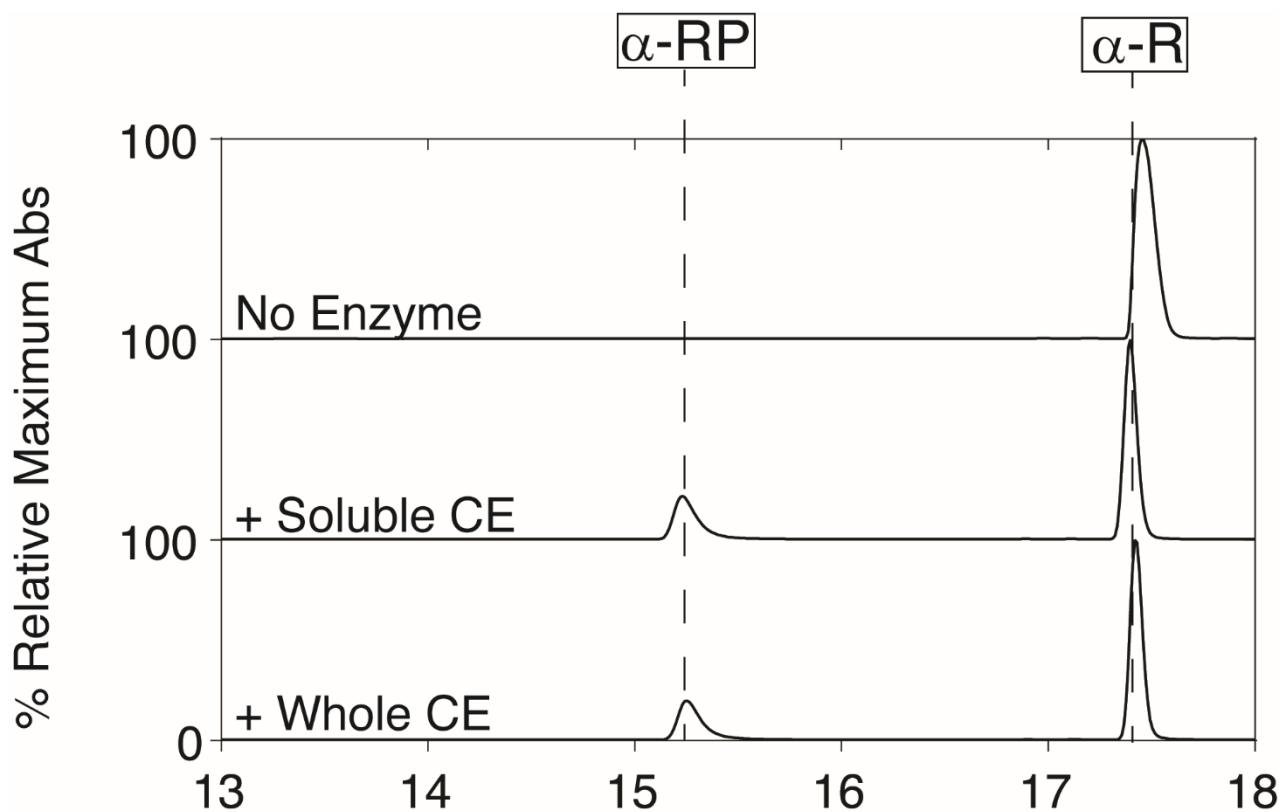


**Figure 5-9. Cell extracts of  $\Delta cobT \Delta cobB / pGkCbITS^+$  (JE17830) can activate  $\alpha$ -R *in vitro*.**

Cell extracts were prepared as described in the *Materials and Methods*. A reaction mixture containing cell extract (10  $\mu$ g), HEPES (pH 7.5), KCl (800 mM), MgCl<sub>2</sub> (5 mM), TCEP (1.25 mM), ATP (1.75 mM), and  $\alpha$ -R (500  $\mu$ M) was incubated for 12 h at 37 °C before shifting to 95 °C. Reactions were separated by HPLC and peaks identified by retention times and confirmed by mass spectrometry. Retention times:  $\alpha$ -RP, 15.1 min;  $\alpha$ -R, 17.2 min.

$\alpha$ -RP was detected in both the whole cell extract (Figure 5-9A) and the soluble extract (Figure 5-9B) in the treatment of  $\alpha$ -R. There was no observable difference in the quantity of  $\alpha$ -RP synthesized. As the reaction occurred above apparent  $K_m$  of *Gk* CblS for  $\alpha$ -R (500  $\mu$ M vs 360  $\mu$ M), indicating that the affinity of *Gk* CblS for  $\alpha$ -R is higher than that of  $\alpha$ -Ado.

**Pseudocobalamin is present in *S. enterica*  $\Delta cobT \Delta cobB$  / p*GkCblTS*<sup>+</sup> corrinoid extracts when  $\alpha$ -Ado is fed at 1  $\mu$ M.**

As noted above,  $\alpha$ -Ado cannot support full density growth, but it can be activated by the cell extracts containing *Gk* CblS and *Gk* CblT. The corrinoids were extracted from cells expressing *Gk* CblS and CblT that are fed  $\alpha$ -Ado to see if pseudoCbl is synthesized. An excess of the ring precursor was provided to saturate the condensation reaction at CobS, which should facilitate utilization of  $\alpha$ -Ado-P. While unexpected, if the adenine-containing pseudoCbl is not detected in the extracted corrinoids, that would suggest that  $\alpha$ -Ado is degraded upon entry to the cell.

JE17830 cells were grown up on minimal NCE ribose medium with an excess of (CN)<sub>2</sub>Cbi (1  $\mu$ M) and one of the following:  $\alpha$ -Ado (1  $\mu$ M),  $\alpha$ -R (1  $\mu$ M), Ade (500  $\mu$ M), or DMB (500  $\mu$ M). The cells were harvested, and the corrinoids were extracted as described (9). A cobamide was considered detected when a given peak appears on both the 367 nm and 525 nm channels on the detector as the deproteinated extracts are separated. (CN)<sub>2</sub>Cbi was found to elute at 14 min in all samples (9). Figure 5-10 contains the trace results at 525 nm for the prepared samples.

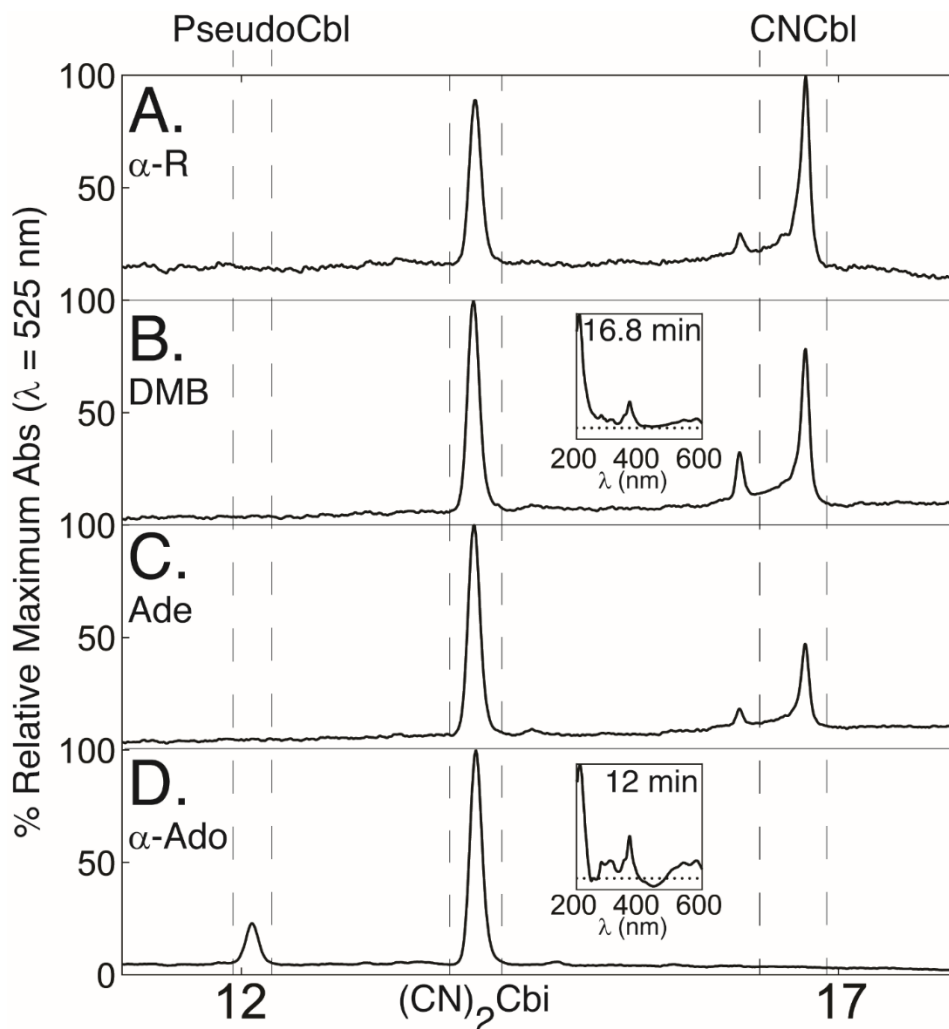


**Figure 5-10. Corrinoid extractions reveal that pseudoCbl is synthesized when  $\Delta cobT \Delta cobB$  /  $pGkCbITS^+$  (JE17830) is fed  $\alpha$ -Ado.** JE17830 ( $CblT^+ CblS^+$ , black bars) was grown on minimal NCE medium containing ribose (22 mM), trace minerals, magnesium sulfate (1 mM), L-arabinose (500  $\mu$ M), ampicillin (100 mg mL<sup>-1</sup>) and (CN)<sub>2</sub>Cbi (1  $\mu$ M).  $\alpha$ -R and  $\alpha$ -Ado were added at 1  $\mu$ M. DMB and Ade were added at 500  $\mu$ M. Corrins were extracted and separated on the HPLC as described in the *Materials and Methods*. The UV-Visible spectra of CNCbl (16.8 min) and pseudoCbl (12 min) are provided in the insets. A. 1  $\mu$ M  $\alpha$ -R. B. 500  $\mu$ M DMB. C. 500  $\mu$ M Ade. D 1  $\mu$ M  $\alpha$ -Ado.

As we expected, when fed  $\alpha$ -R, the cell synthesized Cbl exclusively (Figure 5-10A; 16.8 min, inset). Exclusive synthesis of Cbl is also observed when either the base DMB (Figure 5-10B) or Ade (Figure 5-10C) are provided. The lack of pseudoCbl synthesized in the presence of Ade indicates no  $\alpha$ -Ado is synthesized in the cell, despite the abundance of adenine present.

Strikingly, in the extracts from cells fed  $\alpha$ -Ado, HPLC separation revealed peak formation at approximately 12 minutes (Figure 5-10D), which would correspond to the elution time of pseudoCbl (9). A fraction containing this peak was collected, cleaned up via a SepPak C18 Plus (Waters), and submitted for MALDI mass spectrometry analysis. While we await confirmation, if this peak is indeed pseudoCbl, it would support a hypothesis that the method by which the other benzimidazolyl- $\alpha$ -ribosides are imported into the cell is a barrier to the importation of  $\alpha$ -Ado.

**An *S. enterica*  $\Delta cobT$   $\Delta cobB$  strain expressing the E51A or E98A variants of the *Gk* CblS kinase is an  $\alpha$ -R auxotroph.**

The observed differences in affinities for the  $\alpha$ -ribosides may be the result of specific features of the kinase's active site. Attempts to purify this protein to homogeneity for crystallography to visualize the active site have been unsuccessful, but it may be possible to perform a functional analysis through the generation of catalytic variants.

Generating variants via an unbiased (random) approach. Attempts to use the XL1-Red mutagenic *E. coli* (Agilent) for unbiased mutation of the gene in p*GkCblS3* were unsuccessful. Recapitulation of *Gk* CblS phenotypes in an *E. coli*  $\Delta metE$   $\Delta cobT$  background were unreproducible, necessitating the transfer of the mutagenized vectors to *S. enterica* and passaging through the restriction-deficient *S. enterica* strain JR501. After isolation from the restriction-deficient strain, no transformation was observed in JE12939. In the future, hydroxylamine mutagenesis of a phage

carrying p*GkCblS3* or random mutagenesis by PCR amplification of the gene may be better methods for generating unbiased mutations of the gene.

Generating variants via a biased (targeted) approach. As mentioned earlier, CblS is a member of a family of proteins with other ATP-utilizing proteins like HypE and PurM. Computer annotation identified a conserved ATP-binding domain illustrated in Figure 5-11. Eight residues were selected for site-directed mutagenesis; six were annotated as contributing to ATP-binding (R46, V47, E51, T94, S96, and E98) and the remaining two are conserved glutamates identified in the C-terminal region of the protein (E174 and E180). Of these eight, six alanine-replacement variants were successfully generated in p*GkCblS3* (R46, E51, S96, E98, E174, and E180) and two in the over-expression vector p*GkCblS2* (T94A and E98). No additional work has been done with the p*GkCblS2* variants.

The six *Gk CblS* variants encoded on the modified p*GkCblS3* vectors were transformed into JE12939. As discussed earlier, *Gk CblS*, in the absence of *Gk CblT*, is active in *S. enterica*  $\Delta cobT \Delta cobB$  but cannot scavenge DMB from the medium when (CN)<sub>2</sub>Cbi is limiting. However, it does respond to the addition of the molecule 4,5-dimethyl-1,2-phenylenediamine (DMPDA). DMPDA condenses with R5P to generate DMB and erythrose-4-phosphate (28). By feeding DMPDA (10  $\mu$ M) on medium supplemented with ribose, we can artificially boost endogenous DMB levels and consequently yield  $\alpha$ -R.

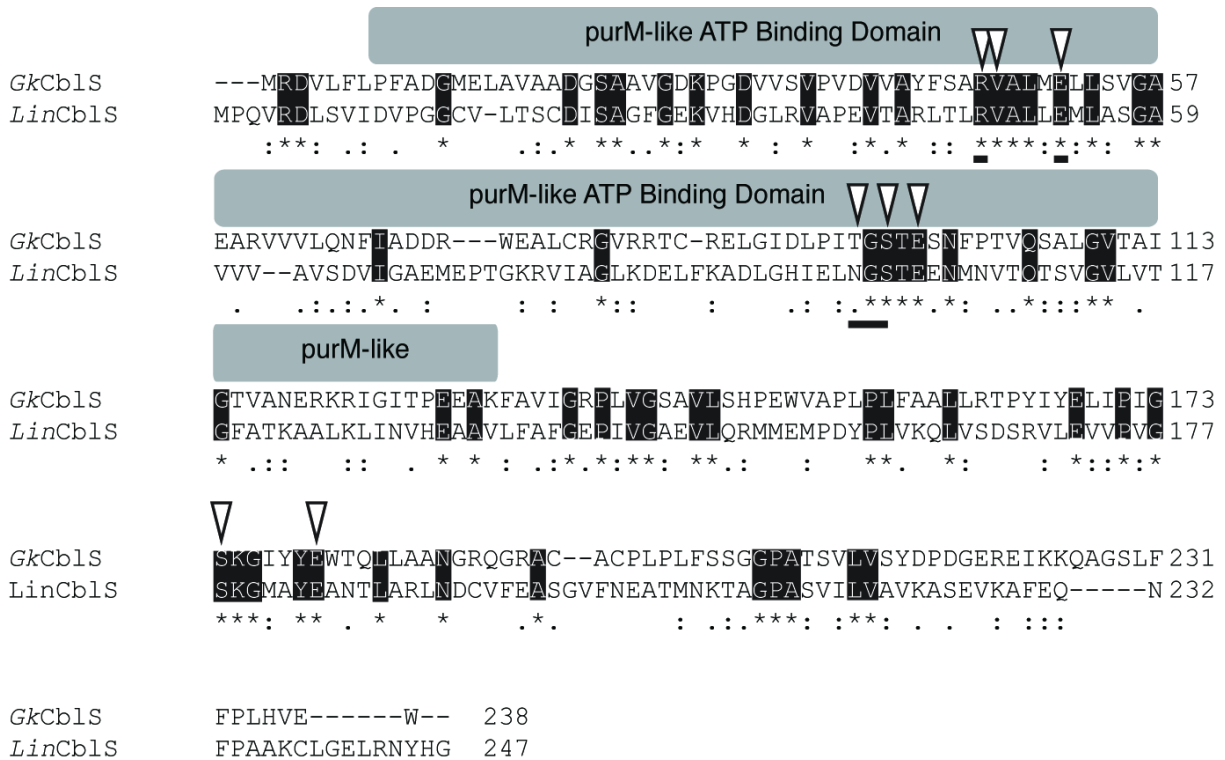


**Figure 5-11. Annotation of a Clustal Omega alignment of Cb1S reveals conserved residues in the ATP binding domain.** A Clustal Omega (29) alignment of *Gk* Cb1S (GK2255) and *L. innocua* Cb1S (LIN1110) revealed conserved residues (black boxes). A conserved PurM-like domain for ATP binding was identified by NCBI (accession ID YP\_148108). The black underlines below the sequences indicate the residues expected to bind ATP (V47, E51, T94, G95, and S96). The white triangles indicate the eight residues targeted for site-directed mutagenesis.

These growth analyses were performed as before, with the modification that JE12939 expressing either wild-type *Gk CblS* or its variants were tested against medium supplemented with varying concentrations of precursors molecules and assessed for growth. Those conditions were: limiting (CN)<sub>2</sub>Cbi (0.25 nM); limiting (CN)<sub>2</sub>Cbi (0.25 nM) + 200 μM DMPDA; limiting (CN)<sub>2</sub>Cbi (0.25 nM) + α-R (300 nM); saturating (CN)<sub>2</sub>Cbi (5 nM); saturating (CN)<sub>2</sub>Cbi (5 nM) + DMPDA (200 μM); saturating (CN)<sub>2</sub>Cbi (5 nM) + DMB (200 μM); saturating (CN)<sub>2</sub>Cbi (5 nM) + DMB (200 μM) + α-R (300 nM); and saturating (CN)<sub>2</sub>Cbi (5 nM) + α-R (300 nM). Generation times of the various variants under the various conditions are reported in Table 5-5. As expected, wild-type *Gk CblS* permitted growth when either (CN)<sub>2</sub>Cbi was not limiting or the medium was supplemented with DMPDA or α-R.

Production of *Gk CblS*<sup>R46A</sup> by JE12939 did not show any significant defects under these conditions. When the variants *Gk CblS*<sup>E51A</sup>, *Gk CblS*<sup>S96A</sup>, *Gk CblS*<sup>E174A</sup>, and *Gk CblS*<sup>I80A</sup> are produced by JE12939, growth is inhibited in the presence of exogenous DMB, but the addition of α-R resolves that blockage. DMB is expected to increase intracellular α-R so inhibition by its addition could suggest a change in the dissociation rate for α-R, or possibly even increased affinity for DMB, blocking binding of the riboside.

The E51A variant also showed a slight growth defect in the absence of either DMPDA or α-R, regardless whether (CN)<sub>2</sub>Cbi was limited or provided in excess. A *ΔcobT ΔcobB* strain producing this variant appears to be unable to detect the endogenous synthesis of DMB, which could potentially be a tool as a positive selection for DMB or α-R synthesis in *S. enterica*.

A *ΔcobT ΔcobB* strain producing *Gk CblS*<sup>E98A</sup> is a complete auxotroph for α-R and cannot scavenge DMB or DMPDA efficiently. It will be necessary to study the E98A variant *in vitro* to understand this phenotype, but most likely, it has a reduced affinity for α-R. As with the E51A

variant, the E98A variant could be used to probe for DMB or  $\alpha$ -R synthesis by positive selection of suppressor mutations.

**Table 5-5. Generation time comparisons of *Gk* CblS variants.** All strains were grown on minimal NCE medium supplemented with trace minerals, ribose (22 mM), MgSO<sub>4</sub> (1 mM), L-arabinose (500  $\mu$ M), and ampicillin (100 mg mL<sup>-1</sup>). (CN)<sub>2</sub>Cbi, DMB, DMPDA, and  $\alpha$ -R were provided at the concentrations indicated. Growth was measured for 24 h. A lower generation time indicates faster growth.

<b>Generation Time (h)</b>	<b><i>Gk</i>CblS<sup>WT</sup></b>	<b>R46A</b>	<b>E51A</b>	<b>S96A</b>	<b>E98A</b>	<b>S174A</b>	<b>E180A</b>
<b>0.5 nM (CN)<sub>2</sub>Cbi (<i>Limiting</i>)</b>	33	27	31	27	32	30	22
<b>+ 200 <math>\mu</math>M DMPDA</b>	1	1	1	1	11	1	1
<b>+ 300 nM <math>\alpha</math>-R</b>	1	1	1	1	1	1	1
<b>5 nM (CN)<sub>2</sub>Cbi (<i>Excess</i>)</b>	1	2	7	2	29	2	2
<b>+ 200 <math>\mu</math>M DMPDA</b>	1	1	1	1	13	1	2
<b>+ 200 <math>\mu</math>M DMB</b>	2	2	39	33	46	33	29
<b>+ 200 <math>\mu</math>M DMB + 300 nM <math>\alpha</math>-R</b>	1	1	1	1	16	2	2
<b>+ 300 nM <math>\alpha</math>-R</b>	1	1	1	1	1	1	1

## DISCUSSION.

In this study, we showed that *Gk* CblS activity depends on the orientation of the N-glycosidic bond of a riboside as the kinase phosphorylates  $\alpha$ -ribosides other than  $\alpha$ -R *in vitro*, including  $\alpha$ -Ado, but not  $\beta$ -ribazole. While all of the  $\alpha$ -ribosides tested could permit growth in a  $\Delta cobT \Delta cobB$  strain producing the kinase, possible transport issues for the charged molecules  $\alpha$ -hydroxyBza-R and  $\alpha$ -Ado were observed. An *S. enterica*  $\Delta cobT \Delta cobB$  producing the kinase could be forced to make pseudoCbl following supplementation with a high concentration of  $\alpha$ -Ado, but supplementation of the purine adenine yields only Cbl, confirming that *S. enterica* does not synthesize  $\alpha$ -Ado. Some initial work to generate catalytic variants of the kinase yielded two variants which may be useful for probing how *S. enterica* makes DMB or  $\alpha$ -R endogenously.

### ***Gk* CblS can activate $\alpha$ -Ado.**

It is clear from this work and our previous report (9) that *S. enterica* does not synthesize  $\alpha$ -Ado endogenously, even when adenine pools are increased by exogenous feeding (Figure 5-10C). Indeed, the deletion of *apt*, which results in accumulation of intracellular adenine (11), in an *S. enterica*  $\Delta cobT \Delta cobB$  strain producing *Gk* CblT and CblS (JE17830) does not recover growth when the ring precursor (CN)<sub>2</sub>Cbi is limited (data not shown).

Previous studies of CblS kinases (8, 9) focused on the DMB- $\alpha$ -riboside,  $\alpha$ -R, because of its ability to enhance growth in *Listeria innocua* (8). Dependence on  $\alpha$ -R presents a unique challenge for *Firmicutes* utilizing the CblT/CblS system, particularly those who lack a DMB: NaMN PRTase, as they appeared dependent on scavenging a specific molecule from the environment. While  $\alpha$ -R may be present in the environment (30), endogenous synthesis could yield a competitive advantage in these organisms.

Activation by *Gk* CblS of non-DMB  $\alpha$ -ribosides, including  $\alpha$ -Ado, indicates that CblT and CblS are responsible for scavenging *any*  $\alpha$ -riboside, not just  $\alpha$ -R. Future study will necessitate understanding how *Salmonella* and other organisms synthesize these ribosides.

***S. enterica* cannot efficiently transport  $\alpha$ -Ado into the cell for activation when the ring is limited.**

When testing feeding of the  $\alpha$ -ribosides, we found inefficient utilization of the  $\alpha$ -ribosides containing charged bases,  $\alpha$ -hydroxyBza-R and  $\alpha$ -Ado. While growth on  $\alpha$ -hydroxyBza-R could be rescued by increasing the concentration in the external medium,  $\alpha$ -Ado did not support robust growth even when provided at 1  $\mu$ M. Treatment with cell extract did not reveal any detectable degradation of the molecule; indeed, we found *Gk* CblS was active in the cell extract and synthesized  $\alpha$ -Ado-P. It is possible that an intact cell could recognize and degrade  $\alpha$ -Ado selectively upon transport, which we bypassed by using cell extract with disrupted membranes, but it is unlikely, as pseudoCbl is (possibly) synthesized when sufficient ring precursor is provided. It may be necessary to test  $\alpha$ -Ado in a Firmicute under conditions where  $\alpha$ -ribosides generate a measurable effect on growth, such as the growth of *L. innocua* on ethanolamine (8).

Another possibility is that the polarity resulting from the amines in ADE and the hydroxyl group of 5-hydroxyBza interferes with whatever mechanism allows the non-polar benzimidazolyl- $\alpha$ -ribosides to be transported so efficiently. The inefficient uptake of these molecules may be why CblT and CblS are present in *Firmicutes*: to efficiently locate, transport, and activate  $\alpha$ -ribosides into the cell through the single membrane, regardless of the base, to enhance scavenging and prevent the  $\alpha$ -ribosides from diffusing back into the environment. In a Gram-negative cell, it is possible that accumulation of the  $\alpha$ -ribosides in the periplasm enables the CblT-independent

growth we observe with *Gk* CblS. Future studies should look at whether non-DMB  $\alpha$ -ribosides are incorporated into corrinoids in *Firmicutes* possessing only the kinase activity.

**The E51A and E98A variants of Gk CblS can be used as tools to probe for DMB and  $\alpha$ -R synthesis in *S. enterica*.**

One aspect of the preference for DMB activation by *Gk* CblS and CblT *S. enterica*  $\Delta cobT \Delta cobB$  is that we can use this as a tool to probe specifically for DMB and  $\alpha$ -R activation in *S. enterica* (9). However, under the conditions where DMB synthesis is required and detected, these probes would require a loss of function mutation. If the activities or functions we seek are redundant or essential, few LOF mutants would be isolated. Our findings that the E51A and E98A variants of *Gk* CblS are  $\alpha$ -R auxotrophs offers a condition for identifying suppressor mutations. By selecting for growth in these backgrounds, we can allow the cell to find a way to make additional DMB or  $\alpha$ -R. Using a combination of transposon mapping and sequencing, we can identify potential targets for further study in the biosynthesis of DMB or  $\alpha$ -R.

**ACKNOWLEDGMENTS.**

The authors declare no conflict of interest. This work was supported by USPHS grant R37 GM040313 to Jorge Escalante-Semerena. We thank Dr. Dennis Phillips and the University of Georgia Proteomics and Mass Spectrometry Core Facility for technical assistance.

**REFERENCES.**

1. Mattes TA, Deery E, Warren MJ, Escalante-Semerena JC. 2017. Cobalamin Biosynthesis and Insertion, p 1-24. In Scott RA (ed), Encyclopedia of Inorganic and Bioinorganic Chemistry doi:10.1002/9781119951438.eibc2489. John Wiley & Sons, Ltd, Chichester, UK.

2. Trzebiatowski JR, O'Toole GA, Escalante-Semerena JC. 1994. The *cobT* gene of *Salmonella typhimurium* encodes the NaMN: 5,6-dimethylbenzimidazole phosphoribosyltransferase responsible for the synthesis of *N*<sup>1</sup>-(5-phospho- $\alpha$ -D-ribose)-5,6-dimethylbenzimidazole, an intermediate in the synthesis of the nucleotide loop of cobalamin. *J Bacteriol* 176:3568-3575.
3. Trzebiatowski JR, Escalante-Semerena JC. 1997. Purification and characterization of CobT, the nicotinate-mononucleotide:5,6-dimethylbenzimidazole phosphoribosyltransferase enzyme from *Salmonella typhimurium* LT2. *J Biol Chem* 272:17662-17667.
4. Cheong CG, Escalante-Semerena JC, Rayment I. 1999. The three-dimensional structures of nicotinate mononucleotide:5,6-dimethylbenzimidazole phosphoribosyltransferase (CobT) from *Salmonella typhimurium* complexed with 5,6-dimethylbenzimidazole and its reaction products determined to 1.9Å resolution. *Biochemistry* 38:16125-16135.
5. Cheong CG, Escalante-Semerena JC, Rayment I. 2001. Structural investigation of the biosynthesis of alternative lower ligands for cobamides by nicotinate mononucleotide: 5,6-dimethylbenzimidazole phosphoribosyltransferase from *Salmonella enterica*. *J Biol Chem* 276:37612-37620.
6. Hazra AB, Tran JL, Crofts TS, Taga ME. 2013. Analysis of substrate specificity in CobT homologs reveals widespread preference for DMB, the lower axial ligand of vitamin B(12). *Chem Biol* 20:1275-1285.
7. Chan CH, Newmister SA, Talyor K, Claas KR, Rayment I, Escalante-Semerena JC. 2014. Dissecting cobamide diversity through structural and functional analyses of the

- base-activating CobT enzyme of *Salmonella enterica*. *Biochim Biophys Acta* 1840:464-475.
8. Gray MJ, Escalante-Semerena JC. 2010. A new pathway for the synthesis of alpha-ribazole-phosphate in *Listeria innocua*. *Mol Microbiol* 77:1429-1438.
  9. Mattes TA, Escalante-Semerena JC. 2017. *Salmonella enterica* synthesizes 5,6-dimethylbenzimidazolyl-(DMB)-alpha-riboside. Why some *Firmicutes* do not require the canonical DMB activation system to synthesize adenosylcobalamin. *Mol Microbiol* 103:269-281.
  10. Torres AC, Vannini V, Bonacina J, Font G, Saavedra L, Taranto MP. 2016. Cobalamin production by *Lactobacillus coryniformis*: biochemical identification of the synthesized corrinoid and genomic analysis of the biosynthetic cluster. *BMC Microbiol* 16:240.
  11. Anderson PJ, Lango J, Carkeet C, Britten A, Kräutler B, Hammock BD, Roth JR. 2008. One pathway can incorporate either adenine or dimethylbenzimidazole as an alpha-axial ligand of B<sub>12</sub> cofactors in *Salmonella enterica*. *J Bacteriol* 190:1160-1171.
  12. Mattes TA, Escalante-Semerena JC. 2018. Facile isolation of alpha-ribazole from vitamin B12 hydrolysates using boronate affinity chromatography. *J Chrom B* 1090:52-55.
  13. Maniatis T, Fritsch EF, Sambrook J. 1982. Introduction of plasmid and bacteriophage lambda into *Escherichia coli*, p 250-251. In Maniatis T, Fritsch EF, Sambrook J (ed), *Molecular cloning: a laboratory manual*. Cold Spring Harbor Laboratory, Cold Spring Harbor, New York.
  14. Rocco CJ, Dennison KL, Klenchin VA, Rayment I, Escalante-Semerena JC. 2008. Construction and use of new cloning vectors for the rapid isolation of recombinant proteins from *Escherichia coli*. *Plasmid* 59:231-237.

15. VanDrisse CM, Escalante-Semerena JC. 2016. New high-cloning-efficiency vectors for complementation studies and recombinant protein overproduction in *Escherichia coli* and *Salmonella enterica*. *Plasmid* 86:1-6.
16. Chan CH, Escalante-Semerena JC. 2011. ArsAB, a novel enzyme from *Sporomusa ovata* activates phenolic bases for adenosylcobamide biosynthesis. *Mol Microbiol* 81:952-967.
17. Guzman LM, Belin D, Carson MJ, Beckwith J. 1995. Tight regulation, modulation, and high-level expression by vectors containing the arabinose PBAD promoter. *J Bacteriol* 177:4121-30.
18. Berkowitz D, Hushon JM, Whitfield HJ, Jr., Roth J, Ames BN. 1968. Procedure for identifying nonsense mutations. *J Bacteriol* 96:215-220.
19. Valero E, Varon R, Garcia-Carmona F. 2000. Kinetics of a self-amplifying substrate cycle: ADP-ATP cycling assay. *Biochem J* 350 Pt 1:237-243.
20. Hazra AB, Han AW, Mehta AP, Mok KC, Osadchiy V, Begley TP, Taga ME. 2015. Anaerobic biosynthesis of the lower ligand of vitamin B12. *Proc Natl Acad Sci U S A* 112:10792-10797.
21. Crofts TS, Hazra AB, Tran JL, Sokolovskaya OM, Osadchiy V, Ad O, Pelton J, Bauer S, Taga ME. 2014. Regiospecific formation of cobamide isomers is directed by CobT. *Biochemistry* 53:7805-7815.
22. Lee J, Filosa S, Bonvin J, Guyon S, Aponte RA, Turnbull JL. 2001. Expression, purification, and characterization of recombinant purine nucleoside phosphorylase from *Escherichia coli*. *Protein Expr Purif* 22:180-8.
23. Zayas CL, Escalante-Semerena JC. 2007. Reassessment of the late steps of coenzyme B<sub>12</sub> synthesis in *Salmonella enterica*: Evidence that dephosphorylation of

- adenosylcobalamin-5'-phosphate by the CobC phosphatase is the last step of the pathway. J Bacteriol 189:2210-2218.
24. Jeter RM, Olivera BM, Roth JR. 1984. *Salmonella typhimurium* synthesizes cobalamin (vitamin B<sub>12</sub>) de novo under anaerobic growth conditions. J Bacteriol 159:206-213.
  25. Jeter RM, Roth JR. 1987. Cobalamin (vitamin B<sub>12</sub>) biosynthetic genes of *Salmonella typhimurium*. J Bacteriol 169:3189-3198.
  26. Escalante-Semerena JC, Roth JR. 1987. Regulation of cobalamin biosynthetic operons in *Salmonella typhimurium*. J Bacteriol 169:2251-2258.
  27. Tsang AW, Escalante-Semerena JC. 1998. CobB, a new member of the SIR2 family of eucaryotic regulatory proteins, is required to compensate for the lack of nicotinate mononucleotide:5,6-dimethylbenzimidazole phosphoribosyltransferase activity in cobT mutants during cobalamin biosynthesis in *Salmonella typhimurium* LT2. J Biol Chem 273:31788-31794.
  28. Maggio-Hall LA, Dorrestein PC, Escalante-Semerena JC, Begley TP. 2003. Formation of the dimethylbenzimidazole ligand of coenzyme B<sub>12</sub> under physiological conditions by a facile oxidative cascade. Org Lett 5:2211-2213.
  29. Sievers F, Wilm A, Dineen D, Gibson TJ, Karplus K, Li W, Lopez R, McWilliam H, Remmert M, Soding J, Thompson JD, Higgins DG. 2011. Fast, scalable generation of high-quality protein multiple sequence alignments using Clustal Omega. Mol Syst Biol 7:539.
  30. Johnson WM, Kido Soule MC, Kujawinski EB. 2016. Evidence for quorum sensing and differential metabolite production by a marine bacterium in response to DMSP. ISME J 10:2304-2316.

CHAPTER 6

INVESTIGATIONS INTO THE ORIGINS OF 5,6-DIMETHYLBENZIMIDAZOLE AND  
ITS  $\alpha$ -RIBOSIDE  $\alpha$ -RIBAZOLE IN *SALMONELLA ENTERICA*<sup>5</sup>

---

<sup>5</sup> Mattes, T.A. and J. C. Escalante-Semerena. To be submitted to *Journal of Bacteriology*.

## ABSTRACT.

The synthesis of a complete cobamide (i.e., coenzyme B<sub>12</sub>) requires the successful synthesis of an activated ring precursor (AdoCbi-GDP) and an  $\alpha$ -N-linked ribotide (i.e.,  $\alpha$ -ribazole-5'-phosphate,  $\alpha$ -RP). While typically the synthesis of the ribotide in *Salmonella enterica* this proceeds through the direct activation of the base (i.e. 5,6-dimethylbenzimidazole) by the DMB: nicotinate mononucleotide (NaMN) phosphoribosyltransferase (PRTase), encoded by CobT, we reported the unexpected finding that *S. enterica* can also synthesize the  $\alpha$ -N-linked riboside as well. Here, we report work to understand how that synthesis occurs and offer a framework for future studies into how *S. enterica* and other organisms synthesize DMB and  $\alpha$ -R.

The loss of the purine/pyrimidine nucleoside phosphorylases (PNPs) and hydrolases, enzymes involved in purine salvaging and possible sources of  $\alpha$ -R, resulted in a loss of ability for *S. enterica*  $\Delta cobT \Delta cobB / pGkCbITS^+$  strain to assimilate DMB from the environment. Complementation of this phenotype has been limited by DMB scavenging inhibition caused by the presence of two vectors in *S. enterica*.

The DMB auxotrophy of an *S. enterica*  $\Delta cobT \Delta cobB / pGkCbITS^+$  strain can be resolved through the addition of other benzimidazoles. Curiously, feeding of 5-hydroxybenzimidazole (hydroxyBza) or 5-methoxybenzimidazole (methoxyBza), intermediates in the anaerobic DMB biosynthetic pathway, yield the DMB-containing cobamide cobalamin instead of hydroxyBza-Cba or methoxyBza-Cba. In the anaerobic synthesis pathway, aminoimidazole-ribotide (AIR), an intermediate of purine biosynthesis, is converted to hydroxyBza. Overproduction of AIR does not appear to resolve a DMB auxotrophy, but that maybe because any modification of purine biosynthesis cause growth in a  $\Delta cobT \Delta cobB / pGkCbITS^+$  strain to be inhibited by DMB supplementation.

## INTRODUCTION.

The ability to make  $\alpha$ -N-linked ribotides is essential in the biosynthesis of coenzyme B<sub>12</sub> (adenosylcobalamin, AdoCbl) (1). Many B<sub>12</sub>-synthesizing prokaryotes generate the  $\alpha$ -ribotide [i.e.,  $\alpha$ -ribose-5'-phosphate ( $\alpha$ -RP)] through the direct activation of a nucleobase [i.e., 5,6-dimethylbenzimidazole (DMB)] (2, 3). This single-step reaction is characterized by the inversion of the N-glycosidic bond as the ribose-5-phosphate (R5P) is transferred from nicotinate mononucleotide (NaMN) to the N1 or N3 position of the imidazole ring of the nucleobase, and is catalyzed by the DMB: NaMN phosphoribosyltransferase (PRTase, EC 2.4.2.21) (4). This DMB: NaMN PRTase is promiscuous, capable of activating a variety of nucleobase compounds [i.e., adenine (Ade)] to the  $\alpha$ -ribotide [i.e.,  $\alpha$ -adenosine-5'-phosphate ( $\alpha$ -AMP)] (5-8). Some organisms use the PRTase to activate phenolic compounds for the synthesis of phenolic cobamides (9, 10).

However, some *Firmicutes*, such as *Listeria innocua*, lack the PRTase. Instead, they host a pair of proteins, the kinase CblS and the transporter CblT, which appear to mediate scavenging of the  $\alpha$ -riboside  $\alpha$ -ribose ( $\alpha$ -R) (11). The transporter helps transfer  $\alpha$ -R from outside the cell to the kinase, where it is activated to the ribotide. While it is unclear how prevalent  $\alpha$ -R is in the environment, there is some precedent for its availability in aqueous environments (12).

There is evidence that  $\alpha$ -R may also be synthesized endogenously in some organisms (13), which would render this system perhaps more robust than previously considered. When produced in a *Salmonella enterica* strain lacking the PRTase, the  $\alpha$ -riboside kinase CblS protein from *Geobacillus kaustophilus* could restore synthesis of  $\alpha$ -ribotides and, consequently, the coenzyme (13). Identification of the coenzyme produced revealed that *S. enterica* synthesizes the DMB-riboside  $\alpha$ -R endogenously, the first time synthesis of  $\alpha$ -ribosides has been observed in any organism. Critically, no adenine-containing pseudocobalamin (PseudoCbl) was detected,

suggesting the kinase could be used to probe for the synthesis of DMB in *S. enterica*, a long-standing question in the field.

Two routes to DMB have been described. In the oxygen-dependent synthesis of DMB, reduced flavin mononucleotide reacts with molecular oxygen in the active site of the protein BluB to generate DMB (14-16). In the anaerobic synthesis, the reaction of S-adenosylmethionine and aminoimidazole-ribotide (AIR) leads to the synthesis of 5'-hydroxybenzimidazole (hydroxyBza) (17), followed by a series of methylation events to generate, in order: 5'-methoxybenzimidazole (methoxyBza), 5'-methoxy-6'-methylbenzimidazole, and DMB (18).

Studies in *S. enterica* have proposed that DMB is not produced under anoxic conditions (19, 20) and that the bacterium utilizes flavin mononucleotide as the precursor to DMB (21). However, no published data exists to indicate that riboflavin can feed a DMB auxotroph. Curiously, the riboflavin in (21) was provided at low concentrations (2-3  $\mu\text{M}$ ) whereas *E. coli* riboflavin auxotrophs have been demonstrated to require two orders of magnitude more of riboflavin (500  $\mu\text{M}$ ) to restore growth on minimal medium (22).

As mentioned above, the replacement of the DMB: NaMN PRTase in *S. enterica* with *G. kaustophilus* CblT and CblS can be exploited as a means for probing DMB biosynthesis in *S. enterica*. At limiting levels of the ring precursor dicyanocobinamide [(CN)<sub>2</sub>Cbi], the cell is auxotrophic for DMB or  $\alpha$ -R, so it may be possible to substitute riboflavin or intermediates of the anaerobic biosynthetic pathway to restore DMB synthesis.

Here, we report that disruptions of multiple enzymes involved in both nucleoside salvaging and purine biosynthesis could disrupt DMB scavenging, including a family of enzymes which may be collectively responsible for  $\alpha$ -R synthesis in the cell. Additionally, an attempt to boost endogenous pools of DMB by supplementing riboflavin was unsuccessful, but two intermediates of the

anaerobic DMB synthesis pathway were found to lead to the synthesis of the DMB-containing coenzyme in *S. enterica*. These findings serve to illustrate the deep metabolic links between purine metabolism and coenzyme B<sub>12</sub> biosynthesis and provide *in vivo* evidence of a potential intermediate in DMB biosynthesis for *S. enterica*.

## **MATERIALS AND METHODS.**

### **Reagents.**

Unless otherwise indicated, chemicals were obtained from Sigma Millipore. Authentic  $\alpha$ -ribose was synthesized as reported (23).  $\alpha$ -hydroxyBza-R and  $\alpha$ -methoxyBza-R were synthesized as described below. The alkaline phosphatase (ALP; from bovine intestinal mucosa; Millipore Sigma) used for dephosphorylating ribotides contains >10 diethanolamine (DEA) units per mg of solid. Immobilized Boronic Acid Gel® (#20244) for purifying ribosides was obtained from Thermo Fisher Scientific.

### **Bacterial strain construction.**

The bacterial strains and plasmids used in this work are found in Table 6-1 (strains) and 6-2 (plasmids). Strains were transformed with plasmids of interest as described (24). Genes were inactivated through the use of Wanner insertions as described (25), using the primers listed in Table 6-3. Insertions were confirmed by PCR, using the primers found in Table 6-4. As necessary, the insertions were resolved as described (25) and deletions verified by PCR.

### **Plasmid construction.**

The sequences of the primers used in this study are listed in Table 6-3. Unless otherwise indicated, DNA amplification, restriction digestion, and ligation were performed according to manufacturer's instructions. The hexahistidine tags of pTEV5 and pTEV18 add the following

protein sequence (~3 kDa) to the N-terminus of the protein: MSYYHHHHHDYDIPTSENL YFQG (26).

### **Type IIS Restriction Cloning.**

The high-efficiency Type IIS cloning (27) was used to insert the following genes into the pCV1 and pCV3 cloning vectors (28): *Rhizobium leguminosarum ribN* (*rl1692*), *Corynebacterium glutamicum pnuX* (*WA5\_0063*), and *Bacillus subtilis fmnP* (*ribU*, *bsu23050*). The following *S. enterica* genes were inserted into the pCV3 and pTEV 18 expression vectors (28): *xapA* (*stm05445*), *udp* (*stm3968*), *rihA* (*stm0661*), *rihC* (*stm0051*), *dlhH* (*stm3967*), and *yaiE* (*ppnP*, *stm0391*). The genes were amplified from genomic DNA using the corresponding primers (Table 6-4, Type IIS Restriction Cloning) and Phusion DNA polymerase (Thermo Fisher Scientific) according to the manufacturer instructions. The resulting DNA product was cloned into the BspQI site of pCV1, pCV3, or pTEV18 as described (28). After colony screening for insertion, the plasmids were certified by sequencing.

### **Restriction Double Digest Cloning.**

Due to the presence of BspQI sites in the *S. enterica* genes *deoA* (*stm4568*) and *deoB* (*stm4569*), these genes were cloned into pBAD33-SD1 (*deoA*) and pTEV5 (*deoA*, *deoB*). pBAD33-SD1 is a modified version of the original arabinose-inducible pBAD33 expression vector (29); a Shine-Dalgarno (AGG AGG) site has been inserted immediately upstream of the NheI site at the 5' end of the multiple cloning site.

The genes were amplified from *S. enterica* genomic DNA using the corresponding primers found in Table 6-5 (Restriction Double Digest Cloning) and Pfu Ultra II DNA polymerase (Agilent) according to the manufacturer's instructions. The amplified products were then cleaned up using a Wizard SV Gel and PCR Clean-Up system (Promega). The products and their target vectors were

digested by restriction enzymes (FastDigest, Thermo Fisher Scientific) in the following pairings: 1) *deoA* + pBAD33-SD1 cut with EcoRI/HindIII, 2) *deoA* + pTEV5 cut with NheI/BamHI, and 3) *deoB* + pTEV5 cut with NheI and XmaI. FastAP (Alkaline phosphatase, Thermo Fisher Scientific) was also added to the digestions of the vectors. The resulting products were ligated together and transformed into *E. coli* DH5 $\alpha$ . Candidates carrying the insertions were identified by PCR and verified by sequencing.

Cloning into pTAC85 proceeded as described above, with the modification that the amplified genes [*S. enterica cobT* (*stm2016*), *G. kaustophilus cblT* (*gk2256*), *G. kaustophilus cblS* (*gk2255*), *Listeria innocua cblT* (*lin1153*), and *L. innocua cblS* (*lin1110*)] and pTAC85 were digested with BamHI and Sall (30). The genes were amplified using the oligonucleotides found in Table 6-5 (pTAC85 cloning).

#### **Site-directed mutagenesis of *S. enterica xapA*.**

The native sequence of *xapA* in *S. enterica* encodes a protein which is unable to facilitate xanthosine scavenging, suggesting it may have limited activity (31). A change of aspartate-72 to a glycine recovers the ability for *S. enterica* to use xanthosine as a carbon and energy source. Site-directed mutagenesis was performed using primers designed using PrimerX (available at <http://www.bioinformatics.org/primerx/>) to modify the codons encoding aspartate-72 to encode glycine.

#### **Preparation of $\alpha$ -hydroxyBza-R and $\alpha$ -methoxyBza-R.**

The CobT enzyme of *S. enterica* was purified as described (2). The reaction mixture (800  $\mu$ L) contained CHES buffer (pH 9.5, 100 mM), enzyme (30  $\mu$ g), base (4 mM), and nicotinate mononucleotide (NaMN; 2.5 mM). The reaction proceeded at 37  $^{\circ}$ C for 16+ h. 10 U of ALP was added to cleave the 5' phosphate, and the reaction was incubated at 37  $^{\circ}$ C for 16+ h. A shift to 100

°C for 15 min followed by centrifugation (15 min; 15k x g) terminated the reactions. The reaction was diluted with loading buffer (1.6 mL) containing ammonium acetate (300 mM, pH 8.8) and magnesium chloride (2 mM), and passed over a column containing equilibrated immobilized boronate resin (0.25 mL; Thermofisher Scientific). Following a wash with five column volumes of loading buffer, the ribosides were eluted with formic acid (1.5 mL). The eluate was lyophilized, resuspended in DMSO (100%), and quantified using absorbance as described (23), using the extinction coefficients of the bases 5-hydroxyBza ( $4398 \text{ M}^{-1} \text{ cm}^{-1}$  at 291 nm) and 5-methoxyBza ( $4223 \text{ M}^{-1} \text{ cm}^{-1}$  at 288 nm) on DMSO.

**Table 6-1. Strains used in this study.**

Strains	Antibiotic resistance	Relevant genotype	Reference or source
<i>E. coli</i> strains <sup>1</sup>			
DH5 $\alpha$ /F'			
JE13607	Km <sup>R</sup>	BL21 ( $\lambda$ DE3) <i>cobT762::kan</i> <sup>+</sup>	(9)
JE24285	Km <sup>R</sup> , Ap <sup>R</sup>	BL21 (DE3) <i>cobT762::kan</i> / pTEV5 (bla+)	
<i>S. enterica</i> strains <sup>2</sup>			
JR501 (JE11492)		( <i>Salmonella enterica</i> ) <i>hsdSA29 hsdSB121 hsdL6 metA22 metE551 trpC2 ilv-452 rpsL120 xyl-404 galE719 H1-b H2-e, n,x (cured of Fels2) fla-66 nm</i>	Lab collection
DM932		<i>purF2085 purR2319 ::Tn10 d(Tc)</i>	D. Downs
DM1024		<i>purE2154 ::MudJ<sup>3</sup> purR2319 ::Tn10 d(Tc)</i>	D. Downs
DM13300		<i>stm4068::cat</i>	D. Downs
TR6583		<i>metE205 ara-9</i>	K. Sanderson via J. Roth
JE7088		$\Delta$ <i>metE2702 ara-9</i>	Lab collection
JE12939		$\Delta$ <i>metE2702 ara-9</i> $\Delta$ <i>cobT1380</i> $\Delta$ <i>cobB1375</i>	Lab collection
E17827	Ap <sup>R</sup>	$\Delta$ <i>metE2702 ara-9</i> $\Delta$ <i>cobT1380</i> $\Delta$ <i>cobB1375</i> / pBAD24	(13)
JE17830	Ap <sup>R</sup>	$\Delta$ <i>metE2702 ara-9</i> $\Delta$ <i>cobT1380</i> $\Delta$ <i>cobB1375</i> / pGkCblTS2	(13)
JE21364	Ap <sup>R</sup>	$\Delta$ <i>metE2702 ara-9</i> $\Delta$ <i>cobT1380</i> $\Delta$ <i>cobB1375</i> / pGkCblS3	(13)
<i>PNP/hydrolase gene analysis</i>			
JE24436		$\Delta$ <i>metE2702 ara-9</i> $\Delta$ <i>cobT1379</i> $\Delta$ <i>cobB1374</i> <i>deoD405::kan</i>	
JE24437	Cm <sup>R</sup>	$\Delta$ <i>metE2702 ara-9</i> $\Delta$ <i>cobT1379</i> $\Delta$ <i>cobB1374</i> <i>rihA57::cat</i>	
JE24438	Cm <sup>R</sup>	$\Delta$ <i>metE2702 ara-9</i> $\Delta$ <i>cobT1379</i> $\Delta$ <i>cobB1374</i> <i>rihC54::kan</i>	
JE24439	Cm <sup>R</sup>	$\Delta$ <i>metE2702 ara-9</i> $\Delta$ <i>cobT1379</i> $\Delta$ <i>cobB1374</i> <i>xapA::cat</i>	
JE24440	Km <sup>R</sup>	$\Delta$ <i>metE2702 ara-9</i> $\Delta$ <i>cobT1379</i> $\Delta$ <i>cobB1374</i> <i>udp221::kan</i>	
JE24467	Km <sup>R</sup> , Cm <sup>R</sup>	$\Delta$ <i>metE2702 ara-9</i> $\Delta$ <i>cobT1379</i> $\Delta$ <i>cobB1374</i> <i>udp221::kan</i> <i>xapA::cat</i>	
JE24468		$\Delta$ <i>metE2702 ara-9</i> $\Delta$ <i>cobT1379</i> $\Delta$ <i>cobB1374</i> $\Delta$ <i>udp222</i> $\Delta$ <i>xapA</i>	
JE24476	Km <sup>R</sup> , Cm <sup>R</sup>	$\Delta$ <i>metE2702 ara-9</i> $\Delta$ <i>cobT1379</i> $\Delta$ <i>cobB1374</i> <i>deoA409::cat</i> <i>deoD405::kan</i>	
JE24492	Km <sup>R</sup> , Cm <sup>R</sup>	$\Delta$ <i>metE2702 ara-9</i> $\Delta$ <i>cobT1379</i> $\Delta$ <i>cobB1374</i> $\Delta$ <i>udp222</i> $\Delta$ <i>xapA</i> <i>deoA409::cat</i> <i>deoD405::kan</i>	
JE24524		$\Delta$ <i>metE2702 ara-9</i> $\Delta$ <i>cobT1379</i> $\Delta$ <i>cobB1374</i> $\Delta$ <i>udp222</i> $\Delta$ <i>xapA</i> $\Delta$ <i>deoA410</i> $\Delta$ <i>deoD411</i> $\Delta$ <i>deoB</i>	
JE24525	Cm <sup>R</sup>	$\Delta$ <i>metE2702 ara-9</i> $\Delta$ <i>cobT1379</i> $\Delta$ <i>cobB1374</i> $\Delta$ <i>udp222</i> $\Delta$ <i>xapA</i> $\Delta$ <i>deoA410</i> $\Delta$ <i>deoD411</i> $\Delta$ <i>deoB</i> <i>rihA57::cat</i>	
JE24526	Km <sup>R</sup>	$\Delta$ <i>metE2702 ara-9</i> $\Delta$ <i>cobT1379</i> $\Delta$ <i>cobB1374</i> $\Delta$ <i>udp222</i> $\Delta$ <i>xapA</i> $\Delta$ <i>deoA410</i> $\Delta$ <i>deoD411</i> $\Delta$ <i>deoB</i> <i>rihC54::kan</i>	
JE24528	Km <sup>R</sup> , Cm <sup>R</sup>	$\Delta$ <i>metE2702 ara-9</i> $\Delta$ <i>cobT1379</i> $\Delta$ <i>cobB1374</i> $\Delta$ <i>udp222</i> $\Delta$ <i>xapA</i> $\Delta$ <i>deoA410</i> $\Delta$ <i>deoD411</i> $\Delta$ <i>deoB</i> <i>rihA57::cat</i> <i>rihC54::kan</i>	

<sup>1</sup> All *E. coli* strains used in this study were derivatives of *E. coli* K-12

<sup>2</sup> All *S. enterica* strains used in this study were derivatives of *S. enterica* sv Typhimurium strain LT2

<sup>3</sup> MudJ is an abbreviation of MudIII1734 (32)

**Table 6-1 (Cont'd). Strains used in this study.**

Strains	Antibiotic resistance	Relevant genotype	Reference or source
JE16692	Cm <sup>R</sup>	<i>ΔmetE2702 ara-9 ΔcobT1380 ΔcobB1375 ΔydjA117 Δfnl26 ΔmdaA126::cat</i>	
JE18872	Km <sup>R</sup>	<i>ΔmetE2702 ara-9 ΔcobT1379 ΔcobB1374 purG::kan</i>	
JE18874	Cm <sup>R</sup>	<i>ΔmetE2702 ara-9 ΔcobT1379 ΔcobB1374 purC::cat</i>	
JE18876	Cm <sup>R</sup>	<i>ΔmetE2702 ara-9 ΔcobT1379 ΔcobB1374 purE::cat</i>	
JE18878	Cm <sup>R</sup>	<i>ΔmetE2702 ara-9 ΔcobT1379 ΔcobB1374 purK::cat</i>	
JE18987	Km <sup>R</sup>	<i>ΔmetE2702 ara-9 ΔcobT1379 ΔcobB1374 purI::MudJ</i>	
JE22191	Km <sup>R</sup>	<i>ΔmetE2702 ara-9 ΔcobT1380 ΔcobB1375 thiC1137::kan</i>	
JE22195	Km <sup>R</sup>	<i>ΔmetE2702 ara-9 ΔcobT1380 ΔcobB1375 purE2154::MudJ</i>	
JE22199	Tc <sup>R</sup>	<i>ΔmetE2702 ara-9 ΔcobT1380 ΔcobB1375 purR2319 ::Tn10d(Tc)</i>	
JE22204	Km <sup>R</sup> , Tc <sup>R</sup>	<i>ΔmetE2702 ara-9 ΔcobT1380 ΔcobB1375 thiC1137::kan purR2319 ::Tn10d(Tc)</i>	
JE22205	Km <sup>R</sup> , Tc <sup>R</sup>	<i>ΔmetE2702 ara-9 ΔcobT1380 ΔcobB1375 purE2154::MudJ purR2319 ::Tn10d(Tc)</i>	
JE22211		<i>ΔmetE2702 ara-9 ΔcobT1380 ΔcobB1375 ΔthiC1225</i>	
JE22212	Km <sup>R</sup>	<i>ΔmetE2702 ara-9 ΔcobT1380 ΔcobB1375 ΔthiC1225 purE2154::MudJ</i>	
JE22216	Km <sup>R</sup> , Tc <sup>R</sup>	<i>ΔmetE2702 ara-9 ΔcobT1380 ΔcobB1375 ΔthiC1225 purE2154::MudJ purR2319 ::Tn10d(Tc)</i>	
JE23961	Cm <sup>R</sup>	<i>ΔmetE2702 ara-9 ΔcobT1379 ΔcobB1374 ΔpurG purC::cat</i>	
JE23965	Cm <sup>R</sup>	<i>ΔmetE2702 ara-9 ΔcobT1379 ΔcobB1374 purI::MudJ purC::cat</i>	
<i>AIR transport</i>			
JE23432	Cm <sup>R</sup>	<i>ΔmetE2702 ara-9 STM4068::cat</i>	
JE23433	Cm <sup>R</sup>	<i>ΔmetE2702 ara-9 ΔcobT1380 ΔcobB1375 STM4068::cat</i>	
JE23434	Km <sup>R</sup> , Cm <sup>R</sup>	<i>ΔmetE2702 ara-9 ΔcobT1380 ΔcobB1375 purE2154::MudJ STM4068::cat</i>	
JE23435	Cm <sup>R</sup>	<i>ΔmetE2702 ara-9 ΔcobT1380 ΔcobB1375 ΔthiC1225 STM4068::cat</i>	
JE23436	Km <sup>R</sup> , Cm <sup>R</sup>	<i>ΔmetE2702 ara-9 ΔcobT1380 ΔcobB1375 ΔthiC1225 purE2154::MudJ STM4068::cat</i>	

Ap<sup>R</sup>, Ampicillin resistance; Cm<sup>R</sup>, chloramphenicol resistance; Km<sup>R</sup>, kanamycin resistance; Tc<sup>R</sup>, tetracycline resistance

**Table 6-2. Plasmids used in this study.**

pBAD24	Ap <sup>R</sup>	Cloning vector with P <sub>araBAD</sub> arabinose-inducible promoter	(29)
pCV1	Ap <sup>R</sup>	Cloning vector with P <sub>araBAD</sub> arabinose-inducible promoter. MCS has been modified from pBAD33 to include a BspQI restriction site.	(28)
pCV3	Cm <sup>R</sup>	Cloning vector with P <sub>araBAD</sub> arabinose-inducible promoter. MCS has been modified from pBAD33 to include an RBS and a BspQI restriction site.	(28)
pTEV18	Ap <sup>R</sup>	TEV protease-cleavable His <sub>6</sub> tag overexpression vector	(26, 28)
pGkCblTS2	Ap <sup>R</sup>	<i>G. kaustophilus cblT</i> <sup>+</sup> <i>cblS</i> <sup>+</sup> in pBAD24	(13)
pGkCblS2	Ap <sup>R</sup>	<i>G. kaustophilus cblS</i> <sup>+</sup> translational fusion to His <sub>6</sub> tag for protein purification in pTEV5	(13)
pGkCblS3	Ap <sup>R</sup>	<i>G. kaustophilus cblS</i> <sup>+</sup> in pBAD24	(13)
pCOBT140	Ap <sup>R</sup>	<i>S. enterica cobT</i> <sup>+</sup> in pBAD24	(13)
pStmDeoD1	Cm <sup>R</sup>	<i>G. kaustophilus cblS</i> <sup>+</sup> in pCV3	
pStmDeoD2	Ap <sup>R</sup>	<i>S. enterica deoD</i> <sup>+</sup> translational fusion to His <sub>6</sub> tag for protein purification in pTEV5	Chapter 4
pStmDeoB	Ap <sup>R</sup>	<i>S. enterica deoB</i> <sup>+</sup> in pTEV18	
pStmXapA1	Cm <sup>R</sup>	<i>S. enterica xapA</i> <sup>+</sup> in pCV3	
pStmXapA2	Ap <sup>R</sup>	<i>S. enterica xapA</i> <sup>+</sup> in pTEV18	
pStmUdp1	Cm <sup>R</sup>	<i>S. enterica udp</i> <sup>+</sup> in pCV3	
pStmUdp2	Ap <sup>R</sup>	<i>S. enterica udp</i> <sup>+</sup> in pTEV18	
pStmRihA1	Cm <sup>R</sup>	<i>S. enterica rihA</i> <sup>+</sup> in pCV3	
pStmRihA2	Ap <sup>R</sup>	<i>S. enterica rihA</i> <sup>+</sup> in pTEV18	
pStmRihC1	Cm <sup>R</sup>	<i>S. enterica rihC</i> <sup>+</sup> in pCV3	
pStmRihC2	Ap <sup>R</sup>	<i>S. enterica rihC</i> <sup>+</sup> in pTEV18	
pTAC85	Ap <sup>R</sup>	Cloning vector with P <sub>tac</sub> IPTG-inducible promoter.	(30)
pGkCblT7	Ap <sup>R</sup>	<i>G. kaustophilus cblT</i> <sup>+</sup> in pTAC85	
pGkCblS7	Ap <sup>R</sup>	<i>G. kaustophilus cblT</i> <sup>+</sup> in pTAC85	
pGkCblTS4	Ap <sup>R</sup>	<i>G. kaustophilus cblT</i> <sup>+</sup> in pTAC85	
pCOBT256	Ap <sup>R</sup>	<i>S. enterica cobT</i> <sup>+</sup> in pTAC85	
pCgPnuX1	Ap <sup>R</sup>	<i>Corynebacterium glutamicum pnuX</i> in pCV1	
pCgPnuX2	Cm <sup>R</sup>	<i>Corynebacterium glutamicum pnuX</i> in pCV3	

Ap<sup>R</sup>, Ampicillin resistance; Cm<sup>R</sup>, chloramphenicol resistance; Km<sup>R</sup>, kanamycin resistance

**Table 6-3. Oligonucleotides used for generating Wanner insertions in this study.**

wanner_purC_5'	CACCCAGGAGTGTTAAAGATGCAAAAGCAAGCTGAGTTGGTGTAGGCTGGAGCTGCTTC
wanner_purC_3'	AGAGCGGTTGCCCCCGGTCAGAAAGCGGAATTAATCTAACATATGAATATCCTCCTTAG
wanner_purG_5'	ATGGAAATTCCTGCGTGGTTCGCGCTGCACTGTCTGCATTTCGTGTAGGCTGGAGCTGCTTC
wanner_purG_3'	CCCTCGTGAAGAGGGGCTTAATGGCTATCGGGCTAATTACATATGAATATCCTCCTTAG
wanner_purK_5'	CAAGTTTGCGTTCCTCGGCAACGGACAACGGGCGGAATGGTGTAGGCTGGAGCTGCTTC
wanner_purK_3'	CAACAGAGAATGCGCCGCCACGCTGTTTTATTTAAGCTTCATATGAATATCCTCCTTAG
wanner_purI_5'	GGCGTCGATATTGATGCGGGTAACGCTCTGGTTGTGTAGGCTGGAGCTGCTTC
wanner_purI_3'	CACACGCTGTTTCGGAATCAGAGGCTTTGATGATACCCATATGAATATCCTCCTTAG
wanner_purE_5'	GTGATGGGGTCCAAAAGCGACTGGGCTACCGTGTAGGCTGGAGCTGCTTC
wanner_purE_3'	GGGATTTTCCAGAACTTCATCGGTTTTCGCGTTTTCGCGCATATGAATATCCTCCTTAG
ribB_Wann_5'	CCCCGCAGAGACGATGACCGTAGAACAGATGGCGTTAACCGTGTAGGCTGGAGCTGCTTC
ribB_Wann_3'	GGAAAACGTGCCCGGACGGTTAAGATCGGACGGTTTTTCCCATATGAATATCCTCCTTAG
xapA_wanner_5'	TTAAATCCGATAGAACAAGGAACTTATGCCTCACGCTGTGTAGGCTGGAGCTGCTTC
xapA_wanner_3'	CCGGGAAAGTTCAGCCGCCGCGGCGTTCGCGCATGGGACATATGAATATCCTCCTTAG
purR_wanner_5'	ATGGCAACAATTAAGATGTAGCGAAACGGGCAGTGTAGGCTGGAGCTGCTTC
purR_wanner_3'	GTCTTTGGGCTGGTGAATCGTCGTCAGCGCCGGCATATGAATATCCTCCTTAG
udp_Wanner_5'	GTTTTATATGTCCAAGTCTGATGTTTTTTCATCTCGGCCTCGTGTAGGCTGGAGCTGCTTC
udp_Wanner_3'	CCGCTTCCACGACGATTTTACCAGCGTGGCTTTCAGTTTGCATATGAATATCCTCCTTAG
deoA_Wanner_5'	TCAGGAGGGTACCGTGTTTCTCGCACAAAGAAATTTATTCGTGTGTAGGCTGGAGCTGCTTC
deoA_Wanner_3'	CAGTAATTCGACGATAGACCGAAGGTGTGCTTGCTGGCGCCATATGAATATCCTCCTTAG
rihC_Wanner_5'	AATGACAGCATCCCTACACATTATTCCTTGATACCGATCCGGTGTAGGCTGGAGCTGCTTC
rihC_Wanner_3'	CATAGGCAAACACCTCAGCCACCCACTGACGAAAACCGTCCATATGAATATCCTCCTTAG
rihA_Wanner_5'	GGAGCCACAATGGCACTGCCATTATTATTGATTGCGATGTGTAGGCTGGAGCTGCTTC
rihA_Wanner_3'	GTATTGCAGCCGTTCCGCCAGCAAATCGACAAATCCCTGCATATGAATATCCTCCTTAG
dlhH_Wanner_5'	ATTTTTTAAGGGTACGGAGAATACCATGACAACGACACATGTGTAGGCTGGAGCTGCTTC
dlhH_Wanner_3'	CAACAAACATCGTAATGCGCTGTGGTTAGCCTTTTTTCCCATATGAATATCCTCCTTAG
yaiE_Wanner_5'	AATTTAATAATGAGACGGGGCTGATTatgCTACAAAGCGTGTAGGCTGGAGCTGCTTC
yaiE_Wanner_3'	TCTCCGCCGAGAGGGGACTCACCGTTACAAATAGCGGCACATATGAATATCCTCCTTAG

**Table 6-4. Sequencing oligonucleotides used in this study.**

purK_wanner_confirm_f	GAACTGCATCAGCGCATTG
purK_wanner_confirm_rev	CGCTGTCGCGTATTGATGATA
purG_wanner_confirm_f	CGGCGCGTCAGATTCTTTAT
purG_wanner_confirm_rev	CTACAACCGCGCTTCCC
purC_wanner_confirm_f	AACCGCTATTTTCGCACCA
purC_wanner_confirm_rev	GGTCAGGCGCAGGATTAC
purI_wanner_confirm_f	ATAACCAGGGCGCAGAC
purI_wanner_confirm_rev	CCCTGAGGGTGCCTTTAAT
purE_wanner_confirm_f	CCTGATTATCATGCTATTCTCTGAC
purE_wanner_confirm_rev	TCTGCATCCAGACCAACC
ribB_Seq_F	CGGATGGGAGAGGGTAAC
ribB_Seq_Rev	ACCATTTCAGCTTATTCGTCGT
STM_deoD_SEQ_5'	ACACACGTTTTGTAGGCCTGA
STM_deoD_SEQ_3'	AGCAATTTACAGTGGGAAGTGC
STM_xapA_SEQ_5'	TGGCTATTGATGACACGTGAA
STM_xapA_SEQ_3'	TTGCCGTGAGATAAAGCCCC
STM_purR_SEQ_5'	CCCTGATGTTGCGATTAGGGT
STM_purR_SEQ_3'	TGGCTGCTGGACTATTTGGG
STM_cobB_SEQ_5'	GCAACTGGCGGAAAGACTG
STM_cobB_SEQ_3'	CGCCAGCGCCATTTATGAAG
STM_cobT_SEQ_5'	GGCGATTTTCATCCTTGGCC
STM_cobT_SEQ_3'	CCAGCGAGAAATGGCTTACC
STM_thiC_SEQ_5'	GATCCGCGGAACCTGATCAG
STM_thiC_SEQ_3'	CTTCCACCTCTTCATCGCGT
STM_purE_SEQ_5'	CGCCTTCCCCCTGTAAATGT
STM_purE_SEQ_3'	TCTCTGCGGTAATGACGCTC
STM_purK_seq_5'	TAAAGCCGGTGCCGCTAAC
STM_purK_seq_3'	TAAGCGGGTATGTGAAGCGG
STM_udp_seq_5'	ACCACATTGCCTTAAAGCGG
STM_udp_seq_3'	AGCCAATCACCGCCCCAG
STM_deoA_seq_5'	GCGCCAGCAGCTACTAAG
STM_deoA_seq_3'	ACCTACGTGCCCCAAAACGAT
STM_rihC_seq_5'	CGTTTTTGCCCATTAGTTCCGT
STM_rihC_seq_3'	TGGGCAGCAGTAAAACCACT
STM_rihA_seq_5'	TCCTTGCGAAAATCCTGCAC
STM_rihA_seq_3'	ATAACGCTGGGACGAAGCAA
STM_dlhH_Seq_5'	TCGGGTTTTGTCAGAAGAAGCA
STM_dlhH_Seq_3'	CGCCGTATATGAATGTCTGGC
STM_yaiE_Seq_5'	GCAACAGTTAATTGATGCCGGA
STM_yaiE_Seq_3'	AGCAGCGCATTCAATTCGTC

**Table 6-5. Cloning oligonucleotides used in this study.**

<i>Type IIS Restriction Cloning</i>	
RibN_bspQI_F	NNGCTCTTCNTTCATGAAAGACATGAATCAG
RibN_bspQI_R	NNGCTCTTCNTTATCAGGCTGGTTTGCGCTC
FmnP_bspQI_F	NNGCTCTTCNTTCGTGAAAGTAAAAAATTA
FmnP_bspQI_R	NNGCTCTTCNTTATTAATGGATATGTGCACT
PnuX_bspQI_F	NNGCTCTTCNTTCATGAATCCTATAACCGAA
PnuX_bspQI_R	NNGCTCTTCNTTATCAGACTGTCACAGACTC
Stm_xapA_pBAD_BspQI_F	NNGCTCTTCNTTCATGCCTCACGCTCTTTTTTCTC
Stm_xapA_BspQI_R	NNGCTCTTCNTTATTAGGCCAGCTTACG
Stm_rihA_pBAD_BspQI_F	NNGCTCTTCNTTCATGGCACTGCCATTATTATTGATTGC
Stm_rihA_BspQI_R	NNGCTCTTCNTTATTATGCGTAGTATTGC
Stm_rihC_pBAD_BspQI_F	NNGCTCTTCNTTCATGACAGCATCCCTAC
Stm_rihC_BspQI_R	NNGCTCTTCNTTATTACGGCGCATAGGC
Stm_udp_pBAD_BspQI_F	NNGCTCTTCNTTCATGTCCAAGTCTGATG
Stm_udp_BspQI_R	NNGCTCTTCNTTATTACAGCAGACGACGGGC
STM_dlhH_BspQI_5'	NNGCTCTTCNTTCATGACAACGACACATCCATCCG
STM_dlhH_BspQI_3'	NNGCTCTTCNTTATTAGCCTTTTTTCCCACCGTACTGC
STM_yaiE_BspQI_5'	NNGCTCTTCNTTCATGCTACAAAGCAATGAATACTTTTCC
STM_yaiE_BspQI_3'	NNGCTCTTCNTTATTACAAATAGCGGCACAGATACG
<i>Restriction Double Digest Cloning</i>	
Stm_deoA_TEV5_NheI_F	NNNGCTAGCATGTTTCTCGCACAAG
Stm_deoA_pTEV5_BamHI_R	NNNGGATCCCTATTTCAGTAATTCGACG
Stm_deoA_pBAD33_EcoRI_F	NNNGAATTCATGTTTCTCGCACAAG
Stm_deoA_pBAD33_HindIII_R	NNNAAGCTTCTATTTCAGTAATTCGACG
STM_deoB_NheI_5'	NNNNGCTAGCATGAAACGTGCATTTATTATGGTGC
STM_deoB_XmaI_3'	NNNNCCCGGGTCACAGCATGTTTACCCTAGTCC
<i>Site-directed mutagenesis of xapA</i>	
STM_xapA_D72G_5'	ATGCTGGTGAACGGTGCCTCGCCATCTGGCGG
STM_xapA_D72G_3'	CCGCCAGATGGCCGAGCACCAGTTCACCAGCAT

**Table 6-5 (Cont'd). Cloning oligonucleotides used in this study.**

<i>pTAC85 cloning</i>	
pTAC85_GkCblS_BamHI_5'	NNNNGGATCCATGCGTGATGTGCTTTTCC
pTAC85_GkCblS_SalI_3'	NNNNGTCGACTTACCACCTCGACGTGCAGTG
pTAC85_GkCblT_BamHI_5'	NNNNGGATCCATGAACCGCCGCTTGGCTT
pTAC85_GkCblT_SalI_3'	NNNNGTCGACGCACATCACGCATGCGGC
pTAC85_SeCobT_BamHI_5'	NNNNGGATCCATGCAGACACTACACGC
pTAC85_SeCobT_SalI_3'	NNNNGTCGACTTATGTTGCGTTTTCGTTTTC
pTAC85_LinCblS_BamHI_5'	NNNNGGATCCATGCCTCAAGTGAGGGATTT
pTAC85_LinCblS_SalI_3'	NNNNGTCGACTTAGTACCCGGCAATTCGTCTT
pTAC85_LinCblT_BamHI_5'	NNNNGGATCCATGAAGATTCAAAAATTAGTATTATGTGCG
pTAC85_LinCblT_SalI_3'	NNNNGTCGACTTAGTACCCGGCAATTCGTCTT

**Growth analyses.**

Strains were grown at 37 °C in no-carbon essential (NCE) minimal medium (33) supplemented with ribose (22 mM) as a carbon and energy source. Minimal medium also contained trace minerals, magnesium sulfate (1 mM), ampicillin (100 µg mL<sup>-1</sup>), L(+)-arabinose (500 µM) and dicyanocobinamide [(CN)<sub>2</sub>Cbi] (as indicated). Bases or ribosides were added as indicated. Growth analyses were performed in 96-well microtiter dishes, with each strain grown under indicated conditions in duplicate. Each well contained 200 µL of medium inoculated with 1% (v/v) of an overnight starter culture grown for at least 20 h on nutrient broth (Difco) to lower the level of residual nutrients in the medium. Cell density was monitored at 650 nm using a computer-controlled BioTek Powerwave XS absorbance plate reader (BioTek Instruments). Readings were acquired every 15 min for 24 h with continuous shaking. Data were analyzed using Microsoft Excel (Microsoft) and the GraphPad Prism v7 software package (GraphPad Software). The natural log of 2 was divided by the specific growth rate  $\mu$  (defined as the change in absorbance in natural log divided by time) to determine generation time.

**Corrinoid Extraction and Separation.**

Flasks (baffled, 500-mL) containing minimal NCE medium (100-mL) were supplemented with trace minerals, magnesium sulfate (1 mM), D-ribose (22 mM), L-arabinose (500 µM),

dicyanocobinamide [(CN)<sub>2</sub>Cbi, 1 μM], and either base (500 μM) or α-riboside (1 μM) were prepared. The medium was inoculated by the addition of 1% (v/v) of an overnight culture of the *S. enterica* strain Δ*cobT* Δ*cobB* / p*GkCblTS2*<sup>+</sup> grown for at least 20 h in nutrient broth (NB, Difco). Cultures were grown for >20 h at 37 °C with shaking (150 rpm) (New Brunswick Innova 44R refrigerated incubator shaker). The cells were then harvested by centrifugation (5,500 × g for 15 min) using a Beckman/Coulter Avanti J25-I centrifuge (JLA-16.250 rotor).

Cell pellets were resuspended in 5 mL of ammonium acetate (100 mM, pH 4) solution containing potassium cyanide (10 mM), and frozen at -20 °C until processed. Corrinoid extraction and isolation proceeded as described (13), with the modifications that samples were resuspended in 100-μL of buffer C [KH<sub>2</sub>PO<sub>4</sub> (100 mM), KCN (10 mM), pH 6.5] before their separation by HPLC. No bioassay was performed.

## RESULTS.

### **Loss of the nucleoside phosphorylases (PNPs) or hydrolases disrupts DMB scavenging in *S. enterica*.**

Typically, *S. enterica* utilizes ribosides as an energy source, cleaving the N-glycosidic bond to release the base and either ribose or ribose-1-phosphate. This cleavage is managed by five phosphorylases (DeoA, DeoD, XapA, Udp, and PpnP) and two hydrolases (RihA, RihC) (34, 35), though XapA activity is limited (31). Following uptake and cleavage, the base is then phosphoribosylated by base-specific phosphoribosyltransferases to the β-ribotide (34). There is no data on α-R degradation and treatment of α-R with purified *S. enterica* DeoD showed no release of DMB *in vitro* (data not shown).

Interestingly, the phosphorylase reactions can run in reverse. While typically the reverse reaction would yield β-ribosides, we considered the possibility that the PNPs can generate α-R

occasionally. (The hydrolase reaction is expected to be irreversible (34), so it is unlikely they can generate  $\alpha$ -R.)  $\alpha$ -R may accumulate in the cytosol, allowing it to be activated by CblS to the ribotide, leading to B<sub>12</sub> biosynthesis.

As mentioned before, *Gk* CblS and *Gk* CblT (13) can substitute for the loss of the two enzymes known to catalyze the activation of bases to the  $\alpha$ -ribotide, CobT (3) and CobB (36), represented by the strain JE12939 ( $\Delta cobT \Delta cobB$ ). The strain lacks MetE, the enzyme catalyzing the final step in cobamide-independent methionine synthesis (19), resulting in a methionine auxotrophy. Under normoxic conditions, the auxotrophy can be satisfied by either cobamides or methionine, permitting growth. The cobamide-dependent methionine synthase enzyme methylates homocysteine using the provided cobamides, satisfying the auxotrophy.

Under normoxic conditions, *S. enterica* does not synthesize the corrin ring (19, 37) as the genes responsible for its synthesis are inactivated in the presence of oxygen (38). Instead, the bacterium can scavenge and activate the ring for condensation with the activated  $\alpha$ -ribotide (i.e.  $\alpha$ -RP). The condensation reaction is catalyzed by the AdoCbl-5'-P synthase CobS and the efficiency of this reaction follows with saturation by one or both substrates (39). Finally, a phosphorylase removes the 5' phosphate from the nucleotide (39, 40), yielding a cobamide and permitting methionine synthesis. The synthesis of  $\alpha$ -RP can be detected under these conditions by providing the ring precursor cobinamide in its cyanated form [(CN)<sub>2</sub>Cbi] at both limiting (0.25 nM) and saturating (5 nM+) concentrations (13).

Wanner insertions (25) were generated in six of the seven genes encoding known nucleoside cleavage proteins (*deoA*, *deoD*, *xapA*, *udp*, *rihA*, *rihC*) (see Table 6-1). To construct a strain carrying disruptions of all six genes, markers encoding different drug markers permitted moving an insertion in *xapA* into a  $\Delta cobT \Delta cobB \text{ udp}::kan$  (JE24440) by P22 phage transduction (41) to

yield  $\Delta cobT \Delta cobB udp::kan xapA::cat$  (JE24467). The insertions were resolved as described (25). Then confirmed insertions in *deoA* and *deoD* (JE24476) were moved by P22 phage transduction into  $\Delta cobT \Delta cobB \Delta udp \Delta xapA$  (JE24492) and resolved. Finally, insertions in *rihA* and *rihC* were moved, sequentially, into  $\Delta cobT \Delta cobB \Delta udp \Delta xapA \Delta deoABD$  (JE24524) to yield JE24528. Resolution of *deoA* and *deoD* results in the loss of the phosphopentomutase DeoB (STM4569, EC 5.4.2.7), which converts D-ribose-5'-phosphate to D- $\alpha$ -ribose-1'-phosphate, a substrate of the PNP reaction.

Expression vectors encoding *G. kaustophilus cblS*<sup>+</sup> and *cblT*<sup>+</sup> (pGkCbITS2) and *S. enterica cobT*<sup>+</sup> were transformed into the strains, as well as the empty vector pBAD24. A list of the strains carrying plasmids can be found in Table D1. These strains were used to test the effect of the disruptions on the cell's ability to synthesize Cbl.

Strains were grown at 37 °C under normoxic conditions. Apparent DMB or  $\alpha$ -R auxotrophy is achieved in the parental strain (JE12939) by growing the cells under conditions where the ring precursor (CN)<sub>2</sub>Cbi is limited (0.25 nM) in availability. DMB (50  $\mu$ M) and  $\alpha$ -R (300 nM) were provided as indicated under limiting (0.25 nM) conditions to satisfy the auxotrophy. The ring precursor (CN)<sub>2</sub>Cbi was also provided at saturating (5 nM) conditions to assess the effect on endogenous DMB or  $\alpha$ -R synthesis. Strains carrying the empty vector failed to grow under any of the conditions tested, as expected because there is no route to  $\alpha$ -RP. When the vector encoding *S. enterica cobT*<sup>+</sup> was present, the strain grew under all of the tested conditions, indicating i)  $\alpha$ -RP synthesis is required for growth, and ii) the PNP disruptions harbored no general effect on the overall viability of the strain.

Table 6-6 reports the results of these experiments in generation time (h). As expected, the parental strain ( $\Delta cobT \Delta cobB$ ) expressing the kinase struggles to grow when limiting amounts of

the ring are provided (10 h), but growth is restored upon provision of either DMB (2 h),  $\alpha$ -R (1 h), or addition ring precursor (1 h). A similar lack of growth was observed for all of the single PNP or hydrolase deletion strains when the ring was limited. Addition of  $\alpha$ -R or additional (CN)<sub>2</sub>Cbi permitted growth across the board, confirming that the PNP disruptions did not affect overall cell viability. Strikingly, the growth suffered under limiting (CN)<sub>2</sub>Cbi conditions when DMB was added for *every* one of the PNP or hydrolase disruptions, indicating a loss of DMB scavenging ability.

Multiple deletions of the genes encoding the four PNPs or the four PNPs plus the two hydrolases resulted in strains which grow *faster* (4-6 h vs. 10 h for the parental strain) under conditions where both the availability of the ring is limited *and* neither base nor riboside is provided. Curiously, these strains remain unable to scavenge DMB, and in fact, grew slower when the base was provided than when it was not. There is no fitness defect when (CN)<sub>2</sub>Cbi is provided at saturating levels (5 nM), indicating  $\alpha$ -R synthesis is likely still occurring. It is not clear why DMB scavenging has been disrupted. Possibilities include dysfunction in DMB transport due to changes in the nucleoside scavenging or a compensatory mutation for the loss of the nucleoside scavenging genes which affects  $\alpha$ -R synthesis. It may be necessary to determine the identity of the corrinoids being synthesized in these backgrounds to confirm it is  $\alpha$ -R being synthesized as seen in the parental strain JE12939 (13).

**Table 6-6. Generation time of the PNP and hydrolase deletion strains in comparison to the parental strain,  $\Delta cobT \Delta cobB$  / pGkCbITS<sup>+</sup> (JE17830).**

Genotype (+ pGkCbITS2)		(CN)2Cbi (0.25 nM)	(CN)2Cbi (0.25 nM) + DMB (50 $\mu$ M)	(CN)2Cbi (0.25 nM) + $\alpha$ -R (300 nM)	(CN)2Cbi (5 nM)
$\Delta cobT \Delta cobB$ (parental strain)	t	10	2	1	1
	SD	0.42	0.09	0.01	0.02
$\Delta cobT \Delta cobB \Delta udp$	t	12	14	1	2
	SD	0.66	0.92	0.01	0.00
$\Delta cobT \Delta cobB \Delta xapA$	t	10	11	1	2
	SD	0.13	0.24	0.19	0.12
$\Delta cobT \Delta cobB \Delta deoA$	t	11	12	2	2
	SD	0.33	0.00	0.02	0.24
$\Delta cobT \Delta cobB \Delta deoD$	t	9	11	2	2
	SD	0.80	0.06	0.01	0.06
$\Delta cobT \Delta cobB \Delta rihA$	t	10	11	1	2
	SD	0.70	0.57	0.04	0.13
$\Delta cobT \Delta cobB \Delta rihC$	t	10	13	1	2
	SD	1.16	2.15	0.01	0.66
$\Delta udp \Delta xapA \Delta deoABD$	t	6	11	2	2
	SD	3.05	0.43	0.36	0.57
$\Delta udp \Delta xapA \Delta deoABD \Delta rihA \Delta rihC$	t	4	11	1	2
	SD	0.22	0.28	0.02	0.11

t= Generation time, in hours; SD = standard deviation

## Use of an IPTG-inducible vector for expression of the transporter and kinase prevents DMB scavenging in *S. enterica*.

The genes encoding PNPs and hydrolases were inserted into a compatible vector to see if co-expression of the PNP with the kinase and transporter restores DMB scavenging, ruling out a secondary mutation. The genes were inserted into pCV3 (28), a compatible expression vector with a pACYC ori (pBAD24 carries a pBR322 ori) (29). The vector containing *S. enterica deoD*<sup>+</sup> was transformed into JE17827 ( $\Delta cobT \Delta cobB$  / pBAD24), JE17828 ( $\Delta cobT \Delta cobB$  / pCOBT140), and JE17830 ( $\Delta cobT \Delta cobB$  / pGkCblTS2) along with the empty vector pCV3. The newly constructed strains were tested for the parental phenotypes as described before (13). Curiously, it was found that addition of the empty vector resulted in a loss of DMB scavenging, even in the parental ( $\Delta cobT \Delta cobB$ ) strain and suffered from slow growth at higher levels of (CN)<sub>2</sub>Cbi (data not shown).

One possibility for the conflict could be that both pCV3 and pBAD24 contain arabinose-inducible promoters, which could lower the amount of the kinase available, resulting in less activation. *Gk cblS*, *Gk cblT*, and *Stm cobT* were cloned into pTAC85 (30), an expression vector with the IPTG-inducible P<sub>tac</sub> promoter, to mitigate this cross-talk and allow for independent induction of each vector. The pTAC85 vectors were transformed into JE12939 ( $\Delta cobT \Delta cobB$ ) and tested under the following conditions: Limiting (CN)<sub>2</sub>Cbi (0.5 nM); Limiting + DMB (50  $\mu$ M); Limiting + DMB (200  $\mu$ M); Limiting +  $\alpha$ -R (300 nM); Saturating (CN)<sub>2</sub>Cbi (5 nM); Saturating + DMB (50  $\mu$ M); Saturating + DMB (200  $\mu$ M); and Saturating +  $\alpha$ -R (300 nM). The NCE minimal medium was supplemented with trace minerals, ribose (22 mM), MgSO<sub>4</sub> (1 mM), and ampicillin (100  $\mu$ g mL<sup>-1</sup>). Each condition was tested with or without induction (100  $\mu$ M IPTG).

The generation times for each condition by strain are listed in Table 6-7, with or without induction. When only the empty vector pTAC85 or the vector encoding *Gk CblT* (pGkCblT7) was

available, no growth was observed as the cell was unable to synthesize the complete coenzyme. Re-introduction of *cobT* on pCOBT256 yielded a robust growth response (1 h generation time) for all conditions, with or without IPTG induction.

When pTAC85 encoding *Gk CblS* (p*GkCblS7*) was present and the ring was limited, the strain became a  $\alpha$ -R auxotroph, requiring the riboside for growth (1 h). Increasing the amount of ring precursor restored growth in the absence of exogenous  $\alpha$ -R. These results are similar to those seen when the kinase was expressed from the arabinose-inducible vector.

Curiously, when *Gk CblS* and *Gk CblT* are co-expressed from pTAC85 (p*GkCblTS4*), the strain was a  $\alpha$ -R auxotroph when the ring is limited, which deviates from what we have observed when expressed from the arabinose-inducible vector (13). These results indicate a possible defect in DMB scavenging, similar to that which we observed when the PNP genes were disrupted. When the amount of ring precursor was increased but no inducer was present, growth improved (2 h). Addition of DMB at 50  $\mu$ M (3 h) and 200  $\mu$ M (6 h) seemed to suppress growth slightly. Oddly, upon induction of p*GkCblTS4*, the strain becomes a  $\alpha$ -R auxotroph at *any* amount of ring precursor. These data suggest that over-induction of the transporter and kinase may cause an issue with DMB scavenging, though the exact cause is not understood at this time. It may be necessary to insert *Gk cblT*, *Gk cblS*, and *Stm cobT* into the chromosome under an inducible promoter, which may reduce any issues related to copy number or cooperation between two vectors.

**Table 6-7. Generation times in response to pTAC85 vectors on minimal medium.**

<b>NO INDUCTION</b>	<b>Vector Only</b>	<b><i>Gk cblT</i>+</b>	<b><i>Gk cblS</i>+</b>	<b><i>Gk cblT</i>+</b> <b><i>cblS</i>+</b>	<b><i>Se cobT</i>+</b>
(CN) <sub>2</sub> Cbi (0.5 nM)	36	27	25	29	1
(CN) <sub>2</sub> Cbi (0.5 nM) + DMB (50 μM)	25	24	28	32	1
(CN) <sub>2</sub> Cbi (0.5 nM) + DMB (200 μM)	32	33	29	35	1
(CN) <sub>2</sub> Cbi (0.5 nM) + α-R (300 nM)	32	27	1	1	1
(CN) <sub>2</sub> Cbi (5 nM)	32	25	2	2	1
(CN) <sub>2</sub> Cbi (5 nM) + DMB (50 μM)	36	32	2	3	1
(CN) <sub>2</sub> Cbi (5 nM) + DMB (200 μM)	35	35	3	6	1
(CN) <sub>2</sub> Cbi (5 nM) + α-R (300 nM)	35	26	1	1	1
<b>100 μM INDUCTION</b>	<b>Vector Only</b>	<b><i>Gk cblT</i>+</b>	<b><i>Gk cblS</i>+</b>	<b><i>Gk cblT</i>+</b> <b><i>cblS</i>+</b>	<b><i>Se cobT</i>+</b>
(CN) <sub>2</sub> Cbi (0.5 nM)	48	41	16	42	1
(CN) <sub>2</sub> Cbi (0.5 nM) + DMB (50 μM)	44	44	22	48	1
(CN) <sub>2</sub> Cbi (0.5 nM) + DMB (200 μM)	42	41	38	50	1
(CN) <sub>2</sub> Cbi (0.5 nM) + α-R (300 nM)	37	21	1	1	1
(CN) <sub>2</sub> Cbi (5 nM)	53	41	2	22	1
(CN) <sub>2</sub> Cbi (5 nM) + DMB (50 μM)	53	44	2	25	1
(CN) <sub>2</sub> Cbi (5 nM) + DMB (200 μM)	44	45	2	11	1
(CN) <sub>2</sub> Cbi (5 nM) + α-R (300 nM)	44	29	1	1	1

### **Addition of riboflavin to the medium does not rescue DMB auxotrophy in *S. enterica*.**

As an alternative to DMB scavenging, it may be possible to try and increase endogenous pools of DMB by increasing flux through its synthesis. It is unclear how *S. enterica* synthesizes the base. Keck and Renz proposed that FMN is the immediate precursor to DMB (20, 21) and that the formation of DMB proceeds similarly to how the reductase BluB converts reduced FMN to DMB (14, 15). Three possible homologs of BluB were identified in *S. enterica*: YdjA (STM1296), NfnB (STM0578), and MdaA (STM0874). However, deletion of all three genes encoding these reductases failed to generate a DMB auxotrophy in an *S. enterica* strain using the *Gk* CblS kinase in place of the PRTase CobT, indicating DMB was still being synthesized (data not shown).

In tracing experiments by Keck and Renz, the labeled riboflavin (RBF) was fed to *S. enterica* at 2-3  $\mu\text{M}$ , and the C1 carbon of riboflavin was found to be incorporated into the DMB moiety of Cbl (21). By increasing the amount of riboflavin by two orders of magnitude (250  $\mu\text{M}$ ), it may be possible to satisfy, under ring-limited conditions, the DMB auxotrophy of the *S. enterica*  $\Delta\text{cobT}$   $\Delta\text{cobB}$  strain (JE12939) expressing the kinase and transporter (JE17830). The kinase and transporter were replaced by *Stm* CobT (JE17828) to account for possible radical damage from free flavin, which should grow under normoxic conditions as long as ring precursor is present. The parent strain carrying the empty vector (JE17827) was also tested to account for kinase-independent growth.

The strains were tested under normoxic conditions at 37 °C as described previously (13). In the minimal ribose medium, the ring was provided at limiting amounts (0.25 nM) to generate a DMB auxotrophy. DMB (200  $\mu\text{M}$ ) or RBF (250  $\mu\text{M}$ ) were added to restore  $\alpha$ -RP synthesis.

As anticipated, when no path to  $\alpha$ -RP is present (JE17827), no growth occurred. The presence of CobT (JE17828) permitted growth under all of the tested growth conditions, indicating no loss of cell viability from free flavin.

The strain expressing the kinase and transporter (JE17830) is auxotrophic for DMB at limiting amounts of the ring precursor and no growth (40 h generation time) was detected. Addition of DMB (200  $\mu$ M) satisfies the auxotrophy (2 h), restoring  $\alpha$ -RP synthesis and permitting growth. When RBF is added (250  $\mu$ M), however, no growth improvement was detected (38 h). These results indicate that *if* riboflavin is being taken up, it is not synthesizing sufficient levels of DMB for conversion to  $\alpha$ -R. It is worth noting that in *E. coli* riboflavin auxotrophs, they require 500  $\mu$ M or more riboflavin (22), suggesting *E. coli* cannot transport the cofactor. It is possible that *S. enterica* also struggles to transport RBF; if so, we may not be providing sufficient amounts of riboflavin.

RBF transporters (22) from three other organisms were cloned into pCV3 (28) to address the possible transport problem: *Rhizobium leguminosarum ribN* (*rl1692*) (42), *Corynebacterium glutamicum pnuX* (*WA5\_0063*) (43), and *Bacillus subtilis fmnP* (*ribU*, *bsu23050*) (43). Expression of *C. glutamicum pnuX* resulted in susceptibility to the riboflavin analog inhibitor roseoflavin (43) in *S. enterica*, even at low concentrations, when tested in minimal NCE medium supplemented with trace minerals, ribose (22 mM), MgSO<sub>4</sub> (1 mM), chloramphenicol (10  $\mu$ g mL<sup>-1</sup>), 200  $\mu$ M L-arabinose, and CNCbl (0.5 nM). At 100  $\mu$ M roseoflavin, the growth rate is diminished 3-fold (3 h doubling time vs. 1 h) in the presence of *Cg PnuX*. RBF is the preferred substrate of PnuX (43). *S. enterica* eventually recovers from roseoflavin toxicity, likely due to competition from endogenously synthesized riboflavin. Once a solution for the DMB scavenging issue with two

vectors has been identified, co-expression of PnuX, the kinase, and transporter could be used to test whether DMB is synthesized directly from RBF.

***S. enterica*  $\Delta cobT \Delta cobB$  / pGkCbITS<sup>+</sup> synthesizes *only* cobalamin in the presence of the anaerobic DMB biosynthetic intermediates 5-hydroxyBza and 5-methoxyBza.**

The lack of response to exogenous riboflavin allows for the possibility that flavins are not the immediate precursor to DMB. The anaerobic biosynthesis of DMB introduced a new branch point for the purine/thiamin intermediate aminoimidazole-ribotide (AIR). Beyond AIR, which requires deletion of the gene *stm4068* in *S. enterica* to be transported (44), the anaerobic pathway generates two commercially available intermediates, 5-hydroxyBza and 5-methoxyBza. If either of these bases can satisfy the DMB auxotrophy of an *S. enterica* utilizing the kinase to synthesize  $\alpha$ -RP from  $\alpha$ -R, it is possible that these bases are modified to DMB *before* its conversion to  $\alpha$ -R.

To account for variations in affinity for the various bases, we determined the amount of DMB necessary to *maximize* the growth rate of JE17830 ( $\Delta cobT \Delta cobB$  / pGkCbITS<sup>+</sup>) under conditions where the strain is auxotrophic for the base. As before, the strains were tested under normoxic conditions at 37 °C. Minimal NCE medium was supplemented with ribose (22 mM), MgSO<sub>4</sub> (1 mM), ampicillin (100  $\mu\text{g}^{-1} \text{mL}^{-1}$ ), L-arabinose (500  $\mu\text{M}$ ), and (CN)<sub>2</sub>Cbi (0.25 nM; limited). DMB was titrated from 20 to 500  $\mu\text{M}$ . In the absence of *Gk* CbIT (JE21364, *Gk cbIS*<sup>+</sup> only) or the empty vector strain (JE17827), no response to DMB was detected.

The results of the experiments are found in Figure 6-1, reported in generation time in hours. At 50  $\mu\text{M}$  DMB, the generation time was reduced by 82% (3 h) compared to growth when no base was provided. A 10-fold increase over 50  $\mu\text{M}$  to 500  $\mu\text{M}$  yielded a 90% reduction in time, down to 2 h. Bases will be added at this level (500  $\mu\text{M}$ ) for the remainder of this work.

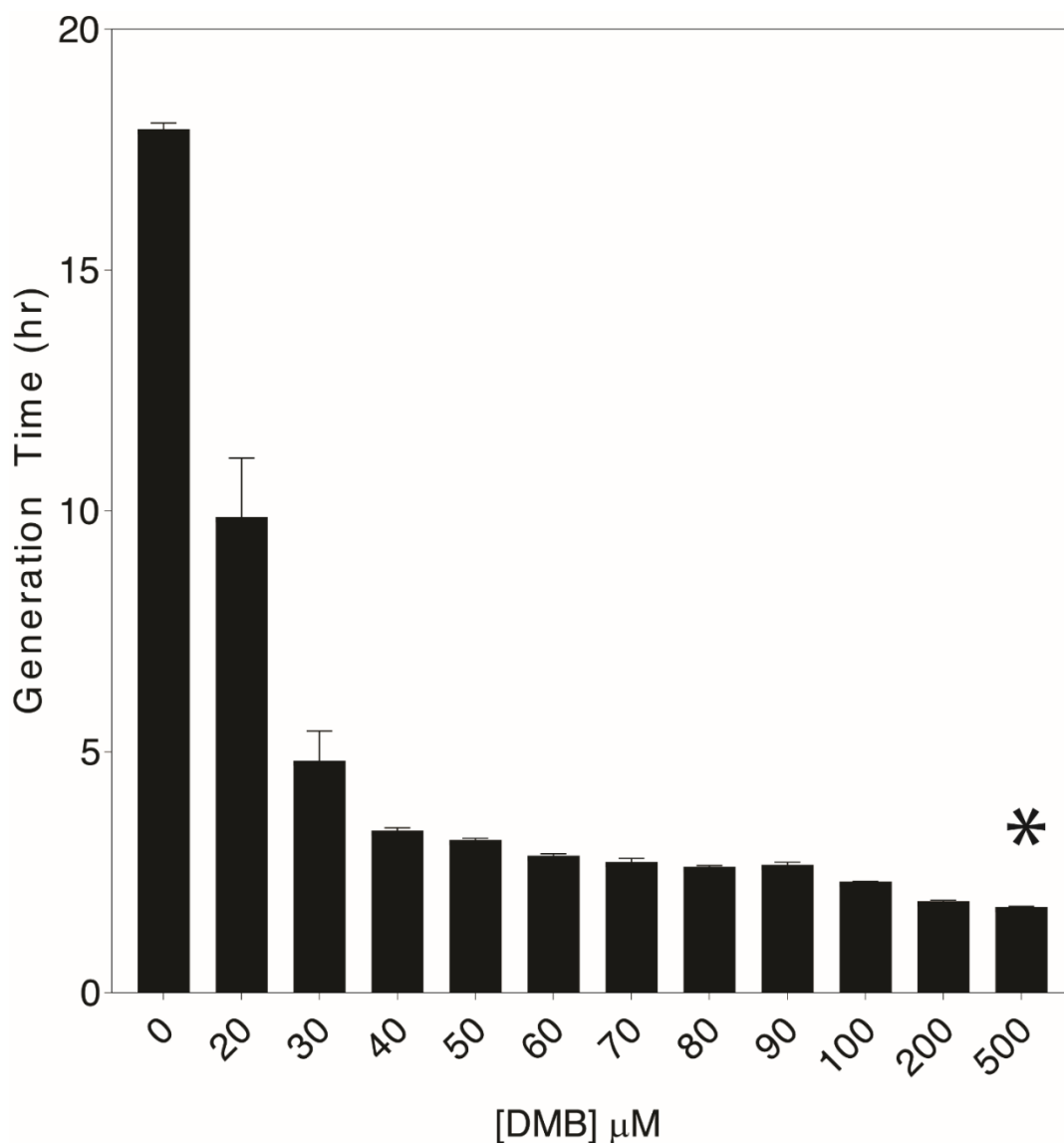


**Figure 6-1. The growth rate of JE17830 varies with the concentration of DMB under limiting conditions.** JE17830 (CbIT<sup>+</sup> CbIS<sup>+</sup>) was grown on minimal NCE medium containing ribose (22 mM), trace minerals, magnesium sulfate (1 mM), L-arabinose (500 mM), ampicillin (100 mg mL<sup>-1</sup>) and (CN)<sub>2</sub>Cbi (0.25 nM). DMB concentration was varied from 0 to 500  $\mu\text{M}$ . The asterisk (\*) indicates the concentration of DMB which maximizes the growth rate.

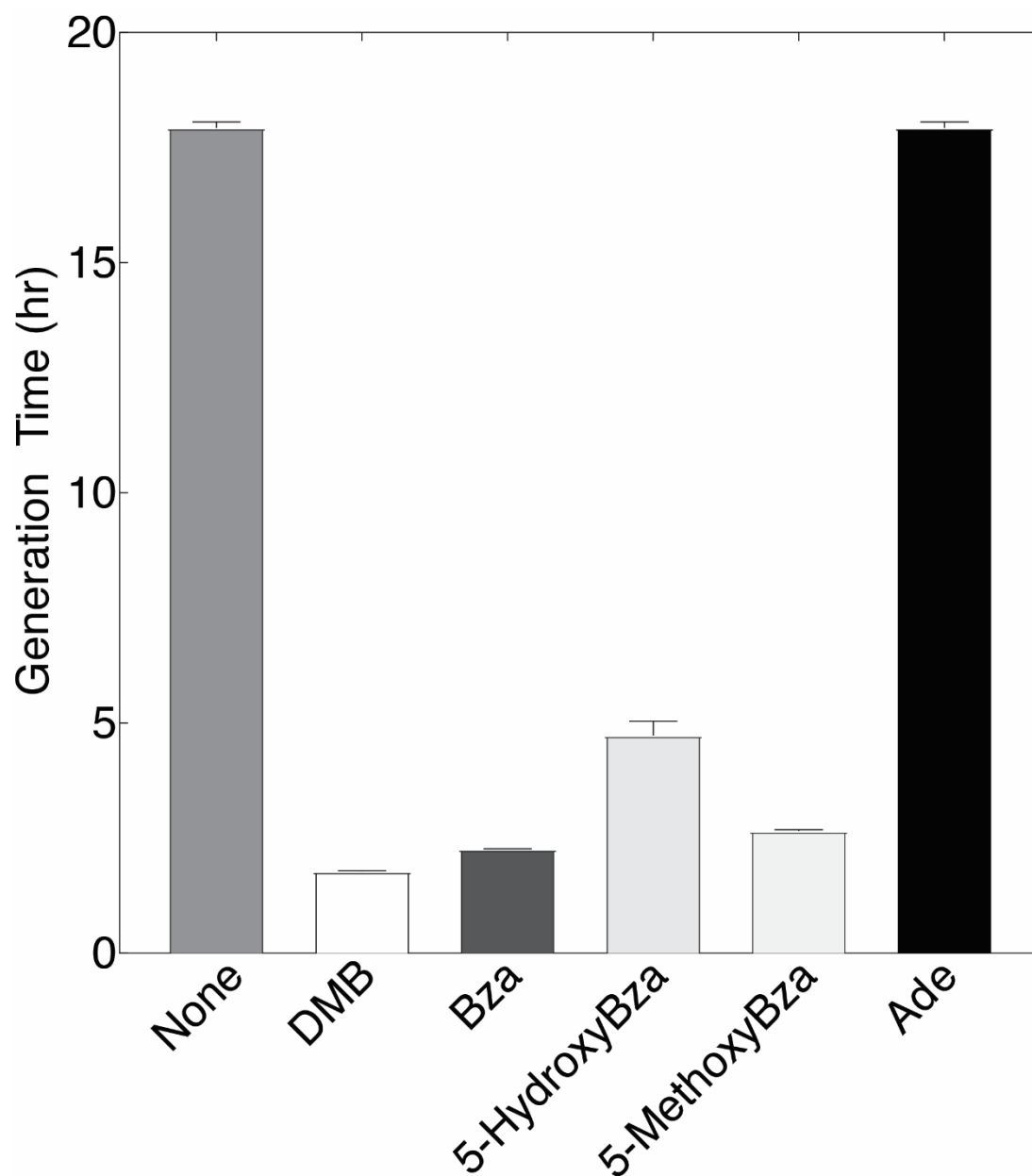


**Figure 6-2. Comparison of generation time (in hours) when fed various bases. JE17830**

(CbIT<sup>+</sup> CbIS<sup>+</sup>) was grown on minimal NCE medium containing ribose (22 mM), trace minerals, magnesium sulfate (1 mM), L-arabinose (500 mM), ampicillin (100 mg mL<sup>-1</sup>) and (CN)<sub>2</sub>Cbi (0.25 nM). Bases were added at 500 μM. Abbreviations: No base added, None; 5,6-dimethylbenzimidazole, DMB; benzimidazole, Bza; 5-hydroxybenzimidazole, 5-hydroxyBza; 5-methoxybenzimidazole, 5-methoxyBza; adenine, Ade

The results of testing whether the bases hydroxyBza, methoxyBza, benzimidazole (Bza), and adenine (Ade) can satisfy a DMB auxotrophy are found in Figure 6-2. Controls for the addition of DMB or no base are included. As expected, no growth is observed when no base is provided (18 h). The addition of DMB yielded a 90% reduction to 2 h. Bza (3 h), methoxyBza (3 h), and hydroxyBza (5 h) were all able to satisfy a DMB auxotrophy and permit growth. Ade (18 h) was unable to restore B<sub>12</sub> biosynthesis. These data indicate both hydroxyBza and methoxyBza are used by *S. enterica* to satisfy the DMB auxotrophy.

The identity of the cobamide synthesized was determined by growing up cells in the presence of hydroxyBza and methoxyBza and extracting the cobamides as described (13). Briefly, JE17830 cells were grown up on minimal NCE ribose medium with an excess of (CN)<sub>2</sub>Cbi (1 μM) and one of the following: nothing, DMB (500 μM), c (500 μM), α-hydroxyBza-R (1 μM), methoxyBza (500 μM), α-methoxyBza-R (1 μM). The cells were harvested, extracted, and separated by HPLC as described (9). A cobamide was considered detected when a given peak appears on both the 367 nm and 525 nm channels on the detector as the deproteinated extracts are separated. (CN)<sub>2</sub>Cbi was found to elute at 14 min in all samples (9). A contaminant from the isolation process can be observed at 525 nm at 16.2 min.

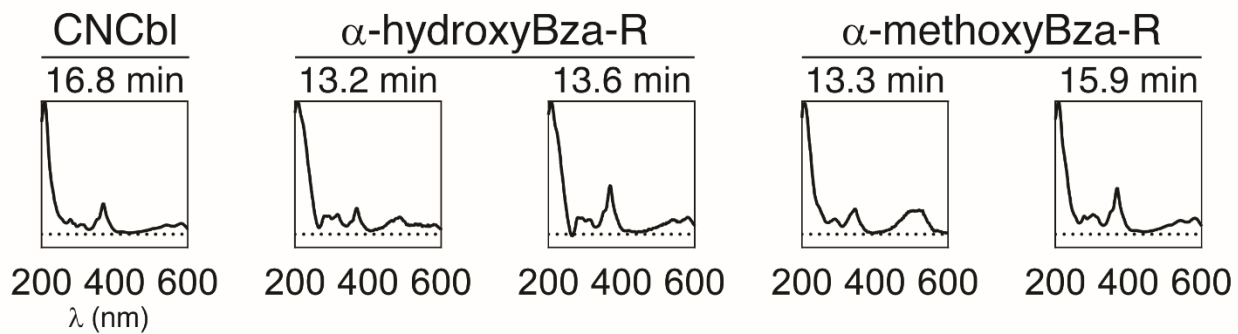
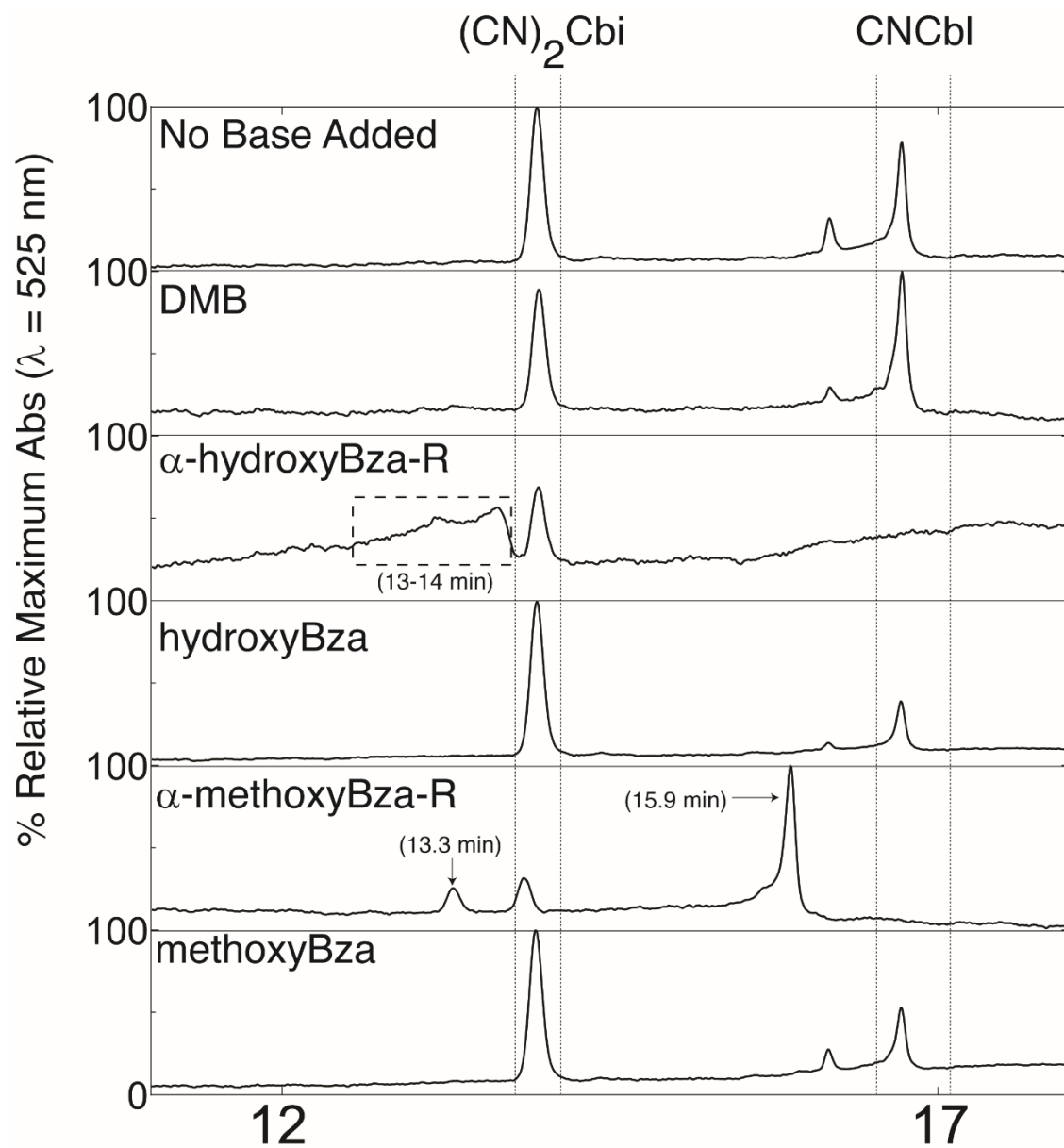
The resulting traces (at 525 nm) are provided in Figure 6-3. When only the ring or the ring and DMB are available, JE17830 synthesizes CNCbl (16.8 min) as expected (13).

When the α-riboside α hydroxyBza-R is incorporated, an elongated peak between 13 and 14 minutes is detected when cobamides are extracted and separated by HPLC. Despite the low resolution, this peak represents hydroxyBza-Cba. Due to the asymmetric nature of hydroxyBza, activation by the DMB: NaMN PRTase can generate α-ribosides with the hydroxyl group at either the 5 or 6 position of the benzene ring (4). The resulting Cbas likely have similar affinities to the

C18 matrix of the HPLC column, causing the low resolution of the peaks. The  $\alpha$ -riboside of another asymmetric benzimidazole, methoxyBza, also results in the appearance of two peaks, though these appear to have different affinities for the matrix. The first peak appears at 13.3 min while a second appears at 15.9 min. Critically, no CNCbl is detected following the addition of either riboside.

Unexpectedly, the addition of the bases hydroxyBza or methoxyBza results in the formation of a *single* peak with a retention time corresponding to the DMB-containing Cba, CNCbl. No other peaks were detected. This finding is incredible as it suggests that somehow hydroxyBza and methoxyBza are being finished to DMB, reactions catalyzed by BzaC, BzaD, and BzaE (18). These results suggest that DMB synthesis in *S. enterica* may proceed from purine biosynthesis rather than reduced FMN.

**Figure 6-3. Corrinoid extractions reveal that CNCbl is synthesized when  $\Delta cobT \Delta cobB / pGkCbITS^+$  (JE17830) is fed hydroxyBza or methoxyBza.** JE17830 ( $CbIT^+ CbIS^+$ ) was grown on minimal NCE medium containing ribose (22 mM), trace minerals, magnesium sulfate (1 mM), L-arabinose (500  $\mu$ M), ampicillin (100 mg mL<sup>-1</sup>) and (CN)<sub>2</sub>Cbi (1  $\mu$ M).  $\alpha$ -hydroxyBza-R and  $\alpha$ -methoxyBza-R were added at 1  $\mu$ M. DMB, hydroxyBza, and methoxyBza were added at 500  $\mu$ M. Corrins were extracted and separated on the HPLC as described in the *Materials and Methods*. The dashed box represents the Cbas synthesized when  $\alpha$ -hydroxyBza-R is provided. The arrows indicate the Cbas synthesized when  $\alpha$ -methoxyBza-R is provided. The UV-Visible spectra of the detected cobamides are provided at the bottom. The CNCbl UV-Vis spectrum is representative of all peaks detected at 16.8 minutes.



**Disruption of purine biosynthesis causes inhibits DMB scavenging in an *S. enterica*  $\Delta cobT$  strain.**

In the anaerobic biosynthetic pathway found in *Eubacterium limosum*, hydroxyBza is synthesized from the reaction of the purine/thiamin precursor AIR and S-adenosyl methionine (SAM). An increase in the amount of AIR available should increase the endogenous pool of DMB, and consequently  $\alpha$ -R. This increase in  $\alpha$ -R should be detectable using the CblS kinase. There are two ways to increase the available AIR: 1) exogenous addition of the riboside form of AIR (AIRs) (44); 2) increasing endogenous synthesis of AIR through gene knockouts.

Increasing flux through the early steps of purine biosynthesis while simultaneously blocking enzymes which use AIR leads to the accumulation of the compound. Purine biosynthesis is regulated by the repressor PurR, which binds products of the pathway, guanine and hypoxanthine (34). By disrupting this regulator, transcription of the genes involved in purine biosynthesis is increased two- to three-fold (45). The genes *thiC* and *purK* (34) encode AIR utilizing enzymes. ThiC converts AIR to 4-amino-5-phosphomethyl-2-methylpyrimidine (HMP-P), the first committed step in thiamin biosynthesis (46). PurK carboxylates AIR to generate N<sup>5</sup>-carboxyaminoimidazole ribonucleotide (N<sup>5</sup>-CAIR) (47). PurK can be bypassed in the presence of CO<sub>2</sub> (34). The next step of the pathway transfers the carboxylate from the N5 position to the C4 of the imidazole to synthesize 4-carboxyaminoimidazole ribonucleotide (CAIR) (47) and is encoded by *purE*. The gene is found upstream of *purK*, and a polar insertion (32) blocks transcription of both genes, enhancing AIR accumulation by reducing escape to CAIR and the rest of purine biosynthesis. Insertions in *purR*, *thiC*, and *purE* were moved into the  $\Delta cobT \Delta cobB$  strain (JE12939) to yield JE22216.

When a  $\Delta cobT \Delta cobB$  strain expressing the kinase and transporter is provided only 50  $\mu\text{M}$  DMB with 500  $\mu\text{M}$  of adenosine, inosine, and guanosine, no DMB scavenging occurs (data not shown). This phenotype could be due to feedback inhibition or issues in transport. Provision of the DMB-forming 4,5-dimethylphenylene-1,2-diamine (DMPDA) (48) at only 10  $\mu\text{M}$  or 50  $\mu\text{M}$  does not suffer from scavenging inhibition in the presence of the purine ribosides.

Insertions were also made in individual purine biosynthetic genes (*purG*, *purI*, *purK*, *purE*, *purC*, and *purR*) to see if the loss of AIR synthesis causes a DMB auxotrophy in the presence of the CblS kinase. The constructed strains are found in Table 6-3. After construction, the vector encoding the kinase CblS and the transporter CblT (*pGkCblTS2*) was transformed into the strains to provide a path to  $\alpha$ -RP and Cbl synthesis.

The strains were cultured overnight at 37 °C on rich medium (nutrient broth, Difco) to exhaust the media. The NCE minimal medium was supplemented with trace minerals, ribose (22 mM),  $\text{MgSO}_4$  (1 mM), ampicillin (100  $\mu\text{g mL}^{-1}$ ), L-arabinose (500  $\mu\text{M}$ ), thiamin (50  $\mu\text{M}$ ), adenosine (500  $\mu\text{M}$ ), guanosine (500  $\mu\text{M}$ ), and inosine (500  $\mu\text{M}$ ). The constructed strains may be purine or thiamin auxotrophs, necessitating the addition of the purines and thiamin (34, 49).  $(\text{CN})_2\text{Cbi}$  was added at either limiting (0.5 nM) or saturating (5 nM) amounts, the base DMB (250  $\mu\text{M}$ ), riboside  $\alpha$ -R (300 nM), and CNCbl (0.5 nM) were added as indicated.

The results are found in Table 6-8, reported as generation times. The parental strain grew as expected, requiring the addition of base (DMB or DMPDA) or  $\alpha$ -R when the ring is limited while requiring no additional base or riboside at higher concentrations of  $(\text{CN})_2\text{Cbi}$ .

When sufficient amounts of ring precursor,  $\alpha$ -R, or DMPDA were present, strains carrying deletions of purine biosynthetic genes were able to synthesize Cbl and allow growth. Curiously, all of these strains, including the strain designed to accumulate AIR, appeared to be inhibited by

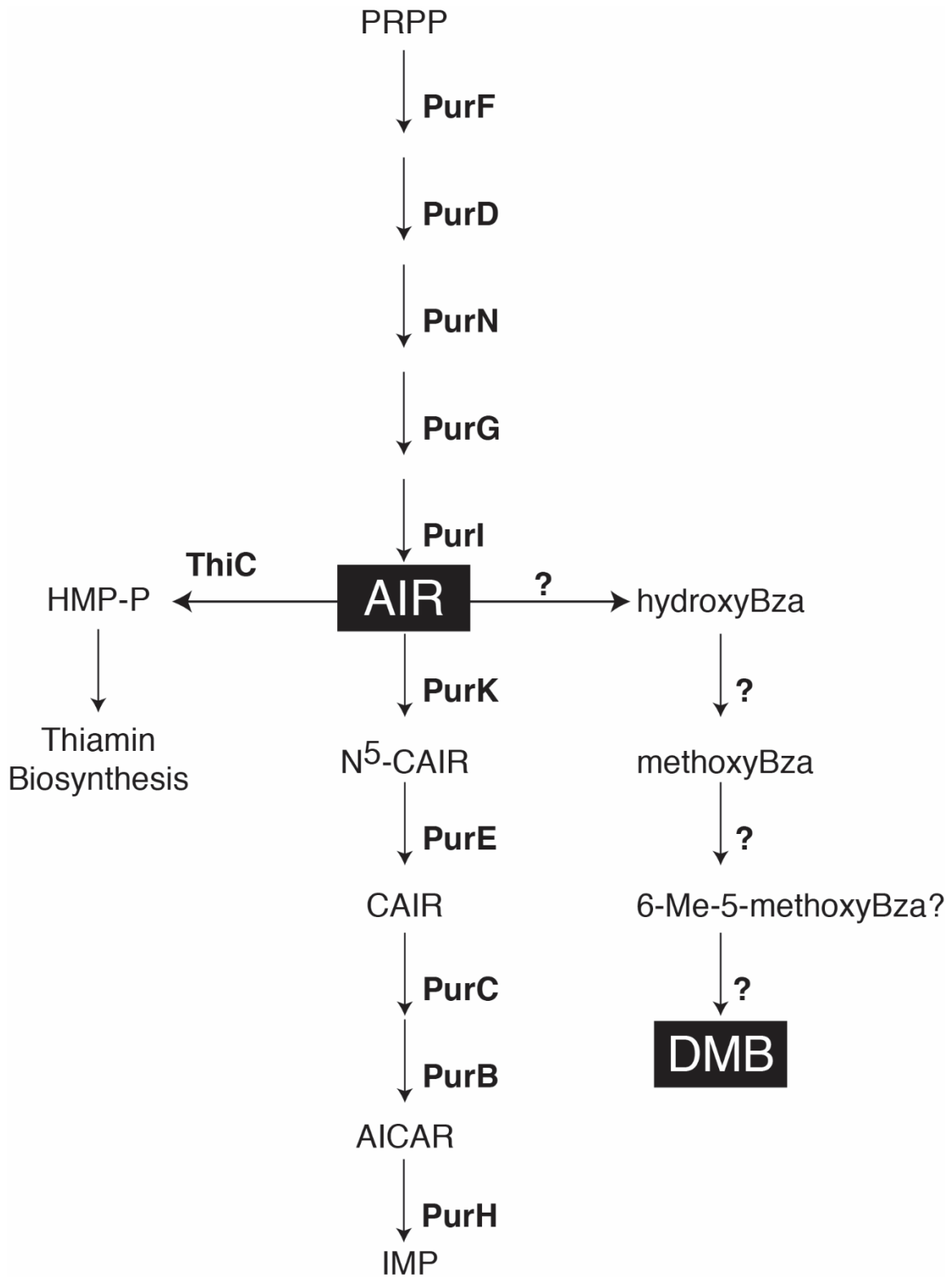
DMB supplementation, regardless of the amount of ring precursor provided. These results suggest that there may be an exacerbation of the blocked DMB scavenging phenotype observed in the wild-type strain when the DMB concentration is an order of magnitude lower than that of the purines, which could be linked to the DMB scavenging phenotype we observed with the PNP genes. Unlike the PNP genes, however, there appear to be varying degrees of growth inhibition. Disruptions of the pre-AIR biosynthetic genes (Figure 6-4; *purG*, *purI*, and *purK*) showed no growth (20 h+) while disruptions of the two post-AIR genes, *purE* (8 h) and *purC* (7 h), showed slightly better growth. N<sup>5</sup>-carboxyaminoimidazole ribonucleotide (N<sup>5</sup>-CAIR) is the common intermediate lost in *purG*, *purI*, and *purK* knockouts, which could suggest N<sup>5</sup>-CAIR is necessary for or inhibitory towards DMB scavenging. No defect was found when a plasmid expressing *S. enterica cobT* was tested (data not shown), indicating these phenotypes are related to the synthesis and activation of  $\alpha$ -R.

Oddly, the AIR overproduction strain (*thiC purE purR*; 16 h) and the insertion in *purR* (11h) were inhibited upon addition of DMB, indicating that the overproduction of AIR or the unregulated synthesis of purines disrupts DMB scavenging and activation. Recalling the observation that the loss of the nucleoside salvaging genes or adding purines at ten-fold higher amounts than DMB also interferes with DMB scavenging, these data indicate a strong link between purine metabolism and  $\alpha$ -R synthesis.

**Table 6-8. Generation times (h) of *pur* gene knockouts in strains carrying pGkCbITS2 (*cbIT*<sup>+</sup>, *cbIS*<sup>+</sup>).**

	$\Delta cobT \Delta cobB$	$\Delta purG$	$\Delta purI$	$\Delta purK$	$\Delta purE$	$\Delta purR$	$\Delta purC$	$\Delta thiC$ $\Delta purE$ $\Delta purR$
(CN)2Cbi (0.25 nM)	32	46	34	31	52	41	27	32
(CN)2Cbi (0.25 nM) + DMB (250 $\mu$ M)	2	86	83	100	79	79	86	66
(CN)2Cbi (0.25 nM) + DMPDA (50 $\mu$ M)	1	1	1	1	1	1	2	1
(CN)2Cbi (0.25 nM) + $\alpha$ -R (300 nM)	1	1	1	1	1	1	1	1
(CN)2Cbi (5 nM)	2	2	3	3	1	2	5	2
(CN)2Cbi (5 nM) + DMB (250 $\mu$ M)	2	20	31	33	8	7	11	16
(CN)2Cbi (5 nM) + $\alpha$ -R (300 nM)	1	1	1	1	1	1	1	1
CNCbl (0.5 nM)	1	1	1	1	1	1	1	1

**Figure 6-4. Purine biosynthetic pathway in *S. enterica* and its possible connection to DMB biosynthesis.** The *de novo* synthesis of purines [reviewed in (34)] proceeds from 5-phospho- $\alpha$ -D-ribose-1-diphosphate (PRPP) through inosine-monophosphate (IMP). The enzymes involved (in **bold**) are regulated by PurR and are repressed by the presence of 6-oxopurines (i.e., guanine, hypoxanthine). The first steps (through PurI) assemble the imidazole ring, yielding 5-amino-1-imidazole ribotide (AIR). AIR serves as a precursor to both purines and the coenzyme thiamin (B<sub>1</sub>). The synthesis of Cbl following the addition of hydroxyBza and methoxyBza suggests AIR may also be a precursor to DMB synthesis in *S. enterica*, though the enzymes responsible remain unknown (indicated by question marks). Abbrev. **PurF**, amidophosphoribosyltransferase; **PurD**, phosphoribosylamine--glycine ligase; **PurN**, phosphoribosylglycinamide formyltransferase; **PurG**, phosphoribosylformylglycinamide synthase; **PurI** (PurM), phosphoribosylformylglycinamide cyclo-ligase; **ThiC**, phosphomethylpyrimidine synthase; **PurK**, N<sup>5</sup>-carboxyaminoimidazole ribonucleotide synthase; **PurE**, N<sup>5</sup>-carboxyaminoimidazole ribonucleotide mutase; **PurC**, phosphoribosylaminoimidazole-succinocarboxamide synthase; **PurB**, adenylosuccinate lyase; **PurH**, bifunctional phosphoribosylaminoimidazolecarboxamide formyltransferase/IMP cyclohydrolase; HMP-P, 4-amino-5-phosphomethyl-2-methylpyrimidine; N<sup>5</sup>-CAIR, N<sup>5</sup>-carboxyaminoimidazole ribonucleotide; CAIR, 4-carboxyaminoimidazole ribonucleotide; AICAR, 5-amino-4-imidazolecarboxamide ribotide.



## DISCUSSION.

In this study, an investigation into the origins of  $\alpha$ -R synthesis in *S. enterica* showed that loss of the purine/pyrimidine phosphorylases involved in nucleoside salvaging results in a disruption to the cell's ability to scavenge exogenous DMB under conditions where the (CN)<sub>2</sub>Cbi ring precursor has been limited. While constructing vectors for complementing the loss of the PNPs, it was found that the cells lose the ability to scavenge DMB in the presence of a second vector (pCV3) or when the IPTG-inducible pTAC85 vector was utilized for expression of the kinase.

An alternative to DMB scavenging to increase endogenous pools of DMB is to enhance its endogenous synthesis. It had been proposed that reduced FMN is the precursor to DMB in *S. enterica*. Riboflavin was fed to an *S. enterica*  $\Delta cobT \Delta cobB / pGkCblTS^+$  strain to attempt to satisfy a DMB auxotrophy, but despite feeding a 100-fold excess over the amount provided during earlier tracing studies, riboflavin failed to restore Cbl synthesis. These data could indicate, much like *E. coli*, that *S. enterica* is unable to transport riboflavin. Riboflavin transporters from *B. subtilis*, *R. leguminosarum*, and *C. glutamicum* were cloned into an expression vector to enable import. It was determined that *C. glutamicum* PnuX was the only one of the three to function in *S. enterica* as expression of PnuX resulted in susceptibility to the toxic analog roseoflavin.

Bacteria evolved a second route to DMB that branches from purine biosynthesis at AIR. Intermediates of this pathway, hydroxyBza and methoxyBza, were demonstrated to satisfy DMB auxotrophy in an *S. enterica*  $\Delta cobT \Delta cobB / pGkCblTS^+$  strain. Unexpectedly, corrinoid extracts from strains fed either of these bases revealed that *S. enterica* failed to synthesize the cobamides carrying these bases. Instead, the DMB-containing Cbl was found, suggesting *S. enterica* makes DMB from those bases. Strains unable to synthesize AIR or which accumulated the compound were constructed to determine if AIR was a precursor to DMB. Unexpectedly, these strains were

inhibited by supplementation with DMB, regardless of how much of the ring precursor was provided. The strains unable to synthesize AIR showed a pattern which seemed to suggest that ability to synthesize N<sup>5</sup>-CAIR is necessary for DMB scavenging, though it is not clear if the compound is inhibitory or a potential substrate.

These data indicate strong links between purine metabolism and DMB activation in *S. enterica*. Figure 6-5 details a new model for the synthesis of Cbl in *S. enterica* when the kinase CblS is present, linking the purine biosynthetic intermediate AIR to DMB.

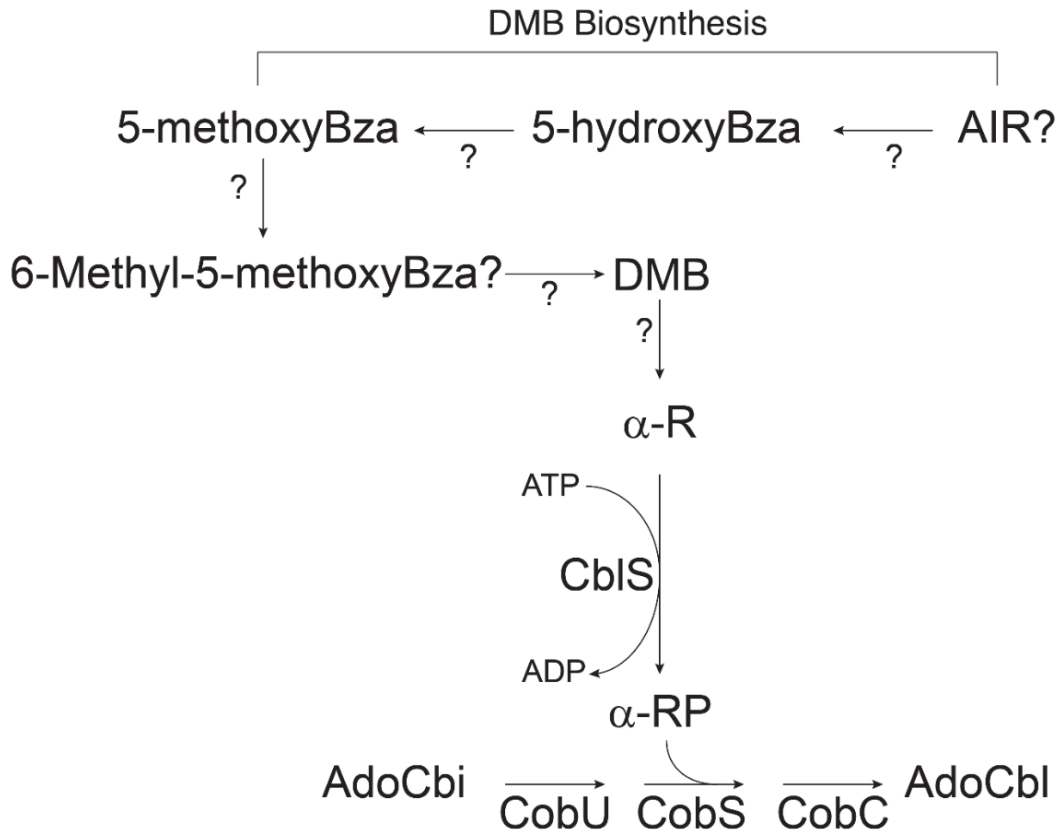


**Figure 6-5. A new model for Cbl biosynthesis in *S. enterica*  $\Delta cobT$  /  $pGkCblS^+$ .** The detection of Cbl in response to feeding with 5-hydroxyBza and 5-methoxyBza suggests that these compounds could be precursors to DMB. After conversion to DMB, the base is converted to  $\alpha$ -R by some unknown manner before being activated by the kinase CblS, yielding  $\alpha$ -RP. The ribotide is condensed with the activated ring to yield the final product, Cbl. These results indicate that 5-aminoimidazole ribotide (AIR), not FMN, is a precursor to DMB. Abbreviations: CobU, NTP:Ado-cobinamide kinase and NTP:Ado-cobinamide-phosphate guanylyltransferase; CobS, AdoCbl-phosphate synthase; CobC, Ado-Cba-P phosphatase

### **Loss of the PNP or hydrolase genes disrupts DMB scavenging but $\alpha$ -R synthesis still occurs.**

The loss of the PNPs results in a strain unable to scavenge DMB. It is difficult to assess if the cause is indirect or direct because it was all six genes resulting in this phenotype. Complementation has thus far been unsuccessful, but it may be possible to move the kinase and transporter into the chromosome, bypassing the issues with using two vectors. If the PNPs or hydrolases can synthesize  $\alpha$ -R, heterologous expression should improve growth when the amounts of DMB or ring precursor are limited. An alternative explanation for the loss of DMB scavenging ability is a compensatory mutation following the loss of the salvaging genes which also inhibits DMB uptake or the synthesis of  $\alpha$ -R. This mutation could be identified through generation of suppressors or whole genome sequencing.

The improved growth observed upon deletion of the hydrolases RihA and RihC could indicate these two are cleaving endogenous pools of  $\alpha$ -R (or other  $\alpha$ -ribosides), and that by deleting those genes, accumulation of  $\alpha$ -ribosides occurs. However, if the hydrolases are only responsible for cleavage of  $\alpha$ -R, why does the loss of either inhibit DMB scavenging? Resolving the co-expression of the PNPs and the kinase would permit determination of whether the effects of RihA or RihC are direct or indirect. If the hydrolases cleave  $\alpha$ -R, overproduction of these should impair growth rates as the enzyme reduces the available riboside.

One additional PNP has not yet been tested, PpnP (formerly YaiE) (35). It is possible that the release of R1P by the other proteins is necessary for the activity of this protein, all of which are expressed at different times. R1P is also generated by the mutase Pgm from R5P, an intermediate of the pentose phosphate pathway. The deletion strains may still be able to synthesize  $\alpha$ -R when the ring precursor is increased 20-fold because the condensation reaction favors the forward reaction and may require less  $\alpha$ -RP to proceed, allowing Cbl synthesis. It is possible that the

deletion of all of the PNPs could abolish  $\alpha$ -R synthesis even when the ring is added to high levels, confirming that it takes the contributions of multiple enzymes to yield sufficient amounts of the riboside in *S. enterica*.

***S. enterica* may not transport riboflavin efficiently enough to restore DMB synthesis.**

Earlier tracing studies indicated that labeled riboflavin at 2.5  $\mu$ M in the exogenous medium was incorporated into the cobalamin molecule in *S. enterica* (21). However, when provided at 100-fold greater amounts, riboflavin failed to satisfy the DMB auxotrophy of JE17830 on limiting levels of (CN)<sub>2</sub>Cbi. One possible cause could be that riboflavin cannot be transported by *S. enterica*, which we attempted to address by cloning riboflavin transporters out of other organisms, but the observed loss of DMB scavenging ability in the presence of multiple vectors complicates this approach. Alternatively, the DMB synthesized by the imported riboflavin could be below the threshold necessary for  $\alpha$ -R synthesis to occur. JE17830 requires 20  $\mu$ M of DMB to grow under limited (CN)<sub>2</sub>Cbi conditions (Figure 6-1). It may be necessary to generate a riboflavin auxotrophy in *S. enterica* and then to assess the effect on DMB synthesis. A *ribB* (encodes the 3,4-dihydroxy-2-butanone-4-phosphate synthase) knockout can be compensated for by the addition of 2,3-butanedione (diacetyl) to the medium (50). It may be possible to use a combination of diacetyl and free riboflavin to assess how much riboflavin is necessary to supply the cell *and* restore DMB biosynthesis, under conditions where Cbl synthesis is necessary.

### **Anaerobic DMB biosynthetic intermediates 5' hydroxybenzimidazole (hydroxyBza) and 5' methoxybenzimidazole (methoxyBza) yield DMB in *S. enterica*.**

The synthesis of Cbl following supplementation with either hydroxyBza or methoxyBza is very compelling. This suggests that *S. enterica* could synthesize DMB from AIR, rather than FMN, or perhaps even more intriguingly, from AIR *or* FMN, depending on the current environment or availability of substrate. The *S. enterica* strain JE17830 should be grown under anoxic conditions in the presence of these bases to determine if DMB is still synthesized in their presence.

Additionally, it may be possible for the conversion of AIR to hydroxyBza, as seen with purified BzaF (17), using *S. enterica* cell extracts. If hydroxyBza or other possible intermediates are recovered, protein fractionation and reverse genetics could be used to identify the enzymes responsible for DMB synthesis. A similar approach could be utilized to see if reduced FMN is converted to DMB.

A complete blockage of AIR synthesis may be necessary to rule out DMB synthesis from that molecule. This can be accomplished by blocking synthesis from PRPP at *purG* or *purI* (34) as well as from histidine biosynthesis via 5-Aminoimidazole-4-carboxamide ribonucleotide (AICAR) by blocking at *purC*, which can take AICAR back to AIR (51, 52).

### **The inability to synthesize N<sup>5</sup>-CAIR inhibits DMB scavenging.**

Curiously, knockouts in the purine biosynthetic pathway generated DMB scavenging phenotypes, with the synthesis of N<sup>5</sup>-CAIR appearing absolutely necessary to growth in the presence of DMB. Deletions in earlier steps (*purG*, *purI*, and *purK*) were completely impaired, while later steps (*purE*) or the regulator (*purR*) appeared less impaired. The AIR overproduction strain, which could accumulate N<sup>5</sup>-CAIR in the presence of CO<sub>2</sub>, also grew slightly better than the deletions in earlier steps. It is possible that accumulation of earlier products of the pathway could

cause the observed impairment, though since expression of the PRTase showed no growth defect, the impairment is limited to  $\alpha$ -R synthesis. Suppressor mutations could reveal the identity of those blocks and illuminate what enzymes specifically are involved in  $\alpha$ -R synthesis from DMB.

Alternatively, N<sup>5</sup>-CAIR could be a substrate or activator of  $\alpha$ -R synthesis. Exogenous N<sup>5</sup>-CAIR or AIR could be provided to the strains lacking the earlier steps to see if DMB scavenging is restored. If N<sup>5</sup>-CAIR is inhibitory, it could cause the parental strain to become auxotrophic for  $\alpha$ -R. *In vitro* testing could determine if the substrates of PurG, PurI, or PurK are inhibitory to CblS.

Overall, this work establishes a framework understanding how these complex interactions lead to the synthesis of DMB and  $\alpha$ -R in *S. enterica*. Determining how DMB is made in *Salmonella* has implications for many other B<sub>12</sub>-synthesizing organisms, as it could indicate the evolution of a *third* route to this very critical molecule. Understanding how DMB is activated to the riboside would not only resolve the outstanding question of how some *Firmicutes* depend on the kinase for Cbl biosynthesis, but it would also mean the introduction of only the second class of enzymes known to synthesize  $\alpha$ -N-glycosidic linkages in nucleosides.

#### **ACKNOWLEDGMENTS.**

The authors declare no conflict of interest. This work was supported by USPHS grant R37 GM040313 to Jorge Escalante-Semerena. We would also like to thank Dr. Diana Downs and members of her group for strains DM932, DM1024, and DM13300, as well as their expertise in purine and thiamin synthesis.

## REFERENCES.

1. Mattes TA, Deery E, Warren MJ, Escalante-Semerena JC. 2017. Cobalamin Biosynthesis and Insertion, p 1-24. In Scott RA (ed), Encyclopedia of Inorganic and Bioinorganic Chemistry doi:10.1002/9781119951438.eibc2489. John Wiley & Sons, Ltd, Chichester, UK.
2. Trzebiatowski JR, Escalante-Semerena JC. 1997. Purification and characterization of CobT, the nicotinate-mononucleotide:5,6-dimethylbenzimidazole phosphoribosyltransferase enzyme from *Salmonella typhimurium* LT2. J Biol Chem 272:17662-17667.
3. Trzebiatowski JR, O'Toole GA, Escalante-Semerena JC. 1994. The *cobT* gene of *Salmonella typhimurium* encodes the NaMN: 5,6-dimethylbenzimidazole phosphoribosyltransferase responsible for the synthesis of *N*<sup>1</sup>-(5-phospho- $\alpha$ -D-ribose)-5,6-dimethylbenzimidazole, an intermediate in the synthesis of the nucleotide loop of cobalamin. J Bacteriol 176:3568-3575.
4. Crofts TS, Hazra AB, Tran JL, Sokolovskaya OM, Osadchiy V, Ad O, Pelton J, Bauer S, Taga ME. 2014. Regiospecific formation of cobamide isomers is directed by CobT. Biochemistry 53:7805-7815.
5. Cheong CG, Escalante-Semerena JC, Rayment I. 2001. Structural investigation of the biosynthesis of alternative lower ligands for cobamides by nicotinate mononucleotide: 5,6-dimethylbenzimidazole phosphoribosyltransferase from *Salmonella enterica*. J Biol Chem 276:37612-37620.

6. Crofts TS, Seth EC, Hazra AB, Taga ME. 2013. Cobamide structure depends on both lower ligand availability and CobT substrate specificity. *Chem Biol* doi:10.1016/j.chembiol.2013.08.006.
7. Hazra AB, Tran JL, Crofts TS, Taga ME. 2013. Analysis of substrate specificity in CobT homologs reveals widespread preference for DMB, the lower axial ligand of vitamin B(12). *Chem Biol* 20:1275-1285.
8. Yan J, Bi M, Bourdon AK, Farmer AT, Wang PH, Molenda O, Quaile AT, Jiang N, Yang Y, Yin Y, Simsir B, Campagna SR, Edwards EA, Löffler FE. 2018. Purinyl-cobamide is a native prosthetic group of reductive dehalogenases. *Nat Chem Biol* 14:8-14.
9. Chan CH, Escalante-Semerena JC. 2011. ArsAB, a novel enzyme from *Sporomusa ovata* activates phenolic bases for adenosylcobamide biosynthesis. *Mol Microbiol* 81:952-967.
10. Chan CH, Newmister SA, Talyor K, Claas KR, Rayment I, Escalante-Semerena JC. 2014. Dissecting cobamide diversity through structural and functional analyses of the base-activating CobT enzyme of *Salmonella enterica*. *Biochim Biophys Acta* 1840:464-475.
11. Gray MJ, Escalante-Semerena JC. 2010. A new pathway for the synthesis of alpha-ribazole-phosphate in *Listeria innocua*. *Mol Microbiol* 77:1429-1438.
12. Johnson WM, Kido Soule MC, Kujawinski EB. 2016. Evidence for quorum sensing and differential metabolite production by a marine bacterium in response to DMSP. *ISME J* 10:2304-2316.
13. Mattes TA, Escalante-Semerena JC. 2017. *Salmonella enterica* synthesizes 5,6-dimethylbenzimidazolyl-(DMB)-alpha-riboside. Why some Firmicutes do not require the

- canonical DMB activation system to synthesize adenosylcobalamin. *Mol Microbiol* 103:269-281.
14. Gray MJ, Escalante-Semerena JC. 2007. Single-enzyme conversion of FMNH<sub>2</sub> to 5,6-dimethylbenzimidazole, the lower ligand of B<sub>12</sub>. *Proc Natl Acad Sci U S A* 104:2921-2926.
  15. Taga ME, Larsen NA, Howard-Jones AR, Walsh CT, Walker GC. 2007. BluB cannibalizes flavin to form the lower ligand of vitamin B<sub>12</sub>. *Nature* 446:449-453.
  16. Campbell GR, Taga ME, Mistry K, Lloret J, Anderson PJ, Roth JR, Walker GC. 2006. *Sinorhizobium meliloti bluB* is necessary for production of 5,6-dimethylbenzimidazole, the lower ligand of B<sub>12</sub>. *Proc Natl Acad Sci U S A* 103:4634-4369.
  17. Mehta AP, Abdelwahed SH, Fenwick MK, Hazra AB, Taga ME, Zhang Y, Ealick SE, Begley TP. 2015. Anaerobic 5-Hydroxybenzimidazole formation from aminoimidazole ribotide: an unanticipated intersection of thiamin and vitamin B<sub>12</sub> biosynthesis. *J Am Chem Soc* doi:10.1021/jacs.5b03576.
  18. Hazra AB, Han AW, Mehta AP, Mok KC, Osadchiy V, Begley TP, Taga ME. 2015. Anaerobic biosynthesis of the lower ligand of vitamin B<sub>12</sub>. *Proc Natl Acad Sci U S A* 112:10792-10797.
  19. Jeter RM, Olivera BM, Roth JR. 1984. *Salmonella typhimurium* synthesizes cobalamin (vitamin B<sub>12</sub>) de novo under anaerobic growth conditions. *J Bacteriol* 159:206-213.
  20. Keck B, Renz P. 2000. *Salmonella typhimurium* forms adenylobamide and 2-methyladenylobamide, but no detectable cobalamin during strictly anaerobic growth. *Arch Microbiol* 173:76-77.

21. Keck B, Munder M, Renz P. 1998. Biosynthesis of cobalamin in *Salmonella typhimurium*: transformation of riboflavin into the 5,6-dimethylbenzimidazole moiety. Arch Microbiol 171:66-68.
22. Gutiérrez-Preciado A, Torres AG, Merino E, Bonomi HR, Goldbaum FA, García-Angulo VA. 2015. Extensive identification of bacterial riboflavin transporters and their distribution across bacterial species. PLoS One 10.
23. Mattes TA, Escalante-Semerena JC. 2018. Facile isolation of alpha-ribazole from vitamin B12 hydrolysates using boronate affinity chromatography. J Chrom B 1090:52-55.
24. Maniatis T, Fritsch EF, Sambrook J. 1982. Introduction of plasmid and bacteriophage lambda into *Escherichia coli*, p 250-251. In Maniatis T, Fritsch EF, Sambrook J (ed), Molecular cloning: a laboratory manual. Cold Spring Harbor Laboratory, Cold Spring Harbor, New York.
25. Datsenko KA, Wanner BL. 2000. One-step inactivation of chromosomal genes in *Escherichia coli* K-12 using PCR products. Proc Natl Acad Sci USA 97:6640-6645.
26. Rocco CJ, Dennison KL, Klenchin VA, Rayment I, Escalante-Semerena JC. 2008. Construction and use of new cloning vectors for the rapid isolation of recombinant proteins from *Escherichia coli*. Plasmid 59:231-237.
27. Galloway NR, Toutkoushian H, Nune M, Bose N, Momany C. 2013. Rapid cloning for protein crystallography using Type IIS restriction enzymes. Crystal Growth & Design 13:2833-2839.
28. VanDrisse CM, Escalante-Semerena JC. 2016. New high-cloning-efficiency vectors for complementation studies and recombinant protein overproduction in *Escherichia coli* and *Salmonella enterica*. Plasmid 86:1-6.

29. Guzman LM, Belin D, Carson MJ, Beckwith J. 1995. Tight regulation, modulation, and high-level expression by vectors containing the arabinose PBAD promoter. *J Bacteriol* 177:4121-30.
30. Marsh P. 1986. Ptac-85, an *E. coli* vector for expression of non-fusion proteins. *Nucleic Acids Res* 14:3603.
31. Hansen MR, Jorgensen JT, Dandanell G. 2006. Xanthosine utilization in *Salmonella enterica* serovar Typhimurium is recovered by a single aspartate-to-glycine substitution in xanthosine phosphorylase. *J Bacteriol* 188:4153-4157.
32. Castilho BA, Olfson P, Casadaban MJ. 1984. Plasmid insertion mutagenesis and *lac* gene fusion with mini-Mu bacteriophage transposons. *J Bacteriol* 158:488-495.
33. Berkowitz D, Hushon JM, Whitfield HJ, Jr., Roth J, Ames BN. 1968. Procedure for identifying nonsense mutations. *J Bacteriol* 96:215-220.
34. Jensen K, Dandanell G, Hove-Jensen B, Willemoes M. 2008. Nucleotides, Nucleosides, and Nucleobases. *EcoSal Plus* doi:doi:10.1128/ecosalplus.3.6.2.
35. Sevin DC, Fuhrer T, Zamboni N, Sauer U. 2017. Nontargeted in vitro metabolomics for high-throughput identification of novel enzymes in *Escherichia coli*. *Nat Methods* 14:187-194.
36. Tsang AW, Escalante-Semerena JC. 1998. CobB, a new member of the SIR2 family of eucaryotic regulatory proteins, is required to compensate for the lack of nicotinate mononucleotide:5,6-dimethylbenzimidazole phosphoribosyltransferase activity in cobT mutants during cobalamin biosynthesis in *Salmonella typhimurium* LT2. *J Biol Chem* 273:31788-31794.

37. Jeter RM, Roth JR. 1987. Cobalamin (vitamin B<sub>12</sub>) biosynthetic genes of *Salmonella typhimurium*. J Bacteriol 169:3189-3198.
38. Escalante-Semerena JC, Roth JR. 1987. Regulation of cobalamin biosynthetic operons in *Salmonella typhimurium*. J Bacteriol 169:2251-2258.
39. Zayas CL, Escalante-Semerena JC. 2007. Reassessment of the late steps of coenzyme B<sub>12</sub> synthesis in *Salmonella enterica*: Evidence that dephosphorylation of adenosylcobalamin-5'-phosphate by the CobC phosphatase is the last step of the pathway. J Bacteriol 189:2210-2218.
40. O'Toole GA, Trzebiatowski JR, Escalante-Semerena JC. 1994. The *cobC* gene of *Salmonella typhimurium* codes for a novel phosphatase involved in the assembly of the nucleotide loop of cobalamin. J Biol Chem 269:26503-26511.
41. Chan RK, Botstein D, Watanabe T, Ogata Y. 1972. Specialized transduction of tetracycline resistance by phage P22 in *Salmonella typhimurium*. II. Properties of a high-frequency-transducing lysate. Virology 50:883-898.
42. Angulo VAG, Bonomi HR, Posadas DM, Serer MI, Torres AG, Zorreguieta Á, Goldbaum FA. 2013. Identification and characterization of RibN, a novel family of riboflavin transporters from *Rhizobium leguminosarum* and other proteobacteria. Journal of bacteriology 195:4611-4619.
43. Vogl C, Grill S, Schilling O, Stulke J, Mack M, Stolz J. 2007. Characterization of riboflavin (vitamin B<sub>2</sub>) transport proteins from *Bacillus subtilis* and *Corynebacterium glutamicum*. J Bacteriol 189:7367-7375.

44. Dougherty M, Downs DM. 2003. The *stm4066* gene product of *Salmonella enterica* serovar Typhimurium has aminoimidazole riboside (AIRs) kinase activity and allows AIRs to satisfy the thiamine requirement of *pur* mutant strains. *J Bacteriol* 185:332-339.
45. He B, Choi KY, Zalkin H. 1993. Regulation of *Escherichia coli* *glnB*, *prsA*, and *speA* by the purine repressor. *J Bacteriol* 175:3598-606.
46. Martinez-Gomez NC, Downs DM. 2008. ThiC is an [Fe-S] cluster protein that requires AdoMet to generate the 4-amino-5-hydroxymethyl-2-methylpyrimidine moiety in thiamin synthesis. *Biochemistry* 47:9054-9056.
47. Meyer E, Leonard NJ, Bhat B, Stubbe J, Smith JM. 1992. Purification and characterization of the *purE*, *purK*, and *purC* gene products: identification of a previously unrecognized energy requirement in the purine biosynthetic pathway. *Biochemistry* 31:5022-32.
48. Maggio-Hall LA, Dorrestein PC, Escalante-Semerena JC, Begley TP. 2003. Formation of the dimethylbenzimidazole ligand of coenzyme B12 under physiological conditions by a facile oxidative cascade. *Org Lett* 5:2211-2213.
49. Koenigskecht MJ, Downs DM. 2010. Thiamine biosynthesis can be used to dissect metabolic integration. *Trends Microbiol* 18:240-247.
50. Crossley RA, Gaskin DJ, Holmes K, Mulholland F, Wells JM, Kelly DJ, van Vliet AH, Walton NJ. 2007. Riboflavin biosynthesis is associated with assimilatory ferric reduction and iron acquisition by *Campylobacter jejuni*. *Appl Environ Microbiol* 73:7819-25.
51. Bazarro JV, Heitman NJ, Downs DM. 2015. Aminoimidazole carboxamide ribotide exerts opposing effects on thiamine synthesis in *Salmonella enterica*. *J Bacteriol* 197:2821-2830.

52. Bazurto JV, Downs DM. 2011. Plasticity in the purine-thiamine metabolic network of *Salmonella*. *Genetics* 187:623-631.

## CHAPTER 7

### CONCLUSIONS AND RECOMMENDATIONS FOR FUTURE WORK

#### SUMMARY

This project began with the intention of leveraging the DMB-riboside specificity of *Geobacillus kaustophilus* CblS to isolate the enzyme(s) responsible for the synthesis of DMB in *S. enterica*. In pursuit of this goal, a new route to  $\alpha$ -ribazole-5'-phosphate in *S. enterica* was discovered, a method for the synthesis of  $\alpha$ -R from cyanocobalamin was improved, and our knowledge of the kinase itself was expanded while probing the connections between DMB activation and purine metabolism. A summary of the major findings of this dissertation follows.

#### ***S. enterica* synthesizes $\alpha$ -R endogenously.**

In Chapter 3, we showed that when *G. kaustophilus* CblS is expressed in an *S. enterica*  $\Delta cobT$   $\Delta cobB$  strain, which lacks the canonical activation route, the strain was still able to synthesize  $\alpha$ -RP, even without the exogenous addition of the  $\alpha$ -riboside, as we had seen with the homologs from *Listeria innocua* (1). When the ring precursor is limited, the strains became DMB or  $\alpha$ -R auxotrophs, suggesting that both molecules are intermediates in a novel route to  $\alpha$ -RP. In the absence of the transporter CblT, DMB could no longer be scavenged but the kinase could still restore growth in a  $\Delta cobT$  strain if additional ring precursor is available, suggesting that CblT enhances the affinity of CblS for  $\alpha$ -R.

***Gk* CblS can activate  $\alpha$ -ribosides other than  $\alpha$ -R, both *in vitro* and when expressed in *S. enterica*.**

In Chapter 4, we reported a method to use boronate affinity chromatography to increase the yield of  $\alpha$ -R from hydrolyzed vitamin B<sub>12</sub>, which enabled synthesis of sufficient amounts of  $\alpha$ -R for studying the activity of the kinase.

In Chapter 5, the initial kinetic characterization of *Gk* CblS is reported. The reaction conditions for a coupled spectrophotometric assay were optimized, and kinetic parameters for the monomeric *Gk* CblS were determined, finding apparent  $K_m$  values for  $\alpha$ -R (360  $\mu$ M) and ATP (300  $\mu$ M). A method for synthesizing  $\alpha$ -ribosides using CobT and  $\beta$ -ribazole using the *S. enterica* purine nucleoside phosphorylase DeoD was reported. These synthesized compounds were used to show that the orientation of the N-glycosidic bond, not the base, determines whether a riboside will be activated by *Gk* CblS, as all of the synthesized  $\alpha$ -ribosides were phosphorylated, but not the  $\beta$ -N-linked ribosides, including  $\beta$ -ribazole. Additionally,  $\alpha$ -ribosides of 5-hydroxybenzimidazole (hydroxyBza) and 5-methoxybenzimidazole (methoxyBza) can replace  $\alpha$ -R and permit growth in a  $\Delta cobT \Delta cobB$  strain expressing the kinase and transporter, confirming *in vivo* activation.

***S. enterica* struggles to transport  $\alpha$ -Ado and does not synthesize it *in vivo*.**

Curiously, in Chapter 5, we showed that *Gk* CblS could phosphorylate  $\alpha$ -adenosine ( $\alpha$ -Ado) *in vitro* and that it could be found in corrinoid extractions when fed to an *S. enterica*  $\Delta cobT \Delta cobB$  strain expressing *Gk* CblT and CblS. However, growth was virtually non-existent when the ring was limiting. *In vitro* assays with cell extracts did not reveal any degradation, indicating that *S. enterica* does not efficiently transport  $\alpha$ -Ado.

In Chapters 3 and Chapter 6, it was demonstrated that feeding of the free base adenine did not restore growth in a DMB auxotroph, indicating *S. enterica* cannot synthesize  $\alpha$ -Ado. These

findings explain why an *S. enterica*  $\Delta cobT \Delta cobB$  strain expressing *Gk* CblITS and CblS only synthesizes cobalamin in the absence of any external base or  $\alpha$ -riboside.

**Blocks in purine metabolism disrupt DMB scavenging of a  $\Delta cobT \Delta cobB$  / *pGkCblITS*<sup>+</sup> strain.**

In Chapter 6, it was determined that blocks in purine scavenging or purine biosynthesis results in inhibition of DMB scavenging. Curiously, this phenotype was somewhat less deleterious in strains which accumulate N<sup>5</sup>-CAIR or when repression of purine biosynthetic genes is prevented.

**Riboflavin supplementation does not satisfy a DMB auxotroph.**

Tracing experiments in *S. enterica* have shown that feeding of labeled riboflavin yields labeled DMB (albeit at 25% of the expected signal, assumed to be due to dilution by endogenous pools of riboflavin) (2). In Chapter 6, the addition of 100-fold more riboflavin than was provided in that study did not satisfy a DMB auxotroph. In the case *S. enterica* does not transport riboflavin (as seen in *E. coli*) (3), it was shown that the riboflavin transporter from *Corynebacterium glutamicum*, PnuX (4), is active in *S. enterica*, and can cause a 67% reduction in growth rate over the empty vector when the toxic riboflavin analog roseoflavin is introduced.

***S. enterica* synthesizes the DMB-cobamide cobalamin when provided 5-hydroxybenzimidazole or 5-methoxybenzimidazole.**

In chapter 5, it was reported that  $\alpha$ -ribosides of hydroxBza and methoxyBza could restore growth under conditions where an *S. enterica*  $\Delta cobT \Delta cobB$  strain expressing *Gk* CblITS and CblS is auxotrophic for  $\alpha$ -R. In Chapter 6, it was determined that feeding of those  $\alpha$ -ribosides results in the synthesis of the corresponding cobamides (hydroxyBza-Cba and methoxyBza-Cba). As asymmetric molecules (5), it was observed that multiple peaks arose when separated either as ribotides (Chapter 5) or as corrinoids (Chapter 6).

Unexpectedly, corrinoid extracts from where an *S. enterica*  $\Delta cobT \Delta cobB$  strain expressing *Gk* CblT and CblS fed excess (CN)<sub>2</sub>Cbi (1  $\mu$ M) and either hydroxyBza or methoxyBza synthesizes cobalamin, not hydroxyBza-Cba or methoxyBza-Cba. This finding suggests *S. enterica* converts hydroxyBza and methoxyBza to DMB, meaning that the purine intermediate 5-aminoimidazole ribotide (AIR) may be a precursor of DMB. Figure 7-1 illustrates how AIR-dependent synthesis of DMB is connected to the synthesis of  $\alpha$ -RP and Cbl.

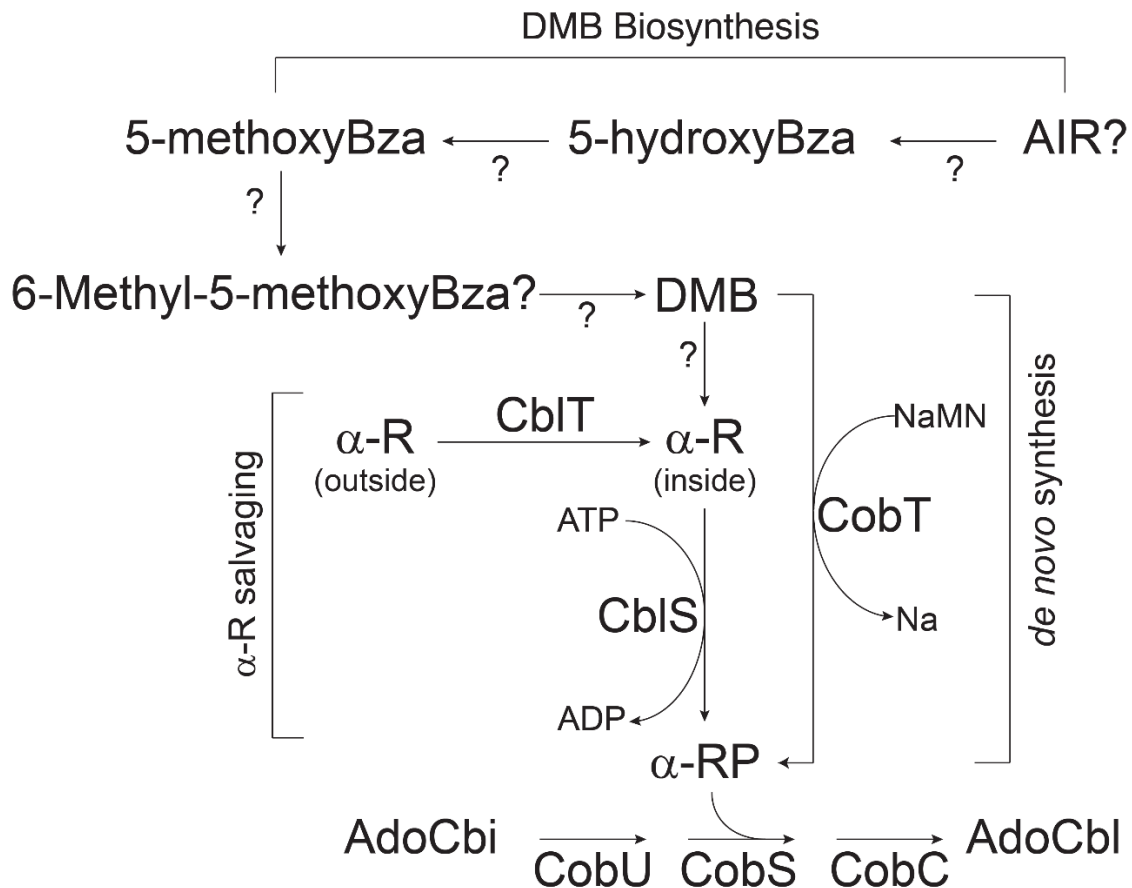


**Figure 7-1. A model for the multiple routes to  $\alpha$ -RP demonstrated in *S. enterica*.** The detection of Cbl in response to feeding with 5-hydroxyBza and 5-methoxyBza suggests that these compounds could be precursors to DMB. After conversion to DMB, the base is converted to  $\alpha$ -R by some unknown manner before being activated by the kinase CbIS, yielding  $\alpha$ -RP. The ribotide is condensed with the activated ring to yield the final product, Cbl. These results indicate that 5-aminoimidazole ribotide (AIR), not FMN, is a precursor to DMB. In this model, the synthesized DMB should be usable either by the kinase CbIS or the PRTase CobT. Abbreviations: CobT, DMB: NaMN phosphoribosyltransferase; CobU, NTP:Ado-cobinamide kinase and NTP:Ado-cobinamide-phosphate guanylyltransferase; CobS, AdoCbl-phosphate synthase; CobC, Ado-Cba-P phosphatase

## **RECOMMENDATIONS FOR FUTURE WORK.**

### **$\alpha$ -R scavenging in a Gram-positive system.**

One of the problems with working with CblS and CblT in *S. enterica* is that this system originates from a Gram-positive organism. As reported in Chapter 5, *S. enterica* does not require the transporter CblT to scavenge  $\alpha$ -R. A Gram-positive system should be identified to study CblT function. For instance, the ethanolamine utilization phenotype in *L. innocua* could be used as a sensor for CblT activity. Genetic systems exist for *L. innocua* (6), making it an excellent candidate for further study.

### **Identification of the enzyme(s) responsible for DMB synthesis.**

The promiscuity of the activation enzymes has limited our ability to identify the enzymes responsible for DMB biosynthesis. However, it may be possible now, by taking advantage of the tools described in this dissertation, to finally isolate genes related to DMB synthesis.

#### Aminoimidazole-ribotide (AIR) origin of DMB.

*S. enterica* appears to be able to convert hydroxyBza and methoxyBza DMB. This conversion can be confirm through *in vitro* synthesis of DMB starting from hydroxyBza or methoxyBza (perhaps using S-adenosylmethionine as a methyl donor, as proposed for BzaC, BzaD, and BzaE (7)) using cell extracts. After activity is detected, reverse genetics can be used to identify the proteins responsible.

A direct test for AIR incorporation into DMB requires the synthesis of AIR. It may be possible to use boronate affinity chromatography to isolate AIR from deproteinated extracts of the *S. enterica* strain designed to overproduce AIR (JE22216). HPLC separation would isolate the compound from other ribosides found in the eluate. The purified AIR is then dephosphorylated and fed to an *S. enterica*  $\Delta cobT \Delta cobB$  strain expressing *Gk* CblTS and CblS carrying a lesion in

*stm4068*, a regulator which prevents transfer of the AIR riboside (8), under conditions causing DMB auxotrophy. If AIR is a precursor of DMB, its presence in the medium should satisfy a DMB requirement. Blocks in *purE* and *thiC* to prevent leakage of the synthesized AIR molecule into other pathways may also be necessary to generate a sufficient amount of DMB from the imported molecule.

#### Riboflavin origin.

To test the possibility that riboflavin is a precursor of DMB, I propose utilizing a riboflavin transporter (*C. glutamicum* PnuX) to feed riboflavin or FMN directly into the cell. If the reduced riboflavin or FMN molecule are the precursors of DMB, feeding of those molecules should satisfy a DMB auxotrophy. It may be necessary to move *G. kaustophilus cblS* and *cblT* into the chromosome in order to express the transporter (or vice versa). A block at *ribB* could be used to prevent endogenous synthesis of riboflavin for future labeling studies, as RibB can be bypassed in the absence of exogenous riboflavin using 2,3-butanedione (diacetyl) (9).

#### Suppressor hunt.

Another possible angle to identifying the genes responsible for DMB biosynthesis would be to use a suppressor hunt. When the ring precursor is limited, an *S. enterica*  $\Delta cobT \Delta cobB$  strain expressing *Gk CblTS* and *CblS* cannot grow. The brief introduction of chemical mutagens could alter metabolic activities to favor the synthesis of DMB (or  $\alpha$ -R) to permit growth without supplementation. Those changes can then be mapped through sequencing.

### Tn-Seq.

The Tn-Seq technique (10) could be useful for identifying the genes required for the synthesis of DMB. By growing cells with and without DMB (or other bases) under conditions where the synthesis of cobalamin is required for growth, we can generate a population of genes which require DMB to grow, narrowing the pool of potential targets.

### **Identification of the enzyme(s) responsible for $\alpha$ -R synthesis.**

In the same vein as above, we can use the tools developed here to probe for  $\alpha$ -R synthesis in *S. enterica*. We can leverage the  $\alpha$ -R auxotrophic variants of *Gk CblS*, E98A to develop suppressor mutations in the *S. enterica*. Because the E98A variants require more  $\alpha$ -R than other variants, a suppressor mutation which increases  $\alpha$ -R would be selected over other mutations.

### **Variant analysis of *Gk CblS*.**

To better understand the kinase and its specificity for the  $\alpha$ -N-glycosidic linkage, mutational analysis of *Gk CblS* should be performed. XL1-Red mutagenesis did not work with p*GkCblS*3, but it may work in other hands. Other methods include hydroxylamine mutagenesis or random PCR mutagenesis. Selection should be performed on minimal NCE medium plates, looking for LOF on  $\alpha$ -R. It would also be interesting to purify other PurM-like kinases and to test whether they are capable of modifying  $\alpha$ -ribosides.

### **CblS Kinase crystal structure.**

In addition to variant analysis, it would be ideal to obtain a 3D structure of the CblS kinase. The specificity for the  $\alpha$ -N-glycosidic bond suggests an active site possess a different configuration than that observed with  $\beta$ -riboside kinases. A crystal structure would also be informative for understanding the role of any modified residues.

## CONCLUSION.

This dissertation has delivered new tools for probing the biosynthesis of DMB in *S. enterica* while expanding our understanding of the flexibility of the  $\alpha$ -riboside kinase from *G. kaustophilus*. We are also starting to understand the implications of the kinase in other organisms lacking the DMB: NaMN PRTase as well as the deep connections between purine metabolism and cobalamin biosynthesis.

## REFERENCES.

1. Gray MJ, Escalante-Semerena JC. 2010. A new pathway for the synthesis of alpha-ribazole-phosphate in *Listeria innocua*. *Mol Microbiol* 77:1429-1438.
2. Keck B, Munder M, Renz P. 1998. Biosynthesis of cobalamin in *Salmonella typhimurium*: transformation of riboflavin into the 5,6-dimethylbenzimidazole moiety. *Arch Microbiol* 171:66-68.
3. Gutiérrez-Preciado A, Torres AG, Merino E, Bonomi HR, Goldbaum FA, García-Angulo VA. 2015. Extensive identification of bacterial riboflavin transporters and their distribution across bacterial species. *PLoS One* 10.
4. Vogl C, Grill S, Schilling O, Stulke J, Mack M, Stolz J. 2007. Characterization of riboflavin (vitamin B2) transport proteins from *Bacillus subtilis* and *Corynebacterium glutamicum*. *J Bacteriol* 189:7367-7375.
5. Crofts TS, Hazra AB, Tran JL, Sokolovskaya OM, Osadchiy V, Ad O, Pelton J, Bauer S, Taga ME. 2014. Regiospecific formation of cobamide isomers is directed by CobT. *Biochemistry* 53:7805-7815.
6. Cossart P, Mengaud J. 1989. *Listeria monocytogenes*. A model system for the molecular study of intracellular parasitism. *Molecular biology & medicine* 6:463-474.

7. Hazra AB, Han AW, Mehta AP, Mok KC, Osadchiy V, Begley TP, Taga ME. 2015. Anaerobic biosynthesis of the lower ligand of vitamin B12. *Proc Natl Acad Sci U S A* 112:10792-10797.
8. Dougherty M, Downs DM. 2003. The *stm4066* gene product of *Salmonella enterica* serovar Typhimurium has aminoimidazole riboside (AIRs) kinase activity and allows AIRs to satisfy the thiamine requirement of *pur* mutant strains. *J Bacteriol* 185:332-339.
9. Crossley RA, Gaskin DJ, Holmes K, Mulholland F, Wells JM, Kelly DJ, van Vliet AH, Walton NJ. 2007. Riboflavin biosynthesis is associated with assimilatory ferric reduction and iron acquisition by *Campylobacter jejuni*. *Appl Environ Microbiol* 73:7819-25.
10. van Opijnen T, Camilli A. 2013. Transposon insertion sequencing: a new tool for systems-level analysis of microorganisms. *Nat Rev Microbiol* 11:435-442.

APPENDIX A

SUPPLEMENTAL INFORMATION FOR

“*SALMONELLA ENTERICA* SYNTHESIZES 5,6-DIMETHYLBENZIMIDAZOYL-(DMB)- $\alpha$ -  
RIBOSIDE. WHY SOME *FIRMICUTES* DO NOT REQUIRE THE CANONICAL DMB  
ACTIVATION SYSTEM TO SYNTHESIZE ADENOSYLCOBALAMIN”<sup>6</sup>

---

<sup>6</sup> Mattes, T.A. and J. C. Escalante-Semerena. 2016. *Molecular Microbiology*. Accepted.  
Reprinted with permission from the publisher.

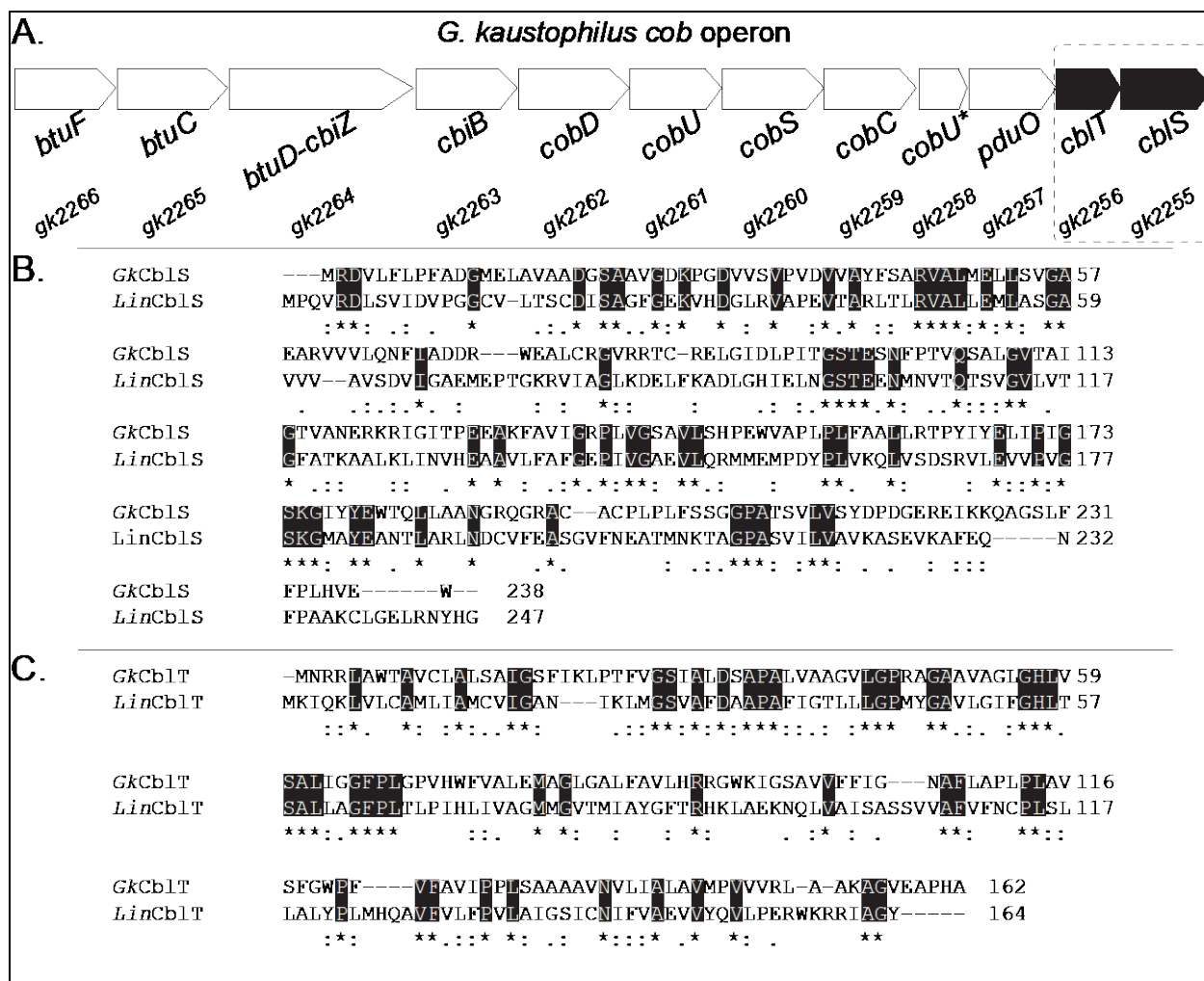


**Figure A-1.** *cbIT* and *cbIS* are found within the *cob* operon of *G. kaustophilus*. Genes and their expected products, based on homology: *btuF*, cobalamin ABC transporter binding protein; *btuC*, cobalamin ABC transporter permease; *btuD-cbiZ*, cobalamin ABC transporter ATP-binding protein/adenosylcobinamide amidohydrolase; *cbiB*, adenosylcobinamide-phosphate synthase; *cobD*, threonine-phosphate decarboxylase; *cobU*, NTP:Ado-cobinamide kinase and NTP:Ado-cobinamide-phosphate guanylyltransferase; *cobS*, adenosylcobalamin-5'-phosphate synthase; *cobC*,  $\alpha$ -RP phosphatase; *pduO*, PduO-type ATP:Co(I)rrinoid adenosyltransferase; *cbIT*,  $\alpha$ -R transporter; *cbIS*,  $\alpha$ -R kinase. B and C. Clustal Omega alignments of *G. kaustophilus* CbIS and CbIT versus their *L. innocua* homologues.

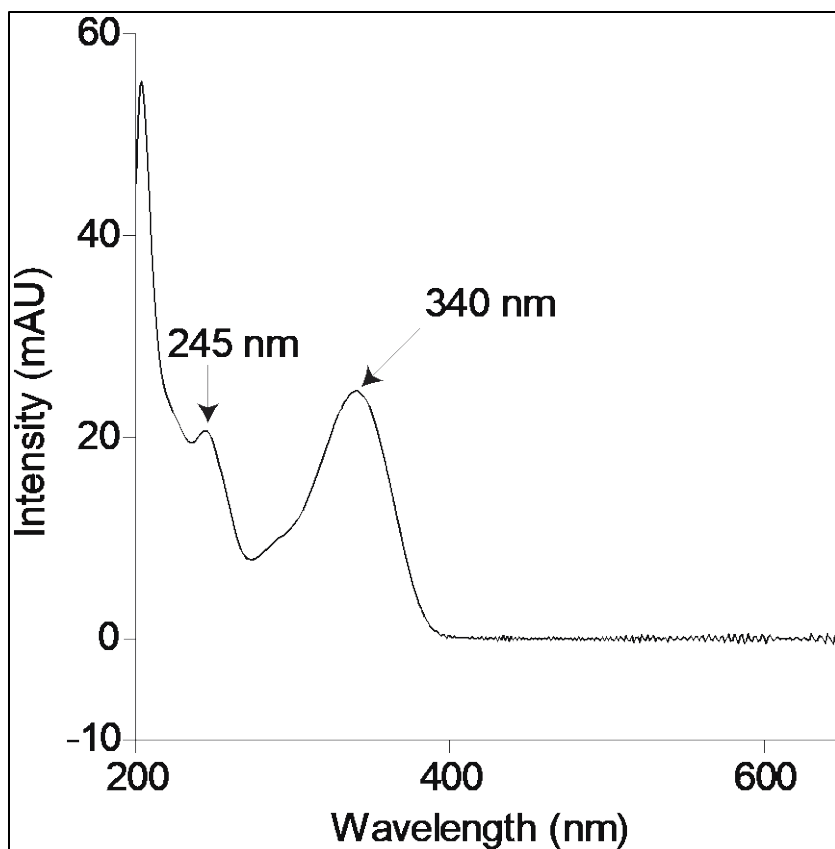


**Figure A-2. UV-visible spectrum of an unknown compound present in all extracted corrinoid mixtures.** Signature absorption maxima of corrinoids in the 500-nm region are missing, indicating that this compound is not a corrinoid. In addition, this compound failed to support Cbl-dependent growth of indicator strain JE8214 (*metE205 ara-9 cobS1312::cat<sup>+</sup>*), which can only grow when supplemented with cobamides like Cbl or pseudoCbl.

APPENDIX B

SUPPLEMENTAL INFORMATION FOR

“FACILE ISOLATION OF  $\alpha$ -RIBAZOLE FROM VITAMIN B<sub>12</sub> HYDROLYSATES USING  
BORONATE AFFINITY CHROMATOGRAPHY”<sup>7</sup>

Theodoric A. Mattes and Jorge C. Escalante-Semerena\*

Department of Microbiology, University of Georgia

---

<sup>7</sup> Mattes, T.A. and J. C. Escalante-Semerena. 2018. *Journal of Chromatography-B*. Accepted.  
This chapter is reprinted with permission from the publisher.

## **SUPPLEMENTAL METHODS**

### **1.1. CNB<sub>12</sub> concentration quantification**

To determine the initial concentration of starting material, dilutions (500-fold and 1000-fold) were made into deionized water (Millipore) and loaded into a 1-cm quartz cuvette. Using the cuvette reader module of an Eon 96-well microplate reader (BioTek Instruments) controlled by a computer, the absorbance at 367 nm was recorded for each CNB<sub>12</sub> dilution and the concentration was determined using the extinction coefficient of dicyanocobinamide in water ( $\epsilon_{367} = 21800 \text{ M}^{-1} \text{ cm}^{-1}$ ) (1).

### **1.2. Quantification of $\alpha$ -R concentrations by fluorescence**

Samples (and dilutions as needed) were diluted 100-fold into Tris-HCl buffer (1M, pH 8). Samples (200- $\mu\text{L}$  each) were loaded into an opaque black Nunc 96-well microtiter plate (ThermoFisher Scientific). Fluorescence was acquired by exciting at 250 nm; fluorescence was measured at 312 nm using a computer-controlled Synergy MX fluorescence plate reader (Biotek Instruments; dynamic range 5 log, a.k.a decades). Concentrations were estimated using the quantum yield of  $\alpha$ -R ( $\Phi_{250,312} = 3.62 \times 10^{13} \text{ RFU/mole}$ ) determined using a standard curve. The linear range for this method was from 320 nM to 6.4  $\mu\text{M}$   $\alpha$ -R.

### **1.3 Quantification of $\alpha$ -R concentrations by absorbance**

#### *1.3.1. Path-length correction*

Path-length corrections for a sample dissolved in DMSO in a 96-well plate were made with some adjustments to the manufacturer's protocol (Biotek Instruments). To determine path-length correction of a sample dissolved in DMSO, it was necessary to determine the k-value of DMSO in a cuvette with a 1-cm path length.

Using such a cuvette, a spectral scan of DMSO was performed between 850 nm and 990 nm using the cuvette reader module of a computer-controlled Eon plate reader (Biotek Instruments) (Figure B-1). A lambda-max at 900 nm and a lambda min of at 930 nm were selected based on the scan. The k-value was calculated as follows:

$$k\text{-value}_{\text{solvent}}: A_{\text{Max } \lambda} - A_{\text{Min } \lambda}$$

A k-value for DMSO of 0.042 was calculated as the difference of A900 and A930.

To correct for path length for a sample dissolved in 100% DMSO, the A900 ( $\lambda$  max) and A930 ( $\lambda$  min) of the sample were obtained and the difference was divided by the k-value of DMSO.

$$\text{Path length}_{\text{sample}}: \frac{(A_{\text{Max } \lambda} - A_{\text{Min } \lambda})_{\text{sample}}}{k\text{-value}_{\text{solvent}}}$$

Finally, to correct the measured absorbance at a given wavelength to 1-cm, we recorded the absorbance for the sample and a blank (*i.e.* A<sub>280</sub>) and divided the difference by the calculated path length of the sample.

$$\text{Corrected } A_{\text{sample}}: \frac{(A_{\text{sample}} - A_{\text{blank}})}{\text{Pathlength}_{\text{sample}}}$$

### 1.3.2. Quantification of $\alpha$ -R using corrected absorbance

100-fold dilutions are prepared of the final product on DMSO. 100-uL aliquots are loaded into wells on a 96-well UV-transparent microtiter plate (acrylic; Corning), along with a DMSO blank. Absorbance of the samples was acquired at 280 nm, 900 nm, and 930 nm on a computer-controlled Eon plate reader (Biotek Instruments). The corrected A<sub>280</sub> value was calculated using 1.3.1. The corrected A<sub>280</sub> value was then multiplied by the dilution factor and divided by the molar extinction coefficient of DMB on DMSO ( $\epsilon_{280} = 6090 \text{ M}^{-1} \text{ cm}^{-1}$  in 96-well plate format) to obtain the estimated molar concentration of the sample, from which the mass yield of the sample was obtained. The linear range for this method was from 10  $\mu\text{M}$  to 1 mM  $\alpha$ -R.

#### 1.4. Corrinoid scavenging bioassay

A corrinoid scavenging bioassay was used to detect the presence of non-hydrolyzed B<sub>12</sub> in samples taken before and after heating, diluted 100x in Tris-HCl buffer (1 M, pH 8). Samples were diluted 10,000x before use. Indicator strains JE8214 (*cobS*; requires either B<sub>12</sub> or L-methionine) or JE12403 (*cobS btuB*; requires L-methionine) (2) were grown under normoxic conditions on minimal no-carbon energy (NCE) growth medium (3) containing ribose (22 mM), trace minerals, magnesium sulfate (1 mM), and antibiotic (JE8214, 10 µg/mL chloramphenicol; JE12403, 25 µg/mL kanamycin). The medium was inoculated with an overnight starter culture (1% vol/vol) grown on nutrient broth (Difco) for ≥20 h to reduce residual nutrients. Growth was observed in 96-well microtiter dishes, with each sample tested in duplicate. Each well contained 190 µL of inoculated medium + 10 µL of sample or controls. Additives of water, B<sub>12</sub> precursor dicyanocobinamide ((CN)<sub>2</sub>Cbi; 150 nM) + α-R (3 µM), CNB<sub>12</sub> (150 nM), and L-methionine (5 mM) were used as controls (Figure B-3). Cell density was monitored at 630 nm on a computer-controlled Powerwave plate reader (Biotek). Readings were acquired every 15 min and final OD<sub>630</sub> and growth rates were determined using the Gen5 2.0 software package.

#### 1.5. α-R scavenging bioassay

To test α-R scavenging, a modification was made to the growth analyses of JE21364 (*metE cobT cobB* / pGkCblS<sup>WT</sup>) described elsewhere (2). A null allele in *metE* renders the strain auxotrophic for methionine or cobamides. In the absence of MetE, the strain requires the B<sub>12</sub>-dependent MetH (4-6) enzyme to methylate homocysteine to methionine. The methionine auxotroph *metE* strain can be rescued by methionine or by complete or incomplete corrinoids (*e.g.*, B<sub>12</sub>, or its precursors cobinamide or cobyrinic acid) (4, 7). The strain (JE12939) possesses null alleles in *cobT* and *cobB* (8, 9). The absence of CobT and CobB renders this strain unable to activate DMB to its ribotide,

blocking de novo synthesis of CoB<sub>12</sub>. Plasmid pGkCbIS3, which contains the wildtype allele of the *Geobacillus kaustophilus* *cbIS* gene inserted into the arabinose-inducible P<sub>araBAD</sub> promoter of pBAD24, was transformed into this genetic background (*metE cobT cobB*) to generate the strain JE21364 (2). Under certain conditions, this strain is auxotrophic for  $\alpha$ -R and can respond to the molecule being present in the medium (2). A strain (JE17827) with the same genetic background (*metE cobT cobB*) but containing the empty cloning vector pBAD24 (10) was used as negative control (2). The positive control (JE17828) carries a plasmid (pCOBT140) encoding the wild-type allele of *S. enterica* *cobT* (2).

These strains were grown under normoxic conditions in minimal no-carbon energy (NCE) medium (3) supplemented with the B<sub>12</sub> precursor dicyanocobinamide ((CN)<sub>2</sub>Cbi)). In the presence of oxygen, *S. enterica* cannot synthesize the corrin ring (4) but it can scavenge the precursor (11-13). (CN)<sub>2</sub>Cbi was present in the medium at 0.25 nM, to saturate the AdoB<sub>12</sub>-5'-P synthase CobS of *S. enterica* (14). Under these conditions strain JE21364 (*cobT cobB* / pGkCbIS3) required  $\alpha$ -R to grow (2). We leveraged this phenotype to assess the purity of  $\alpha$ -R and its biological activity. If the  $\alpha$ -R was impure and at a lower concentration than expected, when compared to an authentic stock of  $\alpha$ -R, it yielded a slower growth rate.

The NCE growth medium was also supplemented with ribose (22 mM), trace minerals, magnesium sulfate (1 mM), L(+)-arabinose (500  $\mu$ M), ampicillin (50  $\mu$ g/mL), and (CN)<sub>2</sub>Cbi (0.25 nM). When required,  $\alpha$ -R or the hydrolysis product was added at 300 nM concentration. Growth was monitored in 96-well microtiter dishes, with each strain growing under the given condition in triplicate. Each well contained 200  $\mu$ L of medium, inoculated with 1% (vol/vol) of an overnight starter culture grown on nutrient broth (Difco) for  $\geq 16$  h to reduce the residual nutrients. Cell density was monitored at 630 nm on a computer-controlled Powerwave plate reader (Biotek).

Readings were acquired every 15 min and final OD<sub>630</sub> and growth rates were determined using the Gen5 2.0 software package.

**Supplemental Table B-1. Bacterial strains and plasmids used in this study.**

Strains	Antibiotic resistance	Relevant genotype	Reference or source
TR6583	none	<i>metE205 ara-9</i>	K. Sanderson via J. Roth
<b>Derivatives of strain TR6583</b>			
JE7088	none	$\Delta metE2702$	Lab collection
JE8214	Cm <sup>R</sup>	<i>metE205 ara-9 cobS1312::cat</i>	Lab collection
JE12403	Km <sup>R</sup>	<i>metE205 ara-9 ΔcobS1313 btuB7::MudJ<sup>3</sup></i>	Lab collection
<b>Derivatives of strain JE7088</b>			
JE12939	none	$\Delta metE2702 \Delta cobT1380 \Delta cobB1375$	Lab collection
JE17827	Ap <sup>R</sup>	$\Delta metE2702 \Delta cobT1380 \Delta cobB1375$ / pBAD24	(2)
JE17828	Ap <sup>R</sup>	$\Delta metE2702 \Delta cobT1380 \Delta cobB1375$ / pCOBT140	(2)
JE21364	Ap <sup>R</sup>	$\Delta metE2702 \Delta cobT1380 \Delta cobB1375$ / pGkCblS3	(2)
<b>Plasmids</b>			
pBAD24	Ap <sup>R</sup>	Cloning vector with P <sub>araBAD</sub> arabinose-inducible promoter	(10)
pGkCblS3	Ap <sup>R</sup>	<i>G. kaustophilus cblS</i> <sup>+</sup> in pBAD24	(2)
pCOBT140	Ap <sup>R</sup>	<i>S. enterica cobT</i> <sup>+</sup> in pBAD24	(2)

<sup>1</sup> All *E. coli* strains used in this study were derivatives of *E. coli* K-12

<sup>2</sup> All *S. enterica* strains used in this study were derivatives of *S. enterica* subsp. *enterica* sv Typhimurium strain LT2

<sup>3</sup> MudJ is an abbreviation of MudIII734 (15)

Ap<sup>R</sup>, Ampicillin resistance; Cm<sup>R</sup>, chloramphenicol resistance; Km<sup>R</sup>, kanamycin resistance

## SUPPLEMENTAL DATA

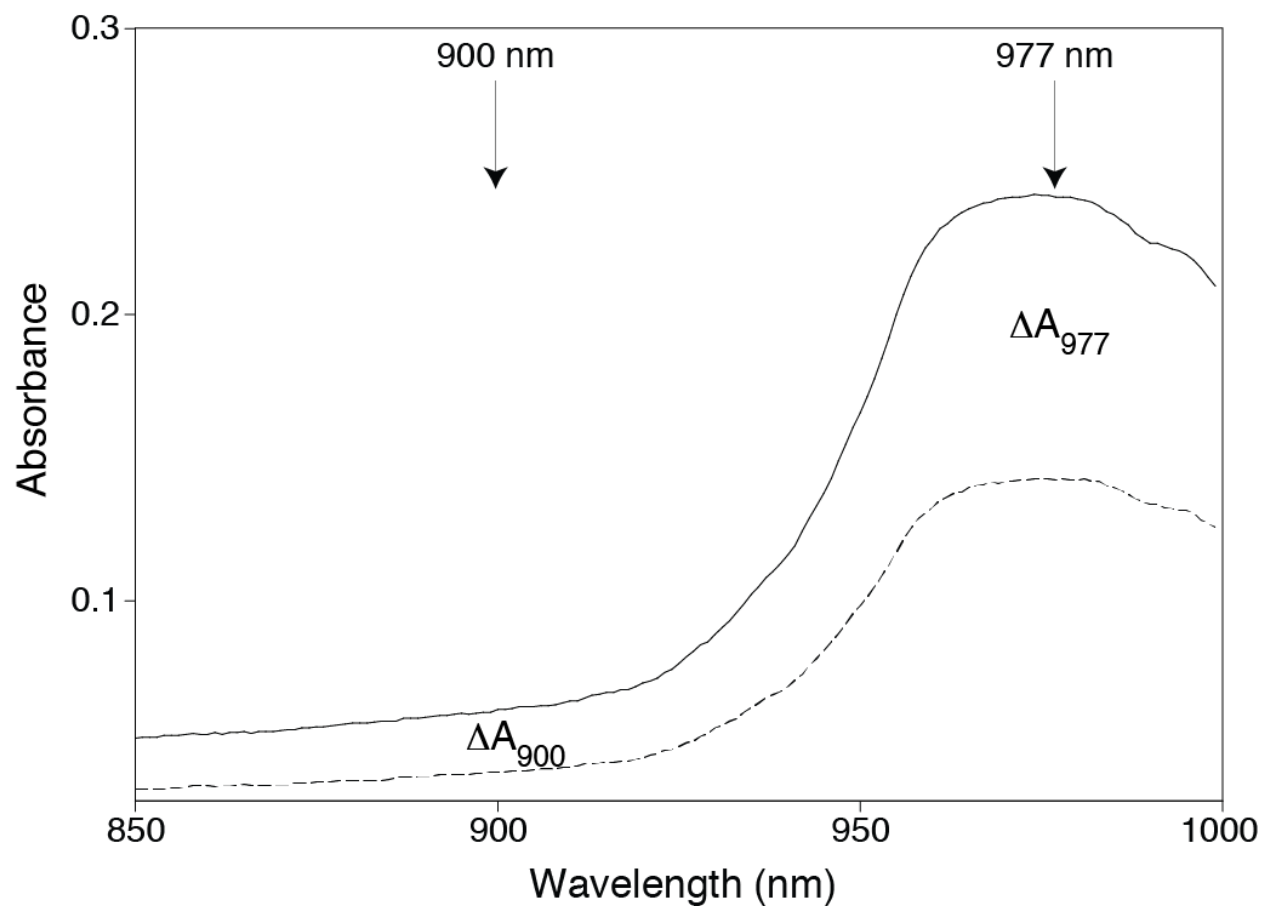


**Figure B-1. UV-Vis spectral scan of water**

The solid line is the UV-Vis spectra of water in a 1-cm path length, 0.580-ml quartz cuvette. The dashed line represents the UV-Vis spectra of water in a UV-transparent 96-well plate. Note the decrease at the  $\lambda$  max at 977 nm and  $\lambda$  min at 900 nm. This difference is used to calculate the path-length correction for samples in water (Suppl. 1.3.1).

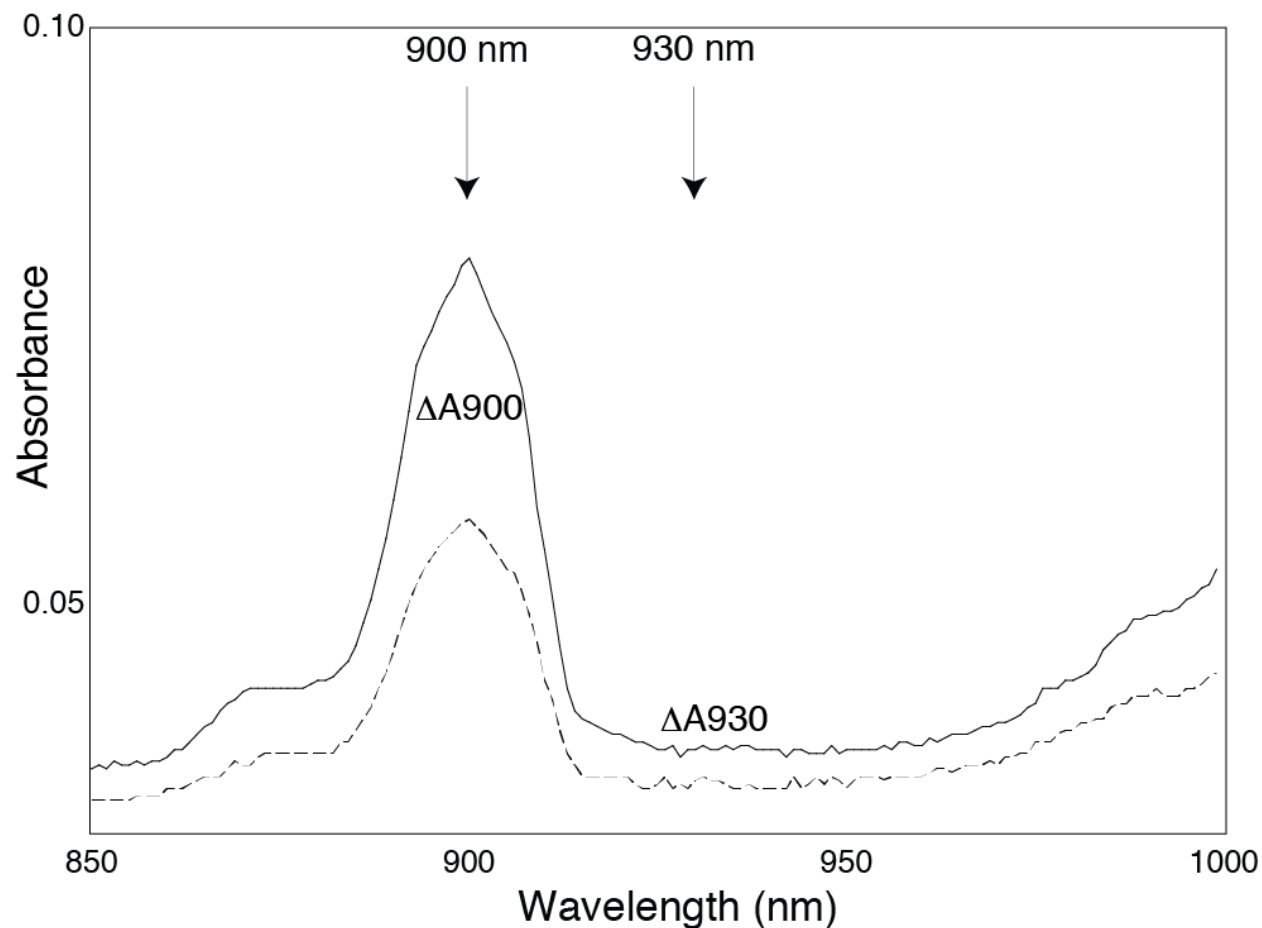


**Figure B-2. UV-Vis spectral scan of DMSO.**

The solid line is the UV-Vis spectra of DMSO in a 1-cm quartz cuvette. The dashed line represents the UV-Vis spectra of DMSO in a UV-transparent 96-well plate. As before, we can see that the overall absorbance decreases. Note the change in maxima, with the  $\lambda$  max occurring at 900 nm and a  $\lambda$  min at 930 nm. This difference is used to calculate the path-length correction for samples in DMSO (Suppl. 1.3.1)

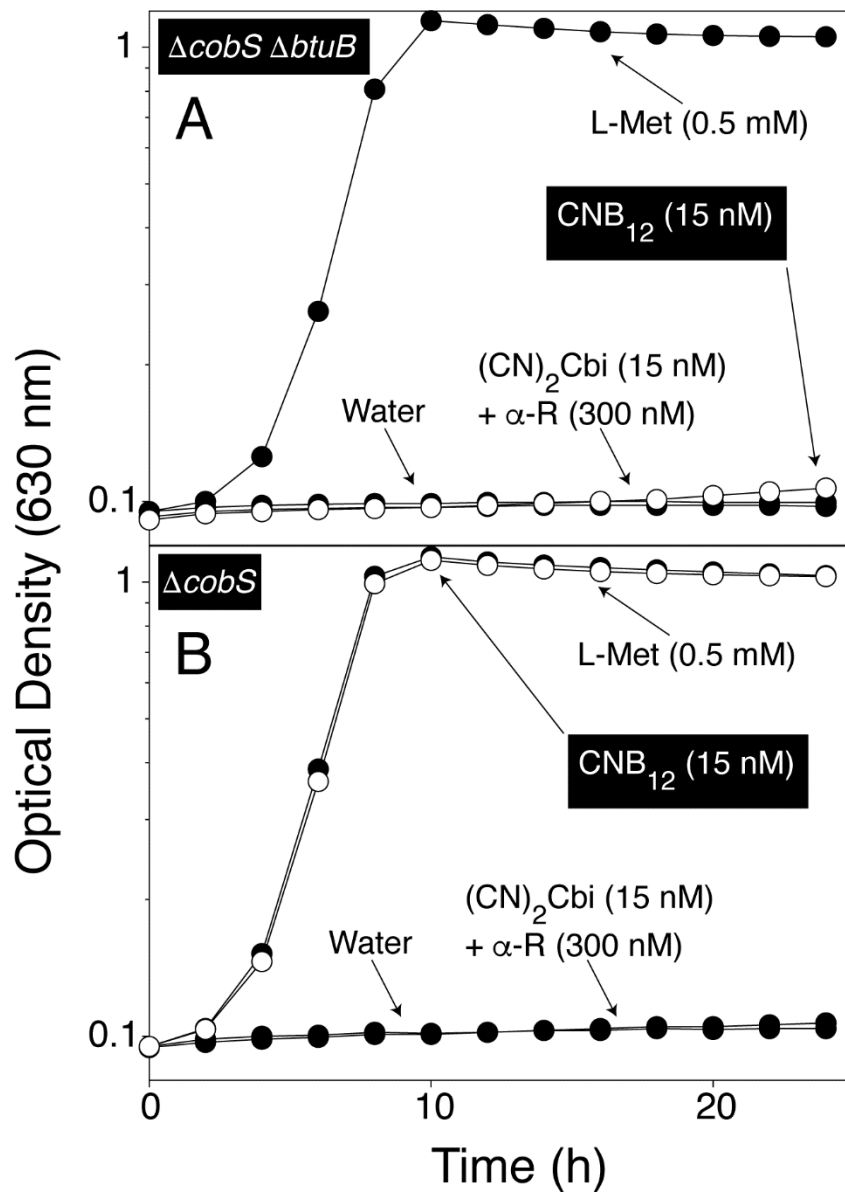


**Figure B-3. Corrinoid scavenging growth assay controls.**

All strains grown on minimal NCE medium containing ribose (22 mM), trace minerals, magnesium sulfate (1 mM), and chloramphenicol (10  $\mu$ g/mL). The white circles represent the response to CNB<sub>12</sub>. Other additives as marked. A. Growth Response of JE12403 ( $\Delta cobS \Delta btuB$ ). B. Growth response of JE8214 ( $\Delta cobS$ ).

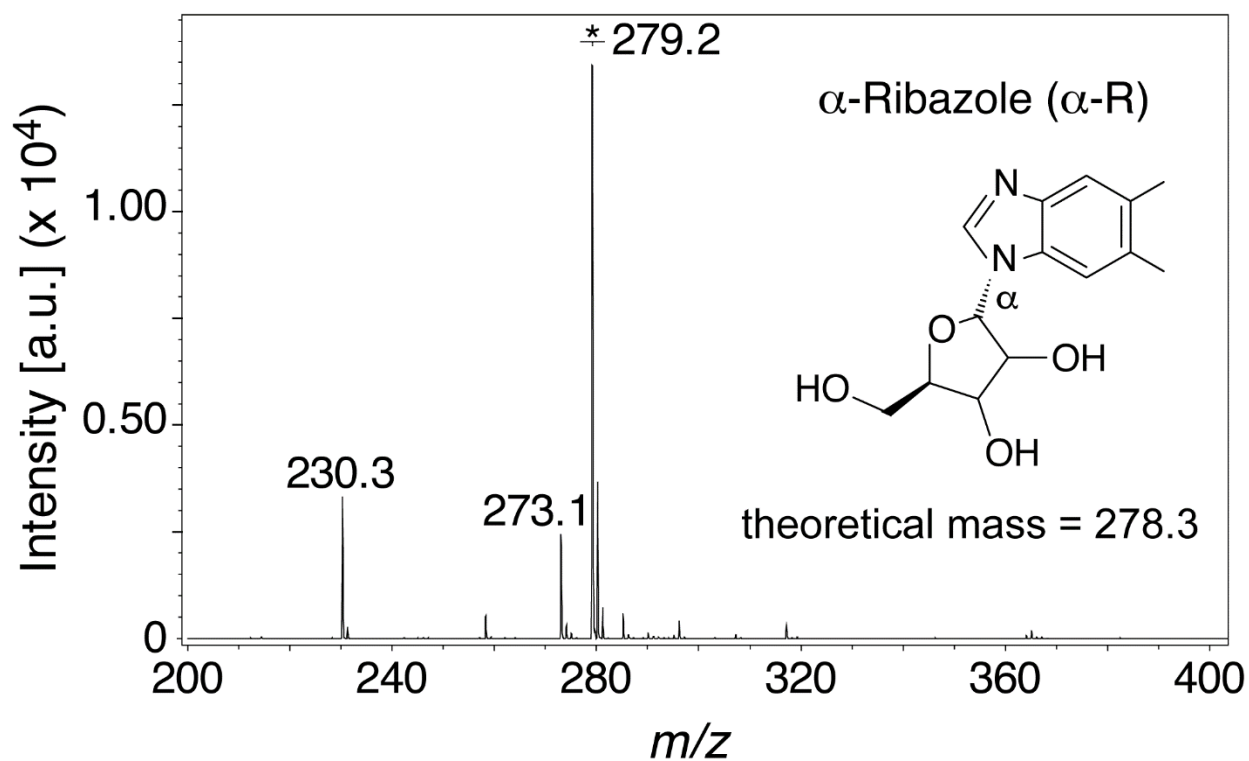


**Figure B-4. Mass spectrometric analysis of final product**

The final product was analyzed by MALDI-TOF mass spectrometry. Shown is the  $[M+1]^+$  ion with a  $m/z = 279.2$

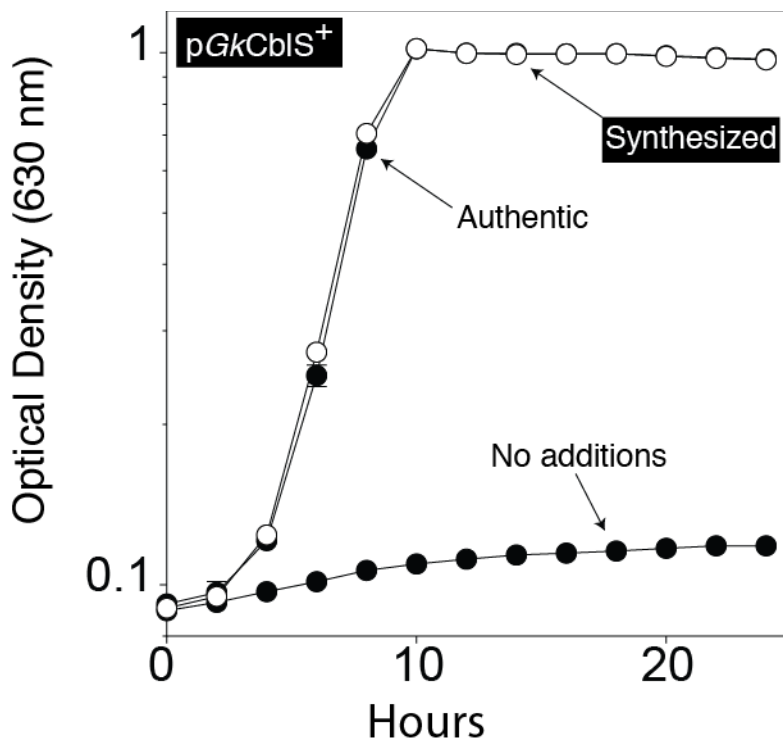


**Figure B-5.  $\alpha$ -R Scavenging Bioassay Results**

Strain JE21364 ( $\Delta metE \Delta cobT \Delta cobB / pGkCbIS^+$ ) was grown on minimal NCE medium containing ribose (22 mM), trace minerals, magnesium sulfate (1 mM), L-(+)-arabinose (0.5 M), ampicillin (50  $\mu\text{g}/\text{mL}$ ), and  $(\text{CN})_2\text{Cbi}$  (0.25 nM). When added,  $\alpha$ -R was diluted to 0.3  $\mu\text{M}$ . The open circle represents the synthesized  $\alpha$ -R following lyophilization.

## REFERENCES

1. C.H. Chan, J.C. Escalante-Semerena, ArsAB, a novel enzyme from *Sporomusa ovata* activates phenolic bases for adenosylcobamide biosynthesis, *Mol. Microbiol.*, 81 (2011) 952-967.
2. T.A. Mattes, J.C. Escalante-Semerena, *Salmonella enterica* synthesizes 5,6-dimethylbenzimidazolyl-(DMB)- $\alpha$ -ribose. Why some *Firmicutes* do not require the

- canonical DMB activation system to synthesize adenosylcobalamin, *Mol. Microbiol.*, 103 (2017) 269-281.
3. D. Berkowitz, J.M. Hushon, H.J. Whitfield, Jr., J. Roth, B.N. Ames, Procedure for identifying nonsense mutations, *J. Bacteriol.*, 96 (1968) 215-220.
  4. R.M. Jeter, B.M. Olivera, J.R. Roth, *Salmonella typhimurium* synthesizes cobalamin (vitamin B<sub>12</sub>) de novo under anaerobic growth conditions, *J. Bacteriol.*, 159 (1984) 206-213.
  5. J.C. Gonzalez, R.V. Banerjee, S. Huang, J.S. Sumner, R.G. Matthews, Comparison of cobalamin-independent and cobalamin-dependent methionine synthases from *Escherichia coli*: two solutions to the same chemical problem, *Biochemistry*, 31 (1992) 6045-6056.
  6. J.T. Drummond, R.G. Matthews, Cobalamin-dependent and cobalamin-independent methionine synthases in *Escherichia coli*: two solutions to the same chemical problem, *Adv. Exp. Med. Biol.*, 338 (1993) 687-692.
  7. K.R. Brushaber, G.A. O'Toole, J.C. Escalante-Semerena, CobD, a novel enzyme with L-threonine-*O*-3-phosphate decarboxylase activity, is responsible for the synthesis of (*R*)-1-amino-2-propanol *O*-2-phosphate, a proposed new intermediate in cobalamin biosynthesis in *Salmonella typhimurium* LT2, *J. Biol. Chem.*, 273 (1998) 2684-2691.
  8. J.R. Trzebiatowski, G.A. O'Toole, J.C. Escalante-Semerena, The *cobT* gene of *Salmonella typhimurium* encodes the NaMN: 5,6-dimethylbenzimidazole phosphoribosyltransferase responsible for the synthesis of *N*<sup>1</sup>-(5-phospho- $\alpha$ -D-ribosyl)-5,6-dimethylbenzimidazole, an intermediate in the synthesis of the nucleotide loop of cobalamin, *J. Bacteriol.*, 176 (1994) 3568-3575.
  9. A.W. Tsang, J.C. Escalante-Semerena, CobB, a new member of the SIR2 family of eucaryotic regulatory proteins, is required to compensate for the lack of nicotinate

- mononucleotide:5,6-dimethylbenzimidazole phosphoribosyltransferase activity in cobT mutants during cobalamin biosynthesis in *Salmonella typhimurium* LT2, J. Biol. Chem., 273 (1998) 31788-31794.
10. L.M. Guzman, D. Belin, M.J. Carson, J. Beckwith, Tight regulation, modulation, and high-level expression by vectors containing the arabinose PBAD promoter, J. Bacteriol., 177 (1995) 4121-4130.
  11. R.M. Jeter, J.R. Roth, Cobalamin (vitamin B<sub>12</sub>) biosynthetic genes of *Salmonella typhimurium*, J. Bacteriol., 169 (1987) 3189-3198.
  12. G.A. O'Toole, M.R. Rondon, J.C. Escalante-Semerena, Analysis of mutants of defective in the synthesis of the nucleotide loop of cobalamin, J. Bacteriol., 175 (1993) 3317-3326.
  13. G.A. O'Toole, J.C. Escalante-Semerena, *cobU*-dependent assimilation of nonadenosylated cobinamide in *cobA* mutants of *Salmonella typhimurium*, J. Bacteriol., 175 (1993) 6328-6336.
  14. C.L. Zayas, J.C. Escalante-Semerena, Reassessment of the late steps of coenzyme B<sub>12</sub> synthesis in *Salmonella enterica*: Evidence that dephosphorylation of adenosylcobalamin-5'-phosphate by the CobC phosphatase is the last step of the pathway, J. Bacteriol., 189 (2007) 2210-2218.
  15. B.A. Castilho, P. Olfson, M.J. Casadaban, Plasmid insertion mutagenesis and *lac* gene fusion with mini-Mu bacteriophage transposons, J. Bacteriol., 158 (1984) 488-495.

APPENDIX C

SUPPLEMENTAL INFORMATION FOR

“FUNCTIONAL STUDIES OF  $\alpha$ -RIBOSIDE ACTIVATION BY THE KINASE CBLs FROM

*GEOBACILLUS KAUSTOPHILUS*”<sup>8</sup>

---

<sup>8</sup> Mattes, T.A. and J. C. Escalante-Semerena. To be submitted to *Journal of Bacteriology*

**Table C1. Riboside (300 pM) feeding generation times (h) for JE17827 (empty vector), JE21364 (*cbIS*<sup>+</sup>), and JE17830 (*cbIT*<sup>+</sup> *cbIS*<sup>+</sup>).** All strains were grown on minimal NCE medium supplemented with trace minerals, ribose (22 mM), MgSO<sub>4</sub> (1 mM), L-arabinose (500 μM), ampicillin (100 mg mL<sup>-1</sup>) and (CN)<sub>2</sub>Cbi (0.25 nM). Ribosides were provided at 300 pM. Growth was measured for 24 h. A lower generation time indicates faster growth.

	<i>ΔcobT ΔcobB</i>	<i>cbIS</i> <sup>+</sup>	<i>cbIT</i> <sup>+</sup> <i>cbIS</i> <sup>+</sup>
No Riboside Added	30	25	32
Authentic α-R	28	3	2
α-R (synthesized with <i>Stm</i> CobT)	33	3	2
α-Bza-R	28	3	2
α-hydroxyBza-R	32	15	15
α-methoxyBza-R	30	3	2
α-Ado	28	25	30
β-Ado	32	20	24

**Table C2. Riboside (300 nM) feeding generation times (h) for JE17827 (empty vector), JE21364 (*cbIS*<sup>+</sup>), and JE17830 (*cbIT*<sup>+</sup> *cbIS*<sup>+</sup>).** All strains were grown on minimal NCE medium supplemented with trace minerals, ribose (22 mM), MgSO<sub>4</sub> (1 mM), L-arabinose (500 μM), ampicillin (100 mg mL<sup>-1</sup>) and (CN)<sub>2</sub>Cbi (0.25 nM). Ribosides were provided at 300 nM. Growth was measured for 24 h. A lower generation time indicates faster growth.

	<i>ΔcobT ΔcobB</i>	<i>cbIS</i> <sup>+</sup>	<i>cbIT</i> <sup>+</sup> <i>cbIS</i> <sup>+</sup>
No Riboside Added	30	25	32
Authentic α-R	25	1	1
α-R (synthesized with <i>Stm</i> CobT)	25	1	1
α-Bza-R	20	2	2
α-hydroxyBza-R	24	2	2
α-methoxyBza-R	25	1	1
α-Ado	23	23	19
β-R	28	24	18
β-Ado	32	32	26

**Table C3.  $\alpha$ -Ado Feeding Generation Times for JE17827 (empty vector) and JE17830**

(*cblT*<sup>+</sup> *cblS*<sup>+</sup>). All strains were grown on minimal NCE medium supplemented with trace minerals, ribose (22 mM), MgSO<sub>4</sub> (1 mM), L-arabinose (500  $\mu$ M), ampicillin (100 mg mL<sup>-1</sup>) and (CN)<sub>2</sub>Cbi (0.25 nM). Ribosides were provided at 300 nM or 1  $\mu$ M. Growth was measured for 24 h. A lower generation time indicates faster growth.

	<i><math>\Delta</math>cobT <math>\Delta</math>cobB</i>	<i>cblT</i> <sup>+</sup> <i>cblS</i> <sup>+</sup>
No Riboside Added	31	29
$\alpha$ -Ado (300 nM)	24	18
$\alpha$ -Ado (300 nM) + $\alpha$ -R (300 nM)	22	1
$\alpha$ -Ado (1 $\mu$ M)	24	10
$\alpha$ -Ado (1 $\mu$ M) + $\alpha$ -R (300 nM)	20	1

**Figure C1. MALDI analysis of synthesized ribosides.** From top to bottom: hydroxybenzimidazole- $\alpha$ -riboside ( $\alpha$ -hydroxyBza-R); methoxybenzimidazole- $\alpha$ -riboside ( $\alpha$ -methoxyBza-R);  $\beta$ -ribazole ( $\beta$ -R);  $\alpha$ -ribazole ( $\alpha$ -R);  $\alpha$ -adenosine ( $\alpha$ -Ado); benzimidazole- $\alpha$ -riboside ( $\alpha$ -Bza-R).

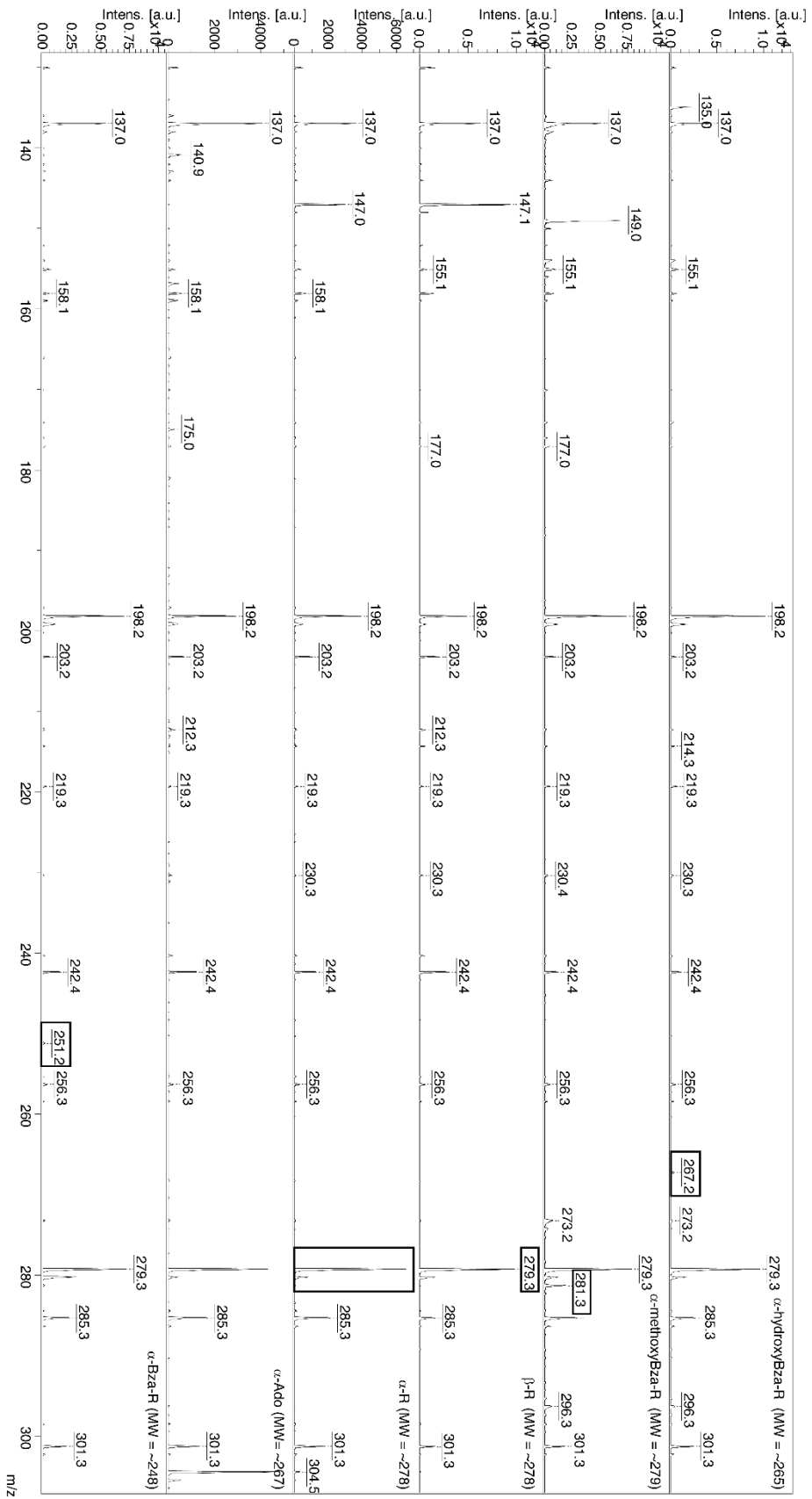


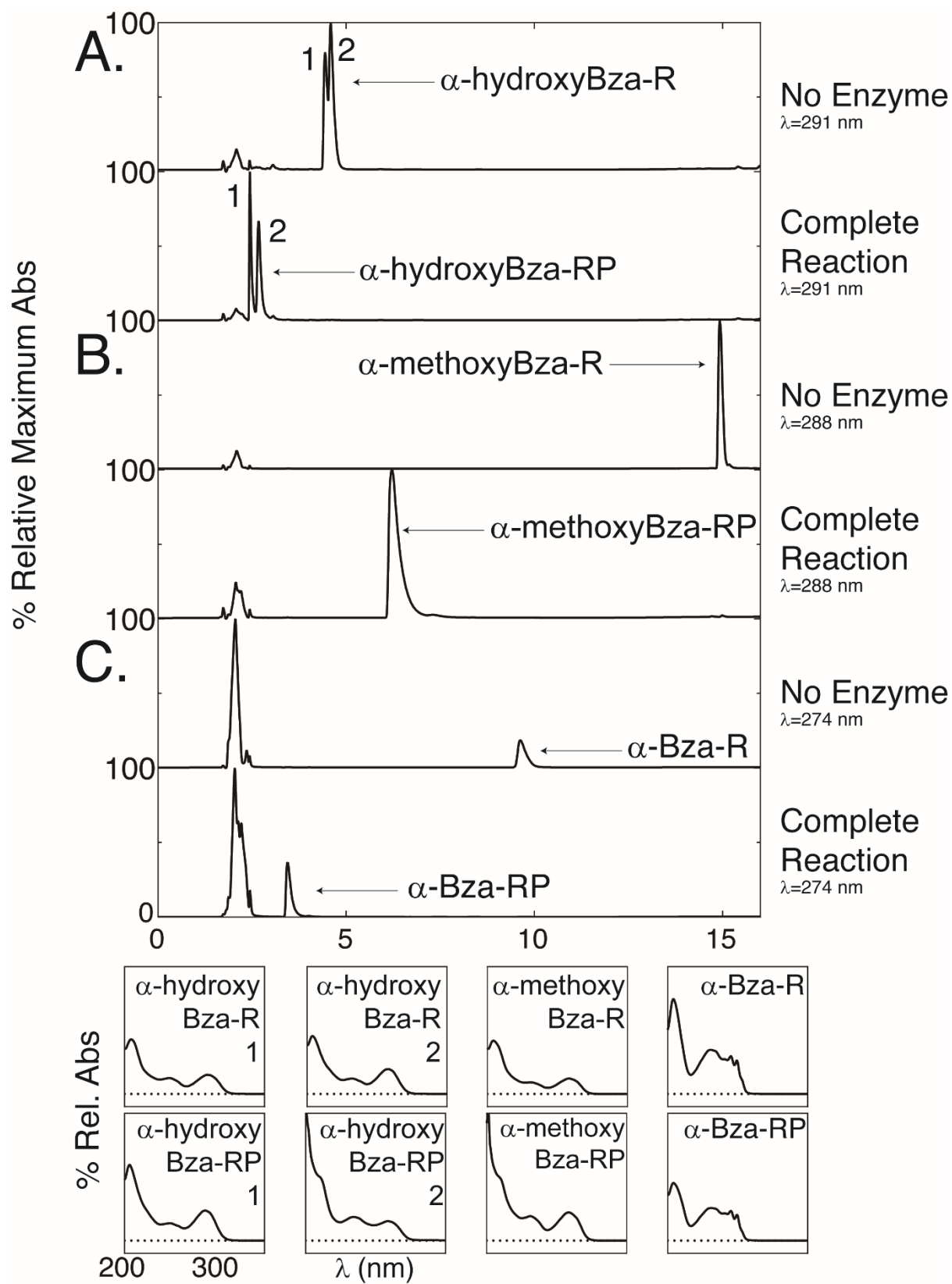
**Figure C2. *Gk* CblS activates  $\alpha$ -hydroxyBza-R,  $\alpha$ -methoxyBza-R, and  $\alpha$ -Bza-R.** A reaction mixture containing *Gk* CblS (2  $\mu$ g), HEPES (pH 7.5), KCl (800 mM), MgCl<sub>2</sub> (5 mM), TCEP (1.25 mM), ATP (1.75 mM), and  $\alpha$ -riboside (500  $\mu$ M) was incubated for 30 min at 37 °C before shifting to 95 °C. The products were then separated by HPLC. The UV-Visible spectra of the ribosides are presented at the bottom. ATP/ADP elute at 2 min (\*).

A. Top: No enzyme + ATP +  $\alpha$ - hydroxyBza-R, Bottom: *Gk* CblS + ATP +  $\alpha$ - hydroxyBza-R.

The two peaks represent the asymmetric synthesis of  $\alpha$ -hydroxyBza-R by the DMB:PRTase, which can generate both 5'- hydroxyBza- $\alpha$ -riboside and 6'- hydroxyBza- $\alpha$ -riboside.

B. Top: No enzyme + ATP +  $\alpha$ - methoxyBza-R, Bottom: *Gk* CblS + ATP +  $\alpha$ - methoxyBza-R.

C. A. Top: No enzyme + ATP +  $\alpha$ -Bza-R, Bottom: *Gk* CblS + ATP +  $\alpha$ -Bza-R.



APPENDIX D

SUPPLEMENTAL INFORMATION FOR

“INVESTIGATIONS INTO THE ORIGINS OF 5,6-DIMETHYLBENZIMIDAZOLE AND  
ITS  $\alpha$ -RIBOSIDE  $\alpha$ -RIBAZOLE IN *SALMONELLA ENTERICA*”<sup>9</sup>

---

<sup>9</sup> Mattes, T.A. and J. C. Escalante-Semerena. To be submitted to *Journal of Bacteriology*

**Table D1. Plasmid-carrying strains used in Chapter 6.**

<b>Strain</b>	<b>Genotype</b>
<b>JE16715</b>	$\Delta metE2702 ara-9 \Delta cobT1380 \Delta cobB1375 \Delta ydjA117 \Delta nfn126 mdaA126::cat/pBAD24 (bla+)$
<b>JE16716</b>	$\Delta metE2702 ara-9 \Delta cobT1380 \Delta cobB1375 \Delta ydjA117 \Delta nfn126 mdaA126::cat/pCOBT48 (S. enterica cobT on pBAD30, bla+)$
<b>JE16717</b>	$\Delta metE2702 ara-9 \Delta cobT1380 \Delta cobB1375 \Delta ydjA117 \Delta nfn126 mdaA126::cat/pGkCblTS2 (Geobacillus kaustophilus cblT and cblS in pBAD24, bla+)$
<b>JE18551</b>	$\Delta metE2702 ara-9 \Delta thiC cobT1379::kan cobB1374::cat$
<b>JE18560</b>	$\Delta metE2702 ara-9 \Delta thiC cobT1379::kan cobB1374::cat / pBAD24 bla+$
<b>JE18561</b>	$\Delta metE2702 ara-9 \Delta thiC cobT1379::kan cobB1374::cat / pCOBT140 (S. enterica cobT+ in pBAD24, bla+)$
<b>JE18562</b>	$\Delta metE2702 ara-9 \Delta thiC cobT1379::kan cobB1374::cat / pGkCBLTS2 (G. kaustophilus cblTS in pBAD24, bla+)$
<b>JE18589</b>	$\Delta metE2702 ara-9 \Delta cobT1380 \Delta cobB1375 \Delta ydjA117 \Delta nfn126 mdaA126::cat/pCOBT140 (S. enterica cobT+ in pBAD24, bla+)$
<b>JE18904</b>	$\Delta metE2702 ara-9 \Delta cobT1379 \Delta cobB1374 purG::kan/pBAD24 (bla+)$
<b>JE18905</b>	$\Delta metE2702 ara-9 \Delta cobT1379 \Delta cobB1374 purG::kan /pGkCBLTS2 (G. kaustophilus cblTS in pBAD24, bla+)$
<b>JE18906</b>	$\Delta metE2702 ara-9 \Delta cobT1379 \Delta cobB1374 purG::kan/pCOBT140 (S. enterica cobT in pBAD24, bla+)$
<b>JE19044</b>	$\Delta metE2702 ara-9 \Delta cobT1379 \Delta cobB1374 purI::MudJ/ pBAD24 (bla+)$
<b>JE19045</b>	$\Delta metE2702 ara-9 \Delta cobT1379 \Delta cobB1374 purI::MudJ /pGkCBLTS2 (G. kaustophilus cblTS in pBAD24, bla+)$
<b>JE19046</b>	$\Delta metE2702 ara-9 \Delta cobT1379 \Delta cobB1374 purI::MudJ/pCOBT140 (S. enterica cobT in pBAD24, bla+)$
<b>JE19070</b>	$\Delta metE2702 ara-9 \Delta cobT1379 \Delta cobB1374 purC::cat/pBAD24 (bla+)$
<b>JE19071</b>	$\Delta metE2702 ara-9 \Delta cobT1379 \Delta cobB1374 purC::cat/pCOBT140 (S. enterica cobT in pBAD24, bla+)$
<b>JE19072</b>	$\Delta metE2702 ara-9 \Delta cobT1379 \Delta cobB1374 purC::cat /pGkCBLTS2 (G. kaustophilus cblTS in pBAD24, bla+)$
<b>JE19075</b>	$\Delta metE2702 ara-9 \Delta cobT1379 \Delta cobB1374 purK::cat/pBAD24 (bla+)$
<b>JE19076</b>	$\Delta metE2702 ara-9 \Delta cobT1379 \Delta cobB1374 purK::cat/pCOBT140 (S. enterica cobT in pBAD24, bla+)$
<b>JE19077</b>	$\Delta metE2702 ara-9 \Delta cobT1379 \Delta cobB1374 purK::cat /pGkCBLTS2 (G. kaustophilus cblTS in pBAD24, bla+)$
<b>JE21671</b>	$\Delta metE2702 ara-9 \Delta thiC1138 ara-9 \Delta cobT1380 ara-9 \Delta cobB1375/pBAD24 (bla+)$
<b>JE21672</b>	$\Delta metE2702 ara-9 \Delta thiC1138 ara-9 \Delta cobT1380 ara-9 \Delta cobB1375/pGkCBLTS2 (G. kaustophilus cblTS in pBAD24, bla+)$
<b>JE21673</b>	$\Delta metE2702 ara-9 \Delta thiC1138 ara-9 \Delta cobT1380 ara-9 \Delta cobB1375/pCOBT140 (S. enterica cobT in pBAD24, bla+)$
<b>JE21676</b>	$\Delta metE2702 ara-9 \Delta cobT1379 \Delta cobB1374 purE::cat/pBAD24 (bla+)$

**Table D1. (Cont'd) Plasmid-carrying strains used in Chapter 6.**

<b>Strain</b>	<b>Genotype</b>
<b>JE21678</b>	$\Delta metE2702 ara-9 \Delta cobT1379 \Delta cobB1374 purE::cat/pCOBT140$ ( <i>S. enterica cobT</i> in pBAD24, bla+)
<b>JE22192</b>	$\Delta metE2702 ara-9 \Delta cobT1380 \Delta cobB1375 thiC1137::kan / pBAD24$ (bla+)
<b>JE22193</b>	$\Delta metE2702 ara-9 \Delta cobT1380 \Delta cobB1375 thiC1137::kan / pCOBT140$ ( <i>S. enterica cobT+</i> in pBAD24, bla+)
<b>JE22194</b>	$\Delta metE2702 ara-9 \Delta cobT1380 \Delta cobB1375 thiC1137::kan / pGkCBLTS2$ ( <i>G. kaustophilus cblTS</i> in pBAD24, bla+)
<b>JE22196</b>	$\Delta metE2702 ara-9 \Delta cobT1380 \Delta cobB1375 purE2154::MudJ / pBAD24$ (bla+)
<b>JE22197</b>	$\Delta metE2702 ara-9 \Delta cobT1380 \Delta cobB1375 purE2154::MudJ / pCOBT140$ ( <i>S. enterica cobT+</i> in pBAD24, bla+)
<b>JE22198</b>	$\Delta metE2702 ara-9 \Delta cobT1380 \Delta cobB1375 purE2154::MudJ / pGkCBLTS2$ ( <i>G. kaustophilus cblTS</i> in pBAD24, bla+)
<b>JE22200</b>	$\Delta metE2702 ara-9 \Delta cobT1380 \Delta cobB1375 purR2319 ::Tn10d(Tc) / pBAD24$ (bla+)
<b>JE22201</b>	$\Delta metE2702 ara-9 \Delta cobT1380 \Delta cobB1375 purR2319 ::Tn10d(Tc) / pCOBT140$ ( <i>S. enterica cobT+</i> in pBAD24, bla+)
<b>JE22202</b>	$\Delta metE2702 ara-9 \Delta cobT1380 \Delta cobB1375 purR2319 ::Tn10d(Tc) / pGkCBLTS2$ ( <i>G. kaustophilus cblTS</i> in pBAD24, bla+)
<b>JE22206</b>	$\Delta metE2702 ara-9 \Delta cobT1380 \Delta cobB1375 purE2154::MudJ purR2319 ::Tn10d(Tc) / pBAD24$ (bla+)
<b>JE22207</b>	$\Delta metE2702 ara-9 \Delta cobT1380 \Delta cobB1375 purE2154::MudJ purR2319 ::Tn10d(Tc) / pCOBT140$ ( <i>S. enterica cobT+</i> in pBAD24, bla+)
<b>JE22208</b>	$\Delta metE2702 ara-9 \Delta cobT1380 \Delta cobB1375 purE2154::MudJ purR2319 ::Tn10d(Tc) / pGkCBLTS2$ ( <i>G. kaustophilus cblTS</i> in pBAD24, bla+)
<b>JE22213</b>	$\Delta metE2702 ara-9 \Delta cobT1380 \Delta cobB1375 \Delta thiC1225 purE2154::MudJ / pBAD24$ (bla+)
<b>JE22214</b>	$\Delta metE2702 ara-9 \Delta cobT1380 \Delta cobB1375 \Delta thiC1225 purE2154::MudJ / pCOBT140$ ( <i>S. enterica cobT+</i> in pBAD24, bla+)
<b>JE22215</b>	$\Delta metE2702 ara-9 \Delta cobT1380 \Delta cobB1375 \Delta thiC1225 purE2154::MudJ / pGkCBLTS2$ ( <i>G. kaustophilus cblTS</i> in pBAD24, bla+)
<b>JE22217</b>	$\Delta metE2702 ara-9 \Delta cobT1380 \Delta cobB1375 \Delta thiC1225 purE2154::MudJ purR2319 ::Tn10d(Tc) / pBAD24$ (bla+)
<b>JE22218</b>	$\Delta metE2702 ara-9 \Delta cobT1380 \Delta cobB1375 \Delta thiC1225 purE2154::MudJ purR2319 ::Tn10d(Tc) / pCOBT140$ ( <i>S. enterica cobT+</i> in pBAD24, bla+)
<b>JE22219</b>	$\Delta metE2702 ara-9 \Delta cobT1380 \Delta cobB1375 \Delta thiC1225 purE2154::MudJ purR2319 ::Tn10d(Tc) / pGkCBLTS2$ ( <i>G. kaustophilus cblTS</i> in pBAD24, bla+)
<b>JE23728</b>	$\Delta metE2702 ara-9 \Delta cobT1380 \Delta cobB1375 / pCgPnuX1$ ( <i>Cornyebacterium glutamicum pnuX</i> inserted in pCV1, bla+)
<b>JE23729</b>	$\Delta metE2702 ara-9 \Delta cobT1380 \Delta cobB1375 / pCgPnuX2$ ( <i>Cornyebacterium glutamicum pnuX</i> inserted in pCV3, cat+)
<b>JE23730</b>	$\Delta metE2702 ara-9 \Delta cobT1380 \Delta cobB1375 / pCgPnuX2$ ( <i>Cornyebacterium glutamicum pnuX</i> inserted in pCV3, cat+) + pBAD24 (bla+)

**Table D1. (Cont'd) Plasmid-carrying strains used in Chapter 6.**

<b>Strain</b>	<b>Genotype</b>
<b>JE23732</b>	$\Delta metE2702 ara-9 \Delta cobT1380 \Delta cobB1375 / pCgPnuX2$ ( <i>Corynebacterium glutamicum pnuX</i> inserted in pCV3, cat+) + pCOBT140 ( <i>Salmonella enterica cobT+</i> in pBAD24, bla+)
<b>JE23743</b>	$\Delta metE2702 ara-9 \Delta cobT1380 \Delta cobB1375 / pSTM\_deoD1$ ( <i>S. enterica deoD+</i> in pCV3, cat+)
<b>JE23744</b>	$\Delta metE2702 ara-9 \Delta cobT1380 \Delta cobB1375 / pSTM\_xapA1$ ( <i>S. enterica xapA+</i> in pCV3, cat+)
<b>JE23745</b>	$\Delta metE2702 ara-9 \Delta cobT1380 \Delta cobB1375 / pGkDeoD1$ ( <i>Geobacillus kaustophilus deoD+</i> in pCV3, cat+)
<b>JE23746</b>	$\Delta metE2702 ara-9 \Delta cobT1380 \Delta cobB1375 / pCV3$ (cat+)
<b>JE23962</b>	$\Delta metE2702 ara-9 \Delta cobT1379 \Delta cobB1374 \Delta purG purC::cat / pBAD24$ (bla+)
<b>JE23963</b>	$\Delta metE2702 ara-9 \Delta cobT1379 \Delta cobB1374 \Delta purG purC::cat / pGkCblTS2$ ( <i>Geobacillus kaustophilus cblTS+</i> in pBAD24, bla+)
<b>JE23964</b>	$\Delta metE2702 ara-9 \Delta cobT1379 \Delta cobB1374 \Delta purG purC::cat / pCOBT140$ ( <i>S. enterica cobT+</i> in pBAD24, bla+)
<b>JE23966</b>	$\Delta metE2702 ara-9 \Delta cobT1379 \Delta cobB1374 purI::MudJ purC::cat / pBAD24$ (bla+)
<b>JE23967</b>	$\Delta metE2702 ara-9 \Delta cobT1379 \Delta cobB1374 purI::MudJ purC::cat / pGkCblTS2$ ( <i>Geobacillus kaustophilus cblTS+</i> in pBAD24, bla+)
<b>JE23968</b>	$\Delta metE2702 ara-9 \Delta cobT1379 \Delta cobB1374 purI::MudJ purC::cat / pCOBT140$ ( <i>S. enterica cobT+</i> in pBAD24, bla+)
<b>JE24142</b>	JR501: <i>hsdSA29 hsdSB121 hsdL6 metA22 metE551 trpC2 ilv-452 rpsL120 xyl-404 galE719 H1-b H2-e, n,x</i> (cured of Fels2) <i>fla-66 nm / pTAC85</i> (bla+)
<b>JE24143</b>	JR501: <i>hsdSA29 hsdSB121 hsdL6 metA22 metE551 trpC2 ilv-452 rpsL120 xyl-404 galE719 H1-b H2-e, n,x</i> (cured of Fels2) <i>fla-66 nm / pGkCblS7</i> ( <i>Geobacillus kaustophilus cblS+</i> in pTAC85, bla+)
<b>JE24144</b>	JR501: <i>hsdSA29 hsdSB121 hsdL6 metA22 metE551 trpC2 ilv-452 rpsL120 xyl-404 galE719 H1-b H2-e, n,x</i> (cured of Fels2) <i>fla-66 nm / pGkCblT7</i> ( <i>Geobacillus kaustophilus cblT+</i> in pTAC85, bla+)
<b>JE24145</b>	JR501: <i>hsdSA29 hsdSB121 hsdL6 metA22 metE551 trpC2 ilv-452 rpsL120 xyl-404 galE719 H1-b H2-e, n,x</i> (cured of Fels2) <i>fla-66 nm / pGkCblTS4</i> ( <i>Geobacillus kaustophilus cblTS+</i> in pTAC85, bla+)
<b>JE24146</b>	JR501: <i>hsdSA29 hsdSB121 hsdL6 metA22 metE551 trpC2 ilv-452 rpsL120 xyl-404 galE719 H1-b H2-e, n,x</i> (cured of Fels2) <i>fla-66 nm / pCOBT256</i> ( <i>S. enterica cobT+</i> in pTAC85, bla+)
<b>JE24147</b>	$\Delta metE2702 ara-9 \Delta cobT1379 \Delta cobB1374 / pTAC85$ (bla+)
<b>JE24148</b>	$\Delta metE2702 ara-9 \Delta cobT1379 \Delta cobB1374 / pGkCblS7$ ( <i>Geobacillus kaustophilus cblS+</i> in pTAC85, bla+)
<b>JE24149</b>	$\Delta metE2702 ara-9 \Delta cobT1379 \Delta cobB1374 / pGkCblT7$ ( <i>Geobacillus kaustophilus cblT+</i> in pTAC85, bla+)
<b>JE24150</b>	$\Delta metE2702 ara-9 \Delta cobT1379 \Delta cobB1374 / pGkCblTS4$ ( <i>Geobacillus kaustophilus cblTS+</i> in pTAC85, bla+)

**Table D1. (Cont'd) Plasmid-carrying strains used in Chapter 6.**

<b>Strain</b>	<b>Genotype</b>
<b>JE24151</b>	$\Delta metE2702 ara-9 \Delta cobT1379 \Delta cobB1374 / pCOBT256$ ( <i>S. enterica cobT+</i> in <i>pTAC85</i> , <i>bla+</i> )
<b>JE24152</b>	$\Delta metE2702 ara-9 \Delta cobT1379 \Delta cobB1374 / pTAC85$ ( <i>bla+</i> ) + <i>pCV3</i> ( <i>cat+</i> )
<b>JE24155</b>	$\Delta metE2702 ara-9 \Delta cobT1379 \Delta cobB1374 / pGkCblS7$ ( <i>Geobacillus kaustophilus cblS+</i> in <i>pTAC85</i> , <i>bla+</i> ) + <i>pCV3</i> ( <i>cat+</i> )
<b>JE24156</b>	$\Delta metE2702 ara-9 \Delta cobT1379 \Delta cobB1374 / pGkCblS7$ ( <i>Geobacillus kaustophilus cblS+</i> in <i>pTAC85</i> , <i>bla+</i> ) + <i>pSTM_deoD1</i> ( <i>S. enterica deoD+</i> in <i>pCV3</i> , <i>cat+</i> )
<b>JE24157</b>	$\Delta metE2702 ara-9 \Delta cobT1379 \Delta cobB1374 / pGkCblS7$ ( <i>Geobacillus kaustophilus cblS+</i> in <i>pTAC85</i> , <i>bla+</i> ) + <i>pSTM_xapA1</i> ( <i>S. enterica xapA+</i> in <i>pCV3</i> , <i>cat+</i> )
<b>JE24158</b>	$\Delta metE2702 ara-9 \Delta cobT1379 \Delta cobB1374 / pGkCblTS4$ ( <i>Geobacillus kaustophilus cblTS+</i> in <i>pTAC85</i> , <i>bla+</i> ) + <i>pCV3</i> ( <i>cat+</i> )
<b>JE24159</b>	$\Delta metE2702 ara-9 \Delta cobT1379 \Delta cobB1374 / pGkCblTS4$ ( <i>Geobacillus kaustophilus cblTS+</i> in <i>pTAC85</i> , <i>bla+</i> ) + <i>pSTM_deoD1</i> ( <i>S. enterica deoD+</i> in <i>pCV3</i> , <i>cat+</i> )
<b>JE24160</b>	$\Delta metE2702 ara-9 \Delta cobT1379 \Delta cobB1374 / pGkCblTS4$ ( <i>Geobacillus kaustophilus cblTS+</i> in <i>pTAC85</i> , <i>bla+</i> ) + <i>pSTM_xapA1</i> ( <i>S. enterica xapA+</i> in <i>pCV3</i> , <i>cat+</i> )
<b>JE24161</b>	$\Delta metE2702 ara-9 \Delta cobT1379 \Delta cobB1374 / pCOBT256$ ( <i>S. enterica cobT+</i> in <i>pTAC85</i> , <i>bla+</i> ) + <i>pCV3</i> ( <i>cat+</i> )
<b>JE24162</b>	$\Delta metE2702 ara-9 \Delta cobT1379 \Delta cobB1374 / pCOBT256$ ( <i>S. enterica cobT+</i> in <i>pTAC85</i> , <i>bla+</i> ) + <i>pSTM_deoD1</i> ( <i>S. enterica deoD+</i> in <i>pCV3</i> , <i>cat+</i> )
<b>JE24163</b>	$\Delta metE2702 ara-9 \Delta cobT1379 \Delta cobB1374 / pCOBT256$ ( <i>S. enterica cobT+</i> in <i>pTAC85</i> , <i>bla+</i> ) + <i>pSTM_xapA1</i> ( <i>S. enterica xapA+</i> in <i>pCV3</i> , <i>cat+</i> )
<b>JE24167</b>	$\Delta metE2702 ara-9 \Delta cobT1379 \Delta cobB1374 / pTAC85$ ( <i>bla+</i> ) + <i>pCgPnuX2</i> ( <i>Corynebacterium glutamicum pnuX</i> inserted in <i>pCV3</i> , <i>cat+</i> )
<b>JE24168</b>	$\Delta metE2702 ara-9 \Delta cobT1379 \Delta cobB1374 / pGkCblS7$ ( <i>Geobacillus kaustophilus cblS+</i> in <i>pTAC85</i> , <i>bla+</i> ) + <i>pCgPnuX2</i> ( <i>Corynebacterium glutamicum pnuX</i> inserted in <i>pCV3</i> , <i>cat+</i> )
<b>JE24169</b>	$\Delta metE2702 ara-9 \Delta cobT1379 \Delta cobB1374 / pGkCblTS4$ ( <i>Geobacillus kaustophilus cblTS+</i> in <i>pTAC85</i> , <i>bla+</i> ) + <i>pCgPnuX2</i> ( <i>Corynebacterium glutamicum pnuX</i> inserted in <i>pCV3</i> , <i>cat+</i> )
<b>JE24170</b>	$\Delta metE2702 ara-9 \Delta cobT1379 \Delta cobB1374 / pCOBT256$ ( <i>S. enterica cobT+</i> in <i>pTAC85</i> , <i>bla+</i> ) + <i>pCgPnuX2</i> ( <i>Corynebacterium glutamicum pnuX</i> inserted in <i>pCV3</i> , <i>cat+</i> )
<b>JE24503</b>	BL21 (DE3) <i>cobT762::kan</i> / <i>pStm_rihA2</i> ( <i>S. enterica rihA</i> in <i>pTEV18</i> , <i>bla+</i> )
<b>JE24504</b>	BL21 (DE3) <i>cobT762::kan</i> / <i>pStm_rihC2</i> ( <i>S. enterica rihC</i> in <i>pTEV18</i> , <i>bla+</i> )
<b>JE24513</b>	BL21 (DE3) <i>cobT762::kan</i> / <i>pStm_DeoD2</i> ( <i>S. enterica deoD</i> in <i>pTEV18</i> , <i>bla+</i> )
<b>JE24514</b>	BL21 (DE3) <i>cobT762::kan</i> / <i>pStm_xapA2</i> ( <i>S. enterica xapA</i> in <i>pTEV18</i> , <i>bla+</i> )
<b>JE24515</b>	BL21 (DE3) <i>cobT762::kan</i> / <i>pStm_udp2</i> ( <i>S. enterica udp</i> in <i>pTEV18</i> , <i>bla+</i> )
<b>JE24516</b>	BL21 (DE3) <i>cobT762::kan</i> / <i>pStm_DeoB1</i> ( <i>S. enterica deoB</i> in <i>pTEV18</i> , <i>bla+</i> )